frontiers | Research Topics

Insights in red blood cell physiology 2023

Edited by
Lars Kaestner and Anna Bogdanova

Published in
Frontiers in Physiology

ISSN 1664-8714
ISBN 978-2-8325-5037-3
DOI 10.3389/978-2-8325-5037-3

About Frontiers

Frontiers is more than just an open access publisher of scholarly articles: it is a pioneering approach to the world of academia, radically improving the way scholarly research is managed. The grand vision of Frontiers is a world where all people have an equal opportunity to seek, share and generate knowledge. Frontiers provides immediate and permanent online open access to all its publications, but this alone is not enough to realize our grand goals.

Frontiers journal series

The Frontiers journal series is a multi-tier and interdisciplinary set of open-access, online journals, promising a paradigm shift from the current review, selection and dissemination processes in academic publishing. All Frontiers journals are driven by researchers for researchers; therefore, they constitute a service to the scholarly community. At the same time, the *Frontiers journal series* operates on a revolutionary invention, the tiered publishing system, initially addressing specific communities of scholars, and gradually climbing up to broader public understanding, thus serving the interests of the lay society, too.

Dedication to quality

Each Frontiers article is a landmark of the highest quality, thanks to genuinely collaborative interactions between authors and review editors, who include some of the world's best academicians. Research must be certified by peers before entering a stream of knowledge that may eventually reach the public - and shape society; therefore, Frontiers only applies the most rigorous and unbiased reviews. Frontiers revolutionizes research publishing by freely delivering the most outstanding research, evaluated with no bias from both the academic and social point of view. By applying the most advanced information technologies, Frontiers is catapulting scholarly publishing into a new generation.

What are Frontiers Research Topics?

Frontiers Research Topics are very popular trademarks of the *Frontiers journals series*: they are collections of at least ten articles, all centered on a particular subject. With their unique mix of varied contributions from Original Research to Review Articles, Frontiers Research Topics unify the most influential researchers, the latest key findings and historical advances in a hot research area.

Find out more on how to host your own Frontiers Research Topic or contribute to one as an author by contacting the Frontiers editorial office: frontiersin.org/about/contact

Insights in red blood cell physiology: 2023

Topic editors

Lars Kaestner — Saarland University, Germany

Anna Bogdanova — University of Zurich, Switzerland

Citation

Kaestner, L., Bogdanova, A., eds. (2024). *Insights in red blood cell physiology: 2023*. Lausanne: Frontiers Media SA. doi: 10.3389/978-2-8325-5037-3

Table of contents

frontiers | Frontiers in Physiology

TYPE Editorial
PUBLISHED 05 June 2024
DOI 10.3389/fphys.2024.1437573

OPEN ACCESS

EDITED AND REVIEWED BY
John D. Imig,
University of Arkansas for Medical Sciences, United States

*CORRESPONDENCE
Anna Bogdanova,
annab@access.uzh.ch
Lars Kaestner,
lars_kaestner@me.com

RECEIVED 23 May 2024
ACCEPTED 27 May 2024
PUBLISHED 05 June 2024

CITATION
Bogdanova A and Kaestner L (2024), Editorial: Insights in red blood cell physiology: 2023. *Front. Physiol.* 15:1437573. doi: 10.3389/fphys.2024.1437573

Editorial: Insights in red blood cell physiology: 2023

Anna Bogdanova[1]* and Lars Kaestner[2,3]*

[1]Red Blood Cell Group, Institute of Veterinary Physiology, University of Zurich, Zurich, Switzerland, [2]Dynamics of Fluids, Experimental Physics, Saarland University, Saarbrücken, Germany, [3]Theoretical Medicine and Biosciences, Medical Faculty, Saarland University, Homburg, Saar, Germany

KEYWORDS

sickle cell disease, drug transport, asplenia, transfusion, extracellular vesicle release, GP.Mur, COVID-19, hemorheology

Editorial on the Research Topic
Insights in red blood cell physiology: 2023

The contributions of the Research Topic "Insights in Red Blood Cell Physiology: 2023" brought to our attention most relevant areas of red blood cell (RBC) research. They include the RBCs as targets and the active players defining the severity of disease manifestation in patients with SARS-CoV-2 (Lechuga et al.; Rogers et al.) and sickle cell disease (Goksel et al.), the possibilities to use RBCs as drug carriers (Biagiotti et al.), the role of RBC membrane dynamics in progression of storage lesions of RBCs (Ghodsi et al.) and in asplenic patients (Dumas et al.), as well as various aspects of optimization of oxygen delivery (Hsu; Wise et al.).

Since the first days of SARS-CoV-2 pandemics, RBC oxidation (Papadopoulos et al., 2022; Bellanti et al., 2023), anemia (Chen et al., 2021) or secondary polycythemia (Yavorkovsky et al., 2023), and increased risk of thrombosis (Vrečko et al., 2022; Bellanti et al., 2023; Farooqui et al., 2023) were reported as confounding factors associated with compromised respiratory function contributing to the severe impairment of oxygen delivery. Also changes in RBC shape and deformability were previously reported for COVID-19 patients (Kubánková et al., 2021; Recktenwald et al., 2022). In their paper Rogers et al. use Lorrca Maxsis to assess the changes in rheological parameters and aggregation index caused by SARS-CoV-2 infection in patients with A and O blood groups and investigated the impact of disease on oxygen transport by hemoglobin. The obtained results reveal the alterations in RBC rheology and oxygen transport capacity in patients with COVID-19 questioning the "protective role" of the blood group O that was claimed by other studies to be associated with milder disease phenotype. A review article by Lechuga et al. summarizes the recent updates on the alterations in RBC caused by "long COVID-19" when symptoms prevail 12 weeks after the disease onset. It is complementary to the review of Papadopulos et al. which focuses on the changes in RBC properties during the acute COVID-19 phase (Papadopoulos et al., 2022). The impact of the interaction of erythroid precursor cells and the circulating cells with the virus itself and the proinflammatory cytokines on RBC indices, deformability, and morphology as well as on the iron metabolism is discussed. Transfusion is a common measure to correct for anemia, also for COVID patients. However, both unstable RBC membranes and stored RBCs release vesicles that may induce a hypercoagulation state (Leal et al., 2018). In their study, Ghodsi et al. show that RBCs of some donors are more prone to vesiculation during storage than those of others. The authors revealed that the two groups of donors differ in the abundance of cholesterol content of plasma membranes suggesting that cholesterol-rich

domains are focal points for the onset of vesiculation. Another type of vesiculation is associated with the release of organelles from reticulocytes during their maturation (Dumas et al.). In this case, theese "vacuoles" are formed that encapsulate the organelles inside the cell and then released from the cells in the process requiring passages through the spleen.

Vesiculation is a challenge for those who try to use RBCs as delivery systems for cytotoxic drugs (Wang et al., 2023). A review dedicated to the recent developments in using RBCs as carriers for drug transport is presented by Biagiotti et al. The optimization of delivery and the possible applications of this delivery system are discussed including modulators of oxygen delivery and immunosuppressive drugs, chemotherapeutics, anti-diabetic and psychoactive drugs.

RBCs are a natural carrier of the compounds regulating vascular tone. The group of Hsu explores the role of anion exchanger-1 in the transport of nitrite into RBCs, where it is reduced to NO by deoxyhemoglobin and released from the cells when they face hypoxic microenvironment causing vasodilatation. Wise et al. discuss plasticity in adjusting oxygen delivery by RBCs from the lungs to hypoxic peripheral tissues by combining vaso-regualtory action with precise control over hemoglobin oxygen affinity. Modulators of hemoglobin's oxygen affinity decreasing the concentration of 2,3-bisphosphoglycerate are currently trialed as symptomatic therapy for patients with sickle cell disease (Parekh et al., 2024). In contrast, from a high-altitude study, it was suggested that hypoxia modulates 2,3-bisphosphoglycerate levels in human RBCs (D'Alessandro et al., 2024). Goksel et al. suggest that inhibitors of phosphodiesterase PDE1 may further contribute to the optimization of oxygen delivery in sickle cell disease patients by making RBC more deformable when exposed to shear stress.

Having a compilation of contributions dealing with basic physiological principles (Wise et al., Hsu), relating to diseases with direct and indirect involvement of RBCs (Goksel et al.; Dumas et al.; Rogers et al.; Lechuga et al.), concerning transfusion medicine-related topics (Ghodsi et al.), and reviewing therapeutic approaches (Biagiotti et al.), we are convinced the series of "Insights in Red Blood Cell Physiology" appearing since 2021 (Kaestner and Bogdanova, 2022) is of utmost relevance and will continue in future.

Author contributions

AB: Writing–original draft. LK: Writing–original draft.

Funding

The author(s) declare that no financial support was received for the research, authorship, and/or publication of this article.

Conflict of interest

The authors declare that the research was conducted in the absence of any commercial or financial relationships that could be construed as a potential conflict of interest.

The author(s) declared that they were an editorial board member of Frontiers, at the time of submission. This had no impact on the peer review process and the final decision.

Publisher's note

References

Bellanti, F., Kasperczyk, S., Kasperczyk, A., Dobrakowski, M., Pacilli, G., Vurchio, G., et al. (2023). Alteration of circulating redox balance in coronavirus disease-19-induced acute respiratory distress syndrome. *J. Intensiv. Care* 11, 30. doi:10.1186/s40560-023-00679-y

Chen, C., Zhou, W., Fan, W., Ning, X., Yang, S., Lei, Z., et al. (2021). Association of anemia and COVID-19 in hospitalized patients. *Futur. Virol.* 16, 459–466. doi:10.2217/fvl-2021–0044

D'Alessandro, A., Earley, E. J., Nemkov, T., Stephenson, D., Dzieciatkowska, M., Hansen, K. C., et al. (2024). Genetic polymorphisms and expression of Rhesus blood group RHCE are associated with 2,3-bisphosphoglycerate in humans at high altitude. *Proc. Natl. Acad. Sci. U. S. Am.* 121, e2315930120. doi:10.1073/pnas.2315930120

Farooqui, A. A., Farooqui, T., Sun, G. Y., Lin, T.-N., Teh, D. B. L., and Ong, W.-Y. (2023). COVID-19, blood lipid changes, and thrombosis. *Biomedicines* 11, 1181. doi:10.3390/biomedicines11041181

Kaestner, L., and Bogdanova, A. (2022). Editorial: Insights in red blood cell physiology: 2021. *Front. Physiol.* 13, 993287. doi:10.3389/fphys.2022.993287

Kubánková, M., Hohberger, B., Hoffmanns, J., Fürst, J., Herrmann, M., Guck, J., et al. (2021). Physical phenotype of blood cells is altered in COVID-19. *Biophys. J.* 120, 2838–2847. doi:10.1016/j.bpj.2021.05.025

Leal, J. K. F., Adjobo-Hermans, M. J. W., and Bosman, G. J. C. G. M. (2018). Red blood cell homeostasis: mechanisms and effects of microvesicle generation in health and disease. *Front. Physiol.* 9, 703. doi:10.3389/fphys.2018.00703

Papadopoulos, C., Spourita, E., Tentes, I., Steiropoulos, P., and Anagnostopoulos, K. (2022). Red blood cell malfunction in COVID-19: molecular mechanisms and therapeutic targets. *Viral Immunol.* 35, 649–652. doi:10.1089/vim.2021.0212

Parekh, D. S., Eaton, W. A., and Thein, S. L. (2024). Recent developments in the use of pyruvate kinase activators as a new approach for treating sickle cell disease. *Blood* 143, 866–871. doi:10.1182/blood.2023021167

Recktenwald, S. M., Simionato, G., Lopes, M. G., Gamboni, F., Dzieciatkowska, M., Meybohm, P., et al. (2022). Cross-talk between red blood cells and plasma influences blood flow and omics phenotypes in severe COVID-19. *Elife* 11, e81316. doi:10.7554/elife.81316

Vrečko, M. M., Rigler, A. A., and Večerić-Haler, Ž. (2022). Coronavirus disease 2019-associated thrombotic microangiopathy: literature review. *Int. J. Mol. Sci.* 23, 11307. doi:10.3390/ijms231911307

Wang, Z., Wang, X., Xu, W., Li, Y., Lai, R., Qiu, X., et al. (2023). Translational challenges and prospective solutions in the implementation of biomimetic delivery systems. *Pharmaceutics* 15, 2623. doi:10.3390/pharmaceutics15112623

Yavorkovsky, L. L., Biller, J. A., and Wallace, K. L. (2023). Pulmonary arteriovenous malformation (with secondary erythrocytosis) A diagnosis hastened by COVID-19 pandemic. *Mayo Clin. Proc.* 98, 443–444. doi:10.1016/j.mayocp.2022.10.020

frontiers | Frontiers in Physiology

TYPE Original Research
PUBLISHED 20 June 2023
DOI 10.3389/fphys.2023.1205493

OPEN ACCESS

EDITED BY
Lars Kaestner,
Saarland University, Germany

REVIEWED BY
Sophie D. Lefevre,
Université Paris Cité, France
Marianna H. Antonelou,
National and Kapodistrian University of Athens, Greece
Helene Guizouarn,
Centre National de la Recherche Scientifique (CNRS), France
Ulrich Salzer,
Medical University of Vienna, Austria

*CORRESPONDENCE
Donatienne Tyteca,
donatienne.tyteca@uclouvain.be

†These authors have contributed equally to this work

RECEIVED 13 April 2023
ACCEPTED 30 May 2023
PUBLISHED 20 June 2023

CITATION
Ghodsi M, Cloos A-S, Mozaheb N, Van Der Smissen P, Henriet P, Pierreux CE, Cellier N, Mingeot-Leclercq M-P, Najdovski T and Tyteca D (2023), Variability of extracellular vesicle release during storage of red blood cell concentrates is associated with differential membrane alterations, including loss of cholesterol-enriched domains.
Front. Physiol. 14:1205493.
doi: 10.3389/fphys.2023.1205493

Variability of extracellular vesicle release during storage of red blood cell concentrates is associated with differential membrane alterations, including loss of cholesterol-enriched domains

Marine Ghodsi[1†], Anne-Sophie Cloos[1†], Negar Mozaheb[2], Patrick Van Der Smissen[1], Patrick Henriet[1], Christophe E. Pierreux[1], Nicolas Cellier[3], Marie-Paule Mingeot-Leclercq[2], Tomé Najdovski[3] and Donatienne Tyteca[1*]

[1]Cell Biology Unit and Platform for Imaging Cells and Tissues, de Duve Institute, UCLouvain, Brussels, Belgium, [2]Cellular and Molecular Pharmacology Unit, Louvain Drug Research Institute, UCLouvain, Brussels, Belgium, [3]Service du Sang, Croix-Rouge de Belgique, Suarlée, Belgium

Transfusion of red blood cell concentrates is the most common medical procedure to treat anaemia. However, their storage is associated with development of storage lesions, including the release of extracellular vesicles. These vesicles affect *in vivo* viability and functionality of transfused red blood cells and appear responsible for adverse post-transfusional complications. However, the biogenesis and release mechanisms are not fully understood. We here addressed this issue by comparing the kinetics and extents of extracellular vesicle release as well as red blood cell metabolic, oxidative and membrane alterations upon storage in 38 concentrates. We showed that extracellular vesicle abundance increased exponentially during storage. The 38 concentrates contained on average 7 × 10^{12} extracellular vesicles at 6 weeks (w) but displayed a ~40-fold variability. These concentrates were subsequently classified into 3 cohorts based on their vesiculation rate. The variability in extracellular vesicle release was not associated with a differential red blood cell ATP content or with increased oxidative stress (in the form of reactive oxygen species, methaemoglobin and band3 integrity) but rather with red blood cell membrane modifications, i.e., cytoskeleton membrane occupancy, lateral heterogeneity in lipid domains and transversal asymmetry. Indeed, no changes were noticed in the low vesiculation group until 6w while the medium and the high vesiculation groups exhibited a decrease in spectrin membrane occupancy between 3 and 6w and an increase of sphingomyelin-enriched domain abundance from 5w and of phosphatidylserine surface exposure from 8w. Moreover, each vesiculation group showed a decrease of cholesterol-enriched domains associated with a cholesterol content increase in extracellular vesicles but at different storage time points. This observation suggested that cholesterol-enriched domains could represent a starting point for vesiculation.

Altogether, our data reveal for the first time that the differential extent of extracellular vesicle release in red blood cell concentrates did not simply result from preparation method, storage conditions or technical issues but was linked to membrane alterations.

KEYWORDS

red blood cell transfusion, intracellular ATP, oxidative stress, spectrin network, cholesterol, phosphatidylserine surface exposure, sphingomyelin-enriched domains, membrane microviscosity

Introduction

Blood conservation outside the bloodstream started a century ago with the discovery of citrate as anticoagulant and the addition of dextrose. From that time, scientists have been trying to improve continuously blood storage conditions and the transfusion efficacy. Nowadays, thanks to leukoreduction and additive solutions such as Saline-Adenine-Glucose-Mannitol (SAGM), red blood cell concentrates (RCCs) can be conserved for 42 days at 2°C–6°C. However, despite these considerable advances, the storage period is characterized by the appearance and the accumulation of detrimental changes in erythrocytes, collectively termed as 'storage lesions' (Garcia-Roa et al., 2017). Among those lesions, the irreversible loss of plasma membrane through the formation and the release of extracellular vesicles (EVs) is particularly problematic as they affect the *in vivo* viability and functionality of transfused red blood cells (RBCs) (Barshtein et al., 2016). In addition, EVs seem to be responsible for adverse post-transfusional complications such as thromboembolic and immunomodulatory events as suggested by *in vitro* studies (Rubin et al., 2012; Rubin et al., 2013). Therefore, it appears essential to carefully investigate EV biogenesis and release mechanisms in RCCs in order to improve RBC quality maintenance and to reduce risks of potential adverse effects upon transfusion.

Vesiculation seems to be the consequence of a series of lesions, supposed to be mainly induced by the development of oxidative stress. Throughout storage, the glycolysis pathway is reduced by the accumulation of lactate as well as the hypothermic and acidic storage conditions. As a result, high energy (ATP) and reducing (NAD(P)H and glutathione) compounds are progressively depleted. Moreover, due to the high concentration of ferrous ions and oxygen, chemical oxidation takes place. Since antioxidant defences are affected by metabolic impairments and the low temperature, they are rapidly overwhelmed, leading to the development of oxidative stress. The produced reactive oxygen species (ROS) then oxidize cytosolic and membrane proteins as well as lipids. This phenomenon has been proposed to (i) disturb the RBC cytoskeleton network and anchorage (Kriebardis et al., 2007), (ii) initiate the lipid peroxidation cycle (D'Alessandro et al., 2012), and (iii) disrupt the transversal membrane asymmetry by triggering the surface exposure of phosphatidylserine (PS), normally confined to the inner leaflet (Lu et al., 2011). In consequence, oxidative stress-related damage might finally lead to plasma membrane loss through vesiculation.

Nevertheless, literature data on vesiculation are difficult to compare due to differential RCC preparation and storage conditions (*e.g.*, different storage solutions or leukoreduction protocols) and varying experimental procedures to evidence the storage lesions. Additionally, we still do not properly understand (i) the precise succession of events, (ii) the exact link between the different parameters due to the labile boundary between cause and effect and (iii) if other mechanisms could be involved in EV biogenesis independently of the oxidative stress (Orlov and Karkouti, 2015; Yoshida et al., 2019).

Among the alternative mechanisms, one could propose the budding of EVs from specific regions of the plasma membrane such as submicrometric lipid domains. We previously showed the coexistence of 3 types of lipid domains at the outer plasma membrane leaflet of resting RBCs: (i) those mainly enriched in cholesterol (chol) (referred below as chol-enriched domains) and mostly located at the high curvature (HC) area of RBCs; (ii) those co-enriched in ganglioside GM1, phosphatidylcholine and chol (referred as GM1-enriched domains), found in the low curvature (LC) area, corresponding to the centre of the RBC; and (iii) those co-enriched in sphingomyelin (SM), phosphatidylcholine and chol (referred as SM-enriched domains), also found in LC areas (Carquin et al., 2014; Carquin et al., 2015; Conrard et al., 2018). During RBC deformation, GM1-enriched domain abundance increases in the LC area concomitantly with calcium influx while chol-enriched domains gather to increase the HC area needed for RBC deformation. After deformation, the SM-enriched domain number rises in parallel to calcium efflux in order to restore the initial discoid shape (Leonard et al., 2017b; Conrard et al., 2018; Leonard et al., 2018).

During the storage of RBCs in K^+/EDTA-coated tubes at 4°C, we observed that, among the 3 types of lipid domains at the RBC area, only those enriched in chol are reduced in abundance (Cloos et al., 2020), suggesting a fine tuning of lipid domain dynamics during storage. This decrease occurs concomitantly with the increase of EV release and is preceded by a transient increase in the membrane microviscosity which could create a line tension between the bulk membrane and lipid domains and lead to their loss by vesiculation (Vind-Kezunovic et al., 2008; Leonard et al., 2018). Although storage of RBCs in K^+/EDTA tubes accelerates and exacerbates the accumulation of lesions, this phenomenon could also occur during storage of RCCs as the chol-binding protein stomatin was found to decrease from RBC membranes and to be enriched in EVs during storage of RCCs (Salzer et al., 2008; Prudent et al., 2018).

The present study aimed at determining the mechanisms behind EV release in 38 RCCs by deciphering the time courses and extents of RBC metabolic (ATP concentration), oxidative (ROS and methaemoglobin (metHb) levels and band3 integrity) and membrane (membrane:cytoskeleton interactions, membrane microviscosity, lateral heterogeneity in lipid domains and transversal asymmetry) alterations. Based on data generated for those RBC parameters, we then evaluated the chol composition as well as the content of some membrane and cytoskeletal proteins in the isolated EVs.

Materials and methods

RBC concentrate preparation and whole blood collection

The study was approved by the Medical Ethics Committee of the Cliniques universitaires Saint-Luc (Brussels, Belgium). Leukoreduced RCCs were prepared by La Croix-Rouge de Belgique (Suarlée, Belgium) according to standard protocols defined by European legislations. Briefly, 450 ± 60 mL of whole blood were drawn by venipuncture from donor volunteers and collected into blood bags containing 63 mL of citrate-phosphate-dextrose solution (anticoagulant). Whole blood units were rapidly cooled and maintained at 18°C–22°C overnight. Next, RBCs were separated from plasma and buffy coat by centrifugation at 4,000 g for 10 min, resuspended in 100 mL of SAGM additive solution, leukoreduced by filtration and stored at 2°C–6°C. In total 38 RCCs from 36 different donors were included into the study. Seven RCCs entered the study immediately after preparation and were stored in our laboratory at 2°C–6°C for 2–70 days, while the 31 others were stored at La Croix-Rouge de Belgique for 2 weeks (w) (n = 3), 3w (n = 12), 4w (n = 5), 5w (n = 4) or 6w (n = 7) before delivery to our laboratory after ordering. All donors provided written consent for the use of their donation for scientific research. Donors were aged between 28 and 64 years and covered 20 men and 16 women. To avoid experimental variability and to determine a basal level for each parameter, a fresh blood tube from a female donor was selected as the internal and reference control for comparison with RCCs. However, as few is known about the *ex vivo* evolution of RBC membrane parameters, we ensured that this reference donor was not significantly different from additional donors (3 men and 5 women aged between 25–35 years). Fresh whole blood tubes were collected by venipuncture after informed consent and corresponded to citrate-coated blood tubes. K^+/EDTA-coated tubes were also used for the measurement of lipid domain abundance (see below).

RBC preparation

Except for EV isolation, metHb and extracellular K^+ and glucose measurements, blood (from tubes) or RBCs (from RCCs) were diluted in the appropriate medium (10-fold and 13-fold, respectively) and washed before experiments, as decribed in (Cloos et al., 2020). Dulbecco's Modified Eagle Medium (DMEM, Invitrogen) was employed for PS surface exposure, lipid domain abundance and membrane microviscosity measurement while Hanks' Balanced Salt Solution (HBSS, Cytiva) without calcium was used for all other experiments.

Particle/EV abundance, size and morphology

Particle/EV isolation was performed as in (Cloos et al., 2020). Briefly, RBCs were centrifuged 2 times at 2,000 g for 15 min at room temperature (RT) to collect the supernatant. Then, 800 µL of supernatant were diluted 8.75-fold in sterile filtered phosphate-buffered saline (PBS, Cytiva) solution and centrifuged one last time at 2,000 g at RT for 10 min. The resulting supernatant was submitted to ultracentrifugation at 20,000 g for 20 min at 4°C to pellet particles. After particle resuspension in sterile PBS, samples were submitted to a second ultracentrifugation step in the same conditions. The final pellet was resuspended in 1 mL of sterile PBS. Particle abundance and size were determined on freshly isolated particle samples by Nanoparticle Tracking Analysis (NTA) with the Zetaview (Particle Metrix). Samples were diluted 5- to 5,000-fold in sterile PBS depending on the initial sample concentration and determined for particle size (in nm) and abundance (in particles/mL). The particle concentration was converted into a particle number/RBC by considering the volume of supernatant engaged and the average number of RBCs/µL in RCCs.

Freshly isolated particles were prepared for electron microscopy as in (Cloos et al., 2020). Briefly, particles were immobilized on poly-L-Lysine (PLL)-coated coverslips at RT, washed with 0.1 M cacodylate, fixed with 1% glutaraldehyde in 0.1 M cacodylate, critical-point dried, sputter-coated with 10 nm of gold and finally observed in a CM12 electron microscope with SED detector at 80 kV.

RBC morphology

RBCs were fixed in suspension for 15 min at RT in a solution containing 4% paraformaldehyde and 0.05% glutaraldehyde (v:v). Fixed RBCs were then washed and dropped off on PLL-coated coverslips for 8 min. Coverslips were finally mounted with Dako (Invitrogen) on SuperFrost Plus adhesion slides (VWR) and observed by light microscopy. RBCs were classified into discocytes, echinocytes and spherocytes. Their respective abundance was assessed through manual counting and expressed as % of the total RBC population.

RBC ATP level

ATP levels were determined with the luminescent ATP detection assay kit (Abcam) as in (Cloos et al., 2020; Pollet et al., 2020). Data were normalised by the Hb content evaluated spectrophotometrically and expressed as % of fresh citrate-coated blood tubes.

RBC reactive oxygen species and methaemoglobin levels

Intracellular ROS levels were detected by using the 2,7-dichlorodihydrofluoresceindiacetate (H_2DCFDA, Invitrogen) probe as in (Cloos et al., 2020), except that the experiment was performed in calcium-free HBSS. The median fluorescence intensity (MFI) for RCCs was expressed as % of the MFI calculated for fresh citrate blood tubes. For positive control, 15×10^7 RBCs from fresh blood tubes were treated with 10 µmol H_2O_2 for 3 min. Intracellular metHb levels were assessed with the automated blood gas analyser ABL-90 (Radiometer) from the Cliniques universitaires Saint-Luc (Brussels, Belgium). As the device detects metHb in whole blood, RBCs were not washed before measurement. The metHb amount was expressed as % of total Hb levels (oxygenated Hb, deoxygenated

Hb, carboxyHb and metHb). The physiological range of metHb levels corresponded to the values provided in the ABL-90 manual. For positive control, 15×10^7 RBCs from fresh blood tubes were treated with 3 µmol H_2O_2 for 15 min.

RBC phosphatidylserine surface exposure

RBCs were labelled with Annexin-V-FITC (Invitrogen) and analysed by flow cytometry as in (Cloos et al., 2020). Since Annexin-V labelling requires the presence of calcium ions, calcium-containing DMEM was used for this experiment. The % of PS-exposing RBCs in fresh citrate-coated blood tubes was subtracted from the % of PS-exposing RBCs in concentrates.

RBC spectrin immunofluorescence

Immunolabelling of α,β-spectrin was performed as in (Cloos et al., 2020; Pollet et al., 2020), except that RBCs were blocked with 3% bovine serum albumin (BSA, Sigma) in PBS for 60 min and that coverslips were mounted with Dako and examined with the Zeiss confocal microscope LSM980 using a plan-Apochromat 63x NA 1.4 oil immersion objective. The illumination settings used were identical for all samples from the same experiment. The membrane spectrin occupancy was determined with the Fiji software and data from RCCs were expressed as % of data obtained on fresh citrate-coated tubes.

RBC cholesterol and sphingomyelin vital imaging

Chol and SM were visualized on living RBCs by fluorescence microscopy using respectively the mCherry-Theta toxin fragment and the fluorescent lipid analog BODIPY-SM (Invitrogen) as detailed in (Conrard et al., 2018; Cloos et al., 2020; Cloos et al., 2021). The mCherry-Theta toxin fragment concentrations ranged from 0.55 to 1.75 µM, due to several productions and purifications during the study. Lipid domain abundance was assessed through manual counting, normalised by the average hemi-RBC area calculated with the Fiji software and finally expressed as % of lipid domain abundance in fresh citrate-coated tubes or K^+/EDTA-coated tubes (usually used in our laboratory for lipid domain imaging). While the abundance of SM-enriched domains was similar whatever the anticoagulant, a 1.5-fold higher abundance of chol-enriched domains was detected in citrate tubes. Therefore, values obtained on K^+/EDTA tubes were multiplied by this factor. For chol-enriched domains, their abundance was either determined for the global hemi-RBC area or separately at HC and LC areas to distinguish domains mainly enriched with chol located in HC areas from those co-enriched with chol and polar lipids in LC areas (Conrard et al., 2018). The HC area corresponds to the periphery of spread RBCs while the LC area represents the centre of spread RBCs (Leonard et al., 2017b).

EV and RBC membrane cholesterol content

Chol content was assessed using the Amplex Red cholesterol assay kit (Invitrogen) in the absence of chol esterase (Grimm et al., 2005; Tyteca et al., 2010). Washed RBCs were lysed in 1 mL of distilled water and diluted 8-fold in the kit reaction buffer while PBS-resuspended EVs were diluted 2-fold. Data on RBCs were normalised by the Hb content evaluated spectrophotometrically and expressed as % of fresh citrate blood tubes while data on EVs were expressed as a chol content (in µg) for 10^9 EVs. Following an internal study in our laboratory, we noticed that the average RBC chol content was consistently higher in women than in men. As a result, the RBC chol content of the female reference control in the study was compared with the one of 2 female and 3 male donors. While the former was very close to the one measured for the two other female donors, it was 1.3-fold higher compared with average RBC chol content for the male donors (data not shown). Data obtained on lysed RBCs from male RCC donors were then corrected by this factor.

RBC membrane microviscosity

RBC membrane microviscosity was studied by fluorescence lifetime imaging (FLIM) technique using a molecular rotor (BODIPY-C10), whose fluorescence lifetime is dependent on the microviscosity of the environment. RBCs were labelled in suspension for 60 min at 37°C with 1 µM of BODIPY-C10 dissolved in 1 mg/mL DMEM-BSA. After incubation, RBCs were washed in fresh DMEM, dropped off in plastic chambers (ibidi) for 8 min at RT. Cells were observed with the Zeiss LSM980 multiphoton microscope, which was equipped with a time-correlated single-photon counting (TCSPC) FLIM module (PicoQuant) for high-resolution microscopy. BODIPY-C10 was excited by a coherent (Chameleon Discovery) pulsed laser (80 MHz) at 800 nm. The emission was captured with a 505–545 nm bandpass filter at a resolution of 512 × 512 pixels. The fluorescence lifetimes for each pixel of the image corresponding to the cells were recorded to create the FLIM images. A minimum of 1,000 photons in the brightest pixel were acquired before stopping the FLIM acquisition. The FLIM images were analyzed using the SymPhoTime64 software (PicoQuant, Germany).

Western blotting

After isolation, EV samples were resuspended in RIPA lysis buffer. RBC ghosts and human platelet lysates were prepared as in (Prausnitz et al., 1993; Octave et al., 2021) respectively. Equal protein amounts (except for plasma samples and platelet lysates) were diluted in a buffer containing 10 mM of dithiothreitol (DTT) and then loaded for sodium dodecylsulfate polyacrylamide gel electrophoresis (Mini-Protean TGX Precast Gels 4%–15% (w/v) SDS-PAGE; BioRad or Novex 4–12% Tris-Glycine Gels, Invitrogen). Then, proteins were transferred to polyvinylidene fluoride (PVDF) membranes and blocked for 2 h. Membranes were incubated overnight with anti-apolipoprotein B100 (Apo B100; BioConnect, SC-13538; 1:500), anti-apolipoprotein A1 (Apo A1; BioConnect, SC-376818; 1:500), anti-CD41 (Abcam, ab134131; 1:2,000), anti-glycophorin A (GPA; Merck, MABF758; 1:1,000), anti-flotillin 1 (BD Biosciences, BD610820; 1:500), anti-ankyrin (Merck, MAB1683; 1:1,000), anti-spectrin (α and β) (Merck,

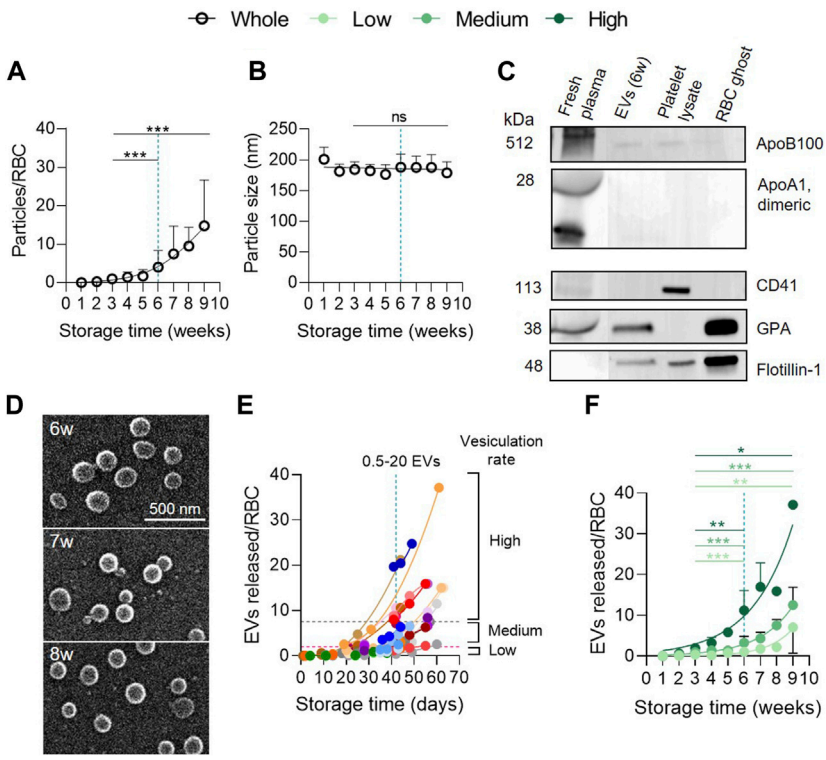

FIGURE 1
RBC vesiculation increases exponentially during storage whatever the donor cohort. **(A,B)** Particle abundance and size in the whole red blood cell concentrate (RCC) cohort. RCCs were centrifuged at low speed to separate cells from supernatants. Then, resulting supernatants were ultracentrifuged to pellet particles. Particle concentration and size were determined with NTA. The concentration was converted into a number of particles expressed in relation to the number of RBCs and the size was expressed in nm. The maximum legal storage period of 6 weeks (w) is indicated by a vertical blue dotted line. **(A)**, Number of particles expressed in relation to the number of RBCs at each week of storage from the 38 RCCs included in the study. Data are expressed as mean ± SD (open symbols). Unpaired *t*-test. Statistical significance is indicated above a line connecting 2 time intervals. **(B)**, Size of particles in nm (n = 38 RCCs). Data are expressed as mean ± SD. Unpaired *t*-test. **(C)** Purity of particle preparations. Western blotting for lipoprotein (apolipoprotein B100 (Apo B100) and apolipoprotein A1 (ApoA1)) and platelet (CD41) contaminations as well as for the presence of RBC (glycophorin A, GPA) and vesicle (flotillin-1) markers. 20 µg/well of particles and RBC ghost proteins. ApoB100 and ApoA1 were revealed on the same cut membrane. CD41 and GPA as well. Flotillin-1 was revealed after GPA membrane stripping. Fresh plasma from blood tubes, platelet lysates and RBC ghosts were used as positive controls. **(D)** Particle morphology. Particles isolated from 2 RCCs stored for the indicated times were laid down on poly-L-Lysine (PLL)-coated coverslips, prepared for and analysed by scanning electron microscopy. **(E)** Comparison of the 38 RCCs for kinetics of EV release during storage. One concentrate, one color. The vesiculation groups were arbitrarily established based on the EV level at 6w of storage: 'high' level with a vesiculation rate ≥7.5 EVs/RBC (area above the grey horizontal dotted line), 'medium' level with a vesiculation rate >2–7.4 EVs/RBC (area between the grey and pink horizontal dotted lines) and 'low' level with a vesiculation rate 0–2 EVs/RBC (area below the pink horizontal dotted line). **(F)** Classification of the whole RCC cohort into 3 groups based on the extent of vesiculation. High level (dark green, n = 9 RCCs), medium level (intermediate green, n = 20 RCCs), low level (light green, n = 9 RCCs). Data are expressed as mean ± SD. Mann Whitney test.

S3396; 1:500), anti-stomatin (Abcam, ab67880; 1:500) or anti-band3 (Invitrogen, MA1-20211; 1:4,000) antibodies. Secondary peroxidase-conjugated goat anti-rabbit or anti-mouse IgGs were then incubated for 1 h and washed. Signal revelation was performed with SuperSignalTM West Pico or Femto (ThermoScientific).

Hemolysis and extracellular potassium and glucose measurements

RCCs were centrifuged at 2,000 g for 10–15 min and the supernatant was collected for Hb and extracellular K^+ content for measurement with the ABL-90. As the device is calibrated for fresh blood samples, RCC supernatants were diluted in SAGM solution if necessary and data corrected for the dilution factor. The physiological range of plasma K^+ levels corresponded to the values provided in the ABL-90 manual. For hematocrit, total Hb and glucose contents, RCCs were directly injected into the device. As RCCs contain the glucose-rich additive SAGM solution, the comparison with blood tubes was not relevant. Data were expressed in mmol/L for K^+ and in mg/dL for glucose. The percentage of hemolysis was calculated as follows: (100-hematocrit) x supernatant Hb/total Hb.

Data presentation and statistical analysis

Kinetics during storage were represented in the form of weekly storage intervals (except in Figure 1E; Supplementary Figure S2; Supplementary Figure S8). The end of the legal storage period is indicated by a vertical blue dotted line. Horizontal black dotted line indicates reference values obtained from fresh blood tubes, mainly

citrate-coated tubes except otherwise stated. The physiological range for metHb and K^+ content in blood is represented by a grey frame while the maximal percentage of hemolysis authorized by the Council of Europe guidelines and the glucose concentration in SAGM and plasma are indicated by horizontal red full and dotted lines. Whenever data for a specific parameter was collected within one storage week from more than one RCC, the mean ± SEM (for most parameters) or ± SD (for EV abundance and size measurements, metHb content, hemolysis and extracellular K^+ and glucose concentrations) for the concerned RCCs was calculated and represented on graphs. Notice that, in some conditions, the error bars are smaller than the size of the symbols.

In Figure 1E, data are presented for each RCC individually through color associations and in the form of the precise storage days in order to identify the 'high', 'medium' and 'low' vesiculation groups. The 3 groups were defined arbitrarily based on the number of EVs released at the legal storage period (42 days). The 'high' vesiculation group contains RCCs with a vesiculation rate ≥7.5 EVs/RBC at 42 days of storage (area above the horizontal grey dotted line), the 'medium' group includes RCCs with >2–7.4 EVs/RBC (area between horizontal pink and grey dotted lines) and the 'low' vesiculation group is composed of RCCs with 0–2 EVs/RBC (area below the horizontal pink dotted line). These groups consisted of 9, 20 and 9 RCCs respectively. To distinguish the different groups, the entire RCC cohort is represented by black opened circles, the high vesiculation by dark green closed circles, the medium vesiculation group by intermediate green closed circles and the low vesiculation group by light green closed circles. In Supplementary Figure S1, data from blood tubes were represented by squares.

To compare the 3 vesiculation cohorts at one specific time point, one-way ANOVA followed by Tukey's multiple comparisons test or Kruskall-Wallis test with Dunn's multiple comparison was performed. The statistical significance of these tests is presented in Supplementary Table S1. For the comparison of 2 time points during storage, an unpaired *t*-test (with Welch's correction if required) or a Mann-Whitney test was performed. Graphically, statistical significance is indicated above a horizontal full line connecting 2 time intervals. Statistical comparison was mainly performed between 3w (corresponding to the storage interval in which RCCs are mostly transfused) and 6w (the maximal legal storage period) or between 3w and 9w (the longest storage period in this study). When necessary and when presenting similar behavior upon time, data from 2 and 3w or 9 and 10w were merged to get sufficient data for statistical analysis. Furthermore, if no data could be collected for these intervals, data from the neighboring intervals were used instead. Finally, to determine whether a difference exists between a reference value/internal control and a specific time point during storage or between a control and a treatment or to evaluate whether the reference blood tube donor is representative of 3 to 5 others, one sample *t*-test or Wilcoxon signed rank test was realized. Graphically, statistical significance is indicated in orange above one specific time interval to give comparison with the reference value/internal control (horizontal black dotted lines). Logarithmic transformation of particles/RBC, ROS, SM-enriched domains/hemi-RBC and the percentage of hemolysis was realized before the statistical test in order to fulfil normality. ***, $p < 0.001$; **, $p < 0.01$; *, $p < 0.05$; ns, not significant.

For correlations, data were transformed when necessary to ensure linearity. Correlation coefficients higher than 0.6 were plotted on graphs.

Results

Study design

A total of 38 RCCs were included into the study and followed for different parameters up to 10w. However, it should be noted that due to specific experiment timelines, all parameters were not assessed on the overall RCC cohort. In addition, 7 RCCs were freshly delivered from La Croix-Rouge de Belgique to our laboratory and evaluated from the first day of storage while 3 RCCs were delivered after 2w of storage, 12 RCCs after 3w, 5 RCCs after 4w, 4 RCCs after 5w and 7 RCCs after 6w. Since the overall RCC cohort could not be studied at all time points, data for most parameters were expressed in relation to values obtained on fresh blood tubes from the same control donor (represented on graphs by horizontal black dotted lines). In this manner, we avoided data misinterpretation due to experimental variability and all RCCs were compared with the same basal level. However, as few is known about control donor RBC membrane parameters routinely measured in our laboratory, we ensured that these parameters were not significantly different between the reference blood tube donor and 3 to 5 additional tube donors (Supplementary Figure S1).

RBC concentrates can be divided into 3 groups based on their extent of vesiculation

Particles in RCC supernatants were concentrated by differential ultracentrifugation and measured by NTA for their abundance and size. As previously shown (Rubin et al., 2008; Roussel et al., 2017; Lauren et al., 2018), the number of particles, expressed in relation to the number of RBCs present in RCCs, increased exponentially during storage, revealing significant differences between 3 and 6w and between 3 and 9w (Figure 1A). However, the size remained stable over storage, at around 180 nm (Figure 1B). At 6w, a mean of 4 particles for one RBC was measured (Figure 1A), corresponding to ~7×10^{12} particles in a 250 mL bag. In reality, this number showed a ~40-fold variability (~0.5–20 particles/RBC) between RCCs. This difference did not result from measurement irreproducibility by NTA, since 4 RCCs which originated from the same 2 donors (2 RCCs from a single donor) showed a similar particle abundance during storage (Supplementary Figure S2). A potential contamination of samples was also excluded, as shown by very few amounts of lipoproteins and platelets (or their vesicles) compared with fresh plasma (Figure 1C; Supplementary Figures S3A, B). Inversely, particles appeared to have an erythrocytic origin, as revealed by the detection of the RBC marker GPA, and exhibited the raft marker flotillin-1, known to be associated with EVs (Salzer and Prohaska, 2001; Freitas Leal et al., 2020). Further analysis with electron microscopy showed vesicle-like structures with a spherical morphology and no aggregates (Figure 1D). Altogether these data indicated that particles were mainly, if not exclusively, EVs and that RCCs released a variable quantity of vesicles upon storage which cannot be explained by technical issues.

To further determine the origin of this variability, RCCs were separated into 3 groups based on their vesiculation rate at the legal storage period of 6w: 'low' rate (0–2 EVs/RBC), 'medium' rate (>2–7.4 EVs/RBC) or 'high' rate (≥7.5 EVs/RBC) (Figures 1E, F). These groups consisted of 9, 20 and 9 RCCs respectively. Each cohort showed an exponential and significant increase of EVs between 3 and 9w

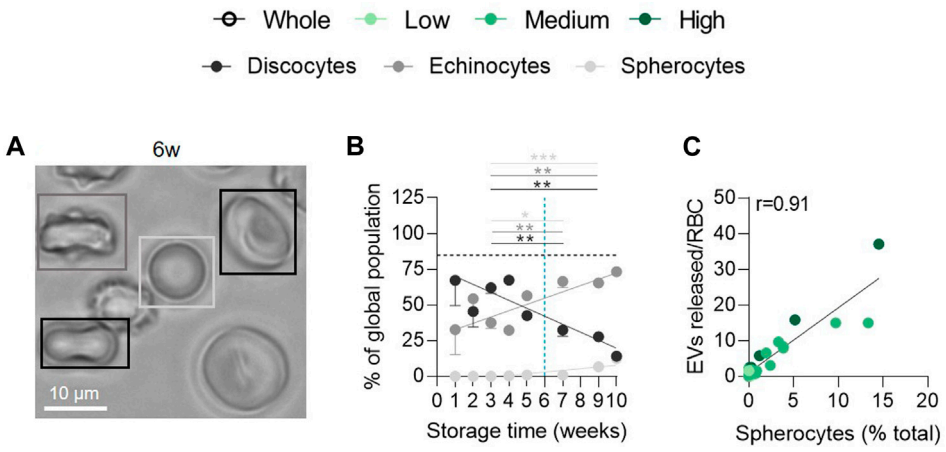

FIGURE 2
The late appearance of spherocytes during storage correlates positively with the extent of EV release. RBCs were fixed in suspension, placed on PLL-coated coverslips and observed by light microscopy. **(A)** Representative image of RBC morphology at 6w of storage. **(B)** Quantification of the relative abundance of discocytes (black), echinocytes (dark grey) and spherocytes (light grey) and expression as % of the global RBC population (n = 15 RCCs). The horizontal black dotted line represents the discocyte abundance of the fresh blood tube. Data are expressed as mean ± SEM. Unpaired *t*-test. **(C)** Correlation between the number of EVs released per RBC and the % of spherocytes in the global population.

(Figure 1F) but was significantly different from each other in terms of amounts of EVs released (Supplementary Table S1, first column). This variability could not be attributed to basic quality measures such as hemolysis and extracellular K^+ and glucose contents, since these parameters were in the expected range and were not different from one cohort to another (Supplementary Figure S4).

Spherocytes appear late during storage and correlate positively with the extent of EV release

Since vesiculation is usually associated with RBC morphological modifications (D'alessandro et al., 2012; Roussel et al., 2017; Alaarg et al., 2013), we next evaluated the relative proportion of discocytes, echinocytes and spherocytes upon time. The abundance of discocytes was already less important than in fresh blood tubes at 1w and further decreased upon storage in favour of echinocytes and a minority of spherocytes (Figures 2A, B). The decrease of discocytes and the increase of spherocytes both correlated with the rise of released EVs for all vesiculation cohorts (data not shown and Figure 2C), suggesting that the relatively late appearance of spherocytes from 6w of storage could be attributed to vesiculation (Roussel et al., 2017).

Intracellular ATP concentration is maintained higher than in fresh tubes until 4 weeks and do not differ at 6 weeks between the 3 vesiculation cohorts

We next wondered whether the high variability in EV abundance between groups could be explained by a differential intracellular ATP concentration. Indeed, ATP levels are known to decrease during storage leading to reorganisation of cytoskeleton, reduction of the antioxidant

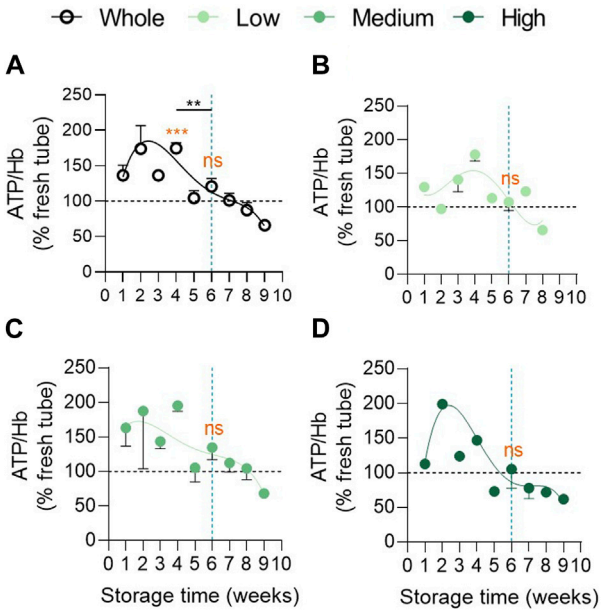

FIGURE 3
Intracellular ATP concentration remains higher in the 3 vesiculation groups in comparison with fresh tubes until 4 weeks of storage and does not differ at 6 weeks. Intracellular ATP concentration was assessed with the luminescent ATP detection assay kit, normalized on the haemoglobin (Hb) content and expressed in % of fresh RBCs in blood tubes. Reference values from fresh blood tubes are represented by horizontal black dotted lines. Evolution of the ATP concentration during storage in the overall RCC population (**(A)**, n = 24 RCCs) and in the 3 cohorts of vesiculation (**(B)**, n = 7; **(C)**, n = 11; **(D)**, n = 6 RCCs). Data are expressed as mean ± SEM. Statistical significance of unpaired *t*-test is indicated above a line connecting 2 time intervals while one sample *t*-test (for the entire cohort) or Wilcoxon signed rank test (for each cohort individually) are indicated in orange above one time interval to give comparison with the internal control (fresh blood tubes).

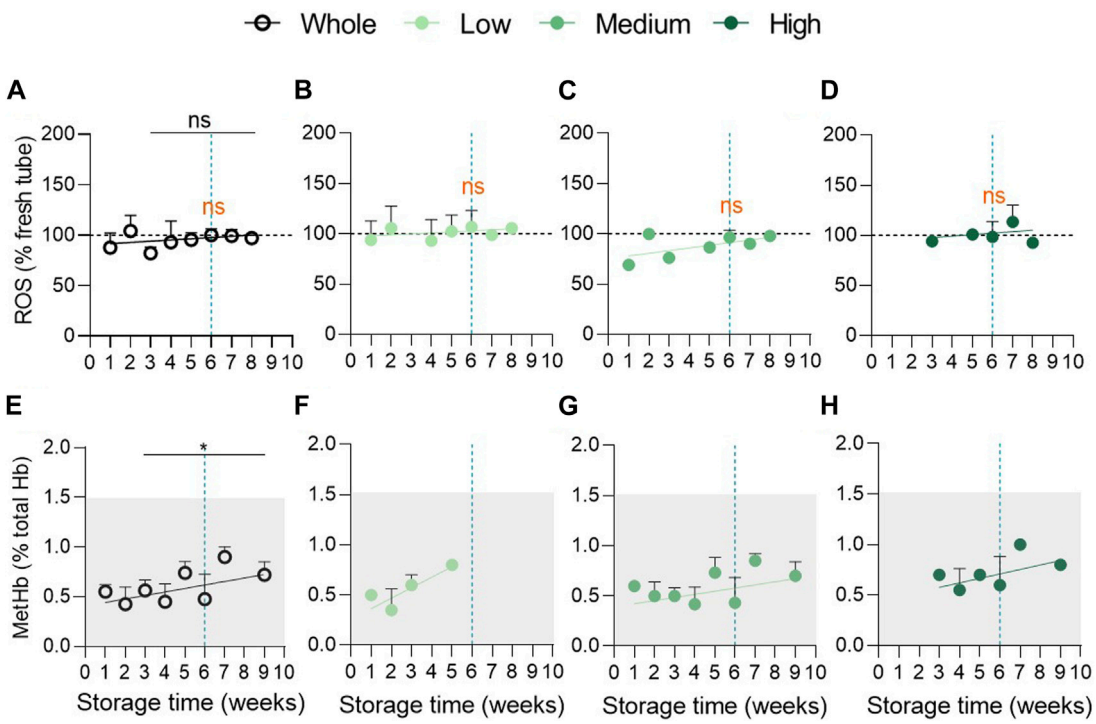

FIGURE 4
Oxidative stress in the form of reactive oxygen species and methaemoglobin does not accumulate during storage. **(A–D)** Intracellular reactive oxygen species levels were detected with the 2,7-dichlorodihydrofluoresceindiacetate (H_2DCFDA) probe in RCCs and in fresh blood tubes and analysed by flow cytometry. The median fluorescence intensity (MFI) for RCCs was expressed as % of the MFI calculated for blood tubes (horizontal black dotted lines). Evolution upon time of the intracellular ROS content in the overall population (**(A)**, n = 17 RCCs) and in the 3 vesiculation cohorts (**(B)**, n = 5; **(C)**, n = 8; **(D)**, n = 4 RCCs). Data are expressed as mean ± SEM. Statistical significance of unpaired *t*-test is indicated above a line connecting 2 time intervals while one sample *t*-test (for the entire cohort) or Wilcoxon signed rank test (for each cohort individually) are indicated in orange above one time interval to give comparison with the internal control (fresh blood tubes). **(E–H)** Intracellular metHb concentration was assessed with the automated blood gas analyser ABL-90 in RCCs and in fresh blood tubes. The metHb amount was expressed as % of total Hb levels. The physiological range of metHb levels is indicated by the clear grey frame. Evolution upon time of the intracellular metHb content in the overall population (**(E)**, n = 13 RCCs) and in the 3 vesiculation cohorts (**(F)**, n = 3; **(G)**, n = 8; **(H)**, n = 2 RCCs). Data are expressed as mean ± SD. Mann-Whitney test (for the entire cohort).

system activities and EV formation (Yoshida et al., 2019). In the overall RCC population, intracellular ATP levels first increased, showing a peak between 1 and 4w of storage, and then decreased progressively (Figure 3A), as observed by Gevi et al. (Gevi et al., 2012). Despite differential kinetics, no significant difference in ATP level could be detected at 6w between groups (Figures 3B–D; Supplementary Table S1, second column). Compared with fresh tubes (horizontal black dotted line), ATP levels in RCCs stayed higher until 4w whatever the cohort (Figure 3). This could be due to the fact that, despite a constant decrease, the glucose content in SAGM never dropped to the plasma level during the whole storage period in each cohort (Supplementary Figures S4I–L). Taken together, these data indicated that the EV abundance variability between the 3 cohorts at 6w could not be explained by a differential intracellular ATP content.

Reactive oxygen species and methaemoglobin do not accumulate during storage in the 3 vesiculation cohorts

As oxidative stress is proposed to be a key player in the development of storage lesions (D'Alessandro et al., 2012; Kriebardis et al., 2008; Gevi et al., 2012; Delobel et al., 2012; Yoshida et al., 2019), we next measured intracellular ROS and metHb contents. Surprisingly, the ROS content was similar in fresh concentrates and in blood tubes and was not modified upon storage (Figure 4A). MetHb levels showed a tendency of constant increase upon storage but stayed in the normal range for fresh blood tubes as defined by the manufacturer of the automated blood gas analyser ABL-90 (grey area at Figure 4E). A technical issue was excluded as ROS and metHb highly increased under H_2O_2 treatment (Supplementary Figure S5) and during the storage of K^+/EDTA blood tubes (Cloos et al., 2020). Moreover, even after cohort division, we were not able to detect accumulation of ROS (Figures 4B–D) or metHb (Figures 4F–H) in RCCs. Overall, oxidative stress did not appear to develop in RCCs at least in the form of ROS and metHb and can therefore not reflect the differences in vesiculation between the 3 groups.

Spectrin occupancy is impaired early during storage and differentially in the 3 vesiculation cohorts

Intrigued by the absence of ROS accumulation, we next wondered whether these reactive species could have attacked other targets than Hb, i.e., the anchorage complex-associated anion transporter band3 and the cytoskeletal protein spectrin (Antonelou et al., 2010;

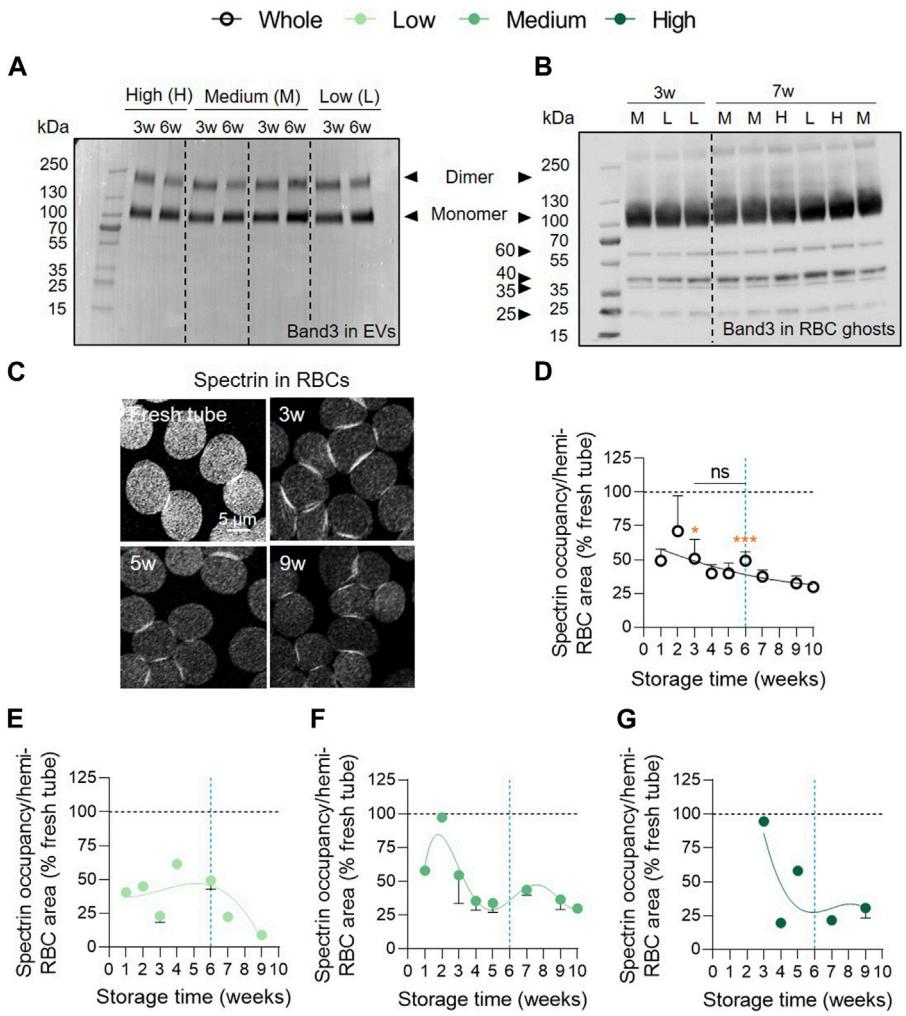

FIGURE 5
The cytoskeleton membrane occupancy is altered early but differentially in the 3 vesiculation groups in contrast to band3 integrity. **(A)** Band3 in EVs. Representative Western blot for the presence of band3 in EVs at 3 and 6w in the 3 vesiculation cohorts (n = 4 RCCs; 1, 2 and 1 RCC(s) from the low, medium and high vesiculation cohort, respectively). 2.4 µg/well of EV proteins. **(B)** Band3 in RBC ghosts. Representative Western blot for the presence of band3 in RBC ghosts at 3 and 7w in the 3 vesiculation cohorts (n = 9 RCCs). 20 µg/well of RBC ghost proteins. L for RBC ghosts from the low vesiculation cohort, M for the medium and H for the high vesiculation cohort. **(C–G)** RBC spectrin membrane occupancy. RBCs were dropped off on PLL-coated coverslips, permeabilised, fixed, immunolabelled for α,β-spectrin and analysed by confocal microscopy. Spectrin-membrane occupancy was determined with Fiji software and expressed as % of fresh blood tubes (horizontal black dotted lines). **(C)**, Representative images of spectrin membrane occupancy during storage. Kinetics of spectrin membrane occupancy during storage in the overall RCC population (**(D)**, n = 17 RCCs) and in the 3 cohorts of vesiculation (**(E)**, n = 4; **(F)**, n = 10; **(G)**, n = 3 RCCs). Data are expressed as mean ± SEM. Statistical significance of unpaired *t*-test is indicated above a line connecting 2 time intervals while one sample *t*-test is indicated in orange above one time interval to give comparison with the internal control (fresh blood tube).

Rinalducci et al., 2012; Prudent et al., 2018), thereby preventing their accumulation and detection. We started by evaluating the presence of band3 in EVs at 3 and 6w of storage by Western blotting in reducing conditions for the 3 vesiculation cohorts. Band3 was found in EVs mainly in the form of monomers but also in dimers at both 3 and 6w whereas no degradation products were detected. However, no obvious differences were visible between 3 and 6w of storage or between the 3 vesiculation cohorts (Figure 5A). We then determined whether band3 dimers were also present in RBC ghosts for each vesiculation cohort. We observed that dimers detected in EVs are present in considerably lower proportions in RBC ghosts when compared with the monomeric form. However, degradation products at approximately 60, 40, 35 and 25 kDa could be visualised (Figure 5B). These band3 fragments were previously reported by Rinalducci et al. and were attributed to oxidative lesions (Rinalducci et al., 2012). Once again, no obvious changes in the profile of band3 could be noticed in the RBC ghosts regarding storage time or according to the vesiculation cohort. The spectrin network was then immunolabelled, visualised by confocal microscopy and quantified for membrane surface occupancy. In the overall RCC population, spectrin occupancy was significantly 2-fold lower than in blood tubes and did not considerably evolve over time (Figures 5C, D). Once cohorts were separated, spectrin occupancy tended to decrease between 2–3 and 5w in the medium and high vesiculation cohorts. In contrast, the low vesiculation cohort showed a stable spectrin occupancy until 6w and then started to decrease (Figures 5E–G). Altogether, these data suggested that the membrane:cytoskeleton interactions were impaired early during

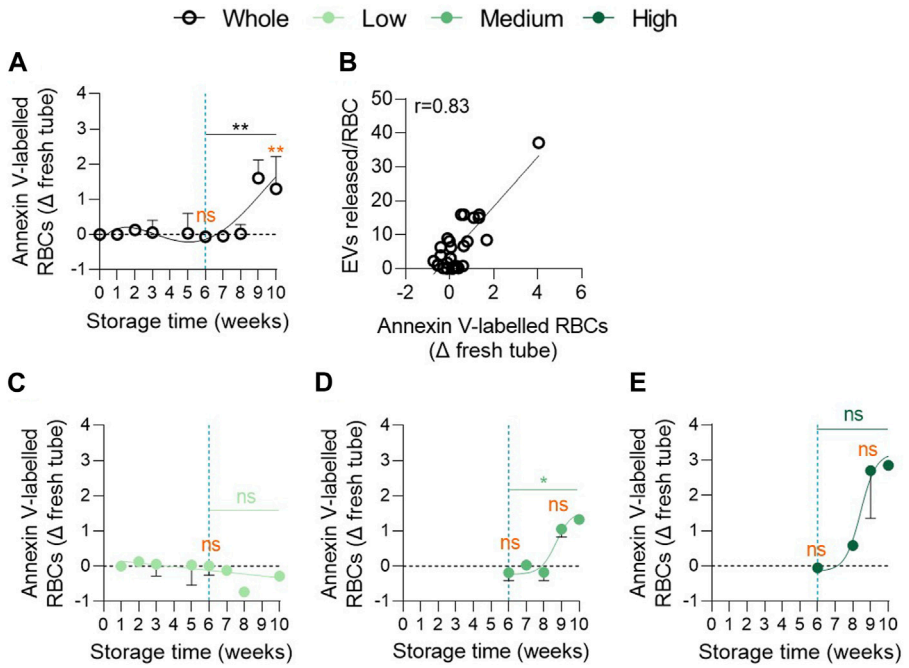

FIGURE 6
The proportion of phosphatidylserine exposing RBCs increases exponentially in the medium and high vesiculation groups from 8 weeks of storage. RBCs were labelled with Annexin-V-FITC and then analysed in flow cytometry. The % of Annexin V-FITC positive RBCs was determined by positioning the cursor at the edge of the labelled cell population for fresh blood tubes. The proportion of labelled RBCs in tubes was subtracted from the percentage of labelled cells in RCCs. **(A,C–E)** Number of PS-exposing RBCs upon time in the overall RCC population (**(A)**, n = 16 RCCs) and in each vesiculation cohort (**(C)**, n = 4; **(D)**, n = 8; **(E)**, n = 4 RCCs). Data are expressed as mean ± SEM. Statistical significance of unpaired *t*-test (for the entire cohort) or Mann-Whitney test (for each cohort individually) is indicated above a line connecting 2 time intervals. In orange, one sample *t*-test (for the entire cohort) or Wilcoxon signed rank test (for each cohort individually) are indicated above one time interval to give comparison with the internal control (fresh blood tube). **(B)** Correlation between EVs released per RBC and the % of Annexin-V-labelled RBCs.

storage which could in part be attributed to oxidative stress. However, whereas spectrin occupancy was differentially altered in the 3 vesiculation groups and evolved over time, it was not the case for band3 alterations.

Membrane transversal asymmetry is altered late during storage and differentially in the 3 vesiculation cohorts

To explore whether cytoskeleton alterations were associated with impairments of membrane transversal asymmetry (Manno et al., 2002), PS externalisation was determined by flow cytometry using Annexin-V labelling. Although PS exposure remained similar to that of fresh blood tubes until 6w of storage, a significant increase was noticed between 6 and 9w with ~2% of PS-exposing RBCs at 9w (Figure 6A). This parameter correlated positively with EV release by RBCs (Figure 6B). More importantly, the 3 cohorts could be discriminated with this parameter. Indeed, the low vesiculation group did not expose PS whatever the storage duration while the medium and high vesiculation groups showed an increase from 8w of storage reaching ~1.5% and ~3% PS exposure at 10w, respectively (Figures 6C–E). Moreover, significant differences were obtained between the low and high groups at 9w of storage (Supplementary Table S1, third column). Taken together, our data revealed that the 3 cohorts could be distinguished by the extent of PS surface exposure. Nevertheless, the kinetics of changes were quite late, occurring during 7–10w. As PS-cytoskeleton interactions are known to modulate membrane stability (Manno et al., 2002), we next wondered whether lateral membrane heterogeneity in domains at the RBC surface could also be altered and contribute to the variability in EV release between groups.

Sphingomyelin-enriched domains rise exponentially upon storage and differentially in the 3 vesiculation cohorts

We therefore analysed the abundance of SM-enriched domains, mostly if not exclusively associated with the LC areas of RBCs (Leonard et al., 2017b). Until 4w of storage in the overall RCC population, this abundance remained stable and was relatively similar to fresh blood tubes. From 5w, SM-enriched domains started to significantly and exponentially increase (Figures 7A, B) and correlated positively with the amount of EVs released (Figure 7C). As for PS exposure, the low vesiculation cohort was protected from this membrane change and showed no correlation between the number of SM-enriched domains and EVs (Figures 7D,G). Conversely, the medium and high vesiculation groups showed a significant exponential increase of SM-enriched domains which correlated with the amount of EVs released (Figures 7E, F, H, I). Nevertheless, no significant difference between the 3 groups could be detected at 9w (Supplementary Table S1, fourth column).

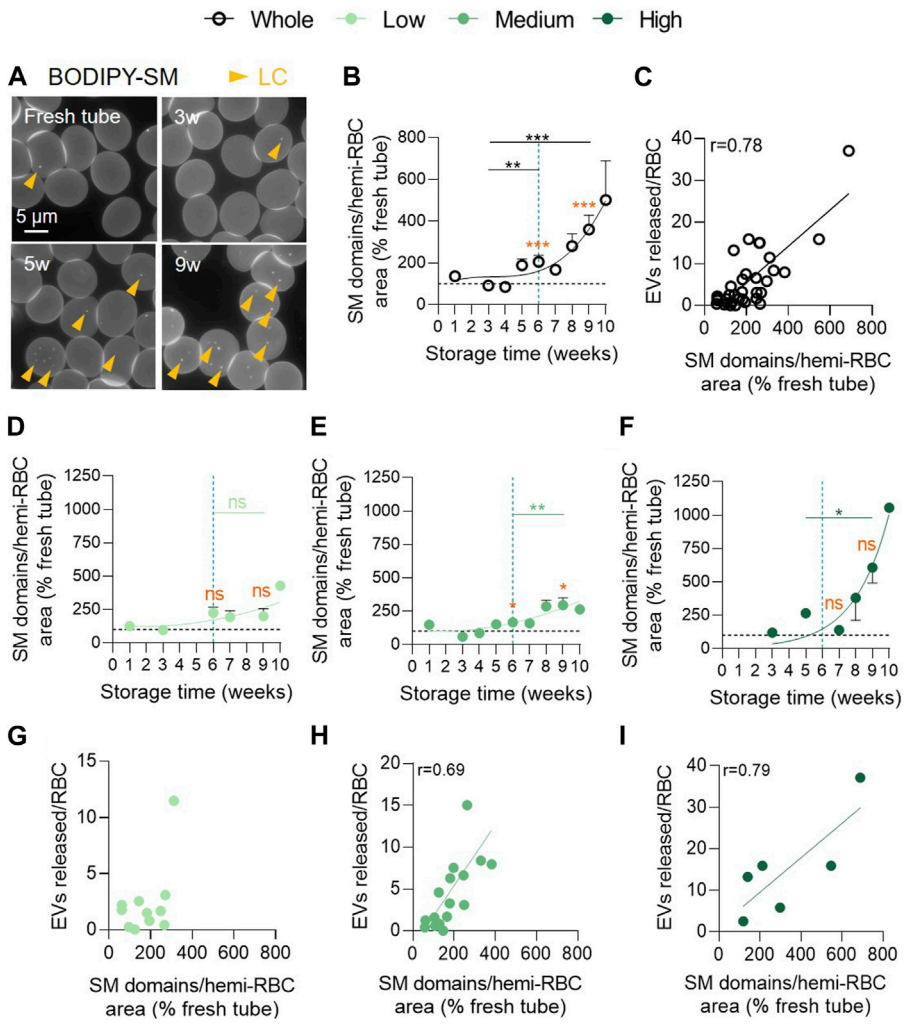

FIGURE 7
Sphingomyelin-enriched domain abundance increases exponentially in the medium and high vesiculation groups and positively correlates with EV accumulation. RBCs were immobilized on PLL-coated coverslips, labelled with BODIPY-SM and then observed by fluorescence microscopy. The domain abundance at the RBC surface in RCCs corresponds to the average number of domains per hemi-RBC area and expressed as % of domain abundance in fresh blood tubes. **(A)** Representative images upon time. Yellow arrowheads, lipid domains in low curvature (LC). **(B,D–F)** Evolution upon time of the number of SM-enriched domains from the overall RCC population (**(B)** n = 15 RCCs) and the 3 cohorts of vesiculation (**(D)**, n = 4; **(E)**, n = 8; **(F)**, n = 3 RCCs). Data are expressed as mean ± SEM. Unpaired *t*-test (for the entire cohort) or Mann-Whitney test (for each cohort individually). Statistical significance is indicated above a line connecting 2 time intervals. In orange, one sample *t*-test (for the entire cohort) or Wilcoxon signed rank test (for each cohort individually) are represented above a precise time interval to give comparison with the internal control (fresh blood tube). **(C,G–I)** Correlation between the number of EVs released by RBC and the SM-enriched domain abundance in the total RCC population **(C)** or in the 3 vesiculation groups **(G–I)**. Correlation coefficients are indicated only if > 0.6.

The decrease of cholesterol-enriched domains from the RBC surface upon storage occurs with differential kinetics in the 3 vesiculation cohorts and is accompanied by an increase of cholesterol in EVs

Next, we evaluated the abundance of chol-enriched domains at the RBC surface in RCCs by fluorescence microscopy. We observed a complex non-significant kinetics with a first transient increase around 2w of storage followed by a decrease between 2 and 5w and a re-increase from 6w of storage. Of note, the number of chol-enriched domains remained lower than in fresh RBCs from blood tubes for the whole storage period (Figures 8A,B). As no statistical difference during storage could be evidenced, we tried to determine from which membrane region the decrease of chol-enriched domains between 2 and 5w could occur. Indeed, we previously showed that lipid domains are preferentially lost from HC areas in K^+/EDTA tubes upon storage (Leonard et al 2017b; Cloos et al., 2020). We therefore differentiated and quantified the domain abundance in HC (red arrowheads) and LC areas (yellow arrowheads) for several RCCs. This analysis showed a significantly lower number of chol-enriched domains in HC but not in LC at 5w compared with fresh tube (Figure 8C), supporting our previous data in K^+/EDTA tubes upon storage (Cloos et al., 2020) and suggesting that chol-enriched domains could be lost by vesiculation from HC areas.

An alternative explanation behind the absence of statistical differences during storage is that the 3 vesiculation cohorts could

10.3389/fphys.2023.1205493

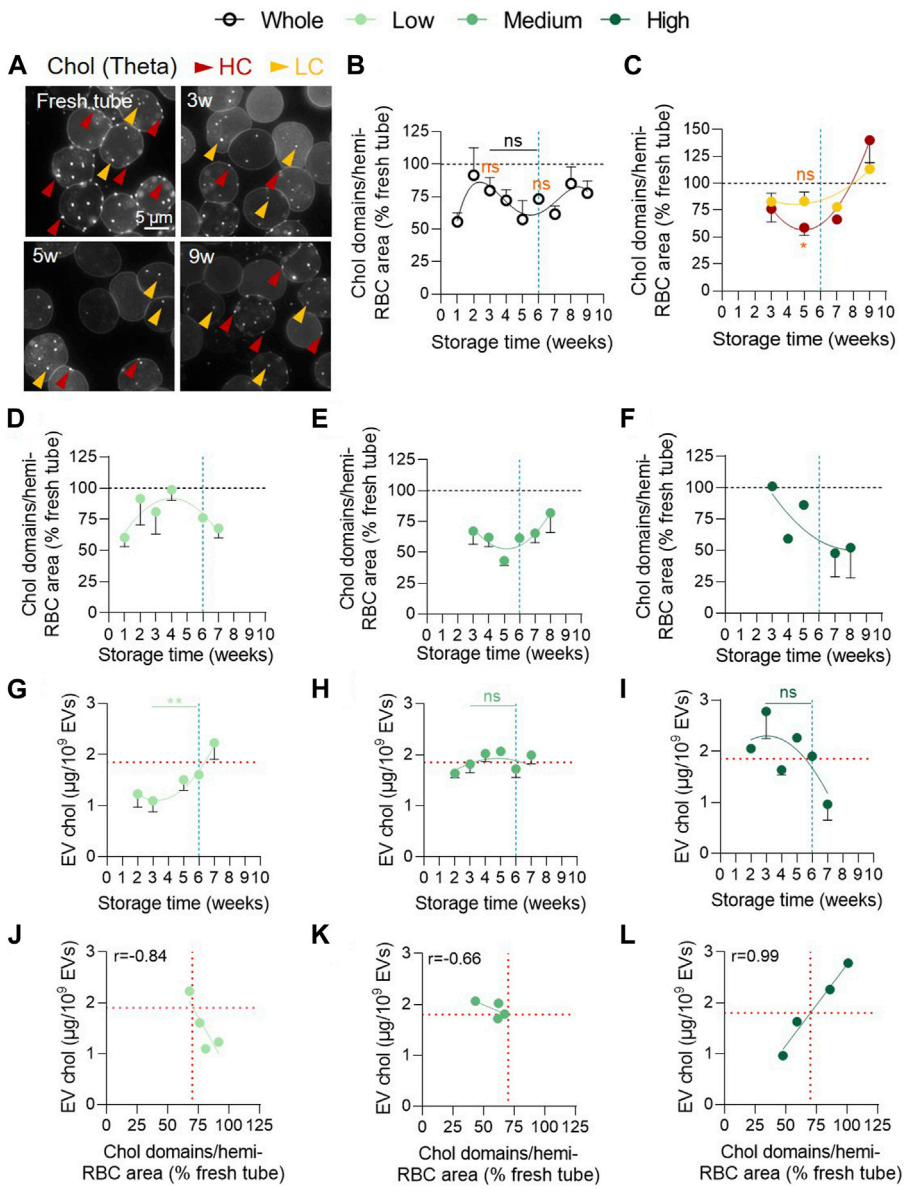

FIGURE 8
The decrease of cholesterol-enriched domain abundance from the RBC surface and the cholesterol association with EVs are observed in the 3 vesiculation cohorts but with differential kinetics. **(A–F)** Abundance of cholesterol (chol)-enriched domains at the RBC surface. RBCs were labelled in suspension with the fluorescent Theta toxin fragment, immobilized on PLL-coated coverslips and then observed by fluorescence microscopy. The domain abundance at the RBC surface in RCCs corresponds to the average number of domains per hemi-RBC area and expressed as % of domain abundance in fresh blood tubes. **(A)** Representative images upon time. Red arrowheads, lipid domains in high curvature (HC) area; yellow arrowheads, lipid domains in low curvature (LC) area. **(B,C)** Kinetics upon storage of the abundance of total chol-enriched domains (**(B)**, n = 18 RCCs) or chol-enriched domains associated with either RBC HC areas (red) or LC areas (yellow) from the overall RCC cohort (**C**, n = 6 RCCs). Data are expressed as mean ± SEM. Mann-Whitney test. Statistical test is indicated above a line connecting 2 time intervals. In orange, Wilcoxon signed rank test is represented above a precise time interval to give comparison with the internal control (fresh blood tube). **(D–F)**, Kinetics of the abundance of content chol-enriched domains in the 3 vesiculation groups (**(D)**, n = 6; **(E)**, n = 8; **(F)**, n = 3 RCCs). Data are expressed as mean ± SEM. **(G–I)**. Evolution of chol content in EVs upon time in the 3 groups of vesiculation (**(G)**, n = 7; **(H)**, n = 16; **(I)**, n = 8 RCCs). Chol was evaluated using the Amplex Red cholesterol assay kit. Data were expressed as a quantity of chol (in µg) for 10^9 EVs and presented as mean ± SEM. Mann-Whitney test. **(J–L)** Correlation between the EV chol content and the abundance of chol-enriched domains in each vesiculation cohort. Horizontal red lines in G-L indicate the EV chol content upon a ~30% decrease of chol-enriched domain abundance.

exhibit differential kinetics of chol-enriched domain alteration. We therefore analysed separately the evolution of chol-enriched domains in the 3 cohorts. Despite different behaviours, the 3 vesiculation groups exhibited a decrease in domain abundance at some time points (Figures 8D–F). To address whether this decrease could be associated with an increase of chol content in EVs, we first evaluated by Western blotting the EV content in stomatin, a chol-binding protein (Salzer et al., 2007). We showed that stomatin was the only protein enriched in EVs compared with RBC ghosts regardless of the storage time. GPA and spectrin were

also present in EVs but not enriched compared with RBC ghosts and ankyrin could not be detected (Supplementary Figures S6A, B). Additionally, stomatin was more enriched in EVs than the raft marker flotillin-1 at 6w except for one RCC from the high vesiculation group (Supplementary Figures S6C, D). Second, we measured the chol content in EVs during storage in the 3 vesiculation groups. A mirror image between the evolution of chol-enriched domains and EV chol content was evident for the 3 groups (Figures 8D–I) and was reflected in the correlations between these two parameters (Figures 8J–L) suggesting that chol-enriched domains could contribute to vesiculation. However, while a negative correlation was observed for the low and medium vesiculation groups as expected, a positive correlation was seen in the high vesiculation group (Figures 8J–L), indicating that lower the abundance of chol-enriched domains, lower the chol content in EVs. Combined with the observations that this high vesiculation cohort presented the highest EV number released, the strongest chol level in EVs at 3w (Figures 8G-I) and a loss of chol content from the RBC membrane (Supplementary Figure S7), this positive correlation suggested that other membrane regions than chol-enriched domains are lost from RBCs in this group.

To confirm the potential contribution of the loss of chol-enriched domains to the vesiculation process whatever the cohort, we looked at the chol content in EVs of the 3 groups for a same chol-enriched domain loss of ~30% (corresponding to the average drop observed for the entire cohort; see Figure 8B and vertical red dotted lines in Figures 8J–L). Such domain decrease was associated with a similar chol content of ~1.9 μg per 10^9 EVs in all 3 groups and was reached only after 6w of storage for the low vesiculation group, between 3 and 4w for the medium vesiculation group and as early as 2w for the high vesiculation group (horizontal red dotted lines in Figures 8G–I). Altogether, these data indicated that the decrease of chol-enriched domains was accompanied by an increase of chol in EVs, suggesting that chol-enriched domains were lost by vesiculation. Moreover, this decrease occurred at differential time points during the storage in the 3 vesiculation cohorts, providing an additional explanation for the non-significant kinetics of chol-enriched domains in the overall cohort besides the differential domain decrease from HC and LC areas.

The RBC membrane microviscosity increases transiently during storage and precedes vesiculation

To then gain insight on the mechanism behind the decrease of chol-enriched domains in the 3 vesiculation groups while addressing the possibility of additional RBC membrane alterations in the high vesiculation group, we measured the RBC membrane microviscosity. For this purpose, fluorescence lifetime of BODIPY-C10 was monitored at 1, 4 and 7w of storage of RBCs from 1 medium and 2 high vesiculation RCCs (Figures 9A, B). The lifetime of this probe correlates with the viscosity of its environment (Mozaheb et al., 2022), a longer lifetime indicating a higher microviscosity of the membrane. After labelling, RCCs were observed by multiphoton microscopy and analysed for the BODIPY-C10 lifetime. Data were expressed as a difference of BODIPY-C10 lifetime *versus* fresh blood tubes. The increase in membrane microviscosity as compared with RBCs from fresh tubes was already present after 1w in the RCC exhibiting the highest vesiculation rate (characterized by the number 2, Figure 9C). It then continued to increase up to 4w and was followed by a decrease in the 3 RCCs (Figures 9A, C). This suggested a transient increase in RBC membrane microviscosity which was reminiscent to the transient rise of ATP concentration (Figures 3C, D). Accordingly, both parameters correlated positively (Figure 9D). Correlation with the EV number was also observed, but was negative between BODIPY-C10 lifetimes and the EV number at the same storage time. Correlation became positive if the lifetimes at 1 and 4w were correlated with EVs released at 4 and 7w respectively (Figures 9E, F). Altogether, these data suggested that the transient increase in membrane microviscosity preceded the release of EVs, at least in the 3 RCCs analysed. The release of EVs and chol from the RBC membrane could in turn affect the RBC membrane in such a way that other membrane regions could be affected.

Discussion

Main observations

The measurement of EV abundance revealed an exponential increase during storage but with a ~40-fold variability between the 38 RCCs included in the study. These RCCs were subsequently classified into 3 cohorts based on their vesiculation rate (Figures 10A–C) and compared for intracellular and membrane parameters (Figures 10D–F). The variability in EV release at 6w was not associated with a differential ATP content or with increased oxidative stress (in the form of ROS, metHb and band3 integrity) but rather with RBC membrane modifications, i.e., cytoskeleton membrane occupancy, lateral heterogeneity in domains and transversal asymmetry, which were not affected simultaneously or with the same rate in each vesiculation group (Figures 10D–F). Among these membrane modifications, the decrease in chol-enriched domain abundance from the RBC surface suggested that those domains could represent a starting point for EV release and prompted us to decipher the mechanism.

The RCCs exhibit an exponential release of EVs characterized by a constant size upon storage

The presence of vesicles in RCCs upon storage is no longer debated (Rubin et al., 2008; Prudent et al., 2018). However, their number and size vary largely between studies. As Rubin et al. and Lauren et al. (Rubin et al., 2008; Lauren et al., 2018), we showed that the EV number increased exponentially during storage. More than 2×10^7 EVs/μL of RCC were measured at 42 days. This value is in concordance with Almizraq et al. who showed by tunable resistive pulse sensing that RCCs stored for 21 days contain between 0.5 and 2.5×10^7 EVs/μL (Almizraq et al., 2017). Likewise, Lauren et al. reported by NTA that the number of EVs climbs up to ~10^7 EVs/μL after 42 days of storage (Lauren et al., 2018). Nevertheless, other groups reported considerably lower numbers, between 650 and 20,000 RBC-derived EVs/μL after 42 days (Rubin et al., 2008;

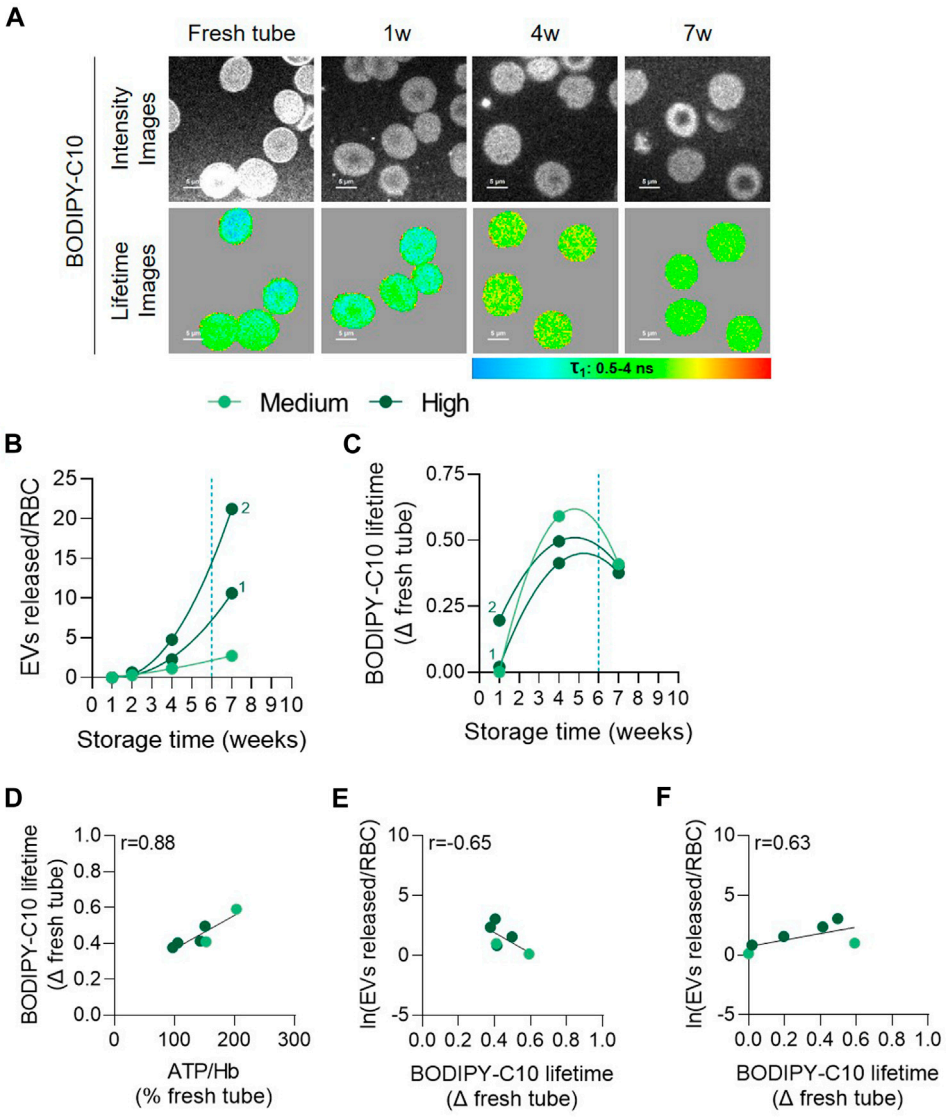

FIGURE 9
The membrane microviscosity increases early during storage and positively correlates with ATP and precedes EV release. RBCs from 3 RCCs were labelled in suspension with BODIPY-C10, washed, dropped off in plastic chamber and examined by confocal microscopy using multiphoton mode. Lifetimes of BODIPY-C10 were determined with SymPhoTime 64 software and expressed as a delta of fresh tube. **(A)** Representative images during storage. The lifetime values (τ) ranged from 0.5 to 4 ns and were shown in pseudocolor-coded images. The longer the lifetime, the higher the membrane microviscosity. **(B)** Number of EVs per RBC at each week of storage from 3 RCCs, 1 from the medium group and 2 from the high vesiculation group (distinguished by a number). **(C)** Evolution of BODIPY-C10 lifetime upon time in the 3 RCCs as a delta of fresh tube. **(D,E)** Correlation between the intracellular ATP content **(D)** and Napierian logarithm of EVs **(E)** with the BODIPY-C10 at the same time intervals. **(F)** Correlation between the Napierian logarithm of EVs and the BODIPY-C10 lifetime in RCCs realized by associating microviscosity at 1w with the EV level at 4w and the microviscosity at 4w with the EV level at 7w.

Almizraq et al., 2017; Roussel et al., 2017; Gamonet et al., 2020). This difference could be related to the flow cytometry-based approaches which have difficulties to detect particles smaller than 200 nm (Serrano-Pertierra et al., 2020). Combined with the fact that optimal RBC markers (mostly GPA) are needed for these approaches, these studies have probably underestimated the number of EVs released in RCCs. Regarding EV size, most studies report an increase over storage (Kriebardis et al., 2008; Bicalho et al., 2016; Almizraq et al., 2017). In our study, the size of vesicles stayed stable all along storage. This difference might be related to different degrees of contamination. Indeed, Bicalho et al. and Almizraq et al. used differential centrifugation at low speed to isolate EVs whereas we observed that 2 steps of ultracentrifugation at 20,000 g were necessary to get rid of lipoprotein and platelet markers (Bicalho et al., 2016; Almizraq et al., 2017). Since both lipoproteins (except chylomicrons) and platelet-derived EVs are supposed to be smaller than EVs produced by RBCs, their presence could influence size measurements, especially at the beginning of storage during which RBC vesiculation is limited (Simonsen, 2017; Lopez et al., 2019).

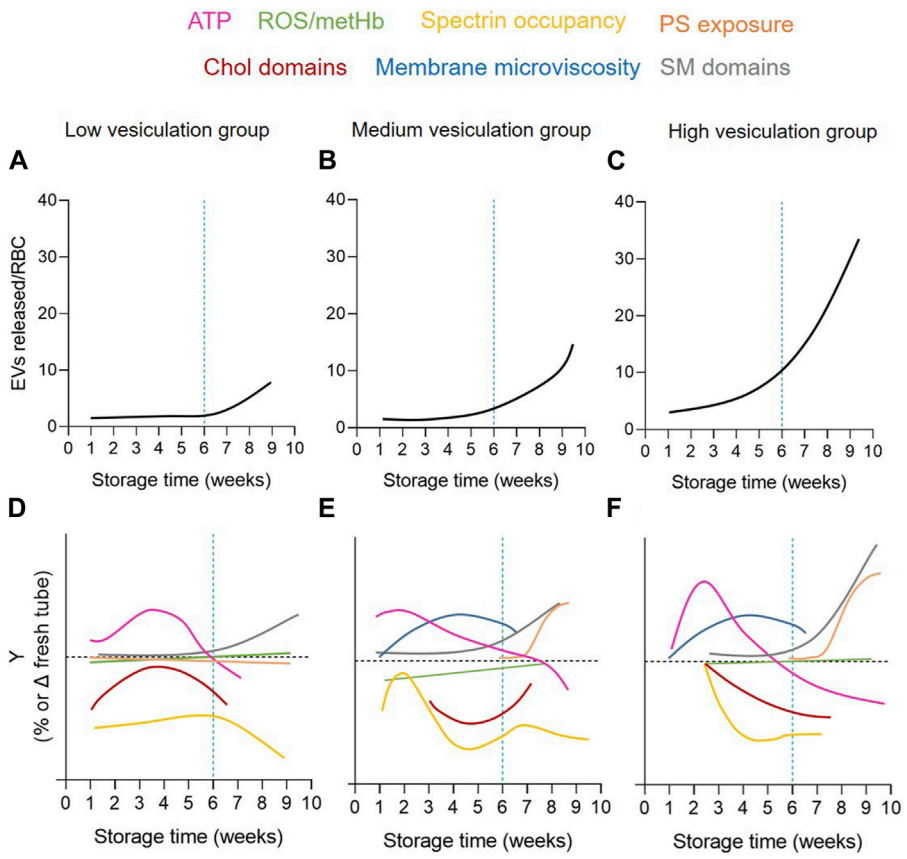

FIGURE 10
Graphical summary of the extent and kinetics of EV release and RBC alterations upon storage in the 3 vesiculation cohorts. The 3 RCC cohorts differed by the extent and kinetics of EV release **(A–C)** but also RBC membrane parameters, including (i) the cytoskeleton membrane occupancy (yellow) and chol-enriched domain abundance (red) during the 1-5w period; (ii) SM-enriched domain abundance (grey) from 5w; and (iii) PS-surface exposure (orange) from 8w **(D–F)**. On the other hand, the RBC membrane microviscosity (blue) and the intracellular ATP content (pink) evolved upon time but were not different between cohorts and ROS/metHb (green) did not appear modified.

The RCCs can be classified into 3 cohorts based on the extent of EV release

The variability in the EV number between RCCs was previously reported and attributed to RCC processing, storage conditions, EV isolation and detection techniques as well as donor characteristics (Rubin et al., 2012; Bicalho et al., 2016; Almizraq et al., 2017; Almizraq et al., 2018; Gamonet et al., 2020; Serrano-Pertierra et al., 2020; Shopsowitz and Shih, 2021). We excluded a variability in RCC preparation as all RCCs were processed by La Croix-Rouge de Belgique. Contaminations and measurement irreproducibility due to EV isolation and detection methods were also dismissed as the comparison of EV kinetics upon storage of 4 RCCs originating from 2 same donors revealed reproducible results with NTA. Regarding donor characteristics, we cross-referenced the data for donor age, gender, BMI and blood group with the number of released EVs at 6w of storage for 25 RCCs. On this specific RCC cohort, no statistical difference could be detected for any of these donor characteristics (data not shown). Confusing data arise in the literature regarding this point. The study of Lelubre et al. showed that female and older donors are associated to increased RBC vesiculation tendency (Lelubre and Vincent, 2013) while the study of Gamonet et al., including 264 RCCs, showed no significant differences in EV abundance according to donor age or gender but described higher EV levels in RCCs from donors with the blood group B and with higher RBC counts (Gamonet et al., 2020). Moreover, in this global picture, the RBC parameters were generally not included, precluding the possibility to better understand the vesiculation mechanism. Here, by classification of RCCs into 3 cohorts based on their extent of vesiculation (Figures 10A–C) we were able to better understand the variability in EV release, both in quantity and kinetics.

The variable EV number between cohorts does not result from differential metabolic impairments or from ROS and metHb accumulation but could be linked to distinct cytoskeleton occupancy alterations

In the medium and high vesiculation groups, the extent of spectrin membrane occupancy was close to fresh blood tubes at

3w of storage before abruptly decreasing. In contrast, in the low vesiculation cohort, this percentage was weaker than in fresh tubes from the beginning of storage and did not evolve until 6w (Figures 10D–F, yellow curves). The lower spectrin membrane occupancy is consistent with the study of Kozlova et al. who reported by atomic force microscopy the apparition of large pores formed in the RBC ghost cytoskeleton from 3w due to the rupture of cytoskeletal filaments (Kozlova et al., 2021; Sherstyukova et al., 2021). This alteration might be responsible for the rapid changes in RBC shape observed from 1w of storage. At this time point, echinocytes represented already more than 25% of RBCs. The abundance of echinocytes then continued to increase and even reached ~60% at 6w.

One possible mechanism for the lower interaction between membrane and cytoskeleton is the ATP-dependent phosphorylation (Manno et al., 1995; Gov and Safran, 2005; Rinalducci et al., 2015). Indeed, Rinalducci et al. observed a substantial increase in the phosphorylation status at 3w of storage in RCCs and visualized by modelling that this event destabilizes interactions between ankyrin and β-spectrin (Rinalducci et al., 2015). In our study, ATP levels increased transiently up to 3w of storage before decreasing progressively. Despite the decrease, ATP levels remained elevated during the whole storage period in the 3 cohorts (Figures 10D–F, pink curves). As a consequence, exaggerated phosphorylation events could occur and alter the cytoskeleton occupancy. The transient increase of ATP agrees with Gevi et al. (Gevi et al., 2012) but is in discordance with other studies that described a slight but constant linear decrease (Burger et al., 2010; Karger et al., 2012; Livshits et al., 2021). During their *ex vivo* storage, RBCs are immersed in a highly concentrated glucose solution. Since the glucose transporter GLUT1 facilitates unidirectional glucose uptake along the concentration gradient, it is not surprising that RBCs react to their new environment and produce high ATP levels (Guizouarn and Allegrini, 2020). In favour of this hypothesis, we found that after 1w of storage the extracellular glucose concentration was ~2-fold reduced, which implicated that half of the disposable glucose in SAGM (900 mg/dL) solution was used within this storage period (Burger et al., 2010). Additionally, it has been proposed that deoxygenated Hb binds to the cytoplasmic tail of band3 inducing the displacement of glycolytic enzymes allowing for their activation (Yoshida et al., 2019).

An alternative hypothesis for the impairment of membrane-cytoskeletal interactions is protein oxidation. Supporting this possibility, oxidative stress in RCCs has been described in the literature mainly in the form of protein and lipid oxidation or through the measurement of antioxidants such as glutathione and urate (D'Alessandro et al., 2012; Kriebardis et al., 2008; Gevi et al., 2012; Delobel et al., 2012). Although we measured variations in ROS content between RCCs, we did not observe any evolution over time (Supplementary Figure S8C; Figures 10D–F, green curves). Furthermore, the metHb content, a major target of ROS, was also not increased. This could be explained by the fact that ROS are extremely reactive and metHb unstable in hypothermic conditions (Shihana et al., 2011; Bardyn et al., 2018). We wondered therefore whether ROS could have attacked lipids or proteins other than Hb. The hypothesis that lipids could have been modified was rapidly discarded. Indeed, during the storage of K^+/EDTA tubes, we previously reported that lipid peroxidation did not significantly increase during storage despite a strong and significant accumulation of ROS and metHb (Cloos et al., 2020). For this reason and since stored blood tubes are an accelerated model for vesiculation, we excluded the possibility that lipid peroxidation would be consequential in stored RCCs. In addition to lipids and Hb, band3, a key component of the membrane-cytoskeleton anchorage complexes, is a preferential target for oxidative attack that leads to its aggregation in membrane and loss in EVs during storage (Prudent et al., 2018). As several research groups, we detected the presence of band3 in EVs from 3w as well as degradation products in RBC ghosts after 3w of storage, suggesting a certain level of oxidative damage at least at the protein level (Rinalducci et al., 2012; Prudent et al., 2018; Freitas Leal et al., 2020). However, band3 dimers in EVs and band3 fragments in RBC ghosts did not accumulate upon storage and showed no obvious differences between the 3 vesiculation cohorts.

The differential EV release in the 3 cohorts is associated with unequal and late impairments of membrane transversal asymmetry during storage

In contrast to the cytoskeleton occupancy, the RBC transversal asymmetry was maintained during the whole legal storage period and started to be altered only after 8w, to reach ~3% of PS-exposing cells in the highest vesiculation group (Figures 10D–F, orange curves). This is in agreement with previous studies which have also reported a limited increase in PS exposure with storage time with maximum levels seen at 7w (Verhoeven et al., 2006; Burger et al., 2010; Dinkla et al., 2014). This very late and limited increase could result from the early loss of PS by vesiculation. Indeed, Freitas Leal et al. observed that nearly 100% of EVs were PS-positive after 3w (Freitas Leal et al., 2020). Alternatively, the use of fluorescent Annexin-V could have underestimated the number of PS-exposing RBCs since Lu et al. detected 18% of PS-exposed RBCs with lactadherin at 6w of storage in RCCs *versus* only 4.5% with Annexin-V (Lu et al., 2011). Nevertheless, low PS exposure in the present storage conditions should be expected and might be explained by the independency of PS exposure from enzymes implicated in transversal asymmetry regulation. In fact, the transversal asymmetry could be largely preserved as calcium is absent in the SAGM solution, preventing the activation of scramblase, and as ATP stores are maintained high until 6w, allowing for flippase activity. Besides calcium, the RBC membrane chol content is also involved in the control of transversal asymmetry and could play a role here. Indeed, in our previous study on RBC storage in K^+/EDTA-coated tubes, we observed that the restoration of the RBC chol content is associated to restored levels of PS exposing RBCs (Cloos et al., 2020). In the present study, we revealed that the highest vesiculation group showed a clear decrease of the RBC chol content, as described for stored RBCs in blood tubes, and the highest increase in PS exposure, which supports this last hypothesis. Nevertheless, even if the mechanism behind PS exposure remains to be elucidated, this alteration was late in all

vesiculation groups, reducing the possibility that it could represent a triggering factor for early EV production.

The variability in EV release in the 3 cohorts is associated with a late and variable increase of SM-enriched domains

The 3 vesiculation cohorts can also be distinguished based on the abundance of SM-enriched domains. The increase in SM-domains abundance was consistent with the maintenance of SM species in stored RBCs and the similar SM enrichment of EVs compared with their parent cells (Lauren et al., 2018; Freitas Leal et al., 2020). Among the triggering factors for SM-enriched domain increase, we can consider the impairment of membrane-cytoskeleton interaction. Indeed, the spectrin membrane occupancy started to decrease at ~6w, 2w and 3w, in the 3 cohorts respectively while the increase in SM-enriched domains started to rise with a delay of 2–3w (Figures 10D–F, grey curves). Additionally, the decrease in chol-enriched domain abundance might represent an another or additional cause for SM-enriched domain alterations, resulting from impairment of RBC global or local membrane fluidity and/or curvature, both regulated by chol (Leonard et al., 2017a).

The differential EV release in the 3 cohorts is associated with a decrease of chol-enriched domains at different times of storage

The chol-enriched domain decrease started from 2w of storage and was specifically observed in RBC HC areas. We therefore asked whether these domains could represent the starting point for EV departure from specific regions of the RBC surface upon storage. Four lines of evidence support this hypothesis. First, the abundance of chol-enriched domains at the HC areas correlated with EV release, at least in the low and medium vesiculation groups (data not shown). Second, as previously shown (Salzer et al., 2008; Freitas Leal et al., 2020), the chol-binding protein stomatin was more enriched in EVs compared with RBC ghosts and with the raft protein flotillin-1 at 6w. This is interesting since stomatin displays a scaffolding function by assembling small membrane microdomains to form larger complexes and to regulate the activity of membrane proteins (Salzer et al., 2007). Third, chol was found in EVs from the 3 cohorts but was more abundant in the high vesiculation group. Finally, the reduction in the abundance of chol-enriched domains was also observed in stored blood tubes in contrast to SM-enriched domains (Cloos et al., 2020). Altogether, our data support the hypothesis that the decrease of chol-enriched domains at the RBC surface did not result from a redistribution of chol in the bilayer but rather from their release by vesiculation.

On a mechanistic point-of-view, based on our previous study on K^+/EDTA tubes upon storage at 4 °C, the increase in membrane microviscosity (Figures 10E,F, blue curves) during storage could represent the starting point for chol-enriched domain loss from the RBC surface. Nevertheless, the opposite hypothesis that loss of chol-enriched domains impacts membrane viscosity cannot be excluded. Such increase in membrane microviscosity was already shown by Kozlova et al. from 4w of storage (Kozlova et al., 2021). The mechanism behind is not clear. Some studies have suggested that it could result from the ATP decrease (Xu et al., 2018). Others rather attributed the decrease to the rupture of cytoskeletal proteins dissociations with the bilayer by phosphorylation and oxidation, leading to the aggregation of membrane components and thickening of cytoskeletal filaments. As a consequence, the membrane organisation and composition change and the cytoskeleton rearrange abnormally with the RBC surface triggering new tensions and an increase in the membrane microviscosity (Kozlova et al., 2021). Additionally, the hypothermic storage could also be implicated as the lower temperature decreases the membrane fluidity (Nozawa, 2011) and the activity of glycolytic and antioxidant enzymes during storage (Yoshida et al., 2019). As a result, lipid peroxidation has been demonstrated through detection of malondialdehyde (D'Alessandro et al., 2012; Bardyn et al., 2018; Collard et al., 2014; Dumaswala et al., 1999), changing membrane composition and organisation. Whatever the mechanism, the increase in microviscosity could cause a line tension at the edges of chol-enriched domains, inducing their release by vesiculation, as previously suggested (Leonard et al., 2017b; Leonard et al., 2018).

Nevertheless, chol-enriched domains started to re-increase from 5w. As this perfectly coincided with the beginning of SM-enriched domain increase in the LC areas and as SM-enriched domains are coenriched in chol (Conrard et al., 2018), one can reasonably propose that the re-increase of chol-enriched domains reflects the increase of SM-enriched domains observed in LC areas from 5w. However, this is probably not the only explanation since chol-enriched domains also re-increased in HC areas. This observation could result from the fact that, after losing chol, the HC area becomes more fluid, facilitating lipid lateral diffusion and allowing new domains to be recruited or to newly form. Those domains could contain polar lipids (e.g., SM or GM1 ganglioside) as well and be lost by vesiculation at later time point, providing a potential explanation behind the positive correlation between the kinetics of chol-enriched domains and EV chol content upon storage in the high vesiculation group. This possibility is supported by the fact that the RBC membrane chol content also specifically decreased in this group upon storage. These data suggested that the decrease of chol-enriched domains represented probably only a part of the global vesiculation mechanism in the high vesiculation group.

Study limitations

Although this study included 38 RCCs from 36 different donors, it encountered limitations. First, most of RCCs were not followed during the whole storage period, meaning that several time intervals did not comprise the exact same RCCs and potentially introducing donor-related issues. However, we did not detect statistical differences for 25 RCCs regarding the following donor characteristics: age, gender, BMI and blood groups. Second, since a large number of RCCs were not studied from day 0, early time points for the different parameters require to be further investigated. This is not easy to implement since RCCs are intended to be transfused at those times. To overcome this difficulty, data for most parameters were expressed in relation to values obtained on fresh whole blood tubes from the same control donor, avoiding data misinterpretation due to experimental variability. To ensure this internal control did not

alter the real kinetics of each RCC, we followed 2 RCCs throughout the whole storage period for the main parameters (i.e., EV abundance, ATP and ROS contents, PS exposure, chol-enriched domain abundance and membrane chol content) and revealed that, whatever the parameter, the 2 RCCs followed the trend of the overall cohort (Supplementary Figure S8). Third, by stratifying our RCC cohort into 3 groups and working with weekly storage intervals, we reduced the number of RCCs studied which complicated the statistical analysis and impacted the probability to reach statistical significance. Nevertheless, despite the absence of statistical analysis or the lack of statistical significance for some parameters, we commented on the observed alterations to encourage the scientific community to further characterize those showing differences between cohorts. Finally, although studying the 8–10w period overtook the acceptable *in vitro* status, it allowed us to confirm that the 3 vesiculation cohorts behave differently, to better understand how and when lesions became substantial and to pave the way for extending the storage time of the low vesiculation cohort.

Conclusion

Our data reveal for the first time that the differential extent of EV release in RCCs did not simply result from RCC preparation method, storage conditions or technical EV-related issues but could be linked to RBC membrane alterations, which are distinct in the 3 cohorts both in terms of extent and kinetics. Among those, the cytoskeleton occupancy changes and the kinetics of SM-enriched domain rise and of PS exposure increase could be distinguished between the 3 groups. Moreover, EV release from specific chol-enriched domains occurs in the 3 vesiculation cohorts but at different time points and they show differential correlation with the EV chol content. These results implicate that chol-enriched domains, combined or not with membrane microviscosity, could represent a potential target to limit EV generation in RCCs since they represent two early membrane alterations. However, in the light of the protective role of EVs in RBC survival and functionality, the contribution of lipid domains in membrane signaling and the significant role of chol in membrane homeostasis, a better understanding of the relationship between those two parameters as well as the precise kinetics in the 3 cohorts is absolutely required.

Data availability statement

The original contributions presented in the study are included in the article/Supplementary Material, further inquiries can be directed to the corresponding author.

Ethics statement

The studies involving human participants were reviewed and approved by the Medical Ethics Committee of the Cliniques universitaires Saint-Luc (Brussels, Belgium). Leukoreduced RCCs were prepared by La Croix-Rouge de Belgique (Suarlée, Belgium) according to standard protocols defined by European legislations. The participants provided their written informed consent to participate in this study.

Author contributions

MG, A-SC, and DT designed the experiments and wrote the manuscript. MG and A-SC performed the experiments and collected the data. Data analysis and interpretation were realized by MG, A-SC, and DT with the help of PH and CP. NM and M-PM-L were in charge of fluorescence lifetime imaging microscopy and quantification. PVDS brought his expertise and helped to acquire data with fluorescence lifetime imaging microscopy and performed the electron microscopy experiments. NC and TN provided RCCs and donor information. All authors contributed to the article and approved the submitted version.

Funding

This work was supported by grants from UCLouvain (FSR and Actions de Recherches concertées, ARC) and the F.R.S-FNRS.

Acknowledgments

We would like to thank Drs. A. Miyawaki, M. Abe, and T. Kobayashi (Riken Brain Science Institute, Saitama, Japan and University of Strasbourg, France) as well as H. Mizuno (KU Leuven, Belgium) for generously supplying the Dronpa-theta-D4 plasmid. The authors also wish to thank Drs. Wim Dehaen (KU Leuven, Belgium) and Tomas Opsomer (KU Leuven, Belgium) for providing us with the BODIPY-C10 probe. We also thank Dr. S. Horman (IREC Institute, UCLouvain) for providing us platelet lysates to confirm purity of EV samples. The Laboratoire central automatisé (Cliniques universitaires Saint-Luc) is acknowledged for the access to the ABL-90 (Radiometer) equipment.

Conflict of interest

The authors declare that the research was conducted in the absence of any commercial or financial relationships that could be construed as a potential conflict of interest.

Publisher's note

Supplementary material

The Supplementary Material for this article can be found online at: https://www.frontiersin.org/articles/10.3389/fphys.2023.1205493/full#supplementary-material

References

Alaarg, A., Schiffelers, R. M., Van Solinge, W. W., and Van Wijk, R. (2013). Red blood cell vesiculation in hereditary hemolytic anemia. *Front. Physiol.* 4, 365. doi:10.3389/fphys.2013.00365

Almizraq, R. J., Holovati, J. L., and Acker, J. P. (2018). Characteristics of extracellular vesicles in red blood concentrates change with storage time and blood manufacturing method. *Transfus. Med. Hemother* 45, 185–193. doi:10.1159/000486137

Almizraq, R. J., Seghatchian, J., Holovati, J. L., and Acker, J. P. (2017). Extracellular vesicle characteristics in stored red blood cell concentrates are influenced by the method of detection. *Transfus. Apher. Sci.* 56, 254–260. doi:10.1016/j.transci.2017.03.007

Antonelou, M. H., Kriebardis, A. G., Stamoulis, K. E., Economou-Petersen, E., Margaritis, L. H., and Papassideri, I. S. (2010). Red blood cell aging markers during storage in citrate-phosphate-dextrose-saline-adenine-glucose-mannitol. *Transfusion* 50, 376–389. doi:10.1111/j.1537-2995.2009.02449.x

Bardyn, M., Tissot, J. D., and Prudent, M. (2018). Oxidative stress and antioxidant defenses during blood processing and storage of erythrocyte concentrates. *Transfus. Clin. Biol.* 25, 96–100. doi:10.1016/j.tracli.2017.08.001

Barshtein, G., Pries, A. R., Goldschmidt, N., Zukerman, A., Orbach, A., Zelig, O., et al. (2016). Deformability of transfused red blood cells is a potent determinant of transfusion-induced change in recipient's blood flow. *Microcirculation* 23, 479–486.

Bicalho, B., Serrano, K., Dos Santos Pereira, A., Devine, D. V., and Acker, J. P. (2016). Blood bag plasticizers influence red blood cell vesiculation rate without altering the lipid composition of the vesicles. *Transfus. Med. Hemotherapy* 43, 19–26. doi:10.1159/000441639

Burger, P., Korsten, H., De Korte, D., Rombout, E., Van Bruggen, R., and Verhoeven, A. J. (2010). An improved red blood cell additive solution maintains 2,3-diphosphoglycerate and adenosine triphosphate levels by an enhancing effect on phosphofructokinase activity during cold storage. *Transfusion* 50, 2386–2392. doi:10.1111/j.1537-2995.2010.02700.x

Carquin, M., Conrard, L., Pollet, H., Van Der Smissen, P., Cominelli, A., Veiga-Da-Cunha, M., et al. (2015). Cholesterol segregates into submicrometric domains at the living erythrocyte membrane: Evidence and regulation. *Cell. Mol. Life Sci.* 72, 4633–4651. doi:10.1007/s00018-015-1951-x

Carquin, M., Pollet, H., Veiga-da-Cunha, M., Cominelli, A., Van Der Smissen, P., N'Kuli, F., et al. (2014). Endogenous sphingomyelin segregates into submicrometric domains in the living erythrocyte membrane. *J. Lipid. Res.* 55, 1331–1342.

Cloos, A. S., Daenen, L. G. M., Maja, M., Stommen, A., Vanderroost, J., Van Der Smissen, P., et al. (2021). Impaired cytoskeletal and membrane biophysical properties of acanthocytes in hypobetalipoproteinemia - a case study. *Front. Physiol.* 12, 638027. doi:10.3389/fphys.2021.638027

Cloos, A. S., Ghodsi, M., Stommen, A., Vanderroost, J., Dauguet, N., Pollet, H., et al. (2020). Interplay between plasma membrane lipid alteration, oxidative stress and calcium-based mechanism for extracellular vesicle biogenesis from erythrocytes during blood storage. *Front. Physiol.* 11, 712. doi:10.3389/fphys.2020.00712

Collard, K., White, D., and Copplestone, A. (2014). The influence of storage age on iron status, oxidative stress and antioxidant protection in paediatric packed cell units. *Blood Transfus.* 12, 210–219. doi:10.2450/2013.0142-13

Conrard, L., Stommen, A., Cloos, A. S., Steinkuhler, J., Dimova, R., Pollet, H., et al. (2018). Spatial relationship and functional relevance of three lipid domain populations at the erythrocyte surface. *Cell. Physiol. Biochem.* 51, 1544–1565. doi:10.1159/000495645

D'alessandro, A., D'amici, G. M., Vaglio, S., and Zolla, L. (2012). Time-course investigation of SAGM-stored leukocyte-filtered red bood cell concentrates: From metabolism to proteomics. *Haematologica* 97, 107–115. doi:10.3324/haematol.2011.051789

Delobel, J., Prudent, M., Rubin, O., Crettaz, D., Tissot, J. D., and Lion, N. (2012). Subcellular fractionation of stored red blood cells reveals a compartment-based protein carbonylation evolution. *J. Proteomics* 76, 181–193. doi:10.1016/j.jprot.2012.05.004

Dinkla, S., Peppelman, M., Van Der Raadt, J., Atsma, F., Novotny, V. M., Van Kraaij, M. G., et al. (2014). Phosphatidylserine exposure on stored red blood cells as a parameter for donor-dependent variation in product quality. *Blood Transfus.* 12, 204–209. doi:10.2450/2013.0106-13

Dumaswala, U. J., Zhuo, L., Jacobsen, D. W., Jain, S. K., and Sukalski, K. A. (1999). Protein and lipid oxidation of banked human erythrocytes: Role of glutathione. *Free Radic. Biol. Med.* 27, 1041–1049. doi:10.1016/s0891-5849(99)00149-5

Freitas Leal, J. K., Lasonder, E., Sharma, V., Schiller, J., Fanelli, G., Rinalducci, S., et al. (2020). Vesiculation of red blood cells in the blood bank: A multi-omics approach towards identification of causes and consequences. *Proteomes* 8, 6. doi:10.3390/proteomes8020006

Gamonet, C., Desmarets, M., Mourey, G., Biichle, S., Aupet, S., Laheurte, C., et al. (2020). Processing methods and storage duration impact extracellular vesicle counts in red blood cell units. *Blood Adv.* 4, 5527–5539. doi:10.1182/bloodadvances.2020001658

Garcia-Roa, M., Del Carmen Vicente-Ayuso, M., Bobes, A. M., Pedraza, A. C., Gonzalez-Fernandez, A., Martin, M. P., et al. (2017). Red blood cell storage time and transfusion: Current practice, concerns and future perspectives. *Blood Transfus.* 15, 222–231. doi:10.2450/2017.0345-16

Gevi, F., D'alessandro, A., Rinalducci, S., and Zolla, L. (2012). Alterations of red blood cell metabolome during cold liquid storage of erythrocyte concentrates in CPD-SAGM. *J. Proteomics* 76, 168–180. doi:10.1016/j.jprot.2012.03.012

Gov, N. S., and Safran, S. A. (2005). Red blood cell membrane fluctuations and shape controlled by ATP-induced cytoskeletal defects. *Biophys. J.* 88, 1859–1874. doi:10.1529/biophysj.104.045328

Grimm, M. O., Grimm, H. S., Patzold, A. J., Zinser, E. G., Halonen, R., Duering, M., et al. (2005). Regulation of cholesterol and sphingomyelin metabolism by amyloid-beta and presenilin. *Nat. Cell. Biol.* 7, 1118–1123. doi:10.1038/ncb1313

Guizouarn, H., and Allegrini, B. (2020). Erythroid glucose transport in health and disease. *Pflugers Arch.* 472, 1371–1383. doi:10.1007/s00424-020-02406-0

Karger, R., Lukow, C., and Kretschmer, V. (2012). Deformability of red blood cells and correlation with ATP content during storage as leukocyte-depleted whole blood. *Transfus. Med. Hemother* 39, 277–282. doi:10.1159/000339809

Kozlova, E., Chernysh, A., Moroz, V., Kozlov, A., Sergunova, V., Sherstyukova, E., et al. (2021). Two-step process of cytoskeletal structural damage during long-term storage of packed red blood cells. *Blood Transfus.* 19, 124–134. doi:10.2450/2020.0220-20

Kriebardis, A. G., Antonelou, M. H., Stamoulis, K. E., Economou-Petersen, E., Margaritis, L. H., and Papassideri, I. S. (2008). RBC-Derived vesicles during storage: Ultrastructure, protein composition, oxidation, and signaling components. *Transfusion* 48, 1943–1953. doi:10.1111/j.1537-2995.2008.01794.x

Kriebardis, A. G., Antonelou, M. H., Antonelou, K. E., Economou-Petersen, E., Margaritis, L. H., and Papassideri, I. S. (2007). Progressive oxidation of cytoskeletal proteins and accumulation of denatured hemoglobin in stored red cells. *J. Cell Mol. Med.* 11, 148–155. doi:10.1111/j.1537-2995.2007.01254.x

Lauren, E., Tigistu-Sahle, F., Valkonen, S., Westberg, M., Valkeajarvi, A., Eronen, J., et al. (2018). Phospholipid composition of packed red blood cells and that of extracellular vesicles show a high resemblance and stability during storage. *Biochim. Biophys. Acta Mol. Cell. Biol. Lipids* 1863, 1–8. doi:10.1016/j.bbalip.2017.09.012

Lelubre, C., and Vincent, J. L. (2013). Relationship between red cell storage duration and outcomes in adults receiving red cell transfusions: A systematic review. *Crit. Care* 17, R66. doi:10.1186/cc12600

Leonard, C., Alsteens, D., Dumitru, A., Mingeot-Leclercq, M., and Tyteca, D. (2017a). "Lipid domains and membrane (re)shaping: From biophysics to biology," in *The biophysics of cell membranes: Biological consequences*. Editors J. Ruysschaert and R. Epand (Springer).

Leonard, C., Conrard, L., Guthmann, M., Pollet, H., Carquin, M., Vermylen, C., et al. (2017b). Contribution of plasma membrane lipid domains to red blood cell (re)shaping. *Sci. Rep.* 7, 4264. doi:10.1038/s41598-017-04388-z

Leonard, C., Pollet, H., Vermylen, C., Gov, N., Tyteca, D., and Mingeot-Leclercq, M. P. (2018). Tuning of differential lipid order between submicrometric domains and surrounding membrane upon erythrocyte reshaping. *Cell. Physiol. Biochem.* 48, 2563–2582. doi:10.1159/000492700

Livshits, L., Barshtein, G., Arbell, D., Gural, A., Levin, C., and Guizouarn, H. (2021). Do we store packed red blood cells under "Quasi-Diabetic" conditions? *Biomolecules* 11, 992. doi:10.3390/biom11070992

Lopez, E., Srivastava, A. K., Burchfield, J., Wang, Y. W., Cardenas, J. C., Togarrati, P. P., et al. (2019). Platelet-derived- extracellular vesicles promote hemostasis and prevent the development of hemorrhagic shock. *Sci. Rep.* 9, 17676. doi:10.1038/s41598-019-53724-y

Lu, C., Shi, J., Yu, H., Hou, J., and Zhou, J. (2011). Procoagulant activity of long-term stored red blood cells due to phosphatidylserine exposure. *Transfus. Med.* 21, 150–157. doi:10.1111/j.1365-3148.2010.01063.x

Manno, S., Takakuwa, Y., and Mohandas, N. (2002). Identification of a functional role for lipid asymmetry in biological membranes: Phosphatidylserine-skeletal protein interactions modulate membrane stability. *Proc. Natl. Acad. Sci. U. S. A.* 99, 1943–1948. doi:10.1073/pnas.042688399

Manno, S., Takakuwa, Y., Nagao, K., and Mohandas, N. (1995). Modulation of erythrocyte membrane mechanical function by beta-spectrin phosphorylation and dephosphorylation. *J. Biol. Chem.* 270, 5659–5665. doi:10.1074/jbc.270.10.5659

Mozaheb, N., Van Der Smissen, P., Opsomer, T., Mignolet, E., Terrasi, R., Paquot, A., et al. (2022). Contribution of membrane vesicle to reprogramming of bacterial membrane fluidity in *Pseudomonas aeruginosa*. *mSphere* 7, e0018722. doi:10.1128/msphere.00187-22

Nozawa, Y. (2011). Adaptive regulation of membrane lipids and fluidity during thermal acclimation in Tetrahymena. *Proc. Jpn. Acad. Ser. B Phys. Biol. Sci.* 87, 450–462. doi:10.2183/pjab.87.450

Octave, M., Pirotton, L., Ginion, A., Robaux, V., Lepropre, S., Ambroise, J., et al. (2021). Acetyl-CoA carboxylase inhibitor CP640.186 increases tubulin acetylation and impairs thrombin-induced platelet aggregation. *Int. J. Mol. Sci.* 22, 13129. doi:10.3390/ijms222313129

Orlov, D., and Karkouti, K. (2015). The pathophysiology and consequences of red blood cell storage. *Anaesthesia* 70 (1), 29–37. doi:10.1111/anae.12891

Pollet, H., Cloos, A. S., Stommen, A., Vanderroost, J., Conrard, L., Paquot, A., et al. (2020). Aberrant membrane composition and biophysical properties impair erythrocyte morphology and functionality in elliptocytosis. *Biomolecules* 10, 1120. doi:10.3390/biom10081120

Prausnitz, M. R., Lau, B. S., Milano, C. D., Conner, S., Langer, R., and Weaver, J. C. (1993). A quantitative study of electroporation showing a plateau in net molecular transport. *Biophys. J.* 65, 414–422. doi:10.1016/S0006-3495(93)81081-6

Prudent, M., Delobel, J., Hubner, A., Benay, C., Lion, N., and Tissot, J. D. (2018). Proteomics of stored red blood cell membrane and storage-induced microvesicles reveals the association of flotillin-2 with band 3 complexes. *Front. Physiol.* 9, 421. doi:10.3389/fphys.2018.00421

Rinalducci, S., Ferru, E., Blasi, B., Turrini, F., and Zolla, L. (2012). Oxidative stress and caspase-mediated fragmentation of cytoplasmic domain of erythrocyte band 3 during blood storage. *Blood Transfus.* 10 (2), s55–s62. doi:10.2450/2012.009S

Rinalducci, S., Longo, V., Ceci, L. R., and Zolla, L. (2015). Targeted quantitative phosphoproteomic analysis of erythrocyte membranes during blood bank storage. *J. Mass Spectrom.* 50, 326–335. doi:10.1002/jms.3531

Roussel, C., Dussiot, M., Marin, M., Morel, A., Ndour, P. A., Duez, J., et al. (2017). Spherocytic shift of red blood cells during storage provides a quantitative whole cell-based marker of the storage lesion. *Transfusion* 57, 1007–1018. doi:10.1111/trf.14015

Rubin, O., Canellini, G., Delobel, J., Lion, N., and Tissot, J. D. (2012). Red blood cell microparticles: Clinical relevance. *Transfus. Med. Hemother* 39, 342–347. doi:10.1159/000342228

Rubin, O., Crettaz, D., Canellini, G., Tissot, J. D., and Lion, N. (2008). Microparticles in stored red blood cells: An approach using flow cytometry and proteomic tools. *Vox Sang.* 95, 288–297. doi:10.1111/j.1423-0410.2008.01101.x

Rubin, O., Delobel, J., Prudent, M., Lion, N., Kohl, K., Tucker, E. I., et al. (2013). Red blood cell-derived microparticles isolated from blood units initiate and propagate thrombin generation. *Transfusion* 53, 1744–1754. doi:10.1111/trf.12008

Salzer, U., Mairhofer, M., and Prohaska, R. (2007). Stomatin: A new paradigm of membrane organization emerges. *Dyn. Cell. Biol.* 1, 20–33.

Salzer, U., and Prohaska, R. (2001). Stomatin, flotillin-1, and flotillin-2 are major integral proteins of erythrocyte lipid rafts. *Blood* 97, 1141–1143. doi:10.1182/blood.v97.4.1141

Salzer, U., Zhu, R., Luten, M., Isobe, H., Pastushenko, V., Perkmann, T., et al. (2008). Vesicles generated during storage of red cells are rich in the lipid raft marker stomatin. *Transfusion* 48, 451–462. doi:10.1111/j.1537-2995.2007.01549.x

Serrano-Pertierra, E., Oliveira-Rodriguez, M., Matos, M., Gutierrez, G., Moyano, A., Salvador, M., et al. (2020). Extracellular vesicles: Current analytical techniques for detection and quantification. *Biomolecules* 10, 824. doi:10.3390/biom10060824

Sherstyukova, E., Chernysh, A., Moroz, V., Kozlova, E., Sergunova, V., and Gudkova, O. (2021). The relationship of membrane stiffness, cytoskeleton structure and storage time of pRBCs. *Vox Sang.* 116, 405–415. doi:10.1111/vox.13017

Shihana, F., Dawson, A. H., and Dissanayake, D. M. (2011). Method of stabilizing blood for the determination of methemoglobin. *J. Clin. Lab. Anal.* 25, 366–368. doi:10.1002/jcla.20487

Shopsowitz, K. E., and Shih, A. W. (2021). How red blood cell quality is starting to carry its weight. *Transfusion* 61, 336–339. doi:10.1111/trf.16264

Simonsen, J. B. (2017). What are we looking at? Extracellular vesicles, lipoproteins, or both? *Circ. Res.* 121, 920–922. doi:10.1161/CIRCRESAHA.117.311767

Tyteca, D., D'auria, L., Van Der Smissen, P., Medts, T., Carpentier, S., Monbaliu, J. C., et al. (2010). Three unrelated sphingomyelin analogs spontaneously cluster into plasma membrane micrometric domains. *Biochim. Biophys. Acta* 1798, 909–927. doi:10.1016/j.bbamem.2010.01.021

Verhoeven, A. J., Hilarius, P. M., Dekkers, D. W., Lagerberg, J. W., and De Korte, D. (2006). Prolonged storage of red blood cells affects aminophospholipid translocase activity. *Vox Sang.* 91, 244–251. doi:10.1111/j.1423-0410.2006.00822.x

Vind-Kezunovic, D., Nielsen, C. H., Wojewodzka, U., and Gniadecki, R. (2008). Line tension at lipid phase boundaries regulates formation of membrane vesicles in living cells. *Biochim. Biophys. Acta* 1778, 2480–2486. doi:10.1016/j.bbamem.2008.05.015

Xu, Z., Zheng, Y., Wang, X., Shehata, N., Wang, C., and Sun, Y. (2018). Stiffness increase of red blood cells during storage. *Microsystems Nanoeng.* 4, 17103. doi:10.1038/micronano.2017.103

Yoshida, T., Prudent, M., and D'alessandro, A. (2019). Red blood cell storage lesion: Causes and potential clinical consequences. *Blood Transfus.* 17, 27–52. doi:10.2450/2019.0217-18

frontiers | Frontiers in Physiology

TYPE Correction
PUBLISHED 18 September 2023
DOI 10.3389/fphys.2023.1291218

OPEN ACCESS

APPROVED BY
Frontiers Editorial Office,
Frontiers Media SA, Switzerland

*CORRESPONDENCE
Donatienne Tyteca,
donatienne.tyteca@uclouvain.be

†These authors have contributed equally to this work

RECEIVED 08 September 2023
ACCEPTED 12 September 2023
PUBLISHED 18 September 2023

CITATION
Ghodsi M, Cloos A-S, Mozaheb N, Van Der Smissen P, Henriet P, Pierreux CE, Cellier N, Mingeot-Leclercq M-P, Najdovski T and Tyteca D (2023), Corrigendum: Variability of extracellular vesicle release during storage of red blood cell concentrates is associated with differential membrane alterations, including loss of cholesterol-enriched domains.
Front. Physiol. 14:1291218.
doi: 10.3389/fphys.2023.1291218

Corrigendum: Variability of extracellular vesicle release during storage of red blood cell concentrates is associated with differential membrane alterations, including loss of cholesterol-enriched domains

Marine Ghodsi[1†], Anne-Sophie Cloos[1†], Negar Mozaheb[2], Patrick Van Der Smissen[1], Patrick Henriet[1], Christophe E. Pierreux[1], Nicolas Cellier[3], Marie-Paule Mingeot-Leclercq[2], Tomé Najdovski[3] and Donatienne Tyteca[1*]

[1]Cell Biology Unit and Platform for Imaging Cells and Tissues, de Duve Institute, UCLouvain, Brussels, Belgium, [2]Cellular and Molecular Pharmacology Unit, Louvain Drug Research Institute, UCLouvain, Brussels, Belgium, [3]Service du Sang, Croix-Rouge de Belgique, Suarlée, Belgium

KEYWORDS

red blood cell transfusion, intracellular ATP, oxidative stress, spectrin network, cholesterol, phosphatidylserine surface exposure, sphingomyelin-enriched domains, membrane microviscosity

A Corrigendum on
Variability of extracellular vesicle release during storage of red blood cell concentrates is associated with differential membrane alterations, including loss of cholesterol-enriched domains

by Ghodsi M, Cloos A-S, Mozaheb N, Van Der Smissen P, Henriet P, Pierreux CE, Cellier N, Mingeot-Leclercq M-P, Najdovski T and Tyteca D (2023). Front. Physiol. 14:1205493. doi: 10.3389/fphys.2023.1205493

In the published article, an **Author name** was incorrectly written as Marie-Paule Mingeot. The correct spelling is Marie-Paule Mingeot-Leclercq.

The authors apologize for this error and state that this does not change the scientific conclusions of the article in any way. The original article has been updated.

Publisher's note

All claims expressed in this article are solely those of the authors and do not necessarily represent those of their affiliated organizations, or those of the publisher, the editors and the reviewers. Any product that may be evaluated in this article, or claim that may be made by its manufacturer, is not guaranteed or endorsed by the publisher.

frontiers | Frontiers in Physiology

TYPE Mini Review
PUBLISHED 24 July 2023
DOI 10.3389/fphys.2023.1203472

OPEN ACCESS

EDITED BY
Lars Kaestner,
Saarland University, Germany

REVIEWED BY
Flavia Dei Zotti,
Columbia University, United States
Angela Risso,
University of Udine, Italy

*CORRESPONDENCE
Salvatore Giovanni De-Simone,
salvatore.simone@fiocruz.br

RECEIVED 10 April 2023
ACCEPTED 10 July 2023
PUBLISHED 24 July 2023

CITATION
Lechuga GC, Morel CM and De-Simone SG (2023), Hematological alterations associated with long COVID-19. *Front. Physiol.* 14:1203472. doi: 10.3389/fphys.2023.1203472

Hematological alterations associated with long COVID-19

Guilherme C. Lechuga[1,2,3], Carlos M. Morel[1] and Salvatore Giovanni De-Simone[1,2,4]*

[1]Center for Technological Development in Health (CDTS)/ National Institute of Science and Technology for Innovation in Neglected Population Diseases (INCT-IDPN), Oswaldo Cruz Foundation (FIOCRUZ), Rio de Janeiro, Brazil, [2]Laboratory of Epidemiology and Molecular Systematics (LESM), Oswaldo Cruz Institute, Oswaldo Cruz Foundation (FIOCRUZ), Rio de Janeiro, Brazil, [3]Laboratory of Cellular Ultrastructure, Oswaldo Cruz Institute, Oswaldo Cruz Foundation (FIOCRUZ), Rio de Janeiro, Brazil, [4]Post-Graduation Program in Science and Biotechnology, Department of Molecular and Cellular Biology, Biology Institute, Federal Fluminense University, Niterói, Brazil

Long COVID-19 is a condition characterized by persistent symptoms lasting beyond the acute phase of COVID-19. Long COVID-19 produces diverse symptomatology and can impact organs and systems, including the hematological system. Several studies have reported, in COVID-19 patients, hematological abnormalities. Most of these alterations are associated with a higher risk of severe disease and poor outcomes. This literature review identified studies reporting hematological parameters in individuals with Long COVID-19. Findings suggest that Long COVID-19 is associated with a range of sustained hematological alterations, including alterations in red blood cells, anemia, lymphopenia, and elevated levels of inflammatory markers such as ferritin, D-dimer, and IL-6. These alterations may contribute to a better understanding of the pathophysiology of Long COVID-19 and its associated symptoms. However, further research is needed to elucidate the underlying mechanisms and potential treatments for these hematological changes in individuals with Long COVID-19.

KEYWORDS

long COVID-19, hematology, post-acute sequelae, SARS-CoV-2, red blood cells, COVID-19

1 Introduction

The COVID-19 pandemic, caused by the SARS-CoV-2 virus, spread rapidly and significantly impacted societies and economies worldwide. Although efforts are ongoing to control the virus's spread and reduce its effects, the successful vaccination strategy significantly decreased morbidity and mortality (Hadj Hassine, 2022). However, the emergence of SARS-CoV-2 variants due to viral mutations produced deep concern in the population. Due to increased transmissibility, some variants became dominant. Furthermore, the spread of Omicron variants, which are more transmissible, demonstrated that these variants also increased resistance to neutralization and vaccination (Hoffmann et al., 2022).

The disease primarily affects the respiratory system. However, COVID-19 can also impact other organs and systems, including the hematological system. Several studies have reported hematological abnormalities in COVID-19 patients. Some alterations include an increase in white blood cell count, a decrease in red blood cell count and hemoglobin levels, an increase in ferritin levels, increase in levels of D-dimer and other markers of coagulation (Słomka et al., 2020; Ye et al., 2020; Al-Saadi and Abdulnabi, 2022; Gajendra, 2022). These

abnormalities are associated with a higher risk of severe disease and worse outcomes (Hariyanto et al., 2021).

The symptoms of COVID-19 can range from mild to severe and can include fever, cough, shortness of breath, fatigue, body aches, loss of taste or smell, and sore throat. It is important to highlight that not all COVID-19 patients experience hematological abnormalities, and the severity of these abnormalities can vary widely among patients (Gajendra, 2022).

Some symptoms can persist for months after the initial infection with COVID-19. In this case, the disease is known as Long COVID, or post-acute sequelae of SARS-CoV-2 infection (PASC). These symptoms can occur even in individuals who have mild or asymptomatic infections. Although Long COVID's effects are still under investigation, the symptoms vary widely. They can include fatigue, shortness of breath, chest pain, joint pain, headaches, brain fog, difficulty concentrating, loss of taste or smell, and mood disorders. Neurological damages are mainly associated with Long COVID (Proal and VanElzakker, 2021). However, people may also experience organ damage, such as heart, lung, or kidney problems (Davis et al., 2023).

Evidence suggests that age, sex, and race can influence the development and severity of Long COVID. Long COVID affects both males and females, but some studies indicate that females have a higher risk (Bai et al., 2022; Perlis et al., 2022; Subramanian et al., 2022). In addition, older individuals are generally more likely to experience persistent symptoms and prolonged recovery (Bai et al., 2022; Perlis et al., 2022). Certain racial and ethnic groups have differences in cognitive symptomology associated with Long COVID (Jacobs et al., 2023). A recent meta-analysis showed that female sex, age, high body mass index, and smoking were associated with an increased risk of developing Long COVID (Tsampasian et al., 2023).

The pathophysiological mechanisms of Long COVID are still under debate and include the effect of immune response to the virus, inflammation, and autoimmune response (Davis et al., 2023). Evidence suggests that the hematological system is altered in Long COVID, with reports of lower hemoglobin levels and increased D-dimer levels that could lead to blood clotting frequently associated with Long COVID (Lehmann et al., 2021). Also, some patients with Long COVID-19 displayed anemia, thrombocytopenia, and lymphopenia (Pasini et al., 2021; Sonnweber et al., 2022). The subsequent sections of this review provide a comprehensive analysis of the hematological alterations in COVID-19 and Long COVID and possible pathological mechanisms.

2 Long COVID-19

Long COVID, or PASC, is a multisystem disorder with multiple persistent or new symptoms (Davis et al., 2023), affecting 10%–30% of infected individuals. However, the exact pathophysiology remains poorly understood. According to the latest definition, Long COVID is considered if symptoms and abnormalities are present beyond 12 weeks of acute COVID-19. Symptoms between weeks 4–12 are defined as 'sub-acute' or 'ongoing symptomatic COVID-19'(Haunhorst et al., 2022).

This morbidity has been associated with debilitating systemic disorders such as cardiovascular disease, cerebrovascular disease, thrombotic events and coagulopathy, type 2 diabetes, and myalgic

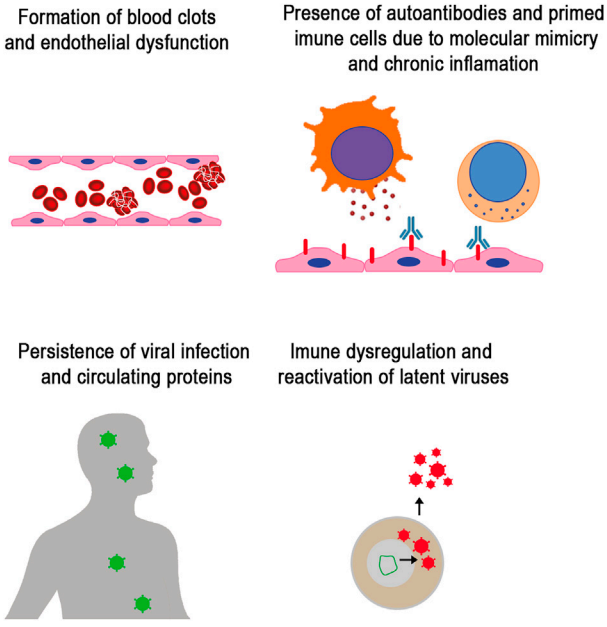

FIGURE 1
Mechanism involved in Long COVID. Studies have identified the main factor in persistent symptoms that characterize Long COVID. Mechanisms include vascular dysfunction and formation of micro clots that lead to thrombosis, immune dysregulation with increased pro-inflammatory response and autoreactive immunity driven by molecular mimicry and bystander activation of lymphocytes, the persistence of viral replication and SARS-CoV-2 proteins circulation, and reactivation of human latent herpes viruses.

TABLE 1 Summary table of most frequent hematological biomarkers of Long COVID.

Hematological parameter	Status in long COVID
Cells and cellular parameters	
RBC	↓(Kubánková et al., 2021; Grau et al., 2022; Lin et al., 2022)
MCV	↑(Lin et al., 2022)
MCHC	↑(Alfadda et al., 2022)
Lymphocytes	↓ (Mandal et al., 2021; Moreno-Pérez et al., 2021; Alfadda et al., 2022); ↔(Darcis et al., 2021)
Blood components and proteins	
Hemoglobin	↓(Kubánková et al., 2021; Pasini et al., 2021; Grau et al., 2022; Pereira-Roche et al., 2022); ↔ (Darcis et al., 2021; Alfadda et al., 2022)
Platelet count	↔ (Mandal et al., 2021; Pasini et al., 2021; Alfadda et al., 2022)
D-dimer	↑ (Mandal et al., 2021; Moreno-Pérez et al., 2021; Pasini et al., 2021; Fan et al., 2022; Kalaivani and Dinakar, 2022)
Ferritin	↑ (Moreno-Pérez et al., 2021; Pasini et al., 2021); ↔(Darcis et al., 2021; Mandal et al., 2021; Alfadda et al., 2022; Pérez-González et al., 2022)
C-reactive protein (C.R.P.)	↑ (Mandal et al., 2021; Pasini et al., 2021; Pérez-González et al., 2022); ↔ (Darcis et al., 2021; Kalaivani and Dinakar, 2022)
Lactate dehydrogenase	↔(Moreno-Pérez et al., 2021; Pasini et al., 2021; Alfadda et al., 2022)
Cytokines	
IL-6	↑ (Fan et al., 2022; Schultheiß et al., 2022); ↓(Williams et al., 2022); ↔ (Kalaivani and Dinakar, 2022; Queiroz et al., 2022)
TNF-α	↑(Peluso et al., 2021; Schultheiß et al., 2022); ↔ (Queiroz et al., 2022; Williams et al., 2022)
IL-1β	↑(Schultheiß et al., 2022); ↔ (Williams et al., 2022)
IL-2	↓ (Williams et al., 2022); ↑ (Queiroz et al., 2022)
IL17	↓ (Williams et al., 2022); ↑(Queiroz et al., 2022)
IFNγ	↓(Williams et al., 2022); ↔ (Queiroz et al., 2022)
IFN-β	↑(Phetsouphanh et al., 2022)
IFN-λ1	↑(Phetsouphanh et al., 2022)
IL-8	↓(Williams et al., 2022); ↔ (Schultheiß et al., 2022); ↑(Phetsouphanh et al., 2022)
IL-10	↔ (Williams et al., 2022); ↓(Queiroz et al., 2022)
IL-4	↓(Queiroz et al., 2022; Williams et al., 2022); ↔(Schultheiß et al., 2022)

Note: ↔ denotes no significant change to a reference value or control group, while ↑ denotes an increase and ↓ denotes a decrease in the parameter.

encephalomyelitis/chronic fatigue syndrome (ME/CFS) (Davis et al., 2021; 2023; Peghin et al., 2021; Xie and Al-Aly, 2022; Xie et al., 2022). Symptoms can persist for years, and for some, symptoms can be expected to be lifelong. Recently, it was suggested that Long COVID could have a more deleterious effect on society and economics. Neurocognitive impairment was linked to loss of productivity and unemployment (Perlis et al., 2023). Neurocognitive disorders are frequently found in PASC, occurring in approximately 70% of individuals. Dysfunction varies from brain fog, depression, anxiety, headaches, insomnia, dizziness, anosmia, and dysgeusia (Davis et al., 2021; Graham et al., 2021; Guo et al., 2022).

Multiple factors may overlap to cause Long COVID. Several hypotheses for its pathogenesis have been suggested (Figure 1). One proposed mechanism is the persistent presence of SARS-CoV-2 in tissues (Sumi and Harada, 2022). In addition, the study demonstrated the presence of Spike protein after 1 year of infection (Swank et al., 2023).

COVID-19 is an immune-mediated disease, and dysregulation of the immune system is also present in Long COVID. Individuals with Long COVID had persistent immune dysregulation, including increased levels of inflammatory cytokines and decreased T cells and B cells (Shuwa et al., 2021)and dysregulation of innate and adaptative immune cells population (Ryan et al., 2022). It was observed that individuals with Long COVID had higher levels of autoantibodies compared to healthy controls (Rojas et al., 2022) and sex-matched patients with other respiratory infections (Son et al., 2022). Molecular mimicry and bystander lymphocyte activation could explain the autoimmune-driven Long COVID hypothesis. Evidence that cytokines could activate $CD8^+$ cell populations without involving TCR has been proposed to explain post-acute COVID-19 complications (Gregorova et al., 2020; Churilov et al., 2022). In addition, the reactivation of latent pathogens, including herpesviruses and others, may contribute to Long COVID (Peluso et al., 2023). Immune-mediated vascular dysfunction is another mechanism proposed in Long COVID that leads to persistent microvascular blood clotting, thrombosis, and thromboembolism (Pretorius et al., 2021). A persistent capillary rarefaction was observed in Long COVID, even after 18 months (Osiaevi et al., 2023). Also, a study demonstrated changes in the size and morphology of red blood cells in Long COVID that potentially can affect oxygen diffusion (Kubánková et al., 2021; Grau et al., 2022). Blood biomarkers can potentially predict Long COVID status and aid the treatment and medical intervention. Changes in hematological parameters and blood biomarkers persist in Long COVID (Brundyn et al., 2022).

3 Hematological alterations in sub-acute and long COVID-19

Different blood alterations occur in COVID-19 and are a predictor of possible biomarkers for outcome and treatment. However, for most infected individuals, hematological parameters return to normal within days after disease onset. However, this parameter remains elevated for a fraction of infected individuals for months and even years. These hematological markers, in some cases, are associated with PASC. Here we list the most relevant alteration in hematological parameters associated with Long COVID (Table 1). The following discussions included studies evaluating hematological alterations in sub-acute (symptoms between 4–12 weeks) and Long COVID-19 (symptoms present beyond 12 weeks).

3.1 Cells

A decrease in lymphocyte count is a common feature in Long COVID (Mandal et al., 2021; Moreno-Pérez et al., 2021; Alfadda et al., 2022). In COVID-19, lymphopenia is a predictor of severity (Illg et al., 2021), and the reduction of T lymphocytes is unusual in viral infections. It is believed that in severe COVID-19, deficient interferon production driven by SARS-CoV-2 can impair T cells, as interferons are important to promote survival and effector functions of T cells (Sa Ribero et al., 2020; Proal and VanElzakker, 2021). Lymphopenia can be caused by direct viral infection since lymphocytes express Angiotensin-converting enzyme 2 (ACE2) (Xu et al., 2020), cytokine storm with a significant increase of IL-6 induce lymphopenia (Tang et al., 2020; Montazersaheb et al., 2022) and lymphocytic infiltration to organs (Proal and VanElzakker, 2021). T-cell exhaustion is also believed to contribute to SARS-CoV-2 persistence (Ramakrishnan et al., 2021).

Alteration in red blood cells (RBC) can occur in COVID-19 (Russo et al., 2022), and despite most studies showing that in the Long COVID normal range is recovered for most individuals (Darcis et al., 2021; Mandal et al., 2021; Moreno-Pérez et al., 2021; Alfadda et al., 2022), evidence suggests a phenotypic change that could be linked to Long COVID (Grau et al., 2022). Pasini et al. (2021) showed a high degree of erythrocyte sedimentation after 2 months of follow-up. Determination of RBC parameters after an average of 60.7 days shows that hemoglobin concentration, mean corpuscular volume (MCV), and mean corpuscular hemoglobin (MCH), were highly altered in COVID-19 and RBC deformability was significantly reduced in post-COVID-19 patients (Grau et al., 2022). Indeed, RBC morphology changes were observed in patients discharged after 4 and 8 months. Alterations include decreased size and deformability of erythrocytes of hospitalized and recovered COVID-19 patients (Kubánková et al., 2021).

These altered physical properties reflect the changes in plasma membranes and cytoskeleton networks. The interaction between SARS-CoV-2 and RBC occurs via the Band-3 and the spike protein, and in the bone marrow, the virus interacts with nascent erythroblasts through CD147 and CD26 (Wang et al., 2020; Kronstein-Wiedemann et al., 2022). Changes in RBC include modifications in shape, size, and deformability, which can alter microvascular perfusion, endothelial cell integrity, blood flow behavior, and hemostasis (Kubánková et al., 2021; Nader et al., 2022; Russo et al., 2022). Reduced deformability of RBCs increases their likelihood of adhering to the vessel wall, resulting in elevated vascular resistance and risk of thrombosis (Weisel and Litvinov, 2019). In addition, vascular endothelial damage can be caused by long-term viral infection, chronic hypoxia, and inflammation (Wang et al., 2022). Also, alteration in RBC structure and metabolism linked to high shear rates, inflammation, and oxidative stress activate scramblase externalizing phosphatidylserine (P.S.) on the outer membrane, P.S. provides a scaffold for coagulation cascade (Whelihan and Mann, 2013; Weisel and Litvinov, 2019), enhances RBC adherence and activation of the endothelium, and increase RBC-microvesicle secretion that enhances the hypercoagulability state (Kim et al., 2018; Leal et al., 2018).

The decrease in deformability can lead to impaired rheology and hemolysis, RBCs from COVID-19 patients may be particularly susceptible to the attack of reactive oxygen species (R.O.S.), leading to cell lysis and reduced oxygen-carrying capacity. The RBC rigidity increases hemolysis and releases free hemoglobin molecules that scavenge nitric oxide leading to platelet activation (Rother et al., 2005; Diederich et al., 2018). During acute SARS-CoV-2 infection, damaged endothelial cells are critical in promoting diffuse microthrombi formation and disrupting various endothelial barriers throughout the body. These microthrombi contribute to multiple organ dysfunction (Wu et al., 2023). These alterations could impair proper circulation, promote hypoxia, and favor coagulopathies, common in Long COVID (Gillespie and Doctor, 2021).

Understanding these complex interactions and their impact on RBCs is crucial for comprehending the hematological changes associated with Long COVID-19, particularly concerning vascular effects and disease severity.

Individuals who followed for 6 months, with at least one Long COVID-19-related symptom, had a significantly higher mean corpuscular hemoglobin concentration (MCHC) than those who recovered with no signs (Alfadda et al., 2022). Higher MCHC can have multiple causes, including autoimmune hemolytic anemia, and rare events have been reported in COVID-19 (Lazarian et al., 2020; Al-Mashdali et al., 2021; Fattizzo et al., 2021).

Changes in blood parameters can be evidenced after 2 years. Most hematologic indicators regarding WBC and platelet counts in COVID-19 convalescents were comparable to those of the healthy control group. However, RBC counts, hemoglobin, red blood cell distribution width-coefficient of variation, and mean corpuscular hemoglobin showed statistical differences. Although indicators related to RBC showed recovery to the normal range, RBC counts were abnormal in 26.4% (20/76) after 1 year and 8.5% (5/59) after 2 years of disease onset. Interestingly, the 2-year follow-up showed the proportion of mean corpuscular volume (MCV) above the normal range increased significantly from 2.6% (2/76) to 37.3% (22/59) (Lin et al., 2022).

3.2 Blood components and proteins

Hemoglobin is responsible for gas exchange in RBCs. COVID-19 hemoglobin levels were reported to be low, compromising oxygen transport of RBCs in COVID-19 patients leading to hypoxia and is related to disease severity (Anai et al., 2021). Several hypotheses were elaborated to explain this viral effect. First, it was evidenced that SARS-CoV-2 can interact with RBC via receptors CD147 and Band 3 (Cosic et al., 2020; Wang et al., 2020), and several structural, including Spike and nucleoprotein and non-structural proteins, can bind hemoglobin and heme (Lechuga et al., 2021), possibly altering protein function. Second, the virus scavenges some molecules like bilirubin and biliverdin, a heme and hemoglobin degradation product, to evade antibodies (Rosa et al., 2021). Third, SARS-CoV-2 was found to infect erythroid precursor cells derived from peripheral $CD34^{+}$ blood stem cells and disrupt hemoglobin biosynthesis (Kronstein-Wiedemann et al., 2022). Another possibility is that the virus triggers an immune response that causes inflammation, the release of cytokines, and oxidative stress, which can lead to the breakdown of RBCs and the release of hemoglobin into the bloodstream. This can decrease hemoglobin

levels, induce hypoxia and anemia (Russo et al., 2022). The chronic hypoxia in Long COVID is mostly related to lung function impairment (Caruso et al., 2021; Cueto-Robledo et al., 2022), but it also provides enhanced release of inflammatory cytokines (Østergaard, 2021). Under the hypoxic stimulus, changes in the erythroid precursor maturation of reticulocytes and young RBC occur. They seem to have low catalase, and increased ROS formation contributes to the preferential destruction of young RBC upon return to normoxia (Risso et al., 2007; Song et al., 2015). These events can promote anemia, inflammation, and iron deficiency in Long COVID (Sonnweber et al., 2022).

In Long COVID, hemoglobin levels tend to return to normal values, but some reports showed that for some patients, this parameter is still altered (Pasini et al., 2021; Pereira-Roche et al., 2022; Lai et al., 2023). Generally, Long COVID symptoms have multiple causes, but low hemoglobin levels and anemia can contribute to fatigue, weakness, and shortness of breath.

Alterations of iron homeostasis can persist in Long COVID-19, markedly hyperferritiemia. Ferritin is a protein composed of two subunits, H and L. Its main function is to store iron, regulating cellular oxygen metabolism (Plays et al., 2021). Ferritin expression and upregulation can be triggered by inflammation and oxidative stress. Serum ferritin levels are increased in COVID-19 due to inflammation and the release of cytokines, particularly IL-6, that stimulate hepcidin synthesis, a master regulator of iron uptake and distribution (Ganz, 2011). Ferritin has immune modulatory functions, mediating inflammation and exerting immunosuppressive effects on T and B cells (Kernan and Carcillo, 2017). Elevated serum levels of ferritin have been found to correlate with the severity of COVID-19 (Kaushal et al., 2022). Iron overload can lead to oxidative stress, lipid peroxidation, and, ultimately, cell death by ferroptosis (Winterbourn, 1995; Girelli et al., 2021).

Additionally, ferritin-increased levels have been linked to interactions between RBCs and platelets in COVID-19 patients, suggesting a role in thrombosis in COVID-19 (Venter et al., 2020) and possibly in Long COVID. After 60 days of follow-up, hyperferritinemia remained elevated in 38% of individuals and was more frequent in patients with severe disease (Pasini et al., 2021). Additionally, persisting ferritin elevation correlated with severe lung disease and iron dysmetabolism contributed to impaired stress resilience at long-term COVID-19 follow-up (Sonnweber et al., 2022).

An analysis of hematological changes in long-COVID19 revealed that in some patients, the increased D-dimer levels are sustained for several months. D-dimer is produced by fibrin degradation. Elevated levels of D-dimer correlate with COVID-19 severity (Yu et al., 2020). A post-COVID follow-up study showed that 30% of patients had elevated D-dimer approximately 54 days after hospital discharge (Mandal et al., 2021). Another study showed that all 75 patients with previously confirmed COVID-19 had increased D-dimer and ferritin 2 months after hospital discharge (Pasini et al., 2021). After a median of 3 months following COVID-19 patients, 15% still had a persistent D-dimer elevation. It was more frequently associated with patients that had severe COVID-19 (Lehmann et al., 2021). After 4 months, increased D-dimer levels (>500 ng/ml) were observed in 25.3% of convalescent patients, but in most (>90%) of this patient's other coagulation markers (prothrombin time, activated partial thromboplastin time, fibrinogen, platelet count) had returned to normal values (Townsend et al., 2021). The D-dimer levels start to decrease but continue high for up to 6 months in patients after discharge from the hospital. The persistence of D-dimer elevated levels is associated with Long COVID symptoms (Kalaivani and Dinakar, 2022). Indeed, thromboembolic complications are a common feature of Long COVID. In this viral infection, the coagulation pathway is activated due to the immune response and cytokine storm leading to the hypercoagulable and pro-inflammatory state (Lazzaroni et al., 2021). RBC could also play a role in the cytokine storm since RBC store and release several cytokines, including pro-inflammatory TNF-α and IL-1β(Karsten et al., 2018).

Additionally, intravascular hemolysis could lead to an inflammatory state and excessive cytokine release, due to oxidative imbalance induced by hemoglobin degradation and the release of heme and iron (Bozza and Jeney, 2020). Iron metabolism is directly influenced by cytokines that trigger the production of hepcidin, which binds to ferroportin, restricting the availability of iron and preventing its export to cells (Ganz, 2011). However, in COVID-19, there is an excess of iron within cells and tissues, accompanied by reduced serum iron levels. Iron dysmetabolism could restrict hemoglobin and RBC synthesis, leading to anemia and sustained hypoxia in Long COVID (Cavezzi et al., 2020; Girelli et al., 2021; Russo et al., 2022).

Several works also showed higher levels of C-reactive protein (CRP), an acute phase protein, in Long COVID (Mandal et al., 2021; Pasini et al., 2021). CRP is produced in the liver after stimulating inflammatory cytokines like IL-6 (Sproston and Ashworth, 2018). This biomarker is sustained increased and is possibly linked to cytokine sustained elevation in Long COVID (Lai et al., 2023). The enzyme lactate dehydrogenase (LDH) is a mark of tissue damage. Levels of this enzyme in some post-acute COVID-19 are also increased. After 2 months of infection, LDH levels were elevated in more than 27% of subjects (Pasini et al., 2021). Multiple factors may contribute to long-term COVID cell lysis, including viral persistence and immune dysregulation (Davis et al., 2023).

3.3 Cytokines

During COVID-19, virus infection induces an intense production of cytokines, the "cytokine storm." This response is implicated in triggering immunopathological reactions. Various cytokines (IFN-γ, IL-1β, IL-6, IL-2, and TNF-α) had altered levels in COVID-19, and the cytokine storms correlate with the severity and progression of COVID-19 (Huang et al., 2020; Chang et al., 2021). However, studies evaluating cytokine levels in Long COVID are contradictory. A Long COVID cohort of 12 individuals showed reductions in circulating levels of cytokines, remarkably Interferon Gamma (IFNγ) and Interleukin-8 (IL-8). Authors proposed that immune exhaustion drives long-COVID (Williams et al., 2022). SARS-CoV-2 expresses proteins that allow it to counteract the induction or escape the antiviral activity of interferons. Additionally, an inadequate or delayed IFN-I response contributes to the disease (Sa Ribero et al., 2020). In contrast,

an increased expression of interferon I (IFN-β) and III (IFN-λ1) was evidenced 8 months after infection. Patients with Long-Covid have higher levels than age- and gender-matched recovered individuals without Long COVID, unexposed donors, and individuals infected with other coronaviruses (Phetsouphanh et al., 2022). The IFN type I and III production imbalance is consistent with the prolonged activation of plasmacytoid dendritic cells, indicating a chronic inflammatory response.

Another study with 135 individuals with PASC revealed that subjects with Long COVID-19 had higher levels of IL-17 and IL-2, and subjects without PASC had higher levels of IL-10, IL-6, and IL- 4 (Queiroz et al., 2022). However, a cohort that followed Long COVID subjects for 8 months observed a different profile. The study showed a long-lasting cytokine signature consisting of elevated levels of interleukin (IL)-1β, IL-6, and tumor necrosis factor (TNF- α) (Schultheiß et al., 2022). Similarly, a study found that IL-6 and TNF-α elevation was sustained in subjects that experienced symptoms at approximately 120 days following COVID-19 (Peluso et al., 2021).

These works confirm that immune dysregulation and sustained pro-inflammatory cytokine production are linked to Long COVID symptomatology. Current data of a cytokine biomarker are relevant as they can serve as diagnostic or prognostic information and be used to monitor Long COVID.

4 Conclusion

This paper highlights the hematological alterations associated with Long COVID-19, which may have important implications for diagnosing, monitoring, and treating this condition. A literature review suggests that Long COVID-19 is a respiratory disease and a systemic disorder affecting multiple organs and systems, including the hematopoietic system. Researchers and clinicians should identify the most frequent and relevant hematological alterations and consider monitoring these parameters in individuals with Long COVID-19. Future research should focus on elucidating the underlying mechanisms of these hematological changes and exploring potential therapeutic interventions to improve outcomes in individuals with Long COVID-19. It is important to note that not all Long COVID-19 patients experience hematological abnormalities. The symptomatology and the severity of these abnormalities can also vary widely among patients. Overall, this paper contributes to a better understanding of the multifaceted nature of Long COVID-19 and highlights the importance of a multidisciplinary approach to managing this condition.

Author contributions

Conceptualization and Investigation: GL, CM, and SD; writing—original draft: GL; review and editing: SD. All authors contributed to the article and approved the submitted version.

Funding

This work was supported by the Brazilian Council for Scientific Research (CNPq #30515-2020-5) and the Carlos Chagas Filho Foundation of Research Support of the State of Rio de Janeiro (FAPERJ #210.780-2021 and #200.960-2022). In addition, funding was also provided by FAPERJ (#210.003-2018) through the National Institutes of Science and Technology Program (INCT) to CM (INCT-IDPN).

Acknowledgments

GL is a Postdoc fellow from the CAPES-FIOCRUZ program.

Conflict of interest

The authors declare that the research was conducted in the absence of any commercial or financial relationships that could be construed as a potential conflict of interest.

Publisher's note

References

Al-Saadi, E. A. K. D., and Abdulnabi, M. A. (2022). Hematological changes associated with COVID-19 infection. *J. Clin. Lab. Anal.* 36, e24064. doi:10.1002/jcla.24064

Alfadda, A. A., Rafiullah, M., Alkhowaiter, M., Alotaibi, N., Alzahrani, M., Binkhamis, K., et al. (2022). Clinical and biochemical characteristics of people experiencing post-coronavirus disease 2019-related symptoms: A prospective follow-up investigation. *Front. Med. (Lausanne)* 9, 1067082. doi:10.3389/fmed.2022.1067082

Al-Mashdali, A. F., Ata, Y. M., and Yassin, M. A. (2021). Concomitant autoimmune hemolytic anemia and pulmonary embolism associated with mild COVID-19: A case report. *Clin. Case Rep.* 9, e04952. doi:10.1002/ccr3.4952

Anai, M., Akaike, K., Iwagoe, H., Akasaka, T., Higuchi, T., Miyazaki, A., et al. (2021). Decrease in hemoglobin level predicts increased risk for severe respiratory failure in COVID-19 patients with pneumonia. *Respir. Investig.* 59, 187–193. doi:10.1016/J.RESINV.2020.10.009

Bai, F., Tomasoni, D., Falcinella, C., Barbanotti, D., Castoldi, R., Mulè, G., et al. (2022). Female gender is associated with long COVID syndrome: A prospective cohort study. *Clin. Microbiol. Infect.* 28, 611.e9–611611.e16. doi:10.1016/j.cmi.2021.11.002-

Bozza, M. T., and Jeney, V. (2020). Pro-inflammatory actions of heme and other hemoglobin-derived DAMPs. *Front. Immunol.* 11, 1323. doi:10.3389/fimmu.2020.01323

Brundyn, J. L., Gillan, J., and Singh, I. (2022). Hematologic abnormalities associated with post-acute COVID-19 sequelae or "long-COVID"-a systematic review. *Int. J. Bio. Lab. Sci.* 11 (1), 23–42.

Caruso, D., Guido, G., Zerunian, M., Polidori, T., Lucertini, E., Pucciarelli, F., et al. (2021). Post-acute sequelae of COVID-19 pneumonia: Six-month chest CT follow-up. *Radiology* 301, E396–E405. doi:10.1148/radiol.2021210834

Cavezzi, A., Troiani, E., and Corrao, S. (2020). COVID-19: Hemoglobin, iron, and hypoxia beyond inflammation. A narrative review. *Clin. Pract.* 10, 1271. doi:10.4081/cp.2020.1271

Chang, S. H., Minn, D., Kim, S. W., and Kim, Y. K. (2021). Inflammatory markers and cytokines in moderate and critical cases of COVID-19. *Clin. Lab.* 67 (9). doi:10.7754/Clin.Lab.2021.210142

Churilov, L. P., Normatov, M. G., and Utekhin, V. J. (2022). Molecular mimicry between SARS-CoV-2 and human endocrinocytes: A prerequisite of post-COVID-19 endocrine autoimmunity? *Pathophysiology* 29, 486–494. doi:10.3390/pathophysiology29030039

Cosic, I., Cosic, D., and Loncarevic, I. (2020). RRM prediction of erythrocyte Band3 protein as alternative receptor for SARS-CoV-2 virus. *Appl. Sci.* 10, 4053. doi:10.3390/app10114053

Cueto-Robledo, G., Porres-Aguilar, M., Puebla-Aldama, D., Barragán-Martínez, M., del, P., Jurado-Hernández, M. Y., et al. (2022). Severe pulmonary hypertension: An important sequel after severe post-acute COVID-19 pneumonia. *Curr. Probl. Cardiol.* 47, 101004. doi:10.1016/j.cpcardiol.2021.101004

Darcis, G., Bouquegneau, A., Maes, N., Thys, M., Henket, M., Labye, F., et al. (2021). Long-term clinical follow-up of patients suffering from moderate-to-severe COVID-19 infection: A monocentric prospective observational cohort study. *Int. J. Infect. Dis.* 109, 209–216. doi:10.1016/j.ijid.2021.07.016

Davis, H. E., Assaf, G. S., McCorkell, L., Wei, H., Low, R. J., Re'em, Y., et al. (2021). Characterizing long COVID in an international cohort: 7 months of symptoms and their impact. *EClinicalMedicine* 38, 101019. doi:10.1016/j.eclinm.2021.101019

Davis, H. E., McCorkell, L., Vogel, J. M., and Topol, E. J. (2023). Long COVID: Major findings, mechanisms and recommendations. *Nat. Rev. Microbiol.* 21, 133–146. doi:10.1038/s41579-022-00846-2

Diederich, L., Suvorava, T., Sansone, R., Keller, T. C. S., Barbarino, F., Sutton, T. R., et al. (2018). On the effects of reactive oxygen species and nitric oxide on red blood cell deformability. *Front. Physiol.* 9, 332. doi:10.3389/fphys.2018.00332

Fan, B. E., Wong, S. W., Sum, C. L. L., Lim, G. H., Leung, B. P., Tan, C. W., et al. (2022). Hypercoagulability, endotheliopathy, and inflammation approximating 1 year after recovery: Assessing the long-term outcomes in COVID-19 patients. *Am. J. Hematol.* 97, 915–923. doi:10.1002/ajh.26575

Fattizzo, B., Pasquale, R., Bellani, V., Barcellini, W., and Kulasekararaj, A. G. (2021). Complement mediated hemolytic anemias in the COVID-19 era: Case series and review of the literature. *Front. Immunol.* 12, 791429. doi:10.3389/fimmu.2021.791429

Gajendra, S. (2022). Spectrum of hematological changes in COVID-19. Available at: www.AJBlood.us/.

Ganz, T. (2011). Hepcidin and iron regulation, 10 years later. *Blood* 117, 4425–4433. doi:10.1182/blood-2011-01-258467

Gillespie, A. H., and Doctor, A. (2021). Red blood cell contribution to hemostasis. *Front. Pediatr.* 9, 629824. doi:10.3389/fped.2021.629824

Girelli, D., Marchi, G., Busti, F., and Vianello, A. (2021). Iron metabolism in infections: Focus on COVID-19. *Semin. Hematol.* 58, 182–187. doi:10.1053/j.seminhematol.2021.07.001

Graham, E. L., Clark, J. R., Orban, Z. S., Lim, P. H., Szymanski, A. L., Taylor, C., et al. (2021). Persistent neurologic symptoms and cognitive dysfunction in non-hospitalized Covid-19 long haulers. *Ann. Clin. Transl. Neurol.* 8, 1073–1085. doi:10.1002/acn3.51350

Grau, M., Ibershoff, L., Zacher, J., Bros, J., Tomschi, F., Diebold, K. F., et al. (2022). Even patients with mild COVID-19 symptoms after SARS-CoV-2 infection show prolonged altered red blood cell morphology and rheological parameters. *J. Cell Mol. Med.* 26, 3022–3030. doi:10.1111/jcmm.17320

Gregorova, M., Morse, D., Brignoli, T., Steventon, J., Hamilton, F., Albur, M., et al. (2020). Post-acute COVID-19 associated with evidence of bystander T-cell activation and a recurring antibiotic-resistant bacterial pneumonia. *Elife* 9, e63430. doi:10.7554/eLife.63430

Guo, P., Benito Ballesteros, A., Yeung, S. P., Liu, R., Saha, A., Curtis, L., et al. (2022). Covcog 2: Cognitive and memory deficits in long COVID: A second publication from the COVID and cognition study. *Front. Aging Neurosci.* 14, 804937. doi:10.3389/fnagi.2022.804937

Hadj Hassine, I. (2022). Covid-19 vaccines and variants of concern: A review. *Rev. Med. Virol.* 32, e2313. doi:10.1002/rmv.2313

Hariyanto, T. I., Japar, K. V., Kwenandar, F., Damay, V., Siregar, J. I., Lugito, N. P. H., et al. (2021). Inflammatory and hematologic markers as predictors of severe outcomes in COVID-19 infection: A systematic review and meta-analysis. *Am. J. Emerg. Med.* 41, 110–119. doi:10.1016/J.AJEM.2020.12.076

Haunhorst, S., Bloch, W., Wagner, H., Ellert, C., Krüger, K., Vilser, D. C., et al. (2022). Long COVID: A narrative review of the clinical aftermaths of COVID-19 with a focus on the putative pathophysiology and aspects of physical activity. *Oxf Open Immunol.* 3, iqac006. doi:10.1093/oxfimm/iqac006

Hoffmann, M., Krüger, N., Schulz, S., Cossmann, A., Rocha, C., Kempf, A., et al. (2022). The Omicron variant is highly resistant against antibody-mediated neutralization: Implications for control of the COVID-19 pandemic. *Cell* 185, 447–456.e11. doi:10.1016/j.cell.2021.12.032

Huang, C., Wang, Y., Li, X., Ren, L., Zhao, J., Hu, Y., et al. (2020). Clinical features of patients infected with 2019 novel coronavirus in Wuhan, China. *Lancet* 395, 497–506. doi:10.1016/S0140-6736(20)30183-5

Illg, Z., Muller, G., Mueller, M., Nippert, J., and Allen, B. (2021). Analysis of absolute lymphocyte count in patients with COVID-19. *Am. J. Emerg. Med.* 46, 16–19. doi:10.1016/j.ajem.2021.02.054

Jacobs, M. M., Evans, E., and Ellis, C. (2023). Racial, ethnic, and sex disparities in the incidence and cognitive symptomology of long COVID-19. *J. Natl. Med. Assoc.* 115, 233–243. doi:10.1016/j.jnma.2023.01.016

Kalaivani, M., and Dinakar, S. (2022). Association between D-dimer levels and post-acute sequelae of SARS-CoV-2 in patients from a tertiary care center. *Biomark. Med.* 16, 833–838. doi:10.2217/bmm-2022-0050

Karsten, E., Breen, E., and Herbert, B. R. (2018). Red blood cells are dynamic reservoirs of cytokines. *Sci. Rep.* 8, 3101. doi:10.1038/s41598-018-21387-w

Kaushal, K., Kaur, H., Sarma, P., Bhattacharyya, A., Sharma, D. J., Prajapat, M., et al. (2022). Serum ferritin as a predictive biomarker in COVID-19. A systematic review, meta-analysis and meta-regression analysis. *J. Crit. Care* 67, 172–181. doi:10.1016/j.jcrc.2021.09.023

Kernan, K. F., and Carcillo, J. A. (2017). Hyperferritinemia and inflammation. *Int. Immunol.* 29, 401–409. doi:10.1093/intimm/dxx031

Kim, Y., Xia, B. T., Jung, A. D., Chang, A. L., Abplanalp, W. A., Caldwell, C. C., et al. (2018). Microparticles from stored red blood cells promote a hypercoagulable state in a murine model of transfusion. *Surgery* 163, 423–429. doi:10.1016/j.surg.2017.09.028

Kronstein-Wiedemann, R., Stadtmüller, M., Traikov, S., Georgi, M., Teichert, M., Yosef, H., et al. (2022). SARS-CoV-2 infects red blood cell progenitors and dysregulates hemoglobin and iron metabolism. *Stem Cell Rev. Rep.* 18, 1809–1821. doi:10.1007/s12015-021-10322-8

Kubánková, M., Hohberger, B., Hoffmanns, J., Fürst, J., Herrmann, M., Guck, J., et al. (2021). Physical phenotype of blood cells is altered in COVID-19. *Biophys. J.* 120, 2838–2847. doi:10.1016/j.bpj.2021.05.025

Lai, Y.-J., Liu, S.-H., Manachevakul, S., Lee, T.-A., Kuo, C.-T., and Bello, D. (2023). Biomarkers in long COVID-19: A systematic review. *Front. Med. (Lausanne)* 10, 1085988. doi:10.3389/fmed.2023.1085988

Lazarian, G., Quinquenel, A., Bellal, M., Siavellis, J., Jacquy, C., Re, D., et al. (2020). Autoimmune haemolytic anaemia associated with COVID-19 infection. *Br. J. Haematol.* 190, 29–31. doi:10.1111/bjh.16794

Lazzaroni, M. G., Piantoni, S., Masneri, S., Garrafa, E., Martini, G., Tincani, A., et al. (2021). Coagulation dysfunction in COVID-19: The interplay between inflammation, viral infection and the coagulation system. *Blood Rev.* 46, 100745. doi:10.1016/j.blre.2020.100745

Leal, J. K. F., Adjobo-Hermans, M. J. W., and Bosman, G. J. C. G. M. (2018). Red blood cell homeostasis: Mechanisms and effects of microvesicle generation in health and disease. *Front. Physiol.* 9, 703. doi:10.3389/fphys.2018.00703

Lechuga, G. C., Souza-Silva, F., Sacramento, C. Q., Trugilho, M. R. O., Valente, R. H., Napoleão-Pêgo, P., et al. (2021). SARS-CoV-2 proteins bind to hemoglobin and its metabolites. *Int. J. Mol. Sci.* 22, 9035. doi:10.3390/ijms22169035

Lehmann, A., Prosch, H., Zehetmayer, S., Gysan, M. R., Bernitzky, D., Vonbank, K., et al. (2021). Impact of persistent D-dimer elevation following recovery from COVID-19. *PLoS One* 16, e0258351. doi:10.1371/journal.pone.0258351

Lin, H., Liu, X., Sun, H., Zhang, J., Dong, S., Liu, M., et al. (2022). Sustained abnormality with recovery of COVID-19 convalescents: A 2-year follow-up study. *Sci. Bull. (Beijing)* 67, 1556–1561. doi:10.1016/j.scib.2022.06.025

Mandal, S., Barnett, J., Brill, S. E., Brown, J. S., Denneny, E. K., Hare, S. S., et al. (2021). 'Long-COVID': A cross-sectional study of persisting symptoms, biomarker and imaging abnormalities following hospitalisation for COVID-19. *Thorax* 76, 396–398. doi:10.1136/thoraxjnl-2020-215818

Montazersaheb, S., Hosseiniyan Khatibi, S. M., Hejazi, M. S., Tarhriz, V., Farjami, A., Ghasemian Sorbeni, F., et al. (2022). COVID-19 infection: An overview on cytokine storm and related interventions. *Virol. J.* 19, 92. doi:10.1186/s12985-022-01814-1

Moreno-Pérez, O., Merino, E., Leon-Ramirez, J.-M., Andres, M., Ramos, J. M., Arenas-Jiménez, J., et al. (2021). Post-acute COVID-19 syndrome. Incidence and risk factors: A mediterranean cohort study. *J. Infect.* 82, 378–383. doi:10.1016/j.jinf.2021.01.004

Nader, E., Nougier, C., Boisson, C., Poutrel, S., Catella, J., Martin, F., et al. (2022). Increased blood viscosity and red blood cell aggregation in patients with COVID-19. *Am. J. Hematol.* 97, 283–292. doi:10.1002/ajh.26440

Osiaevi, I., Schulze, A., Evers, G., Harmening, K., Vink, H., Kümpers, P., et al. (2023). Persistent capillary rarefication in long COVID syndrome. *Angiogenesis* 26, 53–61. doi:10.1007/s10456-022-09850-9

Østergaard, L. (2021). SARS CoV-2 related microvascular damage and symptoms during and after COVID-19: Consequences of capillary transit-time changes, tissue hypoxia and inflammation. *Physiol. Rep.* 9, e14726. doi:10.14814/phy2.14726

Pasini, E., Corsetti, G., Romano, C., Scarabelli, T. M., Chen-Scarabelli, C., Saravolatz, L., et al. (2021). Serum metabolic profile in patients with long-covid (PASC) syndrome: Clinical implications. *Front. Med. (Lausanne)* 8, 714426. doi:10.3389/fmed.2021.714426

Peghin, M., Palese, A., Venturini, M., De Martino, M., Gerussi, V., Graziano, E., et al. (2021). Post-COVID-19 symptoms 6 months after acute infection among hospitalized and non-hospitalized patients. *Clin. Microbiol. Infect.* 27, 1507–1513. doi:10.1016/j.cmi.2021.05.033

Peluso, M. J., Deveau, T.-M., Munter, S. E., Ryder, D., Buck, A., Beck-Engeser, G., et al. (2023). Chronic viral coinfections differentially affect the likelihood of developing long COVID. *J. Clin. Investigation* 133, e163669. doi:10.1172/JCI163669

Peluso, M. J., Lu, S., Tang, A. F., Durstenfeld, M. S., Ho, H., Goldberg, S. A., et al. (2021). Markers of immune activation and inflammation in individuals with postacute sequelae of severe acute respiratory syndrome coronavirus 2 infection. *J. Infect. Dis.* 224, 1839–1848. doi:10.1093/infdis/jiab490

Pereira-Roche, N., Roblejo-Balbuena, H., Marín-Padrón, L. C., Izaguirre-Rodríguez, R., Sotomayor-Lugo, F., Zúñiga-Rosales, Y., et al. (2022). Hematological alterations in patients recovered from SARS-CoV-2 infection in havana, Cuba. *MEDICC Rev.* 24, 7–14. doi:10.37757/mr2022.v24.n2.1

Pérez-González, A., Araújo-Ameijeiras, A., Fernández-Villar, A., Crespo, M., Poveda, E., Cabrera, J. J., et al. (2022). Long COVID in hospitalized and non-hospitalized patients in a large cohort in Northwest Spain, a prospective cohort study. *Sci. Rep.* 12, 3369. doi:10.1038/s41598-022-07414-x

Perlis, R. H., Lunz Trujillo, K., Safarpour, A., Santillana, M., Ognyanova, K., Druckman, J., et al. (2023). Association of post–COVID-19 condition symptoms and employment status. *JAMA Netw. Open* 6, e2256152. doi:10.1001/jamanetworkopen.2022.56152

Perlis, R. H., Santillana, M., Ognyanova, K., Safarpour, A., Lunz Trujillo, K., Simonson, M. D., et al. (2022). Prevalence and correlates of long COVID symptoms among U.S. Adults. *JAMA Netw. Open* 5, e2238804. doi:10.1001/jamanetworkopen.2022.38804

Phetsouphanh, C., Darley, D. R., Wilson, D. B., Howe, A., Munier, C. M. L., Patel, S. K., et al. (2022). Immunological dysfunction persists for 8 months following initial mild-to-moderate SARS-CoV-2 infection. *Nat. Immunol.* 23, 210–216. doi:10.1038/s41590-021-01113-x

Plays, M., Müller, S., and Rodriguez, R. (2021). Chemistry and biology of ferritin. *Metallomics* 13, mfab021. doi:10.1093/mtomcs/mfab021

Pretorius, E., Vlok, M., Venter, C., Bezuidenhout, J. A., Laubscher, G. J., Steenkamp, J., et al. (2021). Persistent clotting protein pathology in Long COVID/Post-Acute Sequelae of COVID-19 (PASC) is accompanied by increased levels of antiplasmin. *Cardiovasc Diabetol.* 20, 172. doi:10.1186/s12933-021-01359-7

Proal, A. D., and VanElzakker, M. B. (2021). Long COVID or post-acute sequelae of COVID-19 (PASC): An overview of biological factors that may contribute to persistent symptoms. *Front. Microbiol.* 12, 698169. doi:10.3389/fmicb.2021.698169

Queiroz, M. A. F., Nevesdas, P. F. M., Lima, S. S., Lopes, J. da C., Torres, M. K. da S., Vallinoto, I. M. V. C., et al. (2022). Cytokine profiles associated with acute COVID-19 and long COVID-19 syndrome. *Front. Cell Infect. Microbiol.* 12, 922422. doi:10.3389/fcimb.2022.922422

Ramakrishnan, R. K., Kashour, T., Hamid, Q., Halwani, R., and Tleyjeh, I. M. (2021). Unraveling the mystery surrounding post-acute sequelae of COVID-19. *Front. Immunol.* 12, 686029. doi:10.3389/fimmu.2021.686029

Risso, A., Turello, M., Biffoni, F., and Antonutto, G. (2007). Red blood cell senescence and neocytolysis in humans after high altitude acclimatization. *Blood Cells Mol. Dis.* 38, 83–92. doi:10.1016/j.bcmd.2006.10.161

Rojas, M., Rodríguez, Y., Acosta-Ampudia, Y., Monsalve, D. M., Zhu, C., Li, Q.-Z., et al. (2022). Autoimmunity is a hallmark of post-COVID syndrome. *J. Transl. Med.* 20, 129. doi:10.1186/s12967-022-03328-4

Rosa, A., Pye, V. E., Graham, C., Muir, L., Seow, J., Ng, K. W., et al. (2021). SARS-CoV-2 can recruit a heme metabolite to evade antibody immunity. *Sci. Adv.* 7, eabg7607. doi:10.1126/sciadv.abg7607

Rother, R. P., Bell, L., Hillmen, P., and Gladwin, M. T. (2005). The clinical sequelae of intravascular hemolysis and extracellular plasma hemoglobin: A novel mechanism of human disease. *JAMA* 293, 1653–1662. doi:10.1001/jama.293.13.1653

Russo, A., Tellone, E., Barreca, D., Ficarra, S., and Laganà, G. (2022). Implication of COVID-19 on erythrocytes functionality: Red blood cell biochemical implications and morpho-functional aspects. *Int. J. Mol. Sci.* 23, 2171. doi:10.3390/ijms23042171

Ryan, F. J., Hope, C. M., Masavuli, M. G., Lynn, M. A., Mekonnen, Z. A., Yeow, A. E. L., et al. (2022). Long-term perturbation of the peripheral immune system months after SARS-CoV-2 infection. *B.M.C. Med.* 20, 26. doi:10.1186/s12916-021-02228-6

Sa Ribero, M., Jouvenet, N., Dreux, M., and Nisole, S. (2020). Interplay between SARS-CoV-2 and the type I interferon response. *PLoS Pathog.* 16, e1008737. doi:10.1371/journal.ppat.1008737

Schultheiß, C., Willscher, E., Paschold, L., Gottschick, C., Klee, B., Henkes, S.-S., et al. (2022). The IL-1β, IL-6, and TNF cytokine triad is associated with post-acute sequelae of COVID-19. *Cell Rep. Med.* 3, 100663. doi:10.1016/j.xcrm.2022.100663

Shuwa, H. A., Shaw, T. N., Knight, S. B., Wemyss, K., McClure, F. A., Pearmain, L., et al. (2021). Alterations in T and B cell function persist in convalescent COVID-19 patients. *Med* 2, 720–735.e4. doi:10.1016/j.medj.2021.03.013

Słomka, A., Kowalewski, M., and Żekanowska, E. (2020). Coronavirus disease 2019 (COVID–19): A short review on hematological manifestations. *Pathogens* 9 (6), 493. doi:10.3390/pathogens9060493

Sonnweber, T., Grubwieser, P., Sahanic, S., Böhm, A. K., Pizzini, A., Luger, A., et al. (2022). The impact of iron dyshomeostasis and anaemia on long-term pulmonary recovery and persisting symptom burden after COVID-19: A prospective observational cohort study. *Metabolites* 12, 546. doi:10.3390/metabo12060546

Son, K., Jamil, R., Chowdhury, A., Mukherjee, M., Venegas, C., Miyasaki, K., et al. (2022). Circulating anti-nuclear autoantibodies in COVID-19 survivors predict long-COVID symptoms. *Eur. Respir. J.* 61, 2200970. doi:10.1183/13993003.00970-2022

Song, J., Yoon, D., Christensen, R. D., Horvathova, M., Thiagarajan, P., and Prchal, J. T. (2015). HIF-mediated increased R.O.S. from reduced mitophagy and decreased catalase causes neocytolysis. *J. Mol. Med.* 93, 857–866. doi:10.1007/s00109-015-1294-y

Sproston, N. R., and Ashworth, J. J. (2018). Role of C-reactive protein at sites of inflammation and infection. *Front. Immunol.* 9, 754. doi:10.3389/fimmu.2018.00754

Subramanian, A., Nirantharakumar, K., Hughes, S., Myles, P., Williams, T., Gokhale, K. M., et al. (2022). Symptoms and risk factors for long COVID in non-hospitalized adults. *Nat. Med.* 28, 1706–1714. doi:10.1038/s41591-022-01909-w

Sumi, T., and Harada, K. (2022). Immune response to SARS-CoV-2 in severe disease and long COVID-19. *iScience* 25, 104723. doi:10.1016/j.isci.2022.104723

Swank, Z., Senussi, Y., Manickas-Hill, Z., Yu, X. G., Li, J. Z., Alter, G., et al. (2023). Persistent circulating severe acute respiratory syndrome coronavirus 2 spike is associated with post-acute coronavirus disease 2019 sequelae. *Clin. Infect. Dis.* 76, e487–e490. doi:10.1093/cid/ciac722

Tang, Y., Liu, J., Zhang, D., Xu, Z., Ji, J., and Wen, C. (2020). Cytokine storm in COVID-19: The current evidence and treatment strategies. *Front. Immunol.* 11, 1708. doi:10.3389/fimmu.2020.01708

Townsend, L., Fogarty, H., Dyer, A., Martin-Loeches, I., Bannan, C., Nadarajan, P., et al. (2021). Prolonged elevation of D-dimer levels in convalescent COVID-19 patients is independent of the acute phase response. *J. Thrombosis Haemostasis* 19, 1064–1070. doi:10.1111/jth.15267

Tsampasian, V., Elghazaly, H., Chattopadhyay, R., Debski, M., Naing, T. K. P., Garg, P., et al. (2023). Risk factors associated with post-COVID-19 condition: A systematic review and meta-analysis. *JAMA Intern Med.* 183, 566–580. doi:10.1001/jamainternmed.2023.0750

Venter, C., Bezuidenhout, J. A., Laubscher, G. J., Lourens, P. J., Steenkamp, J., Kell, D. B., et al. (2020). Erythrocyte, platelet, serum ferritin, and P-selectin pathophysiology implicated in severe hypercoagulation and vascular complications in COVID-19. *Int. J. Mol. Sci.* 21, 8234. doi:10.3390/ijms21218234

Wang, C., Yu, C., Jing, H., Wu, X., Novakovic, V. A., Xie, R., et al. (2022). Long COVID: The nature of thrombotic sequelae determines the necessity of early anticoagulation. *Front. Cell Infect. Microbiol.* 12, 861703. doi:10.3389/fcimb.2022.861703

Wang, K., Chen, W., Zhang, Z., Deng, Y., Lian, J.-Q., Du, P., et al. (2020). CD147-spike protein is a novel route for SARS-CoV-2 infection to host cells. *Signal Transduct. Target Ther.* 5, 283. doi:10.1038/s41392-020-00426-x

Weisel, J. W., and Litvinov, R. I. (2019). Red blood cells: The forgotten player in hemostasis and thrombosis. *J. Thrombosis Haemostasis* 17, 271–282. doi:10.1111/jth.14360

Whelihan, M. F., and Mann, K. G. (2013). The role of the red cell membrane in thrombin generation. *Thromb. Res.* 131, 377–382. doi:10.1016/j.thromres.2013.01.023

Williams, E. S., Martins, T. B., Shah, K. S., Hill, H. R., Coiras, M., Spivak, A. M., et al. (2022). Cytokine deficiencies in patients with long-COVID. *J. Clin. Cell Immunol.* 13, 672.

Winterbourn, C. C. (1995). Toxicity of iron and hydrogen peroxide: The fenton reaction. *Toxicol. Lett.* 82-83, 969–974. doi:10.1016/0378-4274(95)03532-X

Wu, X., Xiang, M., Jing, H., Wang, C., Novakovic, V. A., and Shi, J. (2023). Damage to endothelial barriers and its contribution to long COVID. *Angiogenesis*, 1–18. doi:10.1007/s10456-023-09878-5

Xie, Y., and Al-Aly, Z. (2022). Risks and burdens of incident diabetes in long COVID: A cohort study. *Lancet Diabetes Endocrinol.* 10, 311–321. doi:10.1016/S2213-8587(22)00044-4

Xie, Y., Xu, E., Bowe, B., and Al-Aly, Z. (2022). Long-term cardiovascular outcomes of COVID-19. *Nat. Med.* 28, 583–590. doi:10.1038/s41591-022-01689-3

Xu, H., Zhong, L., Deng, J., Peng, J., Dan, H., Zeng, X., et al. (2020). High expression of ACE2 receptor of 2019-nCoV on the epithelial cells of oral mucosa. *Int. J. Oral Sci.* 12, 8. doi:10.1038/s41368-020-0074-x

Ye, J., Jiao, Y., Zhang, Y., Li, Z., Zeng, X., Deng, H., et al. (2020). Hematological changes in patients with COVID-19 (Review). *Mol. Med. Rep.* 22, 4485–4491. doi:10.3892/mmr.2020.11581

Yu, H.-H., Qin, C., Chen, M., Wang, W., and Tian, D.-S. (2020). D-dimer level is associated with the severity of COVID-19. *Thromb. Res.* 195, 219–225. doi:10.1016/j.thromres.2020.07.047

frontiers | Frontiers in Physiology

TYPE Original Research
PUBLISHED 15 September 2023
DOI 10.3389/fphys.2023.1215835

OPEN ACCESS

EDITED BY
Wassim El Nemer,
French Blood Establishment (EFS), France

REVIEWED BY
John Stanley Gibson,
University of Cambridge, United Kingdom
Thiago Trovati Maciel,
Institut National de la Santé et de la Recherche Médicale (INSERM), France

*CORRESPONDENCE
Ozlem Yalcin,
ozlemyalcin@ku.edu.tr

†These authors have contributed equally to this work and share first authorship

RECEIVED 02 May 2023
ACCEPTED 01 September 2023
PUBLISHED 15 September 2023

CITATION
Goksel E, Ugurel E, Nader E, Boisson C, Muniansi I, Joly P, Renoux C, Gauthier A, Connes P and Yalcin O (2023), A preliminary study of phosphodiesterases and adenylyl cyclase signaling pathway on red blood cell deformability of sickle cell patients.
Front. Physiol. 14:1215835.
doi: 10.3389/fphys.2023.1215835

A preliminary study of phosphodiesterases and adenylyl cyclase signaling pathway on red blood cell deformability of sickle cell patients

Evrim Goksel[1,2,3†], Elif Ugurel[1,2†], Elie Nader[4,5], Camille Boisson[4,5], Ingrid Muniansi[4,5], Philippe Joly[4,5], Celine Renoux[4,5], Alexandra Gauthier[6], Philippe Connes[4,5] and Ozlem Yalcin[1,2*]

[1]Research Center for Translational Medicine (KUTTAM), Koc University, Istanbul, Türkiye, [2]Department of Physiology, School of Medicine, Koc University, Istanbul, Türkiye, [3]Graduate School of Health Sciences, Koc University, Istanbul, Türkiye, [4]Laboratoire Interuniversitaire de Biologie de la Motricité (LIBM) EA7424, Team "Vascular Biology and Red Blood Cell", Université Claude Bernard Lyon 1, Lyon, France, [5]Laboratoire d'Excellence du Globule Rouge (Labex GR-Ex), PRES Sorbonne, Paris, France, [6]Institut Hématologique et Oncologique Pédiatrique (IHOPe), Lyon, France

Sickle cell disease (SCD) is an inherited hemoglobinopathy characterized by chronic anemia, intravascular hemolysis, and the occurrence of vaso-occlusive crises due to the mechanical obstruction of the microcirculation by poorly deformable red blood cells (RBCs). RBC deformability is a key factor in the pathogenesis of SCD, and is affected by various factors. In this study, we investigated the effects of adenylyl cyclase (AC) signaling pathway modulation and different phosphodiesterase (PDE) modulatory molecules on the deformability and mechanical stress responses of RBC from SCD patients (HbSS genotype) by applying 5 Pa shear stress with an ektacytometer (LORRCA). We evaluated RBC deformability before and after the application of shear stress. AC stimulation with Forskolin had distinct effects on RBC deformability depending on the application of 5 Pa shear stress. RBC deformability was increased by Forskolin before shear stress application but decreased after 5 Pa shear stress. AC inhibition with SQ22536 and protein kinase A (PKA) inhibition with H89 increased RBC deformability before and after the shear stress application. Non-selective PDE inhibition with Pentoxifylline increased RBC deformability. However, modulation of the different PDE types had distinct effects on RBC deformability, with PDE1 inhibition by Vinpocetine increasing deformability while PDE4 inhibition by Rolipram decreased RBC deformability after the shear stress application. The effects of the drugs varied greatly between patients suggesting some could benefit from one drug while others not. Developing drugs targeting the AC signaling pathway could have clinical applications for SCD, but more researches with larger patient cohorts are needed to identify the differences in the responses of sickle RBCs.

KEYWORDS

sickle cell disease, deformability, shear stress, adenylyl cyclase, phosphodiesterases, protein kinase A

1 Introduction

Sickle cell disease (SCD) is an inherited hemoglobinopathy characterized by a point mutation in the β-globin gene, resulting in the production of an abnormal hemoglobin (HbS) (Piel et al., 2017). The polymerization of HbS, which occurs in deoxygenated conditions, causes a mechanical distortion of red blood cells (RBC) resulting in a change of cell morphology into a sickle shape (Rees et al., 2010; Connes et al., 2018). Repeated cycles of sickling and unsickling may damage the RBC membrane, deteriorate deformability, increase cell adhesiveness and ultimately lead to vaso-occlusions, intravascular hemolysis, and chronic anemia (Lamarre et al., 2012; Alapan et al., 2014; Connes et al., 2014; Jang et al., 2021). Stiff and poorly deformable sickle RBCs have detrimental effects on the microcirculation by being trapped in the postcapillary venules and impairing blood flow, which may lead to painful vaso-occlusive crises and organ damages (Eaton and Hofrichter, 1987; Chiang and Frenette, 2005; Conran et al., 2009).

RBC deformability depends on intracellular viscosity, surface/volume ratio, and the cytoskeletal interactions with the integral membrane components, as well as ATP levels and redox state (Huisjes et al., 2018; Kuck et al., 2020). ATP is an important energy source for the proper function of ion channels and essential for the intracellular ion balance to maintain cell hydration (Chu et al., 2012; Leal Denis et al., 2016; Gallagher, 2017). Dehydration and reduced ATP levels have been reported in RBCs from SCD patients (Gulley et al., 1982; Banerjee and Kuypers, 2004, Sabina et al., 2009). The impaired production of ATP in sickle RBCs could adversely affect AC signaling pathway. The activation of signaling molecules and enzymes involved in adenylyl cyclase (AC) pathway is dependent on the conversion of ATP to cAMP. Several studies demonstrated a role of AC signaling pathway in the regulation of the deformability of healthy RBCs (Sprague et al., 2001; Muravyov et al., 2009; Muravyov and Tikhomirova, 2013; Semenov et al., 2019). Indeed, ATP levels could affect AC pathway, which may participate to the decrease in RBC deformability in this disease. We have previously shown the potential role of AC pathway for the modulation of RBC deformability in SCD patients and demonstrated that the inhibition of cAMP hydrolysis by phosphodiesterases increased the deformability of RBCs from SCD patients (Ugurel et al., 2019).

Once the AC enzyme is activated by the G protein coupled receptor (GPCR), it catalyzes the conversion of ATP to cAMP that activates cAMP-dependent enzyme (Protein kinase A, PKA). The signal transduction within the cell is carried out depending upon enhanced cAMP levels, and the signal is terminated when cAMP is converted to AMP by phosphodiesterases (PDE). Hence, PDEs provide negative feedback for the signaling pathways. It has also been shown in SCD mice model that activation of PKA through stimulation of $A_{2B}R$ receptor with adenosine promotes cAMP production, leading to RBC sickling (Zhang et al., 2011). Significantly higher RBC cAMP levels have been reported in SCD patients, and correlation with the frequency of painful vaso-occlusive crises has been reported (Hines et al., 2003; Jit et al., 2019). A reduction in cAMP level was also observed in sickle RBCs during hydroxyurea treatment (Bartolucci et al., 2010), a treatment that decrease the risk of vaso-occlusive crises and acute chest syndrome in SCD. Six different PDE types (PDE1, PDE2A, PDE3B, PDE4, PDE5, and PDE9A) have been identified in RBCs to date and are important for the regulation of cAMP or cGMP (Almeida et al., 2008; Adderley et al., 2010; Adderley et al., 2011), however, their distinct roles in the regulation of RBC deformability in SCD are unknown.

In the present study, we hypothesized that RBC deformability from SCD patients is modulated by selective PDE types and AC signaling pathway. We investigated the modulatory effects of AC, PKA, and different PDE types on RBC deformability by incubating SCD RBCs with selective stimulators and inhibitors. Moreover, RBCs undergo various levels of shear stress in the blood circulation that is fundamental for their ability to deform. Shear stress at the physiological level regulates ATP release from RBCs and calcium (Ca^{+2}) influx within RBCs, the latter of which could directly stimulate AC through Ca^{+2}-calmodulin (Halls and Cooper, 2011; Cinar et al., 2015; Danielczok et al., 2017). Indeed, we also exposed RBCs from SCD patients to prolonged shear stress that is physiologically relevant and evaluated mechanical stress responses of RBCs by the changes in deformability, before and after the application of shear stress and with or without drugs known to modulate AC, PKA and PDE signaling pathways.

2 Materials and methods

2.1 Patients and controls

Homozygous SCD patients with HbSS genotype (n = 7) were included in the study: age = 21.4 ± 16.5 years, HbF = 13.1 ± 6.6%, HbS = 83.3 ± 6.0%, Hct = 24.5 ± 3.2%, RBC number = 2.85 ± 0.39 10^{12}/L, MCHC = 347 ± 12.4 g/L, MCV = 87.4 ± 15.9 fl, all under hydroxyurea therapy. The patients were diagnosed and followed at the Sickle Cell Center of the Academic Hospital of Lyon. All patients were at clinical steady state for at least 2 months prior to their inclusion in the study (i.e., no acute episodes of infection, vaso-occlusive crises, acute chest syndrome, stroke, priapism and no blood transfusions in the preceding 3 months). Every donor gave written informed consent before sampling. The study was conducted in accordance with the guidelines set by the Declaration of Helsinki and was approved by the Regional Ethics Committees (CPP Lyon-Est, Hospices Civils de Lyon, L14-127).

2.2 Preparation of blood samples

Peripheral blood was withdrawn from antecubital vein of each donor and taken into EDTA vacuum tubes (15 IU/ml). Hematocrit was set to 40% for the experiments with autologous plasma. Blood samples were treated with the stimulators or inhibitors of the enzymes involved in the PKA pathway. Forskolin (10 μM) and SQ22536 (100 μM) were used for the stimulation and the inhibition of AC, respectively. H-89 (10 μM) and Pentoxifylline (10 μM) were used for the inhibition of PKA and PDEs, respectively. For the selective inhibition of PDEs, Vinpocetine (30 μM), Milrinone (20 μM), and Rolipram (10 μM) were used to block the activities of PDE1, PDE3, and PDE4, respectively. All chemical agents were purchased from Sigma-Aldrich Co (MO, United States) and

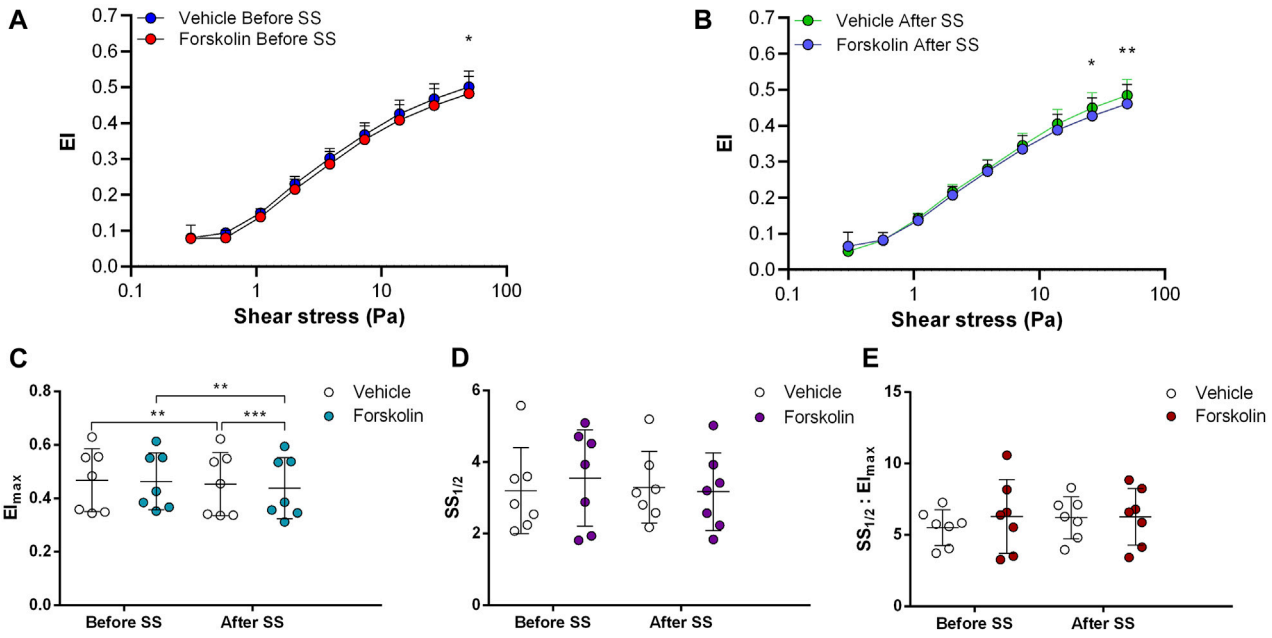

FIGURE 1
Effects of Forskolin on samples before and after shear stress. Changes in elongation index (EI) before continuous 5 Pa shear stress **(A)** and after continuous 5 Pa shear stress **(B)**, maximum elongation index (EI_{max}) **(C)**, and the shear stress required to reach half of maximum elongation index ($SS_{1/2}$) **(D)** are shown. EI_{max}:$SS_{1/2}$ is shown in **(E)**. n = 7, ANOVA, *p < 0.05, **p < 0.01, ***p < 0.001.

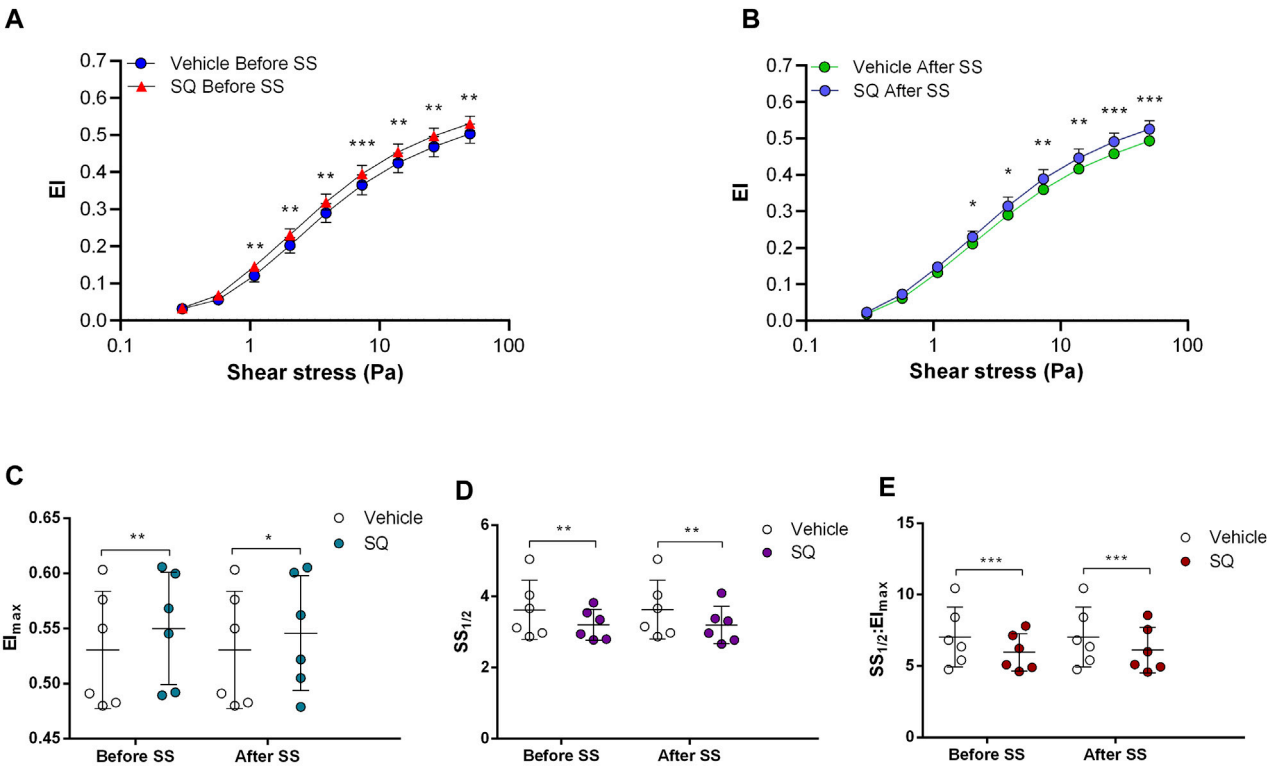

FIGURE 2
Effects of SQ22536 on samples before and after shear stress. Changes in elongation index (EI) before continuous 5 Pa shear stress **(A)** and after continuous 5 Pa shear stress **(B)**, maximum elongation index (EI_{max}) **(C)**, and the shear stress required to reach half of maximum elongation index ($SS_{1/2}$) **(D)** are shown. EI_{max}:$SS_{1/2}$ is shown in **(E)**. n = 6, ANOVA, *p < 0.05, **p < 0.01, ***p < 0.001.

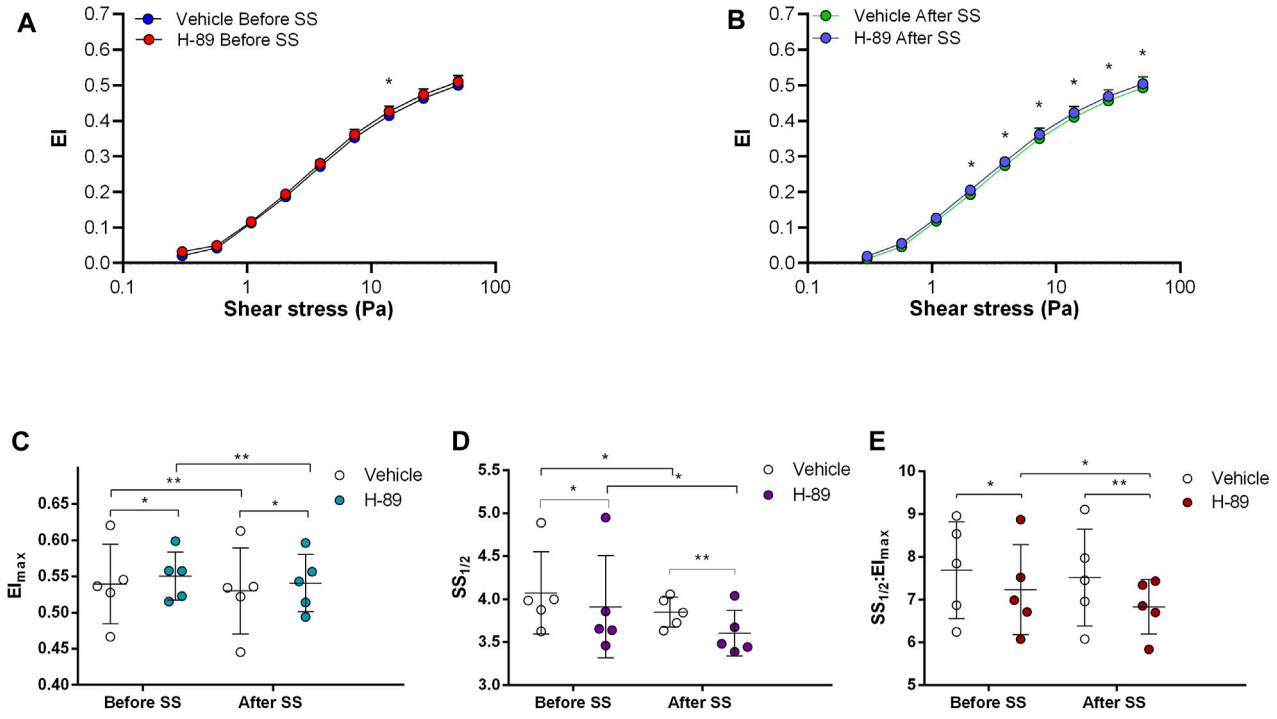

FIGURE 3
Effects of H-89 on samples before and after shear stress. Changes in elongation index (EI) before continuous 5 Pa shear stress **(A)** and after continuous 5 Pa shear stress **(B)**, maximum elongation index (EI_{max}) **(C)**, and the shear stress required to reach half of maximum elongation index ($SS_{1/2}$) **(D)** are shown. EI_{max}:$SS_{1/2}$ is shown in **(E)**. n = 5, ANOVA, *p < 0.05, **p < 0.01, ***p < 0.001.

incubated with blood samples at 37 C for 15 min, except Vinpocetine which was incubated for 30 min. A vehicle (DMSO or PBS) was prepared in the same volume (v/v) and studied under the same conditions as a control. After the incubation with the agents, whole blood samples were measured directly. All experiments were performed within 4 h after blood sampling.

2.3 Measurements of RBC deformability

RBC deformability was measured by ektacytometry, using the laser-assisted optical rotational cell analyzer (LORRCA MaxSis, Mechatronics, Netherlands) at 37°C. The laser integrated device consists of a rotating and a static cylinder that generate shear stresses. Briefly, 2.5 mL iso-osmolar polyvinylpyrrolidone (PVP) solution (360 kDa, 29.9 ± 0.5 mPa s, Mechatronics, Netherlands) was mixed with 12.5 uL of the blood sample and placed into the measuring chamber between the two cylinders. RBC deformability was measured by applying 9 different shear stresses (0.30, 0.57, 1.08, 2.04, 3.87, 7.34, 13.92, 26.38, and 50 Pa). A diffraction pattern of RBCs was generated by the laser beam traversing the blood sample. An Elongation Index (EI) was calculated from the diffraction pattern collected by the camera of the LORRCA, which reflected RBC deformability, such as: (A–B)/(A + B), with A and B corresponding to the vertical and horizontal axis of a theoretical ellipse fitting the diffraction pattern. The Lineweaver-Burke method was used to calculate the maximum elongation index at infinite shear stress (EImax) and the shear stress required to reach half of this maximum elongation index (SS1/2) (Baskurt et al., 2009). In order to normalize SS1/2, the ratio SS1/2/EImax was calculated (Baskurt and Meiselman, 2013).

2.4 Application of prolonged shear stress to blood samples

The effects of prolonged shear stress on the deformability of RBCs treated or not with the different molecules used in this study, were also investigated. Mixed PVP-RBC suspensions were exposed to continuous shear stress of 5 Pa for 300 s using ektacytometry (LORRCA MaxSis, Mechatronics, Hoorn, Netherlands).The shear stress level at 5 Pa corresponds to a physiological shear stress level at arterial walls (Papaioannou and Stefanadis, 2005). RBC deformability was measured before and after the application of shear stress. Data were recorded as curves of EI-shear stresses.

The following experimental procedure was conducted on blood samples with or without chemical agents: (1) RBC suspensions were used to evaluate RBC deformability before continuous shear stress exposure between 0.3 and 50 Pa, (2) after the measurement has been completed, the sample is aspirated from the gap and the cup is cleaned before the replacement of the next sample, (3) the measuring chamber was filled with new suspension, and 300 s of continuous 5 Pa shear stress were applied and, (4) RBC deformability was measured again immediately following the end of the 5 Pa shear stress exposure.

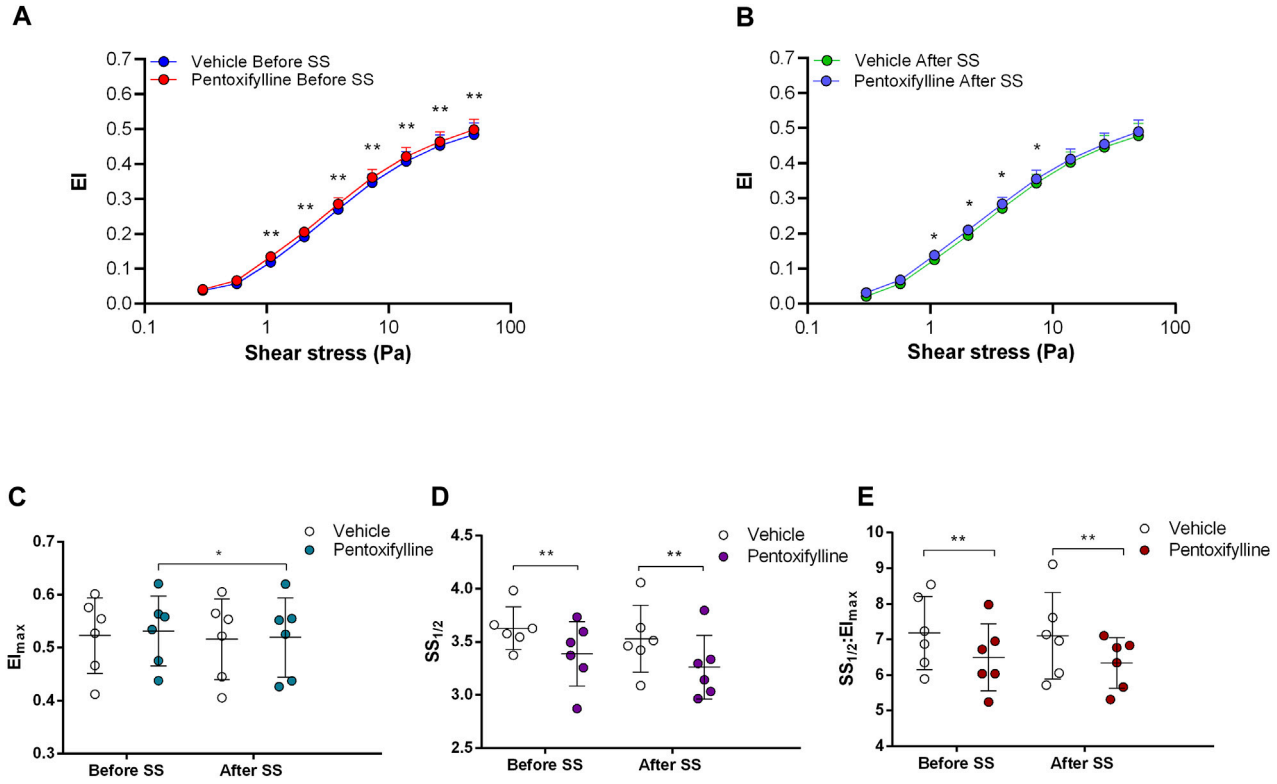

FIGURE 4
Effects of Pentoxifylline on samples before and after shear stress. Changes in elongation index (EI) before continuous 5 Pa shear stress **(A)** and after continuous 5 Pa shear stress **(B)**, maximum elongation index (EI_{max}) **(C)**, and the shear stress required to reach half of maximum elongation index ($SS_{1/2}$) **(D)** are shown. EI_{max}:$SS_{1/2}$ is shown in **(E)**. n = 6, ANOVA, *p < 0.05, **p < 0.01.

2.5 Statistical analysis

Statistical analysis and data presentation using commercial software were performed (Prism, GraphPad Sofware Inc., United States). The results are shown as a mean ± SD. Shapiro-Wilk normality test was applied for all data sets whether they are normally distributed. A non-parametric Wilcoxon test was performed for the matched data sets which were not normally distributed. Deformability measurements were evaluated before and after shear stress application using a two-way ANOVA with repeated measures followed by Bonferroni multiple comparisons test. A p-value less than 0.05 was considered statistically significant.

3 Results

3.1 RBC deformability from SCD patients is improved by the inhibition of adenylyl cyclase and protein kinase A

Adenylyl cyclase (AC) stimulation by Forskolin exerted distinct effects on RBC deformability depending on the application of the constant shear stress of 5 Pa. Deformability was improved before the continuous 5 Pa application by 3.7% but deteriorated after by 4.8%, particularly at high shear stress levels (26.38 Pa and 50 Pa) (Figures 1A, B). Interestingly, EImax decreased with Forskolin treatment before and after the 5 Pa application although SS1/2 and SS1/2:EImax values did not change (Figures 1C–E). On the other hand, AC inhibition by SQ22536 resulted in an increase of RBC deformability by 8%–10% between 1.08 Pa and 50 Pa both before and after the constant 5 Pa application (Figures 2A, B). SQ22536 increased EImax values and decreased SS1/2 and SS1/2:EImax values, which indicates a significant increase in RBC deformability (Figures 2C–E). The inhibition of Protein kinase A (PKA) by H89 slightly increased RBC deformability by 2.7% before the 5 Pa application but only at 13.92 Pa level (Figure 3A). After the 5 Pa application, H89 increased RBC deformability between 2.04 Pa and 50 Pa levels by 4% (Figure 3B). EImax values increased and SS1/2 and SS1/2:EImax values decreased with H89 both before and after the application of the continuous 5 Pa shear stress (Figures 3C–E). These results support a modulatory effect of AC/PKA signaling pathway on RBC deformability in SCD.

3.2 Different PDE types exert distinct effects on sickle cell deformability

Non-selective inhibition of PDEs by Pentoxifylline resulted in an increase of RBC deformability between 1.08 Pa and 50 Pa by 5.5% before the 5 Pa application and between 1.08 Pa and 7.34 Pa after by 4.7% (Figures 4A, B). EImax did not change but SS1/2 and SS1/2:EImax values significantly decreased with Pentoxifylline both before

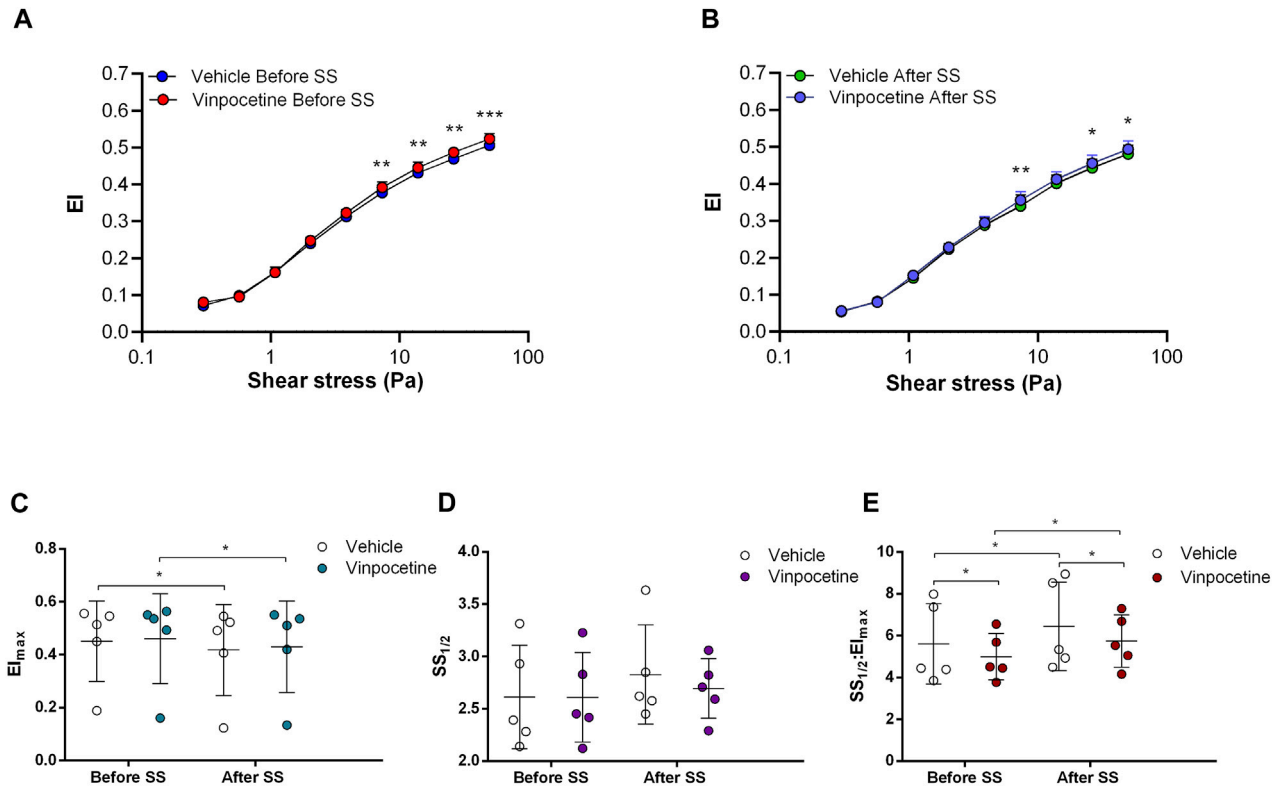

FIGURE 5
Effects of Vinpocetine on samples before and after shear stress. Changes in elongation index (EI) before continuous 5 Pa shear stress **(A)** and after continuous 5 Pa shear stress **(B)**, maximum elongation index (EI_{max}) **(C)**, and the shear stress required to reach half of maximum elongation index ($SS_{1/2}$) **(D)** are shown. EI_{max}:$SS_{1/2}$ is shown in **(E)**. n = 6, ANOVA, *p < 0.05, **p < 0.01.

and after the 5 Pa application (Figures 4C–E). We then investigated the effects of the different types of PDEs on RBC deformability from SCD patients. The inhibition of PDE1 by Vinpocetine significantly increased EI values at high shear stresses (≥7.34 Pa) by 3% both before and after the application of 5 Pa. The inhibition of PDE4 by Rolipram also changed EI values at high shear stresses (≥13.92 Pa). However, Rolipram increased deformability before the 5 Pa application by 4.5% and decreased it after by 6.5% (Figures 5A, B; Figures 6A, B). Vinpocetine decreased SS1/2:EImax ratio but did not change EImax and SS1/2 values (Figures 5C–E). On the contrary, Rolipram did not change SS1/2 and SS1/2:EImax but decreased EImax values both before and after the application of 5 Pa (Figures 6C–E). The inhibition of PDE3 by Milrinone did not significantly affect RBC deformability (data not shown). Figure 7 shows the changes in RBC deformability obtained with the different drugs, before and after the 5 Pa shear stress application, for one SCD patient.

4 Discussion

The salient findings in the present study demonstrate the beneficial effects of the inhibitors of adenylyl cyclase (AC)/Protein kinase A (PKA) signaling pathway on the deformability of RBCs from SCD patients. The inhibition of AC and PKA increased RBC deformability before the application of shear stress, while the stimulation of AC decreased it after the 5 Pa shear stress application. To our knowledge, this is the first study investigating the effects of different PDE families on mechanical stress responses of sickle RBCs. Non-selective phosphodiesterase (PDE) inhibition increased RBC deformability. However, blocking particular PDE families produced divergent results showing that the function of the different PDEs is variable in RBCs from SCD patients.

In SCD, RBC ATP level is reduced, and ATP depletion is associated with increased number of irreversibly sickled RBCs (Jensen et al., 1973; Banerjee and Kuypers, 2004). RBCs are known to release ATP in a response to mechanical stress. Inactivation of AC/PKA signaling pathway attenuates ATP release and improves mechanical stress responses of RBC by increasing deformability (Sprague et al., 2001). Therefore, one may suggest that PKA inhibition could be beneficial for the rheological properties of sickle RBCs. Since PKA activity is dependent on cAMP levels, AC activity is also important for PKA-dependent processes by the conversion of AMP to cAMP. Sickle RBCs are known to contain more than 4-fold cAMP levels compared to healthy RBCs (Hines et al., 2003). The stimulation of AC by Forskolin has been shown to further increase cAMP levels in sickle RBCs, which resulted in increased adhesiveness to laminin (Hines et al., 2003). Our results in the present study demonstrate that AC stimulation by Forskolin lead to a reduction of RBC deformability, plausibly by the enhancement of cAMP levels.

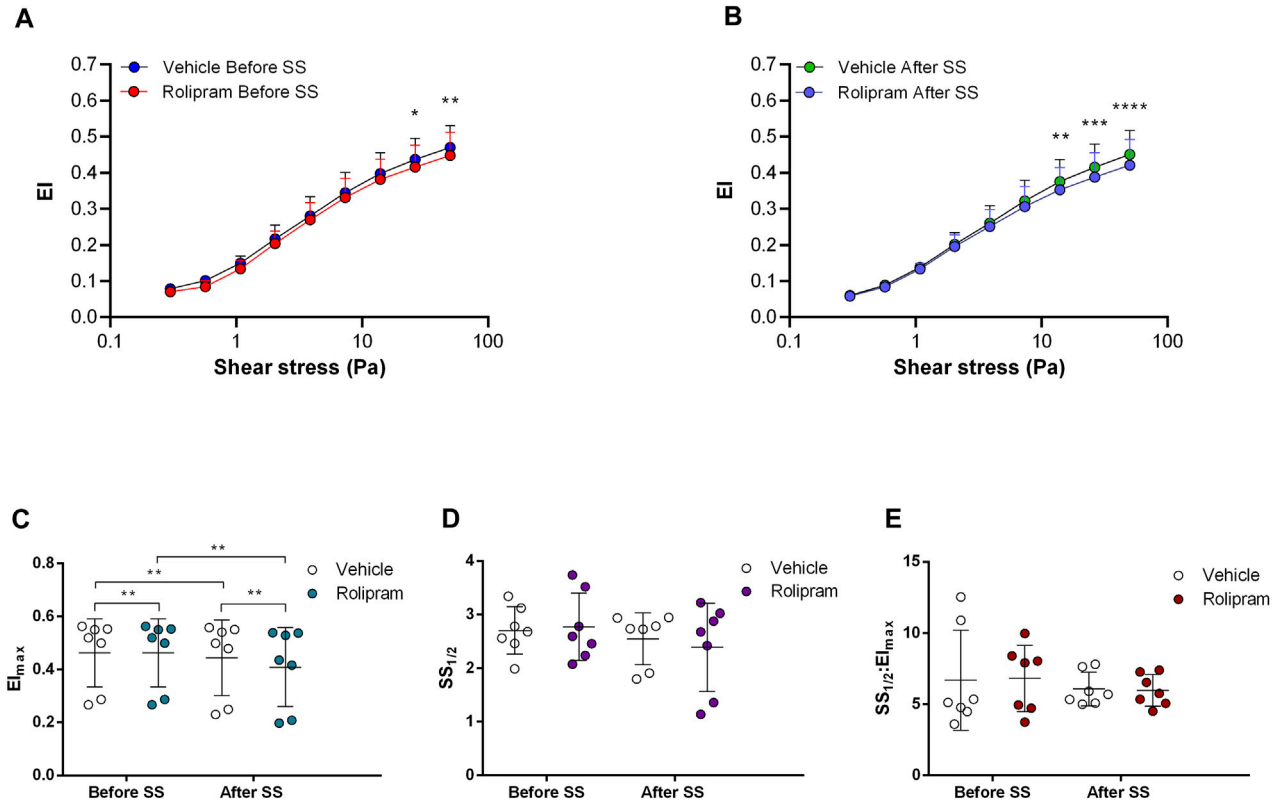

FIGURE 6
Effects of Rolipram on samples before and after shear stress. Changes in elongation index (EI) before continuous 5 Pa shear stress **(A)** and after continuous 5 Pa shear stress **(B)**, maximum elongation index (EI_{max}) **(C)**, and the shear stress required to reach half of maximum elongation index ($SS_{1/2}$) **(D)** are shown. EI_{max}:$SS_{1/2}$ is shown in **(E)**. n = 7, ANOVA and Wilcoxon for EI_{max} data, *p < 0.05, **p < 0.01, ***p < 0.001.

Interestingly, few studies showed that Forskolin increased deformability of healthy RBCs (Muravyov et al., 2009; Muravyov and Tikhomirova, 2013). However, Semenov et al. (2019) demonstrated that the improvement of RBC deformability by Forskolin would be dependent on both the dosage of the drug and the level of shear stress. Similarly, we showed that Forskolin increased RBC deformability before the implementation of constant shear stress; however, RBC deformability was decreased after the 5 Pa application. Physiologically relevant shear stress increases deformability in healthy RBCs (Meram et al., 2013). The impairment of RBC deformability by Forskolin after 5 Pa application in SCD patients could be explained by the calcium influx through shear stress sensing mechanisms that could stimulate AC and lead to the elevation of intracellular cAMP levels (Figure 8). Several nonselective cationic ion channels are present at the membrane of RBCs and can be activated by shear stress, resulting in increased Ca^{2+} influx (Kaestner et al., 2020; Egée and Kaestner, 2021; Nader et al., 2023). The decrease of RBC deformability through AC stimulation was well observed at high shear stresses suggesting that the effect of Forskolin is shear stress dependent.

The inhibition of AC and PKA by SQ22536 and H89, respectively, significantly increased RBC deformability of SCD patients. The improving effects of H89 and SQ22536 on RBC deformability were more pronounced than the effects of Forskolin, which can be observed in $SS_{1/2}$, EI_{max}, and $SS_{1/2}$:EI_{max} parameters. The $SS_{1/2}$ parameter provides a global index of RBC deformability, while EI_{max} indicates the limiting elongation index at infinite shear stress (Baskurt et al., 2009). EI_{max} may be affected by cell shape and membrane properties, however, this parameter is not impacted by cytoplasmic viscosity (Baskurt et al., 2009). A reduced $SS_{1/2}$ often indicates improved RBC deformability, however, this might also be related to a reduced EI_{max}. Therefore, $SS_{1/2}$:EI_{max} ratio should be considered and reflects the dependence of EI on SS independent of EI_{max} alterations (Baskurt and Meiselman, 2013). In our previous study, we also showed that the inhibition of AC/PKA signaling pathway resulted in a rise of RBC deformability in SCD patients (Ugurel et al., 2019). AC inhibition reduces cAMP levels and suppresses PKA activation. PKA targets several membrane proteins and regulates the activities of ion channels. PKA phosphorylates dematin, Protein 4.1 and adducin in RBC membrane that promotes the dissociation of the spectrin network and reduces membrane stability (Cohen and Gascard, 1992; Koshino et al., 2012; Chen et al., 2013). PKA also targets CFTR channel in RBC and regulates Cl efflux (Decherf et al., 2007). This mechanism could affect cell volume with a significant impact on RBC deformability. On the other hand, the enhancement of AC/PKA signaling increases the adhesion of sickle RBCs to endothelium through Lu/BCAM adhesion molecule (Zennadi et al., 2004; Gauthier et al., 2005). Abnormal adherence of sickle RBCs to

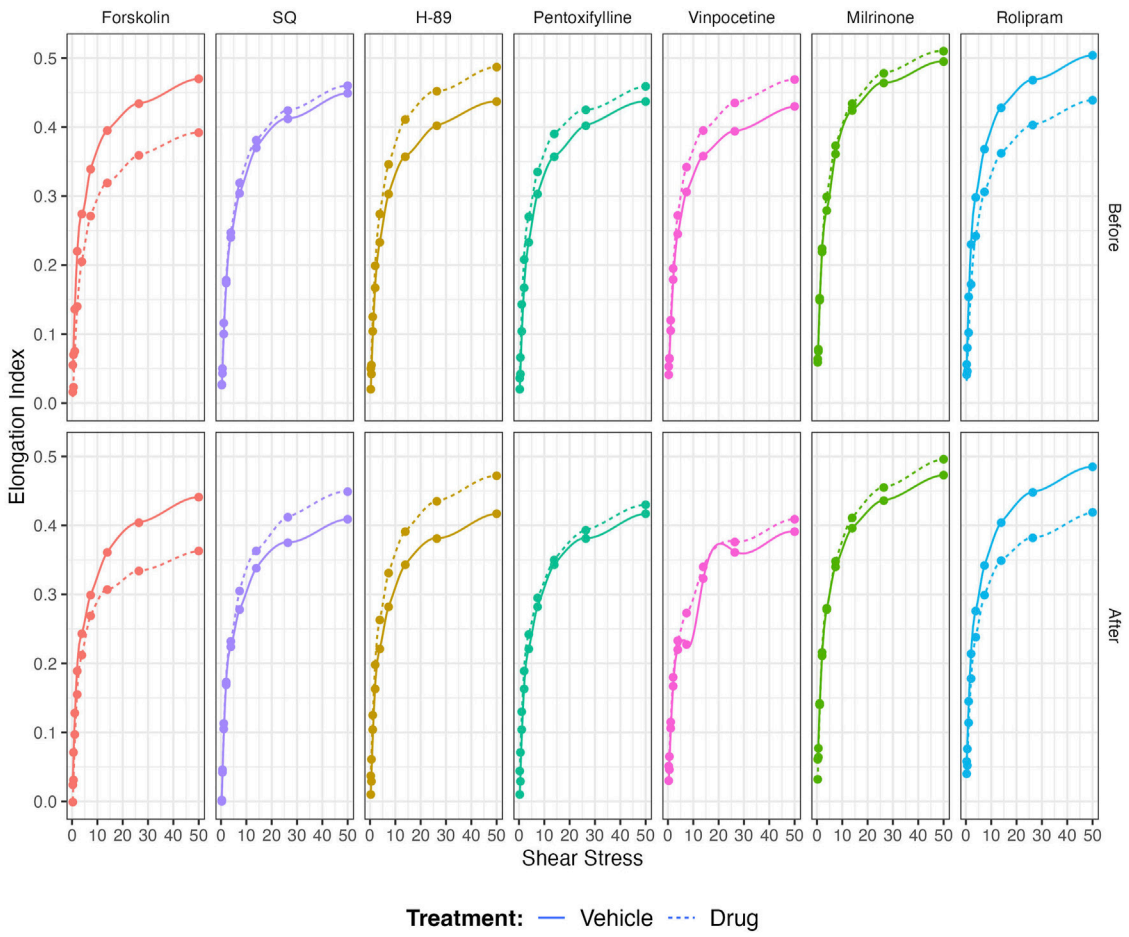

FIGURE 7
Representative figure of the effects of Forskolin, SQ, H-89, Pentoxifylline, Vinpocetine, Milrinone, and Rolipram on a blood sample collected from a patient with sickle cell disease.

endothelial cells was postulated to be important in the initiation and progression of vaso-occlusive crises (Hebbel, 1997; Kaul and Fabry, 2004). AC/PKA signaling pathway also activates ERK1/2 signaling molecule, which phosphorylates ICAM-4 adhesion receptor on RBCs and promotes sickle cell adhesion (Zennadi et al., 2012). This mechanism of action could be reversed by blocking AC or PKA activities that suppresses sickle RBC adhesion to the endothelium (Zennadi et al., 2012).

AC induced synthesis of cAMP requires the stimulation of G protein coupled receptors (GPCR) which includes β2-adrenergic receptors (βAR) and prostacyclin receptors (IPR) in RBCs (Sprague et al., 2008). Intracellular signal transduction is mediated by increased levels of cAMP, which is then carried out by PKA (Figure 8). However, the signal can be attenuated due to the hydrolysis of cAMP by phosphodiesterases (PDEs) (Baillie, 2009). Although 11 different PDE families are present in various cell types, only 6 of them (PDE1, 2, 3, 4, 5, and 9) are defined in mature RBCs or erythroid precursors (Almeida et al., 2008; Adderley et al., 2011). Non-selective inhibition of PDE by Pentoxifylline in the present study significantly increased the deformability of RBCs from SCD patients, both before and after the application of a constant shear stress for prolonged time, which confirms previous findings (Ugurel et al., 2019) but contrast with another study (Cummings and Ballas, 1990). A previous case report in the late seventies showed that Pentoxifylline treatment in a patient with SCD and frequent vaso-occlusive crises improved RBC deformability and decreased blood viscosity (Keller and Leonhardt, 1979). A recent study demonstrated that the elastic modulus of RBC was decreased by Pentoxifylline treatment *in vivo*, which improved blood flow in subjects with cerebrovascular and peripheral arterial diseases (Aifantis et al., 2019). Pentoxifylline is postulated to increase intracellular ATP concentrations, decrease Ca^{2+} concentrations by activation of the Ca^{2+}—Mg^{2+} ATPase and calmodulin, and increase the phosphorylation of proteins into the RBC membrane (Schubotz and Mühlfellner, 1977; Aifantis et al., 2019), which could increase RBC deformability. We previously demonstrated that tyrosine phosphorylation of membrane proteins was increased by the application of Pentoxifylline *in vitro* and was accompanied by an increase of RBC deformability in healthy donors (Ugurel et al., 2022). However, several clinical trials conducted in SCD did not demonstrate any clinical improvement induced by Pentoxifylline, as a preventive molecule, in patients with frequent vaso-occlusive crises (Sherer and Glover, 2000). In contrast, a study demonstrated that the use of Pentoxifylline during the acute phase of vaso-occlusive

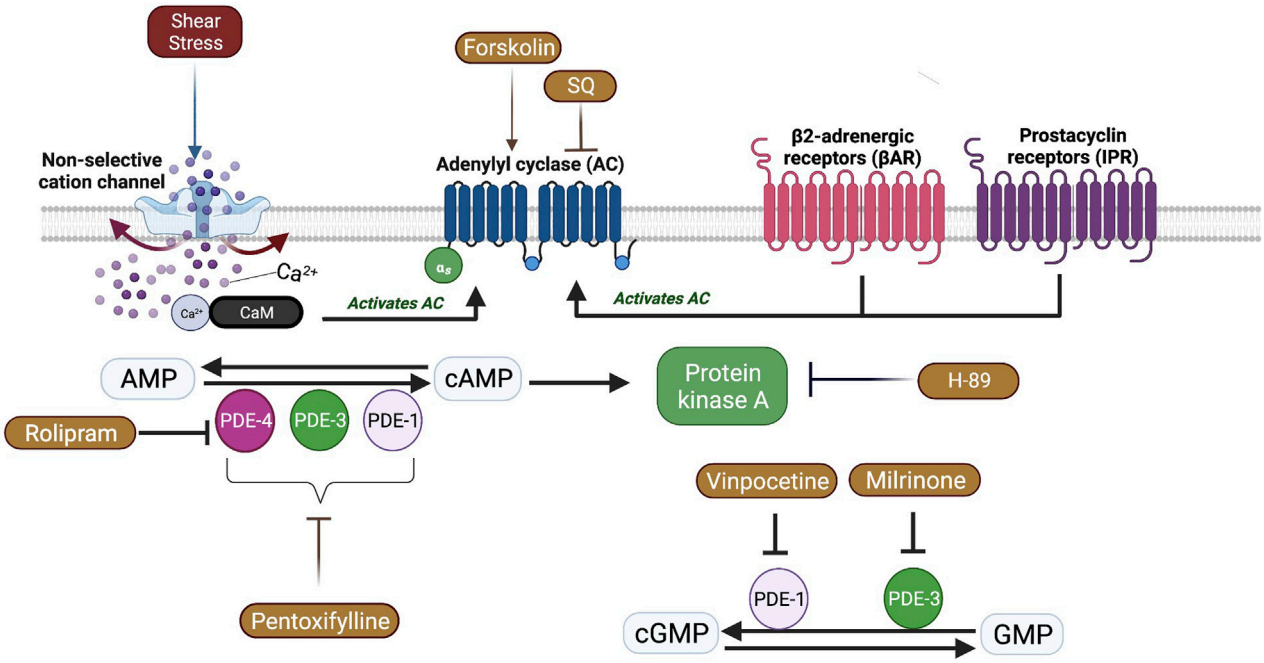

FIGURE 8
A schematic view of Adenylyl cyclase (AC) signaling pathway and the effects of shear stress in red blood cells. Shear stress could activate some non-selective cation channels which causes calcium (Ca^{+2}) entry. Ca^{+2} ions bind Calmodulin (CaM) and activate membrane bound AC which is also activated by β2 adrenergic receptors (βAR) and prostacyclin receptors (IPR). AC catalyzes the conversion of adenosine monophosphate (AMP) to cyclic adenosine monophosphate (Chu et al.) that activates Protein kinase A (PKA). Phosphodiesterases (PDE) facilitate the conversion of cAMP to AMP or cyclic guanosine monophosphate (cGMP) to guanosine monophosphate (GMP).

crisis could be helpful for faster recovery (Poflee et al., 1991). Nevertheless, its clinical impact seems to be rather limited (Sherer and Glover, 2000).

According to the present study, the inhibition of PDE1 by Vinpocetine significantly increased RBC deformability of SCD patients. Vinpocetine was previously shown to improve RBC deformability in healthy subjects and stroke patients (Hayakawa, 1992; Muravyov and Tikhomirova, 2015). This selective inhibitor of PDE1 has no effect on the increase of cAMP in either βAR or IPR pathway suggesting that PDE1 is involved in hydrolysis of cGMP in RBCs (Adderley et al., 2009). The improvement of RBC deformability from SCD patients by PDE1 inhibition could be explained by the elevation of intracellular cGMP levels. PDE4 inhibition by Rolipram decreased RBC deformability from SCD patients. The alterations seem to be more pronounced after the 5 Pa application showing that mechanical stress responses of sickle RBCs are deteriorated by PDE4 inhibition. PDE4 is known to be responsible for hydrolyzing cAMP in healthy RBCs. The selective inhibition of PDE4 by Rolipram increased cAMP levels in RBCs with the stimulation of adrenergic pathway by isoproterenol (Adderley et al., 2009). Rolipram was shown to increase the deformability in healthy RBCs (Muravyov and Tikhomirova, 2015), however we have demonstrated that this drug decreased RBC deformability from SCD patients, particularly at high shear stress. We suspect that the responses of sickle RBCs to mechanical stress would be altered due to the impairment in cAMP signaling. Furthermore, prolonged hypoxia in transgenic SCD mice increased PDE4 levels in lung tissue, which was reversed by Rolipram, preventing the development of pulmonary arterial hypertension (De Franceschi et al., 2008). Rolipram was also shown to reduce ischemic/reperfusion liver injury in transgenic SCD mice most likely by inducing over-expression of Nos3 and reducing vascular activation (Filippini et al., 2008). Although these studies revealed the protective effects of PDE4 inhibition for ischemic injury and hypertension in a SCD model, they did not investigate the efficacy of PDE4 on sickle RBCs. Another PDE family investigated in the present study was PDE3, which hydrolyzes both cAMP and cGMP in a complex manner. The hydrolysis of cGMP by PDE3 can inhibit the hydrolysis of cAMP in various cell types (Degerman et al., 1997; Bender and Beavo, 2006). PDE3 inhibition in RBC had no effect on cAMP levels stimulated by βAR, however PDE3 selectively regulates cAMP synthesis when stimulated by IPR signaling (Hanson et al., 2008; Adderley et al., 2009). We did not initially stimulate βAR or IPR pathways; however, we studied the effects of PDE3 inhibition on sickle RBCs in native conditions. Accordingly, the inhibition of PDE3 by Milrinone did not significantly alter RBC deformability in SCD patients suggesting sickle RBC deformability is not modulated in an IPR dependent way.

5 Conclusion

Although our study showed an effect of most of the drugs used on RBC deformability from SCD patients, the potential clinical relevance is unknown. Most of the changes observed in RBC deformability are rather small in comparison with the effects of other drugs currently used in the context of SCD, such as

Hydroxyurea (Charache et al., 1995; Lemonne et al., 2015) or Voxelotor (Dufu et al., 2018; Migotsky et al., 2022), and where clinical benefits have been reported. The only change we noted, which seems to be physiologically relevant, is the decrease of RBC deformability observed when stimulating AC with Forskolin and blocking PDE4 by Rolipram. Following the application of prolonged shear stress, both drugs reduced the RBC deformability of SCD patients, indicating that the effects of these two compounds might be shear-dependent. However, the results from the present study are preliminary and limited to a small sample size: further studies are needed with a larger group of patients to identify the factors that could be involved in the variability of the responses. Developing drugs targeting the AC signaling pathway mediated by βAR receptors could have potential clinical application but further studies are needed. Nevertheless, the Figure 7 shows the example of a patient with SCD whose *in-vitro* responses to most of the drugs were highly significant from a physiological/rheological point of view, suggesting that the effects of the different drugs tested in the present study are highly variable from one patient to another and that some patients could benefit from one drug while other not. Differential responses of sickle RBCs might be due to variable expression levels of PDEs in each patient, as well. Our next studies will include the quantification of PDEs in RBC samples from SCD patients. Further large *in-vitro* studies are needed to identify why some sickle RBCs could respond more than others.

Data availability statement

The raw data supporting the conclusion of this article will be made available by the authors, without undue reservation.

Ethics statement

The studies involving humans were approved by CPP Lyon-Est, Hospices Civils de Lyon. The studies were conducted in accordance with the local legislation and institutional requirements. Written informed consent for participation in this study was provided by the participants' legal guardians/next of kin.

Author contributions

EG conducted the experiments, performed the data analysis, and drafted the manuscript. EU performed the data analysis, interpreted the data, and wrote the manuscript. EN and PC interpreted the data and wrote the manuscript. AG recruited the patients. IM collected the patient data. CB, PJ, CR, and OY revised the manuscript critically for intellectual content. All authors contributed to the article and approved the submitted version.

Funding

This study was supported by the Turkish Scientific and Technical Council grant SBAG-214S186.

Acknowledgments

The authors gratefully acknowledge the use of the services and facilities of Sickle Cell Center of the Academic Hospital of Lyon and Koç University Research Center for Translational Medicine (KUTTAM).

Conflict of interest

The authors declare that the research was conducted in the absence of any commercial or financial relationships that could be construed as a potential conflict of interest.

Publisher's note

References

Adderley, S. P., Dufaux, E. A., Sridharan, M., Bowles, E. A., Hanson, M. S., Stephenson, A. H., et al. (2009). Iloprost- and isoproterenol-induced increases in cAMP are regulated by different phosphodiesterases in erythrocytes of both rabbits and humans. *Am. J. Physiology-Heart Circulatory Physiology* 296 (5), H1617–H1624. doi:10.1152/ajpheart.01226.2008

Adderley, S. P., Sprague, R. S., Stephenson, A. H., and Hanson, M. S. (2010). Regulation of cAMP by phosphodiesterases in erythrocytes. *Pharmacol. Rep.* 62 (3), 475–482. doi:10.1016/S1734-1140(10)70303-0

Adderley, S. P., Thuet, K. M., Sridharan, M., Bowles, E. A., Stephenson, A. H., Ellsworth, M. I., et al. (2011). Identification of cytosolic phosphodiesterases in the erythrocyte: A possible role for PDE5. *Med. Sci. Monit.* 17 (5), CR241–CR247. doi:10.12659/msm.881763

Aifantis, K. E., Shrivastava, S., Pelidou, S.-H., Ngan, A. H. W., and Baloyannis, S. I. (2019). Relating the blood-thinning effect of pentoxifylline to the reduction in the elastic modulus of human red blood cells: an *in vivo* study. *Biomaterials Sci.* 7 (6), 2545–2551. doi:10.1039/C8BM01691G

Alapan, Y., Little, J. A., and Gurkan, U. A. (2014). Heterogeneous red blood cell adhesion and deformability in sickle cell disease. *Sci. Rep.* 4 (1), 7173. doi:10.1038/srep07173

Almeida, C. B., Traina, F., Lanaro, C., Canalli, A. A., Saad, S. T. O., Costa, F. F., et al. (2008). High expression of the cGMP-specific phosphodiesterase, PDE9A, in sickle cell disease (SCD) and the effects of its inhibition in erythroid cells and SCD neutrophils. *Br. J. Haematol.* 142 (5), 836–844. doi:10.1111/j.1365-2141.2008.07264.x

Baillie, G. S. (2009). Compartmentalized signalling: spatial regulation of cAMP by the action of compartmentalized phosphodiesterases. *FEBS J.* 276 (7), 1790–1799. doi:10.1111/j.1742-4658.2009.06926.x

Banerjee, T., and Kuypers, F. A. (2004). Reactive oxygen species and phosphatidylserine externalization in murine sickle red cells. *Br. J. Haematol.* 124 (3), 391–402. doi:10.1046/j.1365-2141.2003.04781.x

Bartolucci, P., Chaar, V., Picot, J., Bachir, D., Habibi, A., Fauroux, C., et al. (2010). Decreased sickle red blood cell adhesion to laminin by hydroxyurea is associated with inhibition of Lu/BCAM protein phosphorylation. *Blood* 116 (12), 2152–2159. doi:10.1182/blood-2009-12-257444

Baskurt, O. K., Hardeman, M. R., Uyuklu, M., Ulker, P., Cengiz, M., Nemeth, N., et al. (2009). Parameterization of red blood cell elongation index-shear stress curves obtained by ektacytometry. *Scand. J. Clin. Lab. Invest.* 69 (7), 777–788. doi:10.3109/00365510903266069

Baskurt, O. K., and Meiselman, H. J. (2013). Data reduction methods for ektacytometry in clinical hemorheology. *Clin. Hemorheol. Microcirc.* 54, 99–107. doi:10.3233/CH-2012-1616

Bender, A. T., and Beavo, J. A. (2006). Cyclic nucleotide phosphodiesterases: molecular regulation to clinical use. *Pharmacol. Rev.* 58 (3), 488–520. doi:10.1124/pr.58.3.5

Charache, S., Terrin, M. L., Moore, R. D., Dover, G. J., Barton, F. B., Eckert, S. V., et al. (1995). Effect of hydroxyurea on the frequency of painful crises in sickle cell anemia. Investigators of the Multicenter Study of Hydroxyurea in Sickle Cell Anemia. *N. Engl. J. Med.* 332 (20), 1317–1322. doi:10.1056/nejm199505183322001

Chen, L., Brown, J. W., Mok, Y.-F., Hatters, D. M., and McKnight, C. J. (2013). The allosteric mechanism induced by protein kinase A (PKA) phosphorylation of dematin (band 4.9). *J. Biol. Chem.* 288 (12), 8313–8320. doi:10.1074/jbc.M112.438861

Chiang, E. Y., and Frenette, P. S. (2005). Sickle cell vaso-occlusion. *Hematology/Oncology Clin. N. Am.* 19 (5), 771–784. doi:10.1016/j.hoc.2005.08.002

Chu, H., Puchulu-Campanella, E., Galan, J. A., Tao, W. A., Low, P. S., and Hoffman, J. F. (2012). Identification of cytoskeletal elements enclosing the ATP pools that fuel human red blood cell membrane cation pumps. *Proc. Natl. Acad. Sci.* 109 (31), 12794–12799. doi:10.1073/pnas.1209014109

Cinar, E., Zhou, S., DeCourcey, J., Wang, Y., Waugh, R. E., and Wan, J. (2015). Piezo1 regulates mechanotransductive release of ATP from human RBCs. *Proc. Natl. Acad. Sci.* 112 (38), 11783–11788. doi:10.1073/pnas.1507309112

Cohen, C. M., and Gascard, P. (1992). Regulation and post-translational modification of erythrocyte membrane and membrane-skeletal proteins. *Semin. Hematol.* 29 (4), 244–292.

Connes, P., Lamarre, Y., Waltz, X., Ballas, S. K., Lemonne, N., Etienne-Julan, M., et al. (2014). Haemolysis and abnormal haemorheology in sickle cell anaemia. *Br. J. Haematol.* 165 (4), 564–572. doi:10.1111/bjh.12786

Connes, P., Renoux, C., Romana, M., Abkarian, M., Joly, P., Martin, C., et al. (2018). Blood rheological abnormalities in sickle cell anemia. *Clin. Hemorheol. Microcirc.* 68, 165–172. doi:10.3233/CH-189005

Conran, N., Franco-Penteado, C. F., and Costa, F. F. (2009). Newer aspects of the pathophysiology of sickle cell disease vaso-occlusion. *Hemoglobin* 33 (1), 1–16. doi:10.1080/03630260802625709

Cummings, D. M., and Ballas, S. K. (1990). Effects of pentoxifylline and metabolite on red blood cell deformability as measured by ektacytometry. *Angiology* 41 (2), 118–123. doi:10.1177/000331979004100205

Danielczok, J. G., Terriac, E., Hertz, L., Petkova-Kirova, P., Lautenschläger, F., Laschke, M. W., et al. (2017). Red blood cell passage of small capillaries is associated with transient Ca2+-mediated adaptations. *Front. Physiology* 8, 979. doi:10.3389/fphys.2017.00979

De Franceschi, L., Platt, O. S., Malpeli, G., Janin, A., Scarpa, A., Leboeuf, C., et al. (2008). Protective effects of phosphodiesterase-4 (PDE-4) inhibition in the early phase of pulmonary arterial hypertension in transgenic sickle cell mice. *FASEB J.* 22 (6), 1849–1860. doi:10.1096/fj.07-098921

Decherf, G., Bouyer, G., Egée, S., and Thomas, S. L. Y. (2007). Chloride channels in normal and cystic fibrosis human erythrocyte membrane. *Blood Cells, Mol. Dis.* 39 (1), 24–34. doi:10.1016/j.bcmd.2007.02.014

Degerman, E., Belfrage, P., and Manganiello, V. C. (1997). Structure, localization, and regulation of cGMP-inhibited phosphodiesterase (PDE3). *J. Biol. Chem.* 272 (11), 6823–6826. doi:10.1074/jbc.272.11.6823

Dufu, K., Patel, M., Oksenberg, D., and Cabrales, P. (2018). GBT440 improves red blood cell deformability and reduces viscosity of sickle cell blood under deoxygenated conditions. *Clin. Hemorheol. Microcirc.* 70, 95–105. doi:10.3233/CH-170340

Eaton, W., and Hofrichter, J. (1987). Hemoglobin S gelation and sickle cell disease. *Blood* 70 (5), 1245–1266. doi:10.1182/blood.V70.5.1245.1245

Egée, S., and Kaestner, L. (2021). The transient receptor potential vanilloid type 2 (TRPV2) channel–A new druggable Ca2+ pathway in red cells, implications for red cell ion homeostasis. *Front. Physiology* 12, 677573. doi:10.3389/fphys.2021.677573

Filippini, A., Malpeli, G., Janin, A., Platt, O. S., Leboeuf, C., Scarpa, A., et al. (2008). Phosphodiesterase-4 inhibition reduces ischemic/reperfusion liver injury in a mouse model for sickle cell disease. *Blood* 112 (11), 1444. doi:10.1182/blood.V112.11.1444.1444

Gallagher, P. G. (2017). Disorders of erythrocyte hydration. *Blood* 130 (25), 2699–2708. doi:10.1182/blood-2017-04-590810

Gauthier, E., Rahuel, C., Wautier, M. P., El Nemer, W., Gane, P., Wautier, J. L., et al. (2005). Protein kinase A-dependent phosphorylation of Lutheran/basal cell adhesion molecule glycoprotein regulates cell adhesion to laminin alpha5. *J. Biol. Chem.* 280 (34), 30055–30062. doi:10.1074/jbc.M503293200

Gulley, M. L., Ross, D. W., Feo, C., and Orringer, E. P. (1982). The effect of cell hydration on the deformability of normal and sickle erythrocytes. *Am. J. Hematol.* 13 (4), 283–291. doi:10.1002/ajh.2830130403

Halls, M. L., and Cooper, D. M. (2011). Regulation by Ca2+-signaling pathways of adenylyl cyclases. *Cold Spring Harb. Perspect. Biol.* 3 (1), a004143. doi:10.1101/cshperspect.a004143

Hanson, M. S., Stephenson, A. H., Bowles, E. A., Sridharan, M., Adderley, S., and Sprague, R. S. (2008). Phosphodiesterase 3 is present in rabbit and human erythrocytes and its inhibition potentiates iloprost-induced increases in cAMP. *Am. J. Physiology-Heart Circulatory Physiology* 295 (2), H786–H793. doi:10.1152/ajpheart.00349.2008

Hayakawa, M. (1992). Effect of vinpocetine on red blood cell deformability in stroke patients. *Arzneim.* 42 (4), 425–427.

Hebbel, R. P. (1997). Perspectives series: cell adhesion in vascular biology. Adhesive interactions of sickle erythrocytes with endothelium. *J. Clin. Invest.* 99 (11), 2561–2564. doi:10.1172/JCI119442

Hines, P. C., Zen, Q., Burney, S. N., Shea, D. A., Ataga, K. I., Orringer, E. P., et al. (2003). Novel epinephrine and cyclic AMP-mediated activation of BCAM/Lu-dependent sickle (SS) RBC adhesion. *Blood* 101 (8), 3281–3287. doi:10.1182/blood-2001-12-0289

Huisjes, R., Bogdanova, A., van Solinge, W. W., Schiffelers, R. M., Kaestner, L., and van Wijk, R. (2018). Squeezing for life – properties of red blood cell deformability. *Front. Physiology* 9, 656. doi:10.3389/fphys.2018.00656

Jang, T., Poplawska, M., Cimpeanu, E., Mo, G., Dutta, D., and Lim, S. H. (2021). Vaso-occlusive crisis in sickle cell disease: A vicious cycle of secondary events. *J. Transl. Med.* 19 (1), 397. doi:10.1186/s12967-021-03074-z

Jensen, M., Shohet, S. B., and Nathan, D. G. (1973). The role of red cell energy metabolism in the generation of irreversibly sickled cells *in vitro*. *Blood* 42 (6), 835–842. doi:10.1182/blood.V42.6.835.835

Jit, B. P., Mohanty, P. K., Pradhan, A., Purohit, P., Das, K., Patel, S., et al. (2019). Erythrocyte cAMP in determining frequency of acute pain episodes in sickle cell disease patients from odisha state, India. *Hemoglobin* 43 (2), 88–94. doi:10.1080/03630269.2019.1623248

Kaestner, L., Bogdanova, A., and Egee, S. (2020). "Calcium channels and calcium-regulated channels in human red blood cells," in *Calcium signaling*. Editor M. S. Islam (Cham: Springer International Publishing), 625–648.

Kaul, D. K., and Fabry, M. E. (2004). *In vivo* studies of sickle red blood cells. *Microcirculation* 11 (2), 153–165. doi:10.1080/mic.11.2.153.165

Keller, F., and Leonhardt, H. (1979). Amelioration of blood viscosity in sickle cell anemia by pentoxifylline. A case report. *J. Med.* 10 (6), 429–433.

Koshino, I., Mohandas, N., and Takakuwa, Y. (2012). Identification of a novel role for dematin in regulating red cell membrane function by modulating spectrin-actin interaction. *J. Biol. Chem.* 287 (42), 35244–35250. doi:10.1074/jbc.M111.305441

Kuck, L., Peart, J. N., and Simmonds, M. J. (2020). Active modulation of human erythrocyte mechanics. *Am. J. Physiology-Cell Physiology* 319 (2), C250–C257. doi:10.1152/ajpcell.00210.2020

Leal Denis, M. F., Alvarez, H. A., Lauri, N., Alvarez, C. L., Chara, O., and Schwarzbaum, P. J. (2016). Dynamic regulation of cell volume and extracellular ATP of human erythrocytes. *PLOS ONE* 11 (6), e0158305. doi:10.1371/journal.pone.0158305

Lamarre, Y., Romana, M., Waltz, X., Lalanne-Mistrih, M., Tressières, B., Divialle-Doumdo, L., et al. (2012). Hemorheological risk factors of acute chest syndrome and painful vaso-occlusive crisis in children with sickle cell disease. *Haematologica* 97 (11), 1641–1647. doi:10.3324/haematol.2012.066670

Lemonne, N., Charlot, K., Waltz, X., Ballas, S. K., Lamarre, Y., Lee, K., et al. (2015). Hydroxyurea treatment does not increase blood viscosity and improves red blood cell rheology in sickle cell anemia. *Haematologica* 100 (10), e383–e386. doi:10.3324/haematol.2015.130435

Meram, E., Yilmaz, B. D., Bas, C., Atac, N., Yalcin, O., Meiselman, H. J., et al. (2013). Shear stress-induced improvement of red blood cell deformability. *Biorheology* 50 (3-4), 165–176. doi:10.3233/BIR-130637

Migotsky, M., Beestrum, M., and Badawy, S. M. (2022). Recent advances in sickle-cell disease therapies: A review of voxelotor, crizanlizumab, and L-glutamine. *Pharmacy* 10 (5), 123. doi:10.3390/pharmacy10050123

Muravyov, A., and Tikhomirova, I. (2015). Red blood cell microrheological changes and drug transport efficiency. *J. Cell. Biotechnol.* 1 (1), 45–51. doi:10.3233/JCB-15005

Muravyov, A. V., and Tikhomirova, I. A. (2013). Role molecular signaling pathways in changes of red blood cell deformability. *Clin. Hemorheol. Microcirc.* 53, 45–59. doi:10.3233/CH-2012-1575

Muravyov, A. V., Tikhomirova, I. A., Maimistova, A. A., and Bulaeva, S. V. (2009). Extra- and intracellular signaling pathways under red blood cell aggregation and deformability changes. *Clin. Hemorheol. Microcirc.* 43 (3), 223–232. doi:10.3233/ch-2009-1212

Nader, E., Conran, N., Leonardo, F. C., Hatem, A., Boisson, C., Carin, R., et al. (2023). Piezo1 activation augments sickling propensity and the adhesive properties of sickle red blood cells in a calcium-dependent manner. *Br. J. Haematol.* 202, 657–668. n/a(n/a). doi:10.1111/bjh.18799

Papaioannou, T. G., and Stefanadis, C. (2005). Vascular wall shear stress: basic principles and methods. *Hell. J. Cardiol.* 46 (1), 9–15.

Piel, F. B., Steinberg, M. H., and Rees, D. C. (2017). Sickle cell disease. *N. Engl. J. Med.* 376 (16), 1561–1573. doi:10.1056/NEJMra1510865

Poflee, V. W., Gupta, O. P., Jain, A. P., and Jajoo, U. N. (1991). Haemorheological treatment of painful sickle cell crises. Use of pentoxifylline. *J. Assoc. Physicians India* 39 (8), 608–609.

Rees, D. C., Williams, T. N., and Gladwin, M. T. (2010). Sickle-cell disease. *Lancet* 376 (9757), 2018–2031. doi:10.1016/S0140-6736(10)61029-X

Sabina, R. L., Wandersee, N. J., and Hillery, C. A. (2009). Ca^{2+}-CaM activation of AMP deaminase contributes to adenine nucleotide dysregulation and phosphatidylserine externalization in human sickle erythrocytes. *Br. J. Haematol.* 144 (3), 434–445. doi:10.1111/j.1365-2141.2008.07473.x

Schubotz, R., and Mühlfellner, O. (1977). The effect of pentoxifylline on erythrocyte deformability and on phosphatide fatty acid distribution in the erythrocyte membrane. *Curr. Med. Res. Opin.* 4 (9), 609–617. doi:10.1185/03007997709115279

Semenov, A. N., Shirshin, E. A., Muravyov, A. V., and Priezzhev, A. V. (2019). The effects of different signaling pathways in adenylyl cyclase stimulation on red blood cells deformability. *Front. Physiology* 10, 923. doi:10.3389/fphys.2019.00923

Sherer, J. T., and Glover, P. H. (2000). Pentoxifylline for sickle-cell disease. *Ann. Pharmacother.* 34 (9), 1070–1074. doi:10.1345/aph.19397

Sprague, R. S., Bowles, E. A., Hanson, M. S., Dufaux, E. A., Sridharan, M., Adderley, S., et al. (2008). Prostacyclin analogs stimulate receptor-mediated cAMP synthesis and ATP release from rabbit and human erythrocytes. *Microcirculation* 15 (5), 461–471. doi:10.1080/10739680701833804

Sprague, R. S., Ellsworth, M. L., Stephenson, A. H., and Lonigro, A. J. (2001). Participation of cAMP in a signal-transduction pathway relating erythrocyte deformation to ATP release. *Am. J. Physiology-Cell Physiology* 281 (4), C1158–C1164. doi:10.1152/ajpcell.2001.281.4.C1158

Ugurel, E., Connes, P., Yavas, G., Eglenen, B., Turkay, M., Aksu, A. C., et al. (2019). Differential effects of adenylyl cyclase-protein kinase A cascade on shear-induced changes of sickle cell deformability. *Clin. Hemorheol. Microcirc.* 73, 531–543. doi:10.3233/CH-190563

Ugurel, E., Goksel, E., Cilek, N., Kaga, E., and Yalcin, O. (2022). Proteomic analysis of the role of the adenylyl cyclase–cAMP pathway in red blood cell mechanical responses. *Cells* 11 (7), 1250. doi:10.3390/cells11071250

Zennadi, R., Hines, P. C., De Castro, L. M., Cartron, J.-P., Parise, L. V., and Telen, M. J. (2004). Epinephrine acts through erythroid signaling pathways to activate sickle cell adhesion to endothelium via LW-alphavbeta3 interactions. *Blood* 104 (12), 3774–3781. doi:10.1182/blood-2004-01-0042

Zennadi, R., Whalen, E. J., Soderblom, E. J., Alexander, S. C., Thompson, J. W., Dubois, L. G., et al. (2012). Erythrocyte plasma membrane–bound ERK1/2 activation promotes ICAM-4–mediated sickle red cell adhesion to endothelium. *Blood* 119 (5), 1217–1227. doi:10.1182/blood-2011-03-344440

Zhang, Y., Dai, Y., Wen, J., Zhang, W., Grenz, A., Sun, H., et al. (2011). Detrimental effects of adenosine signaling in sickle cell disease. *Nat. Med.* 17 (1), 79–86. doi:10.1038/nm.2280

frontiers | Frontiers in Physiology

TYPE Review
PUBLISHED 11 December 2023
DOI 10.3389/fphys.2023.1308632

OPEN ACCESS

EDITED BY
Lars Kaestner,
Saarland University, Germany

REVIEWED BY
Vassilis L. Tzounakas,
University of Patras, Greece
Vladimir Muzykantov,
University of Pennsylvania, United States

*CORRESPONDENCE
Mauro Magnani,
mauro.magnani@uniurb.it

RECEIVED 06 October 2023
ACCEPTED 27 November 2023
PUBLISHED 11 December 2023

CITATION
Biagiotti S, Pirla E and Magnani M (2023), Drug transport by red blood cells. *Front. Physiol.* 14:1308632. doi: 10.3389/fphys.2023.1308632

Drug transport by red blood cells

Sara Biagiotti, Elena Pirla and Mauro Magnani*

Department of Biomolecular Sciences, University of Urbino, Urbino, Italy

This review focuses on the role of human red blood cells (RBCs) as drug carriers. First, a general introduction about RBC physiology is provided, followed by the presentation of several cases in which RBCs act as natural carriers of drugs. This is due to the presence of several binding sites within the same RBCs and is regulated by the diffusion of selected compounds through the RBC membrane and by the presence of influx and efflux transporters. The balance between the influx/efflux and the affinity for these binding sites will finally affect drug partitioning. Thereafter, a brief mention of the pharmacokinetic profile of drugs with such a partitioning is given. Finally, some examples in which these natural features of human RBCs can be further exploited to engineer RBCs by the encapsulation of drugs, metabolites, or target proteins are reported. For instance, metabolic pathways can be powered by increasing key metabolites (i.e., 2,3-bisphosphoglycerate) that affect oxygen release potentially useful in transfusion medicine. On the other hand, the RBC pre-loading of recombinant immunophilins permits increasing the binding and transport of immunosuppressive drugs. In conclusion, RBCs are natural carriers for different kinds of metabolites and several drugs. However, they can be opportunely further modified to optimize and improve their ability to perform as drug vehicles.

KEYWORDS

red blood cells, drug transport, blood-to-plasma ratio, pharmacokinetic, blood distribution

1 The unique properties of human red blood cells that have an impact on drug transport

Human red blood cells (RBCs) represent 99% of the cellular compartment in the blood and comprise the most numerous cells in the body. One microliter of blood contains approximately 4–5 million RBCs, which means approximately 25 million million RBCs in the total body of an adult human being. Moreover, thanks to their shape and deformability, they can reach almost all organs and tissues and, for this reason, they are considered the carriers par excellence. Mature RBCs mainly contain hemoglobin; thus, it can be argued that RBCs are passive carriers and that their role only relies on oxygen and CO_2 transport (Hsia, 1998). Indeed, a lot of other molecules can be carried by RBCs. As a matter of fact, erythrocytes are not mere gas transporters, but they are also involved in other functions, i.e., vascular function, coagulant pathways, defense processes, and metabolic pathways, thanks to their further contents (Helms et al., 2018; Olver, 2020; Stosik et al., 2020). Regarding vascular function, they are the main source of nitric oxide, and consequently, they are involved in blood pressure homeostasis as well. Concerning metabolism involvement, physiological examples are given by amino acids, in particular the alanine's transport in the so-called glucose–alanine cycle through the muscle tissue and liver. It was demonstrated that the carriage percentage of alanine is higher in whole blood, thanks to the binding with RBCs, than in plasma (Felig et al., 1973). Other examples are nucleosides which are major precursors for nucleotide biosynthesis. RBCs present different specific membrane transport systems for nucleosides, including the equilibrative nucleoside transporter 1

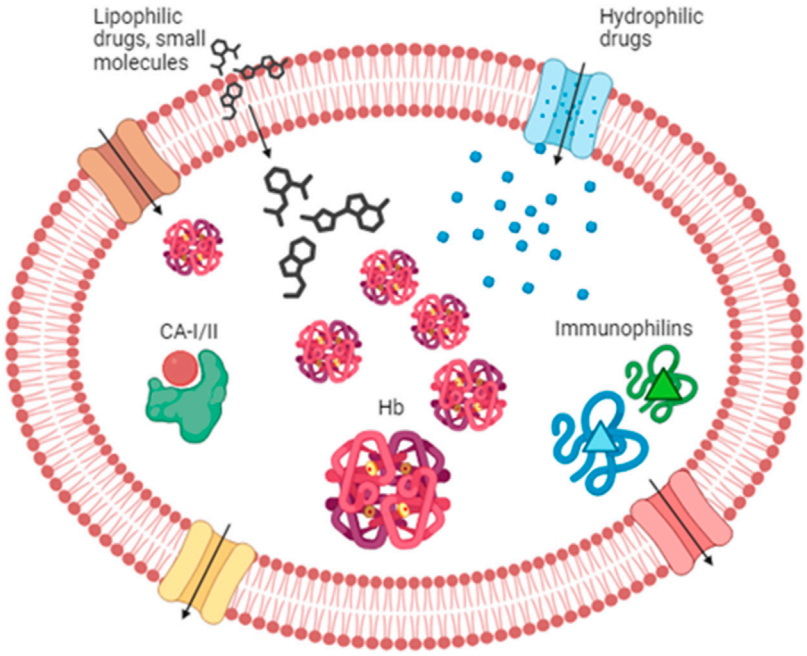

FIGURE 1
Drug partitioning into RBCs. Lipophilic drugs and small molecules can enter the RBC through the lipid bilayer, while hydrophilic compounds can enter via the aqueous channels (in blue) or other transporters such as Glut 1 (in brown). Once in the cytoplasm, drugs can find several binding sites. Among those, we can find hemoglobin, carbonic anhydrase, and immunophilins that possess an affinity for several drugs. RBC partitioning is also affected by drug efflux across several transporters like P-glycoprotein and multidrug resistance-associated protein (MRPs) (in red and yellow, respectively). Hb, hemoglobin; CA-I/II, carbonic anhydrase I and II.

(ENT1), whose absence is related to defective erythropoiesis (Mikdar et al., 2021). Finally, RBCs are also important carriers of hormones, folate, drugs (e.g., valproate, phenytoin, and hydrocortisone), and small metabolites that play key roles in gas exchanges (Highley and De Brujin, 1996). All of these molecules are involved in a complex homeostatic balance between in- and out-flux (Kirk, 2001; Sharma et al., 2001) mediated not only by passive diffusion but also by the use of active transport mechanisms (Sharma et al., 2001), which may be involved in the transport of drugs.

2 RBCs as natural carriers for drugs

The RBC surface area is approximately 163 μm^2 (Beutler et al., 1995), and with a few calculations, we can estimate a total surface area of more than 4,000 m^2. In light of the above, it is quite easy to understand that with a similarly wide area, drugs can easily be distributed into the RBC compartment. In particular, drug molecules can bind to the membrane and/or to proteins into the cytosol. Among the drugs that can bind to the RBC membrane, we can cite codeine, mefloquine, chlorpromazine, imipramine, pyrimethamine (Hinderling, 1997; Dash et al., 2021), and several others. As a matter of fact, the RBC membrane provides an extended surface area that may also be used for anchoring various therapeutic molecules intended to act in the bloodstream. Interested readers can find more information in papers published by Murciano et al. (2009), Muzykantov (2010), Carnemolla et al. (2017), Villa et al. (2018), and Rossi et al. (2019). However, this review will not focus on drugs binding to the RBC membrane but on those that enter into the cell and bind to cytosolic components of RBCs. Indeed, several features affect the partitioning of drugs into RBCs, such as lipophilicity and molecular size. Lipophilic drugs can cross the RBC lipid membrane by simple diffusion, while hydrophilic compounds can enter due to the aqueous channels or other membrane-facilitated or active transport systems such as Glut1 (Dash et al., 2021). Once into the RBC cytoplasm, drugs can find several enzymes and/or proteins to bind to. The most important protein is notably represented by hemoglobin. Hemoglobin represents 10% of the total body proteins of an adult and is able to carry many substances. A review from Hinderling summarized in a table the drugs known to be bound by hemoglobin, and among them, we can find barbiturates, digoxin and derivatives, and salicylic acid (Hinderling, 1997). A more recent review also cites sulfonamides, phenytoin, phenothiazines, phenylbutazones and derivatives, imipramines and derivatives, proquazone, and pyrimethamine (Dash et al., 2021). Some of these drugs may induce allosteric modifications in the hemoglobin structure, changing its affinity for oxygen. In addition to hemoglobin, there are other proteins known to be the binding site for drugs. The nucleoside transporter can bind to draflazine and acetazolamide, while carbonic anhydrase represents the binding site for antidiuretics like chlortalidone, dorzolamide, and methazolamide (Hinderling, 1997). However, the most important example of drug-binding protein is represented by immunophilins (e.g., cyclophilin and FKB12) that bind with very high-affinity immunosuppressive

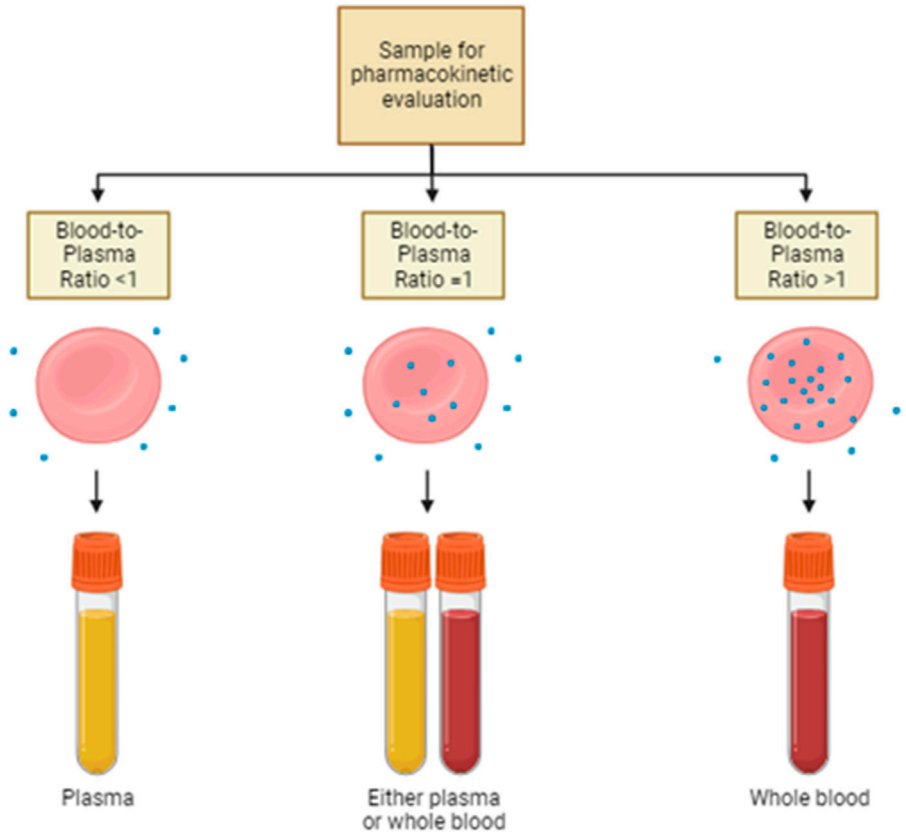

FIGURE 2
Sample choice for pharmacokinetic evaluation. Drug distribution strictly affects the pharmacokinetic properties of the same therapeutic agent. Thus, the choice of the most suitable sample for therapeutic drug monitoring is pivotal. In the case of drugs with a blood-to-plasma ratio lesser than 1, plasma is the sample of choice for pharmacokinetic evaluations. On the contrary, when the blood-to-plasma ratio is higher than 1, whole blood is the recommended sample on which the assessment of drug concentration is performed. Either plasma or whole blood is appropriate if the ratio is around 1.

drugs such as cyclosporine and tacrolimus (Magnani et al., 2012). Finally, drug partitioning into RBCs is affected by the presence of efflux transporters onto the plasma membrane. Evidence showed the presence of P-glycoprotein and breast cancer resistance protein (BCRP) in the RBC membrane. On the contrary, multidrug resistance-associated proteins MRP1, MPR4, and MPR5 are not only involved in the uptake of antimalarial drugs but also in the efflux of some metabolites (e.g., oxidized glutathione conjugates and cyclic nucleotides) (Dash et al., 2021) (Figure 1). Moreover, RBCs can be engineered as drug delivery systems, thanks to their features of biocompatibility, biodegradability, and long-circulating life (Villa et al., 2017). Recently, various types of drug delivery systems based on blood cells have been developed, as well as blood-cell-inspired carriers that mimic the features of native blood cells (Wang et al., 2022). Finally, a new kind of next-generation carrier arising from RBCs has been proposed; this is the case of RBC-derived extracellular vesicles (RBCEVs), which are promising nanosized drug carriers for the intracellular delivery of cargoes (Biagiotti et al., 2023).

Despite the big importance that has been given to plasma protein-binding drugs, the study of RBC partitioning has received much less attention over time. Currently, the routine practice focuses on the systematic investigation of the distribution of drugs into plasma or serum, while it quite completely neglected the measure of the drug distribution into RBCs. Hinderling and other authors have proposed several methods for the measurement of drug partitioning *in vitro* and/or *ex vivo* (Hinderling, 1997). This is very important, especially for the drugs that show high blood-to-plasma ratios. In other words, the plasma concentration of this drug is not at all representative of the real drug bioavailability and pharmacokinetics (Figure 2). In the following paragraphs, some examples are provided.

The drug partitioning rate between RBCs and plasma is calculated using the erythrocyte suspension in plasma and/or buffer after the times required to reach the equilibrium between the compartments and centrifugal separation of the phases. The RBC partitioning rate is calculated by measuring the ratio between the concentrations of the drug in the RBC compartment and those in the plasma or buffer. The partitioning rate in buffer can be considered a measure of the drug's absolute affinity for the RBC-binding sites, while the partitioning rate in plasma indicates the relative drug's affinity for RBC-binding sites with respect to that of the plasma, such as albumin (Hinderling, 1997). Hence, only the unbound fraction in plasma (*i.e.*, drug molecules that are not bound

to albumin or other plasma-binding sites) can partition into RBCs. However, these plasma proteins are saturable; thus, the exceeding drugs' molecules remain unbound in plasma and can additionally partition into RBCs, apparently increasing their affinity for the erythrocyte compartment (Hinderling, 1997). Of note, RBC-associated drugs have a longer life span in circulation compared to the ones portioned in plasma because they are protected by RBCs from macrophage uptake, the liver metabolism, and renal clearance. On the other hand, engineering RBC membranes may induce some feature changes such as an increase rigidity, increasing mechanical stress-induced hemolysis, C-reactive protein activation, and phosphatidylserine (PS) translocation. All these kinds of modifications can lead to precocious clearance of RBCs from the bloodstream if not adequately treated. Several authors have investigated *in vitro* and *in vivo* biocompatibility of membrane-bound molecules, and by appropriate approaches, they have identified the best conditions that do not affect cell clearance (Ferguson et al., 2022) or permit to direct the cargo to the preferred target tissue (Villa et al., 2017; Pan et al., 2018; Glassman et al., 2022). It is worth noting that RBCs can bind to not only drugs but also immune complexes, components of the complement system, biomolecules, small thrombi, and microbial agents, affecting their clearance and eventual transfer to phagocytic cells. In our case, we consider drugs loaded within the inner volume of RBCs, which determine some morphological modifications but do not significantly affect the *in vivo* longevity of the RBC, so they are considered such an optimal drug delivery system able to avoid the liver and spleen metabolisms (Robert et al., 2022). Hence, these drugs can be slowly released into a patient's circulation over a longer period of time (Glassman et al., 2020; 2022). Moreover, RBCs, as drug delivery systems, not only ameliorate the pharmacokinetics drugs' profile but may also represent a new and safe means to deliver therapeutic molecules that otherwise would induce a toxic response (Zaitsev et al., 2006; 2012; Villa et al., 2018).

2.1 Which kind of drugs can bind to RBCs?

In the last years, several drugs have been demonstrated to be able to cross the RBC membrane and highly distribute within them. Thus, RBC partitioning of drugs should be considered at least for these drugs with known RBC affinity. Indeed, the pharmacokinetic profile of those molecules can be extremely affected by this partitioning, and thus, the blood-to-plasma ratio could be opportunely assessed.

2.1.1 Immunosuppressive drugs

Since its first use in the late 80s, cyclosporine A (CsA) has revolutionized the world of transplantation by enabling patients to reduce the possibility of rejection. However, CsA exhibits significant intra- and inter-patient pharmacokinetic variabilities and has limited bioavailability. The tolerability profile of CsA is marked by several potentially severe adverse effects, i.e., acute or chronic nephrotoxicity, hypertension, and neurotoxicity. The primary dose-limiting adverse effect associated with CsA is nephrotoxicity, typically manifested as a reversible decrease in the glomerular filtration rate (Shen et al., 2010). In comparison to CsA, tacrolimus offers greater potency and a more favorable side-effect profile, leading to increased long-term survival in patients (Yang, 2010). Despite its therapeutic efficacy, tacrolimus has a narrow therapeutic window (5–20 ng/mL whole blood 10–12 h post-dose) and frequently displays episodes of toxicity, such as nephrotoxicity, neurotoxicity, and glucose intolerance (Chow et al., 1997). For this reason, therapeutic drug monitoring is highly recommended, and whole blood concentration has been selected as the gold standard pharmacokinetic parameter. As mentioned, immunosuppressive drugs, after their administration in the clinical practice, show the highest blood-to-plasma ratio, owing to an extensive spontaneous binding to RBCs. It is worth noting that these immunophilins are highly expressed in native RBCs, and this confers, to the respective drug, high RBC partitioning. Indeed, more than 70% of CsA binds to erythrocytes at concentrations ranging from 50 to 1,000 ng/mL. The cytosolic form of CsA is specifically bound to the erythrocyte peptidyl–prolyl cis–trans isomerase cyclophilin A (Malaekeh-Nikouei and Davies, 2009). The overall binding capacity of CsA to red blood cells (RBCs) is approximately 43×10^5 nmol per 10^6 RBCs (Malaekeh-Nikouei and Davies, 2009; Sander and Holm, 2009) equivalent to 2 μg CsA/mL in a suspension of RBCs at 40% hematocrit. Notably, FK506 exhibits even higher partitioning into RBCs. In blood, approximately 85% of FK506 associates with erythrocytes, followed by plasma (14%) and lymphocytes (0.46%) (Kim et al., 2008). This elevated RBC fraction is attributed to the presence of at least two types of immunophilins in erythrocytes, binding the drug with really high affinity. Immunophilins are a highly conserved family of proteins with a *cis–trans* peptidyl–prolyl isomerase activity sharing the ability to bind immunosuppressive drugs (Corcoran, 2009). Cyclophilin A was originally discovered as a specific CsA-binding protein, while FK506-binding proteins (FKBPs) as tacrolimus, also known as FK506-binding proteins (Czogalla, 2009; Fukata et al., 2011). In particular, FKBP12 is a 12-kDa cytosolic protein with peptidyl–prolyl *cis–trans* isomerase activity, while FKBP-13 is a 13-kDa membrane-associated protein with 43% amino acid identity with FKBP12 (Lai et al., 2010). A saturable binding capacity has also been calculated for FK506 and amounted to 440 ng/mL of blood (Kim et al., 2008). Furthermore, similar to CsA, FK506 exhibits considerable variability in its pharmacokinetic profile among patients. Consequently, the pharmacokinetics of immunosuppressive drugs heavily relies on their interaction with red cell immunophilins. Additionally, the tolerability of these drugs is influenced by the fraction that is unbound in plasma as the portion transported by red cells does not induce toxic side effects.

Another class of immunosuppressant is represented by the serine/threonine kinase inhibitor; they do not inhibit calcineurin but act by inhibiting mTOR kinase (Mika and Stepnowski, 2016). Sirolimus (rapamycin) is the most representative of this class; chemically, it is a 31-membered macrolide that competes with FK-506 due to the great similarity of their chemical structure. Identically to FK-506, it forms a complex with the cytosolic protein FKBP. However, it establishes a ternary complex involving the pivotal serine/threonine kinase mTOR (mammalian target of rapamycin). Similar to FK-506, sirolimus has a high affinity for erythrocytes, thanks to the presence of high FKBP expression; RBC partitioning reaches 95% of the whole drug concentration (Yatscoff et al., 1995). Hence, the establishment of therapeutic monitoring protocols for the drug is mandatory, and whole blood is the preferred matrix (Figure 2).

2.1.2 Chemotherapeutics

Chemotherapeutic agents undergo oral and parenteral administration and are carried to various tissues via the bloodstream, partitioning into plasma water, plasma proteins, or cells. Red blood cells may be involved in anthracyclines, ifosfamide and its metabolites, topoisomerase I and I/II inhibitor storage, transport, and metabolism. RBCs vehicle these drug molecules to the tumor tissues and release them through different active or passive transport mechanisms. For example, among these classes of anti-tumor drugs that can spontaneously partition into RBCs, there are doxorubicin and daunorubicin. Studies both in patients and rats demonstrated that almost 50% of doxorubicin can be found in the RBC compartment after intravenous administration (Colombo et al., 1981; De Flora et al., 1986). Moreover, when increasing the administered drug dose, the RBC-bound doxorubicin concentration increases, suggesting that their storage capacity is even higher. After partitioning, this drug is released by the RLIP76 transporter, a carrier specialized in the cytotoxic agents' elimination (Schrijvers, 2003). In addition, daunorubicin, another anthracycline drug used in the treatment of solid and liquid cancers, can be found together with its metabolites in RBCs after intravenous administration (Lachâtre et al., 2000). Lastly, the erythrocyte importance in the mercaptopurine transport and metabolism has been demonstrated. Indeed, the mercaptopurine concentration within RBCs has been proven to have a prognostic value in the treatment of childhood acute lymphoblastic leukemia (Schrijvers, 2003). These native features have been widely exploited for drug engineering and will be further analyzed in the following paragraphs.

2.1.3 Metformin

Metformin, an FDA-approved antidiabetic agent, is broadly used every day for the first-line treatment of type 2 diabetes mellitus, even if its therapeutic action is still not well-defined. Remarkably, metformin demonstrated immunomodulatory features in pathological contexts, including cancer, hyper-inflammatory diseases, and infectious disease, and its potential use for other medical conditions is currently being investigated in many clinical trials (Foretz et al., 2023). Recently, its role in hematological tumors has been evaluated, showing that metformin action in lymphomas can be related to glucose metabolism (Bagaloni et al., 2021). Considering drug partitioning, metformin shows a high blood-to-plasma ratio (>10 at C min) in humans; thus, erythrocytes are considered a key distributional compartment for this drug molecule. However, the literature is currently lacking in metformin's intrinsic *in vitro* B/*p* values. Xie F. et al. emphasized on different drug partitioning blood cells in a dynamic *in vivo* system and static *in vitro* values, especially when repartitioning from blood cells is slower than drug clearance in plasma (Xie et al., 2015). These data reveal that the clinical terminal half-life of metformin in plasma (6 h) is three- to four-fold shorter than its half-life in whole blood (18 h) and RBCs (23 h). Despite this, more demonstrative results are still needed.

2.1.4 Berberine

Berberine (BBR) is a naturally occurring benzylisoquinoline alkaloid widely used in traditional Chinese medicine (Ai et al., 2021) and characterized by low concentration and high tissue distribution. Unfortunately, most pharmacokinetic research has focused on the drug's concentration in plasma, making a deep knowledge of its pharmacokinetic process difficult. Yu K. et al. investigated how berberine interacts with RBCs and how it is combined with hemoglobin (Yu et al., 2022). The results indicated that berberine was more concentrated in RBCs than in plasma and the maximum concentration of drug loading was 0.185 g/mL, while higher concentrations have been associated with hemolysis. Actually, co-incubation of berberine and RBCs induced the internalization of the RBC membrane and intracellular vacuole development (Yu et al., 2022). Both *in vitro* and *in silico* findings showed that berberine had a binding affinity for bovine Hb and altered the molecular environment of Hb residues, such as tryptophan and tyrosine, changing the conformation of its secondary and tertiary structures. Molecular docking demonstrated a hydrogen bond-based interaction between berberine and Arg-141 residue, whereas molecular dynamics simulation proposed the establishment of a stable conformation (Wang et al., 2007). Considering all these data together, it is reasonable to assume the existence of an RBC-Hb self-assembly system and a spontaneous system of drug release by RBCs after oral or intravenous administration of this drug, which provided a new understanding of the discrepancy between the high tissue concentration and extremely low plasma concentration of berberine.

2.1.5 Benzodiazepines

Benzodiazepines are among the new psychoactive substances (NPS) that are recently emerging in large numbers. To completely understand their potential benefits and side effects, information about their pharmacological features is necessary. One parameter which is still undescribed is the B/P ratio. Manchester et al. (2022) used gas chromatography tandem to mass spectrometry to determine the blood-to-plasma ratio for the following benzodiazepines: deschloroetizolam, diclazepam, etizolam, meclonazepam, phenazepam, and pyrazolam (Manchester et al., 2022). The results reported various ranges of blood-to-plasma ratios, some of which significantly differ from those found in the literature. As a result, it is incorrect to presume that blood-to-plasma ratios are always assumed to be 1.0 or equivalent to those of other species when they are unknown; instead, they must be determined. It is necessary to determine pharmacodynamics, i.e., the binding affinity to the GABA receptor, as well.

2.1.6 Topiramate

Topiramate is an antiepileptic drug that acts through the inhibition of isoenzymes of carbonic anhydrase (CA). CA-I and CA-II are significantly present in RBCs and, for this reason, may influence the drug pharmacokinetics. Shank RP et al. demonstrated the topiramate linearity of the pharmacokinetics in plasma, while its clearance from whole blood seemed to increase with escalating doses (Shank et al., 2005). In contrast, as the topiramate concentration increased, the B/P ratio decreased from 8 to 2, suggesting a significant and saturable topiramate-RBC binding. Additionally, the kinetic parameter analysis indicated that the overall binding of topiramate could be due to RBC CA-I and CA-II. Consequently, RBCs may function as a reservoir for topiramate, mitigating its loss through clearance from plasma.

3 How we can take advantage in converting RBCs into a drug carrier or improving the delivery of physiological molecules

As is often the case, engineering mimics certain processes that occur spontaneously in nature. For example, many of the cases reported above showed the spontaneous binding of drugs to RBC-binding proteins. However, this binding capacity is usually saturable, owing to the saturation of the available binding sites in the proteins. To overcome this issue, some engineering processes envisage the loading of said binding proteins in order to increase the binding capacity of RBCs. In other cases, the strategy encompasses the engineering of enzymes so as to modify some key metabolites and, thus, modify oxygen release and/or other metabolites.

3.1 Inositol hexaphosphate and oxygen release

As stated above, hemoglobin is the major component of the RBCs and is responsible for oxygen delivery to all tissues of the body. Hemoglobin has a high affinity for oxygen that is physiologically affected by temperature, hydrogen ions, carbon dioxide, and intraerythrocyte 2,3-bisphosphoglycerate (2,3-BPG). Furthermore, a physiological change in hemoglobin affinity for oxygen favors oxygen binding in the lung and oxygen release to peripheral tissues. Based on these simple observations and other experiments, a decrease in O_2 affinity was observed to enhance tissue O_2 delivery (Lenfant et al., 1968). In attempts to produce erythrocytes with a lower oxygen affinity to be administered in a patient in need when normal blood flow is impaired, inositol hexaphosphate (InsP6)-loaded erythrocytes were prepared and investigated (Teisseire et al., 1985). InsP6 cannot diffuse through the erythrocytes' membrane and is the most effective Hb allosteric effector (Benesch et al., 1977), even a thousand times more effective than 2,3-BPG. InsP6 was incorporated into erythrocytes by using a reversed osmotic-lysis process (Ropars et al., 1985) and shown to be effective in mini pig animal models and in sickle transgenic mice (Bourgeaux et al., 2012).

Although these and other data support the possible use of inositol hexaphosphate-loaded erythrocytes as effective treatments to improve the delivery of O_2 to tissues in need, there is an ongoing debate about the advantages of higher or lower hemoglobin–oxygen affinity in humans, particularly during hypoxia (Webb et al., 2021) that require further investigations.

3.2 Engineering RBC metabolism and storage conditions

During their storage at refrigerated temperatures, red blood cells go through several biochemical and morphological modifications known as "storage lesion." Indeed, during this period, 2,3-BPG and other high-energy phosphate compounds gradually decrease because of the reduced glycolytic activity at 1°C–6°C storage temperatures, the acidification of the intracellular pH, and the reversible and irreversible oxidation of the active site of rate-limiting glycolytic enzymes, such as glyceraldehyde 3-phosphate dehydrogenase.

2,3-Bisphosphoglycerate (2,3-BPG) is an intermediate metabolite present in high concentrations in RBCs (approximately 5 mM) and is the principal allosteric effector for hemoglobin (that is present at almost the same concentration as a tetramer), decreasing its affinity for oxygen. During storage conditions, the erythrocyte 2,3-BPG concentration decreases, which impacts the oxygen dissociation curve by shifting it to the left. This means that the oxygen delivery to tissues is reduced. In an attempt to overcome this problem, a number of additives have been proposed to extend 2,3-BPG preservation for weeks. Other authors have suggested that 2,3-BPG preservation should be obtained by modifying red cell metabolism through inhibition of key glycolytic enzymes (Vora, 1987; Beutler et al., 1995). The rationale for this approach is based on observations that patients who have pyruvate kinase deficiency have higher-than-normal levels of 2,3-BPG, while hexokinase-deficient patients have below-normal levels. Several years ago in our laboratory, we confirmed this assumption by loading human RBCs with hexokinase-inactivating antibodies (Magnani et al., 1989). RBCs loaded with these antibodies showed only 20% residual activity and lactate production was only 30% of controls, while the hexose monophosphate pathway was normal under basic conditions but only 12% of controls if the cell was stimulated by the addition of methylene blue. These cells were not able to maintain *in vitro* normal ATP and 2,3-BPG concentrations. In contrast, if RBCs were loaded with human hexokinase, they showed a doubled glycolytic activity, a normal hexose monophosphate pathway, and normal ATP and 2,3-BPG concentrations (Magnani et al., 1988). Storage at 4°C of these cells showed that 2,3-BPG was normal and ATP slightly decreased, proving that encapsulation of key glycolytic enzymes can provide a new way to maintain functionally active RBCs and prevent the loss of the most important hemoglobin effector (2,3-BPG) for several weeks (Magnani et al., 1989).

Furthermore, as the 2,3-BPG concentration decreases and hemoglobin affinity for O_2 increases, there is also an accumulation of reactive species of oxygen (ROS) due to the impaired RBCs' antioxidant capability (Yoshida et al., 2019). So, RBCs cannot face oxidative stress because of the insufficient glutathione synthesis and the inefficient pentose phosphate pathway to produce NADPH, which leads to the irreversible oxidation of key structural and functional proteins such as hemoglobin, band 3, and peroxiredoxin 2 (Bayer et al., 2015; Wither et al., 2016; Reisz et al., 2018). Some studies have exploited some new storage strategies to prevent RBC senescence, which may affect the transfusion efficiency and clinical implications including increased complications and mortality (Jones et al., 2019; Rogers et al., 2021). It was demonstrated that the supplementation of RBCs stored with uric acid and ascorbic acid, both antioxidant molecules, reduces oxidative damage and induces GSH synthesis (Tzounakas et al., 2022; Anastasiadi et al., 2023). Furthermore, washing stored RBCs with PBS seems to reduce senescence pathways, phosphatidylserine and band-3 exposure, and membrane fragility (Pulliam et al., 2021). D'Alessandro et al. proved that hypoxic storage conditions improved 2,3-BPG and GSH synthesis, and ameliorated redox metabolism (D'Alessandro et al., 2020). Moreover, donor selection could influence the

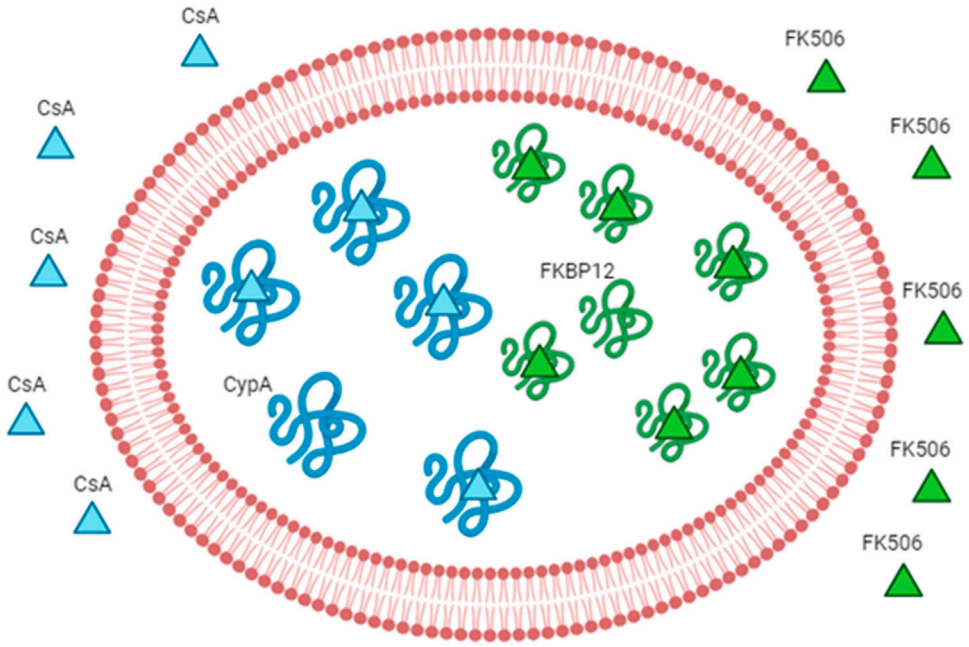

FIGURE 3
Engineered RBCs as immunophilin carriers. The figure schematizes how we can increase the drug-binding capacity of RBCs by increasing the concentration of the intracellular receptor (binding site). The example of immunosuppressants and immunophilins is given as a proof-of-concept. The immunophilin FKBP12 is known to bind to the immunosuppressant FK506 (also known as tacrolimus); thus, the overloading of the recombinant protein FKBP12 can increase the affinity for the same drug. The overloading of cyclophilin A can increase the affinity for cyclosporine A. Abbreviation in the figure: FKBP12, FK506-binding protein; CypA, cyclophilin A; CsA, cyclosporine A.

transfusion efficiency. For example, the enrollment of G6PD deficiency donors might result in increased hemolysis, mechanical fragility, and ROS accumulation after the transfusion, even if their adjustment to oxidative stress could make them better recipients of RBCs long-stored rather than donors (García-Roa et al., 2017; Putter and Seghatchian, 2017).

3.3 Immunophilin-loaded RBCs

Biagiotti et al. first reported the pioneering use of engineered RBCs overloaded with cyclophilin A or FKBP12 as the drug delivery system for CsA or FKBP12, respectively (Biagiotti et al., 2011). As they can be spontaneously recruited into RBCs, our strategy is designed to increment the FK506 or CsA's levels in RBCs by the augmentation of the cytosolic concentration of FKBP12 or cyclophilin A, respectively (Figure 3). In order to do that, recombinant FKBP12 and cyclophilin A were produced. Furthermore, a new approach is intended to enhance the FK506/CsA amount carried by erythrocytes. This involves recombinant forms of human FKBP12 and cyclophilin A loaded into RBCs through a process of hypotonic dialysis and isotonic resealing. Thus, engineered RBCs have the capacity to bind up to an order of magnitude more drugs than their native counterparts. In summary, our findings suggest that diffusible immunosuppressants could be sequestered into red blood cells by loading the respective target proteins. This proposes the potential use of immunophilin-loaded RBCs as a promising delivery system for immunosuppressive agents.

Moreover, a patent application has been filed by Magnani et al. (2010). The patent suggests two different uses of immunophilin-loaded RBCs: the first one proposes the loaded-RBC reinfusion into patients in need of immunosuppressive drugs after their *ex vivo* incubation with the drug of interest. In this way, the drug is not freely administrated, and the carriers slowly release the drug in circulation, which could eventually bind endogenous immunophilins. In contrast, according to the second modality, the patient will receive, first, the immunophilin-loaded red blood cells that can remain in circulation for months and then the drug (in any administration way). Thus, a significant portion of free drugs will be carried preferentially by the engineered cells due to their higher affinity. Both strategies are used in treating patients in need of immunosuppressive therapy, but which one is better in pharmacokinetics is still not known. However, the initial administration of immunophilin-loaded erythrocytes should coincide with the erythrocytes' binding capacity saturation time with the selected drug. Once in circulation, the loaded erythrocytes will release the captured drug. Given their prolonged stay in circulation, they may also bind and transport other immunosuppressive drugs circulating in the system. In a further application, the patient's RBCs could be loaded with more than one immunophilin simultaneously (i.e., FKBP12 and cyclophilin A), either separately or in combination with the same RBC. This approach aims to increase the quantity of immunosuppressive

drugs administered to a patient without inducing pharmacological side effects.

The abovementioned example is potentially applicable to all human "druggable" proteins, that is, proteins that have been demonstrated to be able to bind a drug. The primary limiting step seems to lie in obtaining the recombinant forms of the selected proteins, produced under Good Manufacturing Practice (GMP) conditions and at a reasonable cost. According to the literature, single-protein domains or a combination thereof, can be exploited to create engineered RBCs to bind and transport all necessary drugs to a patient. Moreover, since the drug's rate of dissociation from its protein-binding partner is determined by the protein's affinity for the drug of choice, it may, one day, be possible to modify the specific site of the protein so that the drug would be released at a predetermined rate, maintaining the proper concentration of free drug in the bloodstream. Hence, by taking advantage of the potential erythrocytes loading with specific drug-binding proteins, then we will have new means to administer almost all drugs in patients.

3.4 RBC-mediated delivery of anti-tumor drugs

Anthracycline antibiotics are effective anti-cancer agents widely used for the treatment of different cancer diseases. Given that their high toxicity may provoke serious side effects, researchers are proposing different ways to reduce their toxicity without decreasing their efficacy. One of them is to extend the time of the drug in the bloodstream so that its dosage can be reduced. So, clinical studies evaluated the pharmacokinetics of RBC-bound daunorubicin and doxorubicin, in patients with acute leukemia and lymphoma, respectively. The results will be summarized in the following sections.

3.4.1 Erythrocyte-bound daunorubicin

Pharmacokinetics of erythrocyte-bound daunorubicin (EBD) has been evaluated in 14 patients with acute leukemia, after the drug's loading into RBCs (Skorokhod et al., 2004). Daunorubicin-loaded RBCs were prepared in order to have a final dose of 45 or 60 mg/m^2 of the patient body surface, and the erythrocytes' deformability was not affected during the EBD preparation. The results highlighted an increase in the average plasma and blood daunorubicin concentrations for the EBD compared to its standard free form, during the chemotherapy course. Moreover, EBD was better tolerated by patients, and in nine of them, side effects were uncommon, unlike those treated with the free form of daunorubicin. Although the primary purpose of this study was not to assess the antileukemic efficacy of EBD, it is worth mentioning that remission was achieved in eight out of 10 patients who received three infusions. Hence, the clinical application of daunorubicin-loaded red blood cells looks bright.

3.4.2 Erythrocyte-bound doxorubicin

Intact RBCs can naturally bind anthracycline antibiotics in isotonic media (Kravtzoff et al., 1990; Ataullakhanov et al., 1992). Despite that, this binding is weak, so anthracycline antibiotics need to be immobilized by the use of glutaraldehyde (Ataullakhanov et al., 1994; Skorokhod et al., 2004). The use of engineered doxorubicin-loaded erythrocytes (DLEs) increased the drug's presence in the bloodstream and facilitated its targeted delivery to the spleen, liver, and lungs, thereby reducing the doxorubicin load on other organs (Zocchi et al., 1989; Tonetti et al., 1990). Yet, glutaraldehyde treatment likely induced an unpredictable variation in antibiotic toxicity, and the DLE efficacy seems to be independent of the solidity of the binding between antibiotics and cells. Hence, DLE prepared without glutaraldehyde pharmacokinetics was evaluated in patients with lymphoproliferative disorders (Tonetti et al., 1992; Ataullakhanov et al., 1997). DLEs were set up to achieve a final dose of 25 or 50 mg/m^2 post-infusion. The mixture was incubated at 37°C for 60 min and then infused into patients immediately thereafter. Compared to the standard administration of doxorubicin, the concentration over time of DLE administration was approximately five-fold higher for blood and six-fold higher for plasma (Ataullakhanov et al., 1997). Furthermore, DLE was well-tolerated in patients as neither prolonged or severe myelosuppression was observed nor evidence of cardiotoxicity was seen. Once more, these results refer to the delivery of anthracycline antibiotics through erythrocytes as a promising tumor treatment.

More recently, Lucas et al. submitted a methodology for the synthesis of DOX-loaded red blood cells (RBC-DOX) through electrophoresis (Lucas et al., 2019). The strategy has been tested both in *in vitro* models and in preclinical models, manifesting the faculty of RBCs to carry higher doses of DOX and limit cardiac toxicity with superior antitumorigenic effects.

3.5 Conclusion

In conclusion, human RBCs are not only hemoglobin-containing bags involved in gas exchanges but may have great importance in drug transport. This opens the way to two fields of investigation. On one hand, being that RBC partitioning has an enormous impact on drug pharmacokinetics, clinicians must take into account the therapeutic drug monitoring in whole blood for those drugs showing a high blood-to-plasma ratio. On the other hand, biomedical researchers can set up innovative strategies that are aimed at increasing the RBC power to bind and transport selected drugs by exploiting some of their natural features.

Author contributions

SB: conceptualization, visualization, and writing–original manuscript. EP: data curation and writing–original manuscript. MM: conceptualization, supervision, validation, and writing–review and editing.

Funding

The author(s) declare financial support was received for the research, authorship, and/or publication of this article. This work has been funded by the European Union—NextGenerationEU—under the Italian Ministry of University and Research (MUR) National Innovation Ecosystem grant ECS00000041—VITALITY—CUP [H33C22000430006].

Conflict of interest

The authors declare that the research was conducted in the absence of any commercial or financial relationships that could be construed as a potential conflict of interest.

The author(s) declared that they were an editorial board member of Frontiers, at the time of submission. This had no impact on the peer review process and the final decision.

Publisher's note

References

Ai, X., Yu, P., Peng, L., Luo, L., Liu, J., Li, S., et al. (2021). Berberine: a review of its pharmacokinetics properties and therapeutic potentials in diverse vascular diseases. *Front. Pharmacol.* 12, 762654. doi:10.3389/fphar.2021.762654

Anastasiadi, A. T., Stamoulis, K., Papageorgiou, E. G., Lelli, V., Rinalducci, S., Papassideri, I. S., et al. (2023). The time-course linkage between hemolysis, redox, and metabolic parameters during red blood cell storage with or without uric acid and ascorbic acid supplementation. *Front. Aging* 4, 1161565. doi:10.3389/fragi.2023.1161565

Ataullakhanov, F. I., Batasheva, T. V., and Vitvitskii, V. M. (1994). Effect of temperature, daunorubicin concentration and suspension hematocrit on daunorubicin binding by human erythrocytes. *Antibiot. Khimioter* 39 (9-10), 26–29.

Ataullakhanov, F. I., Isaev, V. G., Kohno, A. V., Kulikova, E. V., Parovichnikova, E. N., Savchenko, V. G., et al. (1997). Pharmacokinetics of doxorubicin in patients with lymphoproliferative disorders after infusion of doxorubicin-loaded erythrocytes. *Erythrocytes as Drug Carriers Med.*, 137–142. doi:10.1007/978-1-4899-0044-9_18

Ataullakhanov, F. I., Vitvitsky, V. M., Kovaleva, V. L., and Mironova, S. B. (1992). Rubomycin loaded erythrocytes in the treatment of mouse tumor P388. *Adv. Exp. Med. Biol.* 326, 209–213. doi:10.1007/978-1-4615-3030-5_26

Bagaloni, I., Visani, A., Biagiotti, S., Ruzzo, A., Navari, M., Etebari, M., et al. (2021). Metabolic switch and cytotoxic effect of metformin on burkitt lymphoma. *Front. Oncol.* 11, 661102. doi:10.3389/fonc.2021.661102

Bayer, S. B., Hampton, M. B., and Winterbourn, C. C. (2015). Accumulation of oxidized peroxiredoxin 2 in red blood cells and its prevention. *Transfusion* 55 (8), 1909–1918. doi:10.1111/trf.13039

Benesch, R. E., Edalji, R., and Benesch, R. (1977). Reciprocal interaction of hemoglobin with oxygen and protons. The influence of allosteric polyanions. *Biochemistry* 16 (12), 2594–2597. doi:10.1021/bi00631a003

Beutler, E., Lichtman, M. A., Coller, B. S., and Kipos, T. J. (1995). *Williams hematology*.

Biagiotti, S., Abbas, F., Montanari, M., Barattini, C., Rossi, L., Magnani, M., et al. (2023). Extracellular vesicles as new players in drug delivery: a focus on red blood cells-derived EVs. *Pharmaceutics* 15 (2), 365. doi:10.3390/pharmaceutics15020365

Biagiotti, S., Rossi, L., Bianchi, M., Giacomini, E., Pierige, F., Serafini, G., et al. (2011). Immunophilin-loaded erythrocytes as a new delivery strategy for immunosuppressive drugs. *J. Control Release* 154 (3), 306–313. doi:10.1016/j.jconrel.2011.05.024

Bourgeaux, V., Aufradet, E., Campion, Y., De Souza, G., Horand, F., Bessaad, A., et al. (2012). Efficacy of homologous inositol hexaphosphate-loaded red blood cells in sickle transgenic mice. *Br. J. Haematol.* 157 (3), 357–369. doi:10.1111/j.1365-2141.2012.09077.x

Carnemolla, R., Villa, C. H., Greineder, C. F., Zaitsev, S., Patel, K. R., Kowalska, M. A., et al. (2017). Targeting thrombomodulin to circulating red blood cells augments its protective effects in models of endotoxemia and ischemia-reperfusion injury. *FASEB J.* 31 (2), 761–770. doi:10.1096/fj.201600912R

Chow, F. S., Piekoszewski, W., and Jusko, W. J. (1997). Effect of hematocrit and albumin concentration on hepatic clearance of tacrolimus (FK506) during rabbit liver perfusion. *Drug Metabolism Dispos.* 25 (5), 610–616. doi:10.1016/1043-6618(95)86427-x

Colombo, T., Broggini, M., Garattini, S., and Donelli, M. G. (1981). Differential adriamycin distribution to blood components. *Eur. J. Drug Metabolism Pharmacokinet.* 6 (2), 115–122. doi:10.1007/BF03189477

Corcoran, T. (2009). Aerosol drug delivery in lung transplant recipients. *Expert Opin. Drug Deliv.* 6 (2), 139–148. doi:10.1517/17425250802685332

Czogalla, A. (2009). Oral cyclosporine A - the current picture of its liposomal and other delivery systems. *Cell. Mol. Biol. Lett.* 14 (1), 139–152. doi:10.2478/s11658-008-0041-6

D'Alessandro, A., Yoshida, T., Nestheide, S., Nemkov, T., Stocker, S., Stefanoni, D., et al. (2020). Hypoxic storage of red blood cells improves metabolism and post-transfusion recovery. *Transfusion* 60 (4), 786–798. doi:10.1111/trf.15730

Dash, R. P., Veeravalli, V., Thomas, J. A., Rosenfeld, C., Mehta, N., and Srinivas, N. R. (2021). Whole blood or plasma: what is the ideal matrix for pharmacokinetic-driven drug candidate selection? *Future Med. Chem.* 13 (2), 157–171. doi:10.4155/fmc-2020-0187

De Flora, A., Benatti, U., Guida, L., and Zocchi, E. (1986). Encapsulation of Adriamycin in human erythrocytes. *Proc. Natl. Acad. Sci. U. S. A.* 83 (18), 7029–7033. doi:10.1073/pnas.83.18.7029

Felig, P., Wahren, J., and Raf, L. (1973). Evidence of inter organ amino acid transport by blood cells in humans. *Proc. Natl. Acad. Sci. U. S. A.* 70 (6), 1775–1779. doi:10.1073/pnas.70.6.1775

Ferguson, L. T., Hood, E. D., Shuvaeva, T., Shuvaev, V. V., Basil, M. C., Wang, Z., et al. (2022). Dual affinity to RBCs and target cells (DART) enhances both organ- and cell type-targeting of intravascular nanocarriers. *ACS Nano* 16 (3), 4666–4683. doi:10.1021/acsnano.1c11374

Foretz, M., Guigas, B., and Viollet, B. (2023). Metformin: update on mechanisms of action and repurposing potential. *Nat. Rev. Endocrinol.* 19 (8), 460–476. doi:10.1038/s41574-023-00833-4

Fukata, N., Uchida, K., Kusuda, T., Koyabu, M., Miyoshi, H., Fukui, T., et al. (2011). The effective therapy of cyclosporine A with drug delivery system in experimental colitis. *J. Drug Target* 19 (6), 458–467. doi:10.3109/1061186X.2010.511224

García-Roa, M., Del Carmen Vicente-Ayuso, M., Bobes, A. M., Pedraza, A. C., González-Fernández, A., Martín, M. P., et al. (2017). Red blood cell storage time and transfusion: current practice, concerns and future perspectives. *Blood Transfus.* 15 (3), 222–231. doi:10.2450/2017.0345-16

Glassman, P. M., Villa, C. H., Marcos-Contreras, O. A., Hood, E. D., Walsh, L. R., Greineder, C. F., et al. (2022). Targeted *in vivo* loading of red blood cells markedly prolongs nanocarrier circulation. *Bioconjugate Chem.* 33 (7), 1286–1294. doi:10.1021/acs.bioconjchem.2c00196

Glassman, P. M., Villa, C. H., Ukidve, A., Zhao, Z., Smith, P., Mitragotri, S., et al. (2020). Vascular drug delivery using carrier red blood cells: focus on RBC surface loading and pharmacokinetics. *Pharmaceutics* 12 (5), 440. doi:10.3390/pharmaceutics12050440

Helms, C. C., Gladwin, M. T., and Kim-Shapiro, D. B. (2018). Erythrocytes and vascular function: oxygen and nitric oxide. *Front. Physiology* 9 (2), 125. doi:10.3389/fphys.2018.00125

Highley, M. S., and De Brujin, E. A. (1996). Erythrocytes and the transport of drugs and endogenous compounds. *Pharm. Res.* 13, 186–195. doi:10.1023/a:1016074627293

Hinderling, P. H. (1997). Red blood cells: a neglected compartment in pharmacokinetics and pharmacodynamics. *Pharmacol. Rev.* 49 (3), 279–295.

Hsia, C. C. W. (1998). Respiratory function of hemoglobin. *N. Engl. J. Med.* 338 (4), 239–247. doi:10.1056/NEJM199801223380407

Jones, A. R., Patel, R. P., Marques, M. B., Donnelly, J. P., Griffin, R. L., Pittet, J. F., et al. (2019). Older blood is associated with increased mortality and adverse events in massively transfused trauma patients: secondary analysis of the PROPPR trial. *Ann. Emerg. Med.* 73 (6), 650–661. doi:10.1016/j.annemergmed.2018.09.033

Kim, J., Chung, K. H., Lee, C. M., Seo, Y. S., Song, H. C., and Lee, K. Y. (2008). Lymphatic delivery of 99mTc-labeled dextran acetate particles including cyclosporine A. *J. Microbiol. Biotechnol.* 18 (9), 1599–1605.

Kirk, K. (2001). Membrane transport in the malaria-infected erythrocyte. *Physiol. Rev.* 81 (2), 495–537. doi:10.1152/physrev.2001.81.2.495

Kravtzoff, R., Ropars, C., Laguerre, M., Muh, J. P., and Chassaigne, M. (1990). Erythrocytes as carriers for L-asparaginase - methodological and mouse invivo studies. *J. Pharm. Pharmacol.* 42 (7), 473–476. doi:10.1111/j.2042-7158.1990.tb06598.x

Lachâtre, F., Marquet, P., Ragot, S., Gaulier, J. M., Cardot, P., and Dupuy, J. L. (2000). Simultaneous determination of four anthracyclines and three metabolites in human serum by liquid chromatography-electrospray mass spectrometry. *J. Chromatogr. B Biomed. Sci. Appl.* 738 (2), 281–291. doi:10.1016/s0378-4347(99)00529-0

Lai, J., Lu, Y., Yin, Z., Hu, F., and Wu, W. (2010). Pharmacokinetics and enhanced oral bioavailability in beagle dogs of cyclosporine A encapsulated in glyceryl monooleate/poloxamer 407 cubic nanoparticles. *Int. J. Nanomedicine* 5, 13–23. doi:10.2147/ijn.s8311

Lenfant, C., Torrance, J., English, E., Finch, C. A., Reynafarje, C., Ramos, J., et al. (1968). Effect of altitude on oxygen binding by hemoglobin and on organic phosphate levels. *J. Clin. Invest.* 47 (12), 2652–2656. doi:10.1172/JCI105948

Lucas, A., Lam, D., and Cabrales, P. (2019). Doxorubicin-loaded red blood cells reduced cardiac toxicity and preserved anticancer activity. *Drug Deliv.* 26 (1), 433–442. doi:10.1080/10717544.2019.1591544

Magnani, M., Pierigè, F., and Rossi, L. (2012). Erythrocytes as a novel delivery vehicle for biologics: from enzymes to nucleic acid-based therapeutics. *Ther. Deliv.* 3 (3), 405–414. doi:10.4155/tde.12.6

Magnani, M., Rossi, L., Biagiotti, S., and Bianchi, M. (2010). *Drug delivery systems*. Patent 2763695.

Magnani, M., Rossi, L., Bianchi, M., Fornaini, G., Benatti, U., Guida, L., et al. (1988). Improved metabolic properties of hexokinase-overloaded human erythrocytes. *Biochim. Biophys. Acta* 972 (1), 1–8. doi:10.1016/0167-4889(88)90095-x

Magnani, M., Rossi, L., Bianchi, M., Serafini, G., Zocchi, E., Laguerre, M., et al. (1989). Improved stability of 2,3-bisphosphoglycerate during storage of hexokinase-overloaded erythrocytes. *Biotechnol. Appl. Biochem.* 11 (5), 439–444. doi:10.1111/j.1470-8744.1989.tb00069.x

Malaekeh-Nikouei, B., and Davies, N. (2009). Double loading of cyclosporine A in liposomes using cyclodextrin complexes. *PDA J. Pharm. Sci. Technol.* 63 (2), 139–148.

Manchester, K. R., Waters, L., Haider, S., and Maskell, P. D. (2022). The blood-to-plasma ratio and predicted GABA(A)-binding affinity of designer benzodiazepines. *Forensic Toxicol.* 40 (2), 349–356. doi:10.1007/s11419-022-00616-y

Mika, A., and Stepnowski, P. (2016). Current methods of the analysis of immunosuppressive agents in clinical materials: a review. *J. Pharm. Biomed. Anal.* 127, 207–231. doi:10.1016/j.jpba.2016.01.059

Mikdar, M., González-Menéndez, P., Cai, X., Zhang, Y., Serra, M., Dembele, A. K., et al. (2021). The equilibrative nucleoside transporter ENT1 is critical for nucleotide homeostasis and optimal erythropoiesis. *Blood* 137 (25), 3548–3562. doi:10.1182/blood.2020007281

Murciano, J. C., Higazi, A. A. R., Cines, D. B., and Muzykantov, V. R. (2009). Soluble urokinase receptor conjugated to carrier red blood cells binds latent pro-urokinase and alters its functional profile. *J. Control. Release* 139 (3), 190–196. doi:10.1016/j.jconrel.2009.07.003

Muzykantov, V. R. (2010). Drug delivery by red blood cells: vascular carriers designed by mother nature. *Expert Opin. Drug Deliv.* 7 (4), 403–427. doi:10.1517/17425241003610633

Olver, C. S. (2020). "Erythrocyte structure and function," in *Schalm's veterinary hematology*. Seventh Edition.

Pan, D. C., Myerson, J. W., Brenner, J. S., Patel, P. N., Anselmo, A. C., Mitragotri, S., et al. (2018). Nanoparticle properties modulate their attachment and effect on carrier red blood cells. *Sci. Rep.* 8 (1), 1615. doi:10.1038/s41598-018-19897-8

Pulliam, K. E., Joseph, B., Makley, A. T., Caldwell, C. C., Lentsch, A. B., Goodman, M. D., et al. (2021). Washing packed red blood cells decreases red blood cell storage lesion formation. *Surg. (United States)* 169 (3), 666–670. doi:10.1016/j.surg.2020.07.022

Putter, J. S., and Seghatchian, J. (2017). Cumulative erythrocyte damage in blood storage and relevance to massive transfusions: selective insights into serial morphological and biochemical findings. *Blood Transfus.* 15 (4), 348–356. doi:10.2450/2017.0312-16

Reisz, J. A., Nemkov, T., Dzieciatkowska, M., Culp-Hill, R., Stefanoni, D., Hill, R. C., et al. (2018). Methylation of protein aspartates and deamidated asparagines as a function of blood bank storage and oxidative stress in human red blood cells. *Transfusion* 58 (12), 2978–2991. doi:10.1111/trf.14936

Robert, M., Laperrousaz, B., Piedrahita, D., Gautier, E. F., Nemkov, T., Dupuy, F., et al. (2022). Multiparametric characterization of red blood cell physiology after hypotonic dialysis based drug encapsulation process. *Acta Pharm. Sin. B* 12 (4), 2089–2102. doi:10.1016/j.apsb.2021.10.018

Rogers, S. C., Ge, X., Brummet, M., Lin, X., Timm, D. D., d'Avignon, A., et al. (2021). Quantifying dynamic range in red blood cell energetics: evidence of progressive energy failure during storage. *Transfusion* 61 (5), 1586–1599. doi:10.1111/trf.16395

Ropars, C., Chassaigne, M., Villereal, M. C., Avenard, G., Hurel, C., and Nicolau, C. (1985). Resealed red blood cells as a new blood transfusion product. *Bibl. Haematol.* 51, 82–91. doi:10.1159/000410231

Rossi, L., Fraternale, A., Bianchi, M., and Magnani, M. (2019). Red blood cell membrane processing for biomedical applications. *Front. Physiology* 10, 1070. doi:10.3389/fphys.2019.01070

Sander, C., and Holm, P. (2009). Porous magnesium aluminometasilicate tablets as carrier of a cyclosporine self-emulsifying formulation. *Aaps Pharmscitech* 10 (4), 1388–1395. doi:10.1208/s12249-009-9340-0

Schrijvers, D. (2003). Role of red blood cells in pharmacokinetics of chemotherapeutic agents. *Clin. Pharmacokinet.* 42 (9), 779–791. doi:10.2165/00003088-200342090-00001

Shank, R. P., Doose, D. R., Streeter, A. J., and Bialer, M. (2005). Plasma and whole blood pharmacokinetics of topiramate: the role of carbonic anhydrase. *Epilepsy Res.* 63 (2-3), 103–112. doi:10.1016/j.eplepsyres.2005.01.001

Sharma, R., Singhal, S. S., Cheng, J. Z., Yang, Y. S., Sharma, A., Zimniak, P., et al. (2001). RLIP76 is the major ATP-dependent transporter of glutathione-conjugates and doxorubicin in human erythrocytes. *Archives Biochem. Biophysics* 391 (2), 171–179. doi:10.1006/abbi.2001.2395

Shen, J., Deng, Y. P., Jin, X. F., Ping, Q. N., Su, Z. G., and Li, L. J. (2010). Thiolated nanostructured lipid carriers as a potential ocular drug delivery system for cyclosporine A: improving *in vivo* ocular distribution. *Int. J. Pharm.* 402 (1-2), 248–253. doi:10.1016/j.ijpharm.2010.10.008

Skorokhod, O. A., Garmaeva, T., Vitvitsky, V. M., Isaev, V. G., Parovichnikova, E. N., Savchenko, V. G., et al. (2004). Pharmacokinetics of erythrocyte-bound daunorubicin in patients with acute leukemia. *Med. Sci. Monit.* 10 (4), PI55–64.

Stosik, M., Tokarz-Deptuła, B., Deptuła, J., and Deptuła, W. (2020). Immune functions of erythrocytes in osteichthyes. *Front. Immunol.* 11, 1914. doi:10.3389/fimmu.2020.01914

Teisseire, B. P., Ropars, C., Vallez, M. O., Herigault, R. A., and Nicolau, C. (1985). Physiological effects of high-P50 erythrocyte transfusion on piglets. *J. Appl. Physiol.* 58 (6), 1810–1817. doi:10.1152/jappl.1985.58.6.1810

Tonetti, M., Astroff, B., Satterfield, W., De Flora, A., Benatti, U., and DeLoach, J. R. (1990). Construction and characterization of adriamycin-loaded canine red blood cells as a potential slow delivery system. *Biotechnol. Appl. Biochem.* 12 (6), 621–629. doi:10.1111/j.1470-8744.1990.tb00136.x

Tonetti, M., Zocchi, E., Guida, L., Polvani, C., Benatti, U., Biassoni, P., et al. (1992). Use of glutaraldehyde treated autologous human erythrocytes for hepatic targeting of doxorubicin. *Adv. Exp. Med. Biol.* 326, 307–317. doi:10.1007/978-1-4615-3030-5_37

Tzounakas, V. L., Anastasiadi, A. T., Arvaniti, V. Z., Lelli, V., Fanelli, G., Paronis, E. C., et al. (2022). Supplementation with uric and ascorbic acid protects stored red blood cells through enhancement of non-enzymatic antioxidant activity and metabolic rewiring. *Redox Biol.* 57, 102477. doi:10.1016/j.redox.2022.102477

Villa, C. H., Cines, D. B., Siegel, D. L., and Muzykantov, V. (2017). Erythrocytes as carriers for drug delivery in blood transfusion and beyond. *Transfus. Med. Rev.* 31 (1), 26–35. doi:10.1016/j.tmrv.2016.08.004

Villa, C. H., Pan, D. C., Johnston, I. H., Greineder, C. F., Walsh, L. R., Hood, E. D., et al. (2018). Biocompatible coupling of therapeutic fusion proteins to human erythrocytes. *Blood Adv.* 2 (3), 165–176. doi:10.1182/bloodadvances.2017011734

Vora, S. (1987). Metabolic manipulation of key glycolytic enzymes: a novel proposal for the maintenance of red cell 2,3-DPG and ATP levels during storage. *Biomed. Biochim. Acta* 46 (2-3), S285–S289.

Wang, S., Han, K., Ma, S., Qi, X., Guo, L., and Li, X. (2022). Blood cells as supercarrier systems for advanced drug delivery. *Med. Drug Discov.* 13, 100119. doi:10.1016/j.medidd.2021.100119

Wang, Y. Q., Zhang, H. M., Zhang, G. C., Liu, S. X., Zhou, Q. H., Fei, Z. H., et al. (2007). Studies of the interaction between paraquat and bovine hemoglobin. *Int. J. Biol. Macromol.* 41 (3), 243–250. doi:10.1016/j.ijbiomac.2007.02.011

Webb, K. L., Dominelli, P. B., Baker, S. E., Klassen, S. A., Joyner, M. J., Senefeld, J. W., et al. (2021). Influence of high hemoglobin-oxygen affinity on humans during hypoxia. *Front. Physiol.* 12, 763933. doi:10.3389/fphys.2021.763933

Wither, M., Dzieciatkowska, M., Nemkov, T., Strop, P., D'Alessandro, A., and Hansen, K. C. (2016). Hemoglobin oxidation at functional amino acid residues during routine storage of red blood cells. *Transfusion* 56 (2), 421–426. doi:10.1111/trf.13363

Xie, F., Ke, A. B., Bowers, G. D., and Zamek-Gliszczynski, M. J. (2015). Metformin's intrinsic blood-to-plasma partition ratio (B/P): reconciling the perceived high *in vivo* B/P > 10 with the *in vitro* equilibrium value of unity. *J. Pharmacol. Exp. Ther.* 354 (2), 225–229. doi:10.1124/jpet.115.225698

Yang, S. G. (2010). Biowaiver extension potential and IVIVC for BCS class II drugs by formulation design: case study for cyclosporine self-microemulsifying formulation. *Archives Pharmacal Res.* 33 (11), 1835–1842. doi:10.1007/s12272-010-1116-2

Yatscoff, R. W., Wang, P., Chan, K., Hicks, D., and Zimmerman, J. (1995). Rapamycin: distribution, pharmacokinetics, and therapeutic range investigations. *Ther. Drug Monit.* 17 (6), 666–671. doi:10.1097/00007691-199512000-00020

Yoshida, T., Prudent, M., and D'Alessandro, A. (2019). Red blood cell storage lesion: causes and potential clinical consequences. *Blood Transfus.* 17 (1), 27–52. doi:10.2450/2019.0217-18

Yu, Q., Li, M., Chen, H., Xu, L., Cheng, J., Lin, G., et al. (2022). The discovery of berberine erythrocyte-hemoglobin self-assembly delivery system: a neglected carrier underlying its pharmacokinetics. *Drug Deliv.* 29 (1), 856–870. doi:10.1080/10717544.2022.2036870

Zaitsev, S., Danielyan, K., Murciano, J. C., Ganguly, K., Krasik, T., Taylor, R. P., et al. (2006). Human complement receptor type 1-directed loading of tissue plasminogen activator on circulating erythrocytes for prophylactic fibrinolysis. *Blood* 108 (6), 1895–1902. doi:10.1182/blood-2005-11-012336

Zaitsev, S., Kowalska, M. A., Neyman, M., Carnemolla, R., Tliba, S., Ding, B. S., et al. (2012). Targeting recombinant thrombomodulin fusion protein to red blood cells provides multifaceted thromboprophylaxis. *Blood* 119 (20), 4779–4785. doi:10.1182/blood-2011-12-398149

Zocchi, E., Tonetti, M., Polvani, C., Guida, L., Benatti, U., and De Flora, A. (1989). Encapsulation of doxorubicin in liver-targeted erythrocytes increases the therapeutic index of the drug in a murine metastatic model. *Proc. Natl. Acad. Sci. U. S. A.* 86 (6), 2040–2044. doi:10.1073/pnas.86.6.2040

frontiers | Frontiers in Physiology

TYPE Mini Review
PUBLISHED 18 December 2023
DOI 10.3389/fphys.2023.1324463

OPEN ACCESS

EDITED BY
Anna Bogdanova,
University of Zurich, Switzerland

REVIEWED BY
Emeric Stauffer,
Hospices Civils de Lyon, France

*CORRESPONDENCE
Camille Roussel,
camille.roussel@inserm.fr

†These authors have contributed equally to this work

RECEIVED 19 October 2023
ACCEPTED 22 November 2023
PUBLISHED 18 December 2023

CITATION
Dumas L, Roussel C and Buffet P (2023), Intra-erythrocytic vacuoles in asplenic patients: elusive genesis and original clearance of unique organelles. *Front. Physiol.* 14:1324463. doi: 10.3389/fphys.2023.1324463

Intra-erythrocytic vacuoles in asplenic patients: elusive genesis and original clearance of unique organelles

Lucie Dumas[1,2], Camille Roussel[1,2,3*†] and Pierre Buffet[1,2,4†]

[1]Université Paris Cité and Université des Antilles, Inserm, Biologie Tissulaire du Globule Rouge, Paris, France, [2]Laboratoire d'Excellence GR-Ex, Paris, France, [3]Laboratoire d'Hématologie, Hôpital Universitaire Necker Enfants Malades, Assistance Publique–Hôpitaux de Paris (AP-HP), Paris, France, [4]Université Paris Cité, Service de Maladies Infectieuses et Tropicales Hôpital Universitaire Necker Enfants Malades, Assistance Publique–Hôpitaux de Paris (AP-HP), IHU Imagine, Paris, France

The spleen plays a dual role of immune response and the filtration of red blood cells (RBC), the latter function being performed within the unique microcirculatory architecture of the red pulp. The red pulp filters and eliminates senescent and pathological RBC and can expell intra-erythrocytic rigid bodies through the so-called pitting mechanism. The loss of splenic function increases the risk of infections, thromboembolism, and hematological malignancies. However, current diagnostic tests such as quantification of Howell-Jolly Bodies and splenic scintigraphy lack sensitivity or are logistically demanding. Although not widely available in medical practice, the quantification of RBC containing vacuoles, i.e., pocked RBC, is a highly sensitive and specific marker for hyposplenism. The peripheral blood of hypo/asplenic individuals contains up to 80% RBC with vacuoles, whereas these pocked RBC account for less than 4% of RBC in healthy subjects. Despite their value as a spleen function test, intraerythrocytic vacuoles have received relatively limited attention so far, and little is known about their origin, content, and clearance. We provide an overview of the current knowledge regarding possible origins and mechanisms of elimination, as well as the potential function of these unique and original organelles observed in otherwise "empty" mature RBC. We highlight the need for further research on pocked RBC, particularly regarding their potential function and specific markers for easy counting and sorting, which are prerequisites for functional studies and wider application in medical practice.

KEYWORDS

spleen, hyposplenism, asplenia, red blood cell, pocked RBC, pitted RBC, vacuoles

Introduction

The spleen displays a dual immunologic and cell filtering function, and its parenchyma contains white pulp and red pulp. The marginal/perifollicular zone lies in between and likely connects these distinct functions. The white pulp and the marginal/perifollicular zone initiate the innate and adaptative immune responses. The latter traps and removes blood-borne antigens from the circulation. Based on a unique microvasculature architecture, the red pulp eliminates intact RBC (culling mechanism), ghosts, or small cellular components (pitting mechanism). Pitting is a

spleen-specific process whereby intra-erythrocyte rigid bodies (i.e., Howell Jolly bodies, Pappenheimer bodies, dead malaria parasites, or intraerythrocytic vacuoles, Figure 1; Howell, 1890, Pappenheimer et al., 1945, Jauréguiberry et al., 2014, Box 1) are expelled from the RBC without lysis. These spleen functions can be partially or totally impaired, leading to hyposplenism or asplenia, respectively. The main cause of asplenia is splenectomy which is mainly performed for traumatic spleen injury, pancreatic cancer, hematologic malignancy, or inherited or auto-immune hematologic diseases. The main medical conditions that lead to a partial or complete loss of splenic function are sickle cell disease (SCD), celiac and inflammatory bowel diseases, and auto-immune disorders (William and Corazza, 2007; Corazza et al., 1982). The loss of splenic function is associated with an increased risk of infections with encapsulated bacteria (including the rare but very severe Overwhelming Post-Splenectomy Infection Syndrome) and a higher incidence of thromboembolism and cancer (Kristinsson et al., 2014). Reference methods to measure spleen filtering function are splenic scintigraphy and quantification of Howell Jolly Bodies (HJB). Scintigraphy requires the infusion of (mildly) radioactive material and is expensive. Results are semi-quantitative and few patients/guardians now accept this procedure. The quantification of HJB (that are DNA-containing intra-erythrocytic bodies) (Felka et al., 2007) is performed on venous blood and is also semi-quantitative. It lacks sensitivity,

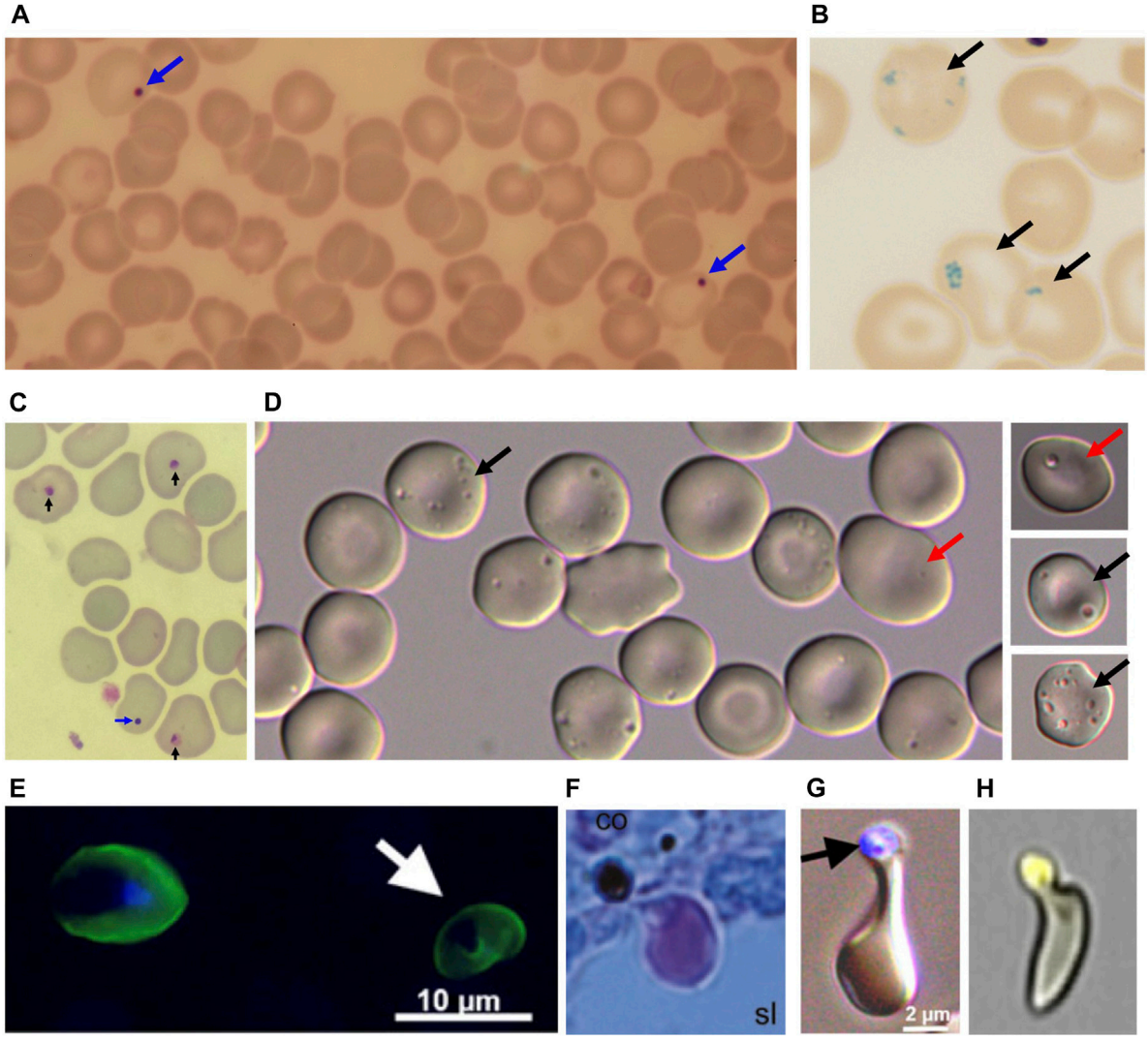

FIGURE 1
(A) Blue arrows: Howell Jolly Bodies (HJB) following Giemsa coloration. **(B)** Dark arrows: Pappenheimer bodies after Prussian blue coloration. **(C)** Blue arrow: HJB, Dark arrows: dead malaria parasites after Giemsa coloration. **(D)** pocked RBC with one vacuole (dark arrows) or multiple vacuoles (red arrows). **(E)** Left: Plasmodium falciparum-infected RBC by epifluorescence, visualized by anti-Resa antibody, staining the plasma membrane, and the DNA marker DAPI staining the intracellular parasite nucleus. Right (White arrow): Once-infected RBC stained by the anti-Resa antibody, from which the parasite has been expelled by pitting, hence the absence of DAPI staining. **(F)**. P. falciparum-infected RBC, pre-exposed to artesunate before perfusion ex-vivo in a human spleen, squeezing through an inter-endothelial slit with the dead parasite remnant retained upstream from the slit (Giemsa-stained histological section). **(G)** Same aspect generated by filtration through layers of microspheres (Epifluorescence and bright field, with dead parasite remnant stained with DAPI). **(H)** "Herniated" RBC from a patient with sickle cell disease. The cell trace yellow-stained vacuole looks almost expelled from the RBC. **(E and G)** from Ndour et al JID 2015; **(F)** from Buffet at al. Blood 2006; **(H)** from Sissoko et al. AJH 2022, with permission.

and is operator-dependent (Casper et al., 1976; Sills and Oski, 1979), although optimized quantification methods have recently emerged (El Hoss et al., 2018). Though not widely used, another specific and sensitive marker exists (Sills et al., 1988). This marker, conventionally called "pitted cells", more accurately "pocked RBC" (Holroyde et al., 1969), corresponds to RBC containing vacuoles and has been observed for the first time by Koyama in 1962 (Koyama, 1962). Sissoko *et al.* compared specificity and sensitivity of pocked RBC and HJB. ROC curves in healthy and splenectomized subjects (Sissoko et al., 2022) showed that the most effective thresholds for the best diagnostic performance were 0.15% of RBC for HJB and 10% for pocked RBC. With these threshold, specificity and sensitivity of pocked RBC counts as a diagnostic test for hyposplenism were 100% for pocked RBC, and 96% and 91% for HJB, respectively (Sissoko et al., 2022). Patients with asplenia have impaired splenic filtration of RBC but also defective immune functions, as indicated by abnormal levels of lymphocytes subpopulations and tuftsin, a soluble marker. Tuftsin, that stimulates phagocytosis, displays decreased plasma levels in splenectomized patients compared to healthy subjects (Constantopoulos et al., 1973). Its activity is negatively correlated with the concentration of pocked RBC (Zoli et al., 1994). The concentration of memory B cells (switched and unswitched) is lower in splenectomized than in control subjects (Cameron et al., 2011; Lammers et al., 2012). This review is focused on RBC-related markers of hyposplenism.

BOX 1 | Relevance of models to study pitting

An *in vivo* spleen model relevant to human physiology would be helpful to study the mechanism of pitting and the genesis of vacuoles. Spleen anatomy and function differ between animal species, including *Homo sapiens*. Spleens of equine and feline are reservoirs of RBC unlike those of humans, rabbits, dogs and mice. Spleens of humans, rats and dogs display a sinusal structure as opposed to spleens of mice, cats and horses (Bowdler, 2001). In splenectomized mice, rats, and rabbits, vacuoles have been observed in RBC but their proportion increase only slightly, to less than 10% of all RBC after splenectomy (Buchanan et al., 1987; Shet et al., 2008). In mice and rats, the mean proportion of pocked RBC quantified by DIC was 0.4% and 3%, 63 days and 100 days post-splenectomy, respectively (Buchanan et al., 1987; Shet et al., 2008). In rabbits, a transient increase from 2.5% to 10% in the first 45 days was observed, but the proportion returned to baseline 90 days after splenectomy (Buchanan et al., 1987). Only dogs showed proportions similar to those observed in humans with pocked RBC reaching a plateau at 100 days post-splenectomy. However, the maximal rate of pocked RBC was lower than in humans (13%–39% at 100 days) (Buchanan et al., 1987). The most accurate observations are thus performed in human subjects and/or human tissues. *Ex-vivo* perfusion of human spleens preserves key RBC filtering functions, including pitting, but is a demanding, very low throughput model (Buffet et al., 2006).

Although more than half of circulating RBC in asplenic patient contain vacuoles, little is known about their genesis, content and clearance. We review here current knowledge about possible origins and mechanisms of elimination of these unique and original organelles, observed in otherwise "empty" mature RBC.

Methods

Articles reviewed here were selected on google scholar using the following keywords: "pocked cells" OR "pitted cells" OR "pocked red blood cells" OR "pitted red blood cells" AND "sickle cell disease" OR "splenectomy" as of 21 July 2023. Additional articles not found by these keywords-based queries were selected from references of the selected articles, and personal collection of the authors.

Pocked red blood cells counts to quantify hyposplenism

To quantify pocked RBC, whole blood is collected in tubes containing EDTA or heparin (de Haan et al., 1988; Reinhart and Chien, 1988). Pocked RBC are fixed in 0.1%–3% PBS-buffered glutaraldehyde (Pearson et al., 1979; Sills and Oski, 1979) or in 2% PBS-buffered paraformaldehyde (Nardo-Marino et al., 2022). Counts are against 250 to 2000 RBC under the oil-immersion objective (x1000) using differential interference contrast microscope (DIC Nomarski optics) (Pearson et al., 1979; Sills and Oski, 1979). Such fixed RBC can be stored for at least 1 month at room temperature, and at least 24 months at 4°C, after glutaraldehyde fixation (Holroyde and Gardner, 1970), and 6 weeks at 37°C or room temperature after paraformaldehyde fixation (Nardo-Marino et al., 2022). Recently, two automated quantification methods of pocked RBC were published: one using deep neural network analysis (Nardo-Marino et al., 2022), the other imaging flow cytometry after fluorescent labeling (Sissoko et al., 2022). Marino *et al.* generated a learning model from DIC pictures (Nardo-Marino et al., 2022). This automated count was reliable and correlated with manual counts (albeit with lower performance when the proportion of pocked RBC was high). Sissoko *et al.* observed the presence of spotted RBC after labeling with Cell Trace Yellow. The proportion of these spotted RBC correlated with the proportion of pocked RBC counted manually by DIC (Sissoko et al., 2022).

In healthy subjects, pocked RBC generally account for less than 4% of RBC (Holroyde et al., 1969; Holroyde and Gardner, 1970; Casper et al., 1976) while in splenectomized patients, the proportion of pocked RBC varies between 20% and 80% (Koyama, 1962; Holroyde and Gardner, 1970). There is a good correlation between splenic scintigraphy, HJB, and pocked RBC (Rogers et al., 2011; El Hoss et al., 2019) but HJB are generally not observed when pocked RBC counts are lower than 8% (Phoon, 1997). The marked difference in proportions of pocked RBC between controls and hyposplenic subjects makes it a robust quantitative method (Phoon, 1997). Phoon *et al.* defined hyposplenism by the presence of 3.5%–10% pocked RBC, and asplenia by the presence of more than 12% of pocked RBC (Phoon, 1997). However, none of the thresholds published so far have been validated by large-scale clinical studies correlating them with the risk of long-term complications. Of note, this marker is irrelevant in neonates where 5%–40% of RBC are pocked (Holroyde et al., 1969; Kim et al., 1980). This high rate is probably associated with spleen developmental immaturity. The proportion of pocked RBC returns to normal (low) levels during the first month of life.

Vacuoles are morphologically diverse

Vacuoles in pocked RBC appear by DIC microscopy as punctate light or dark craters (Figure 1) (Koyama, 1962). Pocked RBC contain single or multiple vacuoles in hyposplenic subjects (0.2µm–1.5 µm

diameter) and only a single and generally small vacuole in healthy subjects (0.2µm–0.8 µm diameter) (Holroyde and Gardner, 1970; Sills and Oski, 1979). By transmission electron microscopy (TEM), Reinhart *et al.* observed that 13% of RBC pictures contained small vacuoles (40 and 330 nm) in healthy subject, either empty (1.7% of RBC) or containing small grainy material (11.3% of RBC) (Reinhart and Chien, 1988). In the same study, RBC pictures with small vacuoles were four times more frequent in splenectomized patients than in healthy individuals (42.5% of RBC pictures) and were empty (36.2% of RBC pictures) or containing dense material (6.3% of RBC pictures). In these patients, the authors also observed low proportions of RBC with large vacuoles (diameter >300 nm) and clusters of small vacuoles (3.2% and 2.6% respectively). Kent *et al.* described by TEM larger vacuoles (200–1000 nm), containing electron dense material, in healthy subjects as well as in patients with anemia, with or without splenectomy (Kent et al., 1966). Large vacuoles seen optically may correspond to the coalescence of small vacuoles seen by TEM, which may ultimately fuse to generate a single large vacuole (Holroyde and Gardner, 1970; Reinhart and Chien, 1988). When vacuoles content was studied by TEM (Kent et al., 1966; Holroyde and Gardner, 1970; Schnitzer et al., 1971), they appeared either empty or heterogeneous, and sometimes contained material identified as altered organelles like mitochondria, ribosomes and smooth internal membranes surrounded by an external membrane (Kent et al., 1966; Holroyde and Gardner, 1970; Schnitzer et al., 1971). These observations were based exclusively on morphological characteristics and, so far, no immunostaining has confirmed that these structures are altered organelles. Other vacuoles have a homogenous internal structure, similar to the cytoplasm in aspect and density, which suggests that they may contain hemoglobin (Kent et al., 1966; Schnitzer et al., 1971). Another subtype of iron-containing vacuoles has been observed, that may correspond to Pappenheimer bodies (Kent et al., 1966). Finally, few autophagic vacuoles with a phosphatase acid activity have been described (Kent et al., 1966). These observations do not robustly establish the origin of vacuoles and their content.

This wealth of morphological observations leaves indeed significant knowledge gaps (Please see Box 2). There is currently no method to sort pocked RBC or to isolate vacuoles. Therefore, it remains uncertain whether all TEM observations of vacuoles correspond to those observed by DIC. As mentioned above, several subtypes of vacuoles have been observed by TEM, suggesting that vacuoles may have multiple origins. Small (<400 nm) vacuoles observed by TEM cannot be seen by DIC and have been observed in RBC from healthy subject in which the proportion of pocked RBC is usually very low. Largest vacuoles containing structures identified as altered organelles may correspond to remnants of reticulocyte multivesicular bodies but, as mentioned, no direct staining has confirmed this hypothesis so far.

BOX 2 | Knowledge gaps and current research questions

1. The fine mechanism of pitting, responsible for vacuole clearance, is only partially understood. It may involve inter-endothelial slits, splenic macrophages, or a synergistic contribution of both.

(Continued in next column)

BOX 2 (*Continued*) | Knowledge gaps and current research questions

2. The origin and composition of small vacuoles present in almost all RBC is unknown.
3. The origin and composition of large, complex vacuoles, containing organelle-like remnants is unknown.
4. How the coalescence of small vacuoles generates larger, optically observable, vacuoles is not known.
5. The role of these vacuoles in the RBC physiology is unknown.
6. The theranostic value of pocked RBC is not robustly established.

Genesis of vacuoles: confronting hypotheses

Following splenectomy, a gradual increase in the proportion of pocked RBC is observed, and the plateau is reached after 60–100 days (Koyama, 1962; Zago et al., 1986; Buchanan et al., 1987), or 130 days in one study (de Haan et al., 1988). Vacuoles may appear during erythropoiesis and persist as remnants in mature RBC. Alternatively, they may be created *de novo* in circulating RBC (Reinhart and Chien, 1988). To solve the quandary, searchers have quantified vacuoles in young *versus* old RBC (de Haan et al., 1988; Reinhart and Chien, 1988). Young and old RBC were separated based on density using microhematocrit tubes (Reinhart and Chien, 1988), or angle-head centrifugation (de Haan et al., 1988). Using DIC microscopy on RBC from splenectomized subjects, Reinhart *et al.* found 2.6 times more pocked RBC in old than in young cells (52.2% vs 20.8%). De Haan *et al.* reported a similar difference (42.2% vs 27.6%) as well as a continuous increase of pocked RBC both in young and old RBC between 10 and 130 days after splenectomy (de Haan et al., 1988). A positive correlation between the proportion of pocked RBC and levels of glycated hemoglobin (HbA1c), a marker of RBC aging, was also observed (de Haan et al., 1988). Selective case reports also support the hypothesis that most vacuoles appear *de novo* in mature RBC. In two patients with idiopathic autoimmune hemolytic anemia unresponsive to splenectomy (that had been performed 17 and 54 months previously), Zago *et al.* observed that therapy with corticosteroids improved RBC survival and reduced reticulocytosis. In parallel, 12 weeks after starting treatment, the proportion of pocked RBC had increased from 5.5% to 29.8% in one patient; and from 13% to 47.4% in the other (Holroyde and Gardner, 1970). Similarly, when a splenectomized patient was transfused with normal RBC for pure red cell aplasia, Holroyde *et al.* observed a dilution of pocked RBC immediately after transfusion (from 44% to 26% of RBC) followed by a rapid increase and return to high baseline proportions in about 20 days, suggesting that vacuoles had appeared in transfused RBC, which were most likely mature in vast majority (Holroyde and Gardner, 1970).

A theoretical argument against the hypothesis of *de novo* appearance of vacuoles is the elusive mechanism of their (potential) creation in mature RBC, a highly differentiated enucleated cell entity devoid of organelles and endocytosis machinery. The formation of intracellular vacuoles is a well-known mechanism in erythroid precursors but the mechanism

underlying their suspected appearance in mature RBC remains currently an enigma. Several teams have tried to replicate experimentally this process *in vitro* (Reinhart and Chien, 1988; Sills et al., 1988; Colin and Schrier, 1991). Incubating RBC with 0.5 mM chlorpromazine for 2 min at 37°C induced the appearance of vacuoles similar in shape and size (40–234 nm) to that observed in healthy subjects, as observed by TEM (Reinhart and Chien, 1988). In a more physiological approach, Sills *et al.* compared the creation of vacuoles *in vitro* (upon incubation of normal RBC for 6 days at 37°C in physiologic buffer or plasma), to the *in vivo* formation of vacuoles during the same period immediately after splenectomy (Sills et al., 1988). The proportion of vacuoles increased at a similar pace in these two groups: from 0.3% to 4.9% *in vitro* and 0.4%–4.1% in patients, suggesting that vacuoles do appear in mature RBC. The experience *in vitro* could not be extended further because of the increasing crenation of RBC (echinocytosis) when they were incubated for more than a week. Crenation impairs an accurate visualization of vacuoles. Colin *et al.* performed the same experiment with and without FITC-BSA in order to determine whether vacuoles could be created by the invaginations of the plasma membrane (Colin and Schrier, 1991). No fluorescence was observed inside RBC, despite the appearance of vacuoles after 144 h of incubation in medium containing FITC-BSA. Conversely, in the presence of the antimalarial drug primaquine, the appearance of vacuoles was accompanied by intra-erythrocytic fluorescence, which strongly suggested that these primaquine-induced vacuoles, unlike "spontaneous" vacuoles, were created by internalization of the plasma membrane (Colin and Schrier, 1991). How vacuoles spontaneously appear *in vitro* and *in vivo* is therefore still mysterious. Spontaneous appearance of vacuoles in Eagle's modified buffer was not inhibited by the addition of sodium vanadate (that inhibits ATPase activity required for drug-induced endocytosis), NaF (that inhibits ATP production by glycolysis thereby blocking endocytosis), or NaCN (which inhibits transferrin receptor-mediated endocytosis). The process is therefore ATP- and transferrin receptor-independent, and, in the absence of primaquine (to which splenectomized patients are generally not exposed), is probably not due to plasma membrane invagination (Colin and Schrier, 1991). If the experimental appearance of intra-erythrocytic vacuoles *in vitro* replicates the natural mechanism in action in hypo- or a-splenic patients, they are not generated by an endocytosis-like mechanism. One hypothesis that reconciles all currently available information would be the progressive coalescence (both *in vitro* or *in vivo*) of preexisting smaller vacuoles created during erythropoiesis (Reinhart and Chien, 1988). They would "appear" optically in mature RBC but from elements already present, too small to be seen by DIC, but observable by TEM.

As a further source of complexity, vacuoles are morphologically diverse. The different types may therefore stem from different mechanisms. Empty vacuoles and those containing homogenous material resembling RBC cytoplasm may be "created" (probably by coalescence, see above) *de novo* in circulation, and would be removed rapidly by the spleen, except in subjects with hyposplenism. Larger and more complex vacuoles containing organelle-like components may be remnants from erythropoiesis never removed from the mature RBC in asplenic subjects. Indeed, no known autonomous, active process enabling their expulsion persists in mature RBC. As summarized at the previous section, the appearance of optically visible vacuoles in mature RBC is supported by several observations (Holroyde and Gardner, 1970; de Haan et al., 1988; Reinhart and Chien, 1988). That the minority of "complex" vacuoles are remnants from erythropoiesis is a logical assumption but leans only on TEM pictures (Kent et al., 1966; Holroyde and Gardner, 1970; Schnitzer et al., 1971). Currently, there is no way to differentiate these two types of vacuoles by other methods.

Clearance of intra-erythrocytic vacuoles

The observation that high proportions of pocked RBC are present only in splenectomized subjects strongly suggests that vacuoles are eliminated by the spleen (Koyama, 1962; Kent et al., 1966). The demonstration was made in humans by Holroyde *et al.* who transfused a normal subject with ^{51}Cr labelled RBC from splenectomized donor having 49.5% of pocked RBC (Holroyde and Gardner, 1970). Seventy hours after transfusion, 90% of ^{51}Cr RBC were still in circulation in the recipient, while the proportion of pocked RBC had dropped to 0 (Holroyde and Gardner, 1970). Buchanan *et al.* performed the same experiment in dogs: pocked RBC counts decreased from 6.5% to 1% in 170 h after transfusion while transfused RBC were still in circulation (Buchanan et al., 1987). This persistence of labeled RBC with disappearance of pocked RBC is strongly reminiscent of a prior observation by Crosby using RBC containing Pappenheimer bodies (Crosby and Benjamin, 1957) that forged the concept of pitting. Pitting was later observed with malaria parasites, with initial suggestive pictures by TEM (Schnitzer et al., 1972) later confirmed by RBC labeling (Angus et al., 1997; Chotivanich et al., 2002). Searchers in Thailand observed a rapid parasite clearance (in less than a week) in spleen-intact malaria patients treated with artemisinins, followed by the appearance in circulation of uninfected RBC labeled with a parasitic protein, called RESA (Ring-Erythrocyte Surface Antigen) (Angus et al., 1997; Chotivanich et al., 2002). This peculiar subpopulation was called "once-infected RBC". This process was later replicated in human spleens perfused *ex-vivo* (Buffet et al., 2006) enabling the visualization on histological sections of infected RBC squeezing through narrow splenic slits with the dead parasite remnant laying upstream from the slit (Figure 1). In splenectomized subjects, post-treatment parasite clearance is much longer, often lasting several weeks, without appearance of "once infected" RESA-positive RBC in circulation (Angus et al., 1997; Chotivanich et al., 2002). This suggests that vacuoles are eliminated from RBC by pitting, enabling the almost intact pitted RBC to go back into circulation. A similar process is likely operating for Howell-Jolly bodies and Pappenheimer bodies. Pitting likely requires squeezing through inter-endothelial slits of the spleen, selective engulfment of the vacuole by macrophages, or the synergistic contribution of both mechanisms. Ndour *et al.* performed microsphiltration experiments, where layers of microspheres of different sizes mimic inter-endothelial slits (Ndour et al., 2015). Using RBC infected by the malaria parasite *Plasmodium falciparum* and exposed to artesunate, they quantified "once-infected" RESA-positive RBC, before and after microsphiltration. A low (<5%) rate of pitting was observed, lower than the rate observed *in vivo*, generally greater than 50% (Ndour et al., 2015). Anyona *et al.* co-incubated infected RBC with THP1 monocytes and observed the appearance of uninfected, RESA-positive RBC (Anyona et al., 2006). Pocked RBC are also pitted by the spleen and a similar uncertainty exists regarding the specific cellular

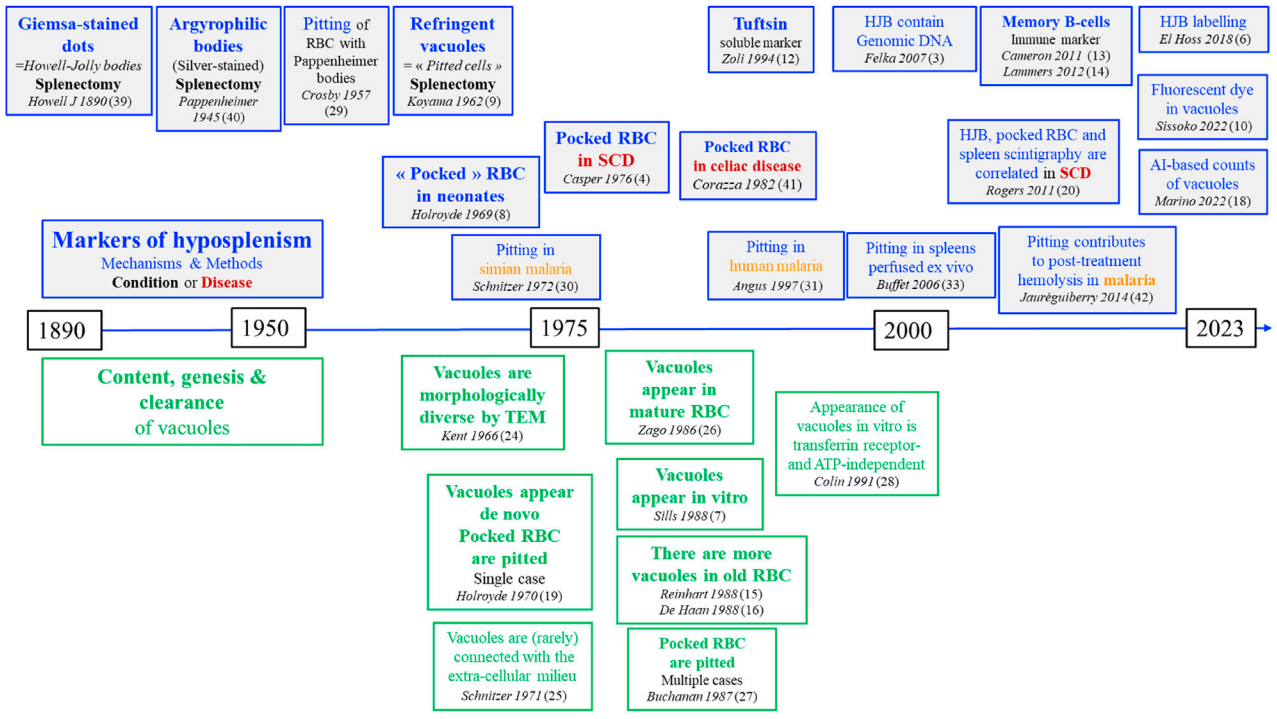

FIGURE 2
Timeline of the main discoveries on markers of splenic function.

mechanism leading to this expulsion of vacuoles (Nagelkerke et al., 2018).

Discussion

Pocked RBC were first reported in 1962 and have since received relatively limited attention. Large studies to validate their quantitative theranostic value are still missing. Their clearance, or, more accurately said, the clearance of their vacuoles by pitting is better understood than their genesis (Figure 2). Several teams have shown that vacuoles, rather than being former intra-erythroblastic organelles, may appear in circulating mature RBC, likely by a process distinct from conventional endocytosis. Yet, by TEM, residues resembling organelles are observed in a proportion of vacuoles. "Empty" vacuoles, which are the majority, likely appear by coalescence in mature RBC, whereas the minority of more complex and large vacuoles may be remnants from erythropoiesis. Not least, the possible function of intra-erythrocytic vacuoles (if there is any) has been poorly explored so far. Small vacuoles (visible only by TEM) are present in almost all RBC, including those from healthy subjects, which suggests they may have a (yet to be identified) physiological role. Because of their high numbers in asplenic individual, a pathogenic (e.g., procoagulant) role is also conceivable. A better knowledge of the composition of each subtype of vacuoles would help identify specific markers, for simple counting and sorting, as prerequisite for functional studies and wider use in medical practice.

Author contributions

LD: Writing–original draft. CR: Writing–review and editing. PB: Writing–review and editing.

Funding

The author(s) declare that no financial support was received for the research, authorship, and/or publication of this article.

Conflict of interest

The authors declare that the research was conducted in the absence of any commercial or financial relationships that could be construed as a potential conflict of interest.

Publisher's note

All claims expressed in this article are solely those of the authors and do not necessarily represent those of their affiliated organizations, or those of the publisher, the editors and the reviewers. Any product that may be evaluated in this article, or claim that may be made by its manufacturer, is not guaranteed or endorsed by the publisher.

References

Angus, B. J., Chotivanich, K., Udomsangpetch, R., and White, N. J. (1997). *In vivo* removal of malaria parasites from red blood cells without their destruction in acute falciparum malaria. *Blood* 90 (5), 2037–2040. doi:10.1182/blood.v90.5.2037

Anyona, S. B., Schrier, S. L., Gichuki, C. W., and Waitumbi, J. N. (2006). Pitting of malaria parasites and spherocyte formation. *Malar. J.* 5 (1), 64. doi:10.1186/1475-2875-5-64

Bowdler, A. J. (2001). The complete spleen: structure, function, and clinical disorders. *Springer Sci. Bus. Media*, 334.

Buchanan, G. R., Holtkamp, C. A., and Horton, J. A. (1987). Formation and disappearance of pocked erythrocytes: studies in human subjects and laboratory animals. *Am. J. Hematol.* 25 (3), 243–251. doi:10.1002/ajh.2830250303

Buffet, P. A., Milon, G., Brousse, V., Correas, J. M., Dousset, B., Couvelard, A., et al. (2006). *Ex vivo* perfusion of human spleens maintains clearing and processing functions. *Blood* 107 (9), 3745–3752. doi:10.1182/blood-2005-10-4094

Cameron, P. U., Jones, P., Gorniak, M., Dunster, K., Paul, E., Lewin, S., et al. (2011). Splenectomy associated changes in IgM memory B cells in an adult spleen registry cohort. *PLOS ONE* 6 (8), e23164. doi:10.1371/journal.pone.0023164

Casper, J. T., Koethe, S., Rodey, G. E., and Thatcher, L. G. (1976). A new method for studying splenic reticuloendothelial dysfunction in sickle cell disease patients and its clinical application: a brief report. *Blood* 47 (2), 183–188. doi:10.1182/blood.v47.2.183.bloodjournal472183

Chotivanich, K., Udomsangpetch, R., McGready, R., Proux, S., Newton, P., Pukrittayakamee, S., et al. (2002). Central role of the spleen in malaria parasite clearance. *J. Infect. Dis.* 185 (10), 1538–1541. doi:10.1086/340213

Colin, F. C., and Schrier, S. L. (1991). Spontaneous endocytosis in human neonatal and adult red blood cells: comparison to drug-induced endocytosis and to receptor-mediated endocytosis. *Am. J. Hematol.* 37 (1), 34–40. doi:10.1002/ajh.2830370108

Constantopoulos, A., Najjar, V. A., Wish, J. B., Necheles, T. H., and Stolbach, L. L. (1973). Defective phagocytosis due to tuftsin deficiency in splenectomized subjects. *Am. J. Dis. Child.* 125 (5), 663–665. doi:10.1001/archpedi.1973.04160050017004

Corazza, G. R., Lazzari, R., Frisoni, M., Collina, A., and Gasbarrini, G. (1982). Splenic function in childhood coeliac disease. *Gut* 23 (5), 415–416. doi:10.1136/gut.23.5.415

Crosby, W. H., and Benjamin, N. R. (1957). Siderocytes and the spleen. *Blood* 12 (2), 165–170. doi:10.1182/blood.v12.2.165.165

de Haan, L. D., Werre, J. M., Amth, R., Huls, A. H., de Gier, J., and Staal, G. E. J. (1988). Vacuoles in red cells from splenectomized subjects originate during cell life: association with glycosylated haemoglobin? *Eur. J. Haematol.* 41 (5), 482–488. doi:10.1111/j.1600-0609.1988.tb00231.x

El Hoss, S., Cochet, S., Marin, M., Lapouméroulie, C., Dussiot, M., Bouazza, N., et al. (2019). Insights into determinants of spleen injury in sickle cell anemia. *Blood Adv.* 3 (15), 2328–2336. doi:10.1182/bloodadvances.2019000106

El Hoss, S., Dussiot, M., Renaud, O., Brousse, V., and El Nemer, W. (2018). A no*vel non*-invasive method to measure splenic filtration function in humans. *Haematologica* 103 (10), e436–e439. doi:10.3324/haematol.2018.188920

Felka, T., Lemke, J., Lemke, C., Michel, S., Liehr, T., and Claussen, U. (2007). DNA degradation during maturation of erythrocytes – molecular cytogenetic characterization of Howell-Jolly bodies. *Cytogenet. Genome Res.* 119 (1–2), 2–8. doi:10.1159/000109611

Holroyde, C. P., and Gardner, F. H. (1970). Acquisition of autophagic vacuoles by human erythrocytes. Physiological role of the spleen. *Blood* 36 (5), 566–575. doi:10.1182/blood.v36.5.566.566

Holroyde, C. P., Oski, F. A., and Gardner, F. H. (1969). The "pocked" erythrocyte. Red-cell surface alterations in reticuloendothelial immaturity of the neonate. *N. Engl. J. Med.* 281 (10), 516–520. doi:10.1056/NEJM196909042811002

Howell, W. H. (1890). The life-history of the formed elements of the blood, especially the red blood corpuscles. *J. Morphol.* IV, 57–116. doi:10.1002/jmor.1050040105

Jauréguiberry, S., Ndour, P. A., Roussel, C., Ader, F., Safeukui, I., Nguyen, M., et al. (2014). Postartesunate delayed hemolysis is a predictable event related to the lifesaving effect of artemisinins. *Blood* 124 (2), 167–175. doi:10.1182/blood-2014-02-555953

Kent, G., Minick, O. T., Volini, F. I., and Orfei, E. (1966). Autophagic vacuoles in human red cells. *Am. J. Pathol.* 48 (5), 831–857.

Kim, K. Y., Choi, J. W., Sohn, Y. M., and Chung, K. S. (1980). A prospective study of development of splenic reticuloendothelial function in premature and term infants. *Yonsei Med. J.* 21 (2), 110–115. doi:10.3349/ymj.1980.21.2.110

Koyama, S. (1962). Postsplenectomy vacuole,a new erythrocytic inclusion boby. *Mie Med. J.* 11 (3), 425–443.

Kristinsson, S. Y., Gridley, G., Hoover, R. N., Check, D., and Landgren, O. (2014). Long-term risks after splenectomy among 8,149 cancer-free American veterans: a cohort study with up to 27 years follow-up. *Haematologica* 99 (2), 392–398. doi:10.3324/haematol.2013.092460

Lammers, A. J. J., de Porto, APNA, Bennink, R. J., van Leeuwen, E. M. M., Biemond, B. J., Goslings, J. C., et al. (2012). Hyposplenism: comparison of different methods for determining splenic function. *Am. J. Hematol.* 87 (5), 484–489. doi:10.1002/ajh.23154

Nagelkerke, S. Q., Bruggeman, C. W., den Haan, J. M. M., Mul, E. P. J., van den Berg, T. K., van Bruggen, R., et al. (2018). Red pulp macrophages in the human spleen are a distinct cell population with a unique expression of Fc-γ receptors. *Blood Adv.* 2 (8), 941–953. doi:10.1182/bloodadvances.2017015008

Nardo-Marino, A., Braunstein, T. H., Petersen, J., Brewin, J. N., Mottelson, M. N., Williams, T. N., et al. (2022). Automating pitted red blood cell counts using deep neural network analysis: a new method for measuring splenic function in sickle cell anaemia. *Front. Physiology* 13, 859906. doi:10.3389/fphys.2022.859906

Ndour, P. A., Lopera-Mesa, T. M., Diakité, S. A. S., Chiang, S., Mouri, O., Roussel, C., et al. (2015). Plasmodiumfalciparum clearance is rapid and pitting independent in immune Malian children treated with artesunate for malaria. *J. Infect. Dis.* 211 (2), 290–297. doi:10.1093/infdis/jiu427

Pappenheimer, A. M., Molloy, E., and Rose, H. M. (1945). Presence of granules resembling elementary bodies in yolk cells of normal eggs. *Proc. Soc. Exp. Biol. Med.* 58 (4), 313–315. doi:10.3181/00379727-58-14936

Pearson, H. A., McIntosh, S., Ritchey, A. K., Lobel, J. S., Rooks, Y., and Johnston, D. (1979). Developmental aspects of splenic function in sickle cell diseases. *Blood* 53 (3), 358–365. doi:10.1182/blood.v53.3.358.358

Phoon, C. K. L. (1997). Where's the spleen? Looking for the spleen and assessing its function in the syndromes of isomerism. *Cardiol. Young* 7 (3), 347–357. doi:10.1017/s1047951100004297

Reinhart, W. H., and Chien, S. (1988). Red cell vacuoles: their size and distribution under normal conditions and after splenectomy. *Am. J. Hematol.* 27 (4), 265–271. doi:10.1002/ajh.2830270407

Rogers, Z. R., Wang, W. C., Luo, Z., Iyer, R. V., Shalaby-Rana, E., Dertinger, S. D., et al. (2011). Biomarkers of splenic function in infants with sickle cell anemia: baseline data from the BABY HUG Trial. *Blood* 117 (9), 2614–2617. doi:10.1182/blood-2010-04-278747

Schnitzer, B., Rucknagel, D. L., Spencer, H. H., and Aikawa, M. (1971). Erythrocytes: pits and vacuoles as seen with transmission and scanning electron microscopy. *Science* 173 (3993), 251–252. doi:10.1126/science.173.3993.251

Schnitzer, B., Sodeman, T., Mead, M. L., and Contacos, P. G. (1972). Pitting function of the spleen in malaria: ultrastructural observations. *Science* 177 (4044), 175–177. doi:10.1126/science.177.4044.175

Shet, A. S., Hoffmann, T. J., Jirouskova, M., Janczak, C. A., Stevens, J. R. M., Adamson, A., et al. (2008). Morphological and functional platelet abnormalities in Berkeley sickle cell mice. *Blood Cells, Mol. Dis.* 41 (1), 109–118. doi:10.1016/j.bcmd.2008.01.008

Sills, R. H., and Oski, F. A. (1979). RBC surface pits in the sickle hemoglobinopathies. *Am. J. Dis. Child.* 133 (5), 526–527. doi:10.1001/archpedi.1979.02130050070014

Sills, R. H., Tamburlin, J. H., Barrios, N. J., Yeagle, P. L., and Glomski, C. A. (1988). Physiologic formation of intracellular vesicles in mature erythrocytes. *Am. J. Hematol.* 28 (4), 219–226. doi:10.1002/ajh.2830280403

Sissoko, A., Fricot-Monsinjon, A., Roussel, C., Manceau, S., Dumas, L., Capito, C., et al. (2022). Erythrocytic vacuoles that accumulate a fluorescent dye predict spleen size and function in sickle cell disease. *Am. J. Hematol.* 97 (11), E385–E388. doi:10.1002/ajh.26690

William, B. M., and Corazza, G. R. (2007). Hyposplenism: a comprehensive review. Part I: basic concepts and causes. *Hematology* 12 (1), 1–13. doi:10.1080/10245330600938422

Zago, M. A., Covas, D. T., Figueiredo, M. S., and Bottura, C. (1986). Red cell pits appear preferentially in old cells after splenectomy. *Acta Haematol.* 76 (1), 54–56. doi:10.1159/000206019

Zoli, G., Corazza, G. R., D'Amato, G., Bartoli, R., Baldoni, F., and Gasbarrini, G. (1994). Splenic autotransplantation after splenectomy: tuftsin activity correlates with residual splenic function. *BJS Br. J. Surg.* 81 (5), 716–718. doi:10.1002/bjs.1800810530

frontiers | Frontiers in Physiology

TYPE Original Research
PUBLISHED 03 January 2024
DOI 10.3389/fphys.2023.1320697

OPEN ACCESS

EDITED BY
Lars Kaestner,
Saarland University, Germany

REVIEWED BY
Asya Makhro,
University of Zurich, Switzerland
Ozlem Yalcin,
Koç University, Türkiye
Roland Pittman,
Virginia Commonwealth University,
United States

*CORRESPONDENCE
Allan Doctor,
adoctor@som.umaryland.edu

RECEIVED 12 October 2023
ACCEPTED 06 December 2023
PUBLISHED 03 January 2024

CITATION
Rogers SC, Brummet M, Safari Z, Wang Q, Rowden T, Boyer T and Doctor A (2024), COVID-19 impairs oxygen delivery by altering red blood cell hematological, hemorheological, and oxygen transport properties.
Front. Physiol. 14:1320697.
doi: 10.3389/fphys.2023.1320697

COVID-19 impairs oxygen delivery by altering red blood cell hematological, hemorheological, and oxygen transport properties

Stephen C. Rogers, Mary Brummet, Zohreh Safari, Qihong Wang, Tobi Rowden, Tori Boyer and Allan Doctor*

Divisions of Critical Care Medicine and the Center for Blood Oxygen Transport and Hemostasis, Department of Pediatrics, University of Maryland School of Medicine, Baltimore, MD, United States

Introduction: Coronavirus disease 2019 (COVID-19) is characterized by impaired oxygen (O_2) homeostasis, including O_2 sensing, uptake, transport/delivery, and consumption. Red blood cells (RBCs) are central to maintaining O_2 homeostasis and undergo direct exposure to coronavirus *in vivo*. We thus hypothesized that COVID-19 alters RBC properties relevant to O_2 homeostasis, including the hematological profile, Hb O_2 transport characteristics, rheology, and the hypoxic vasodilatory (HVD) reflex.

Methods: RBCs from 18 hospitalized COVID-19 subjects and 20 healthy controls were analyzed as follows: (i) clinical hematological parameters (complete blood count; hematology analyzer); (ii) O_2 dissociation curves (p50, Hill number, and Bohr plot; Hemox-Analyzer); (iii) rheological properties (osmotic fragility, deformability, and aggregation; laser-assisted optical rotational cell analyzer (LORRCA) ektacytometry); and (iv) vasoactivity (the RBC HVD; vascular ring bioassay).

Results: Compared to age- and gender-matched healthy controls, COVID-19 subjects demonstrated 1) significant hematological differences (increased WBC count—with a higher percentage of neutrophils); RBC distribution width (RDW); and reduced hematocrit (HCT), Hb concentration, mean corpuscular volume (MCV), and mean corpuscular hemoglobin concentration (MCHC); 2) impaired O_2-carrying capacity and O_2 capacitance (resulting from anemia) without difference in p50 or Hb–O_2 cooperativity; 3) compromised regulation of RBC volume (altered osmotic fragility); 4) reduced RBC deformability; 5) accelerated RBC aggregation kinetics; and (6) no change in the RBC HVD reflex.

Discussion: When considered collectively, homeostatic compensation for these RBC impairments requires that the cardiac output in the COVID cohort would need to increase by ~135% to maintain O_2 delivery similar to that in the control cohort. Additionally, the COVID-19 disease RBC properties were found to be exaggerated in blood-type O hospitalized COVID-19 subjects compared to blood-type A. These data indicate that altered RBC features in hospitalized COVID-19 subjects burden the cardiovascular system to maintain O_2 delivery homeostasis, which appears exaggerated by blood type (more pronounced with blood-type O) and likely plays a role in disease pathogenesis.

KEYWORDS

red blood cell, coronavirus disease 2019, oxygen, rheology, osmotic fragility, deformability, aggregation, vasoactivity

Introduction

Red blood cells (RBCs), the most abundant cells in the body (Sender et al., 2016), play an essential role in oxygen (O_2) homeostasis (i.e., O_2 sensing, uptake, transport, and delivery). Whilst the RBC number and hemoglobin concentration (Hb) define blood O_2-carrying capacity, homeostatic modulation of Hb–O_2 affinity ultimately regulates O_2 capture/release in a manner that stabilizes O_2 delivery in the setting of reduced O_2 availability (i.e., hypoxia and anemia) or increased consumption (i.e., stress and disease). This effect is achieved via the production of allosteric effectors (i.e., 2,3 DPG and ATP) and adjustment of the RBC internal milieu (i.e., pH and anion concentration) in response to external stimuli (i.e., temperature and CO_2 tension). In addition to modulating Hb–O_2 affinity, RBCs play a direct but less well-appreciated role in O_2 delivery homeostasis by regulating blood flow itself. This includes both active signaling, whereby RBCs control the bioavailability of vasoactive factors that modulate vessel caliber in an O_2-dependent manner (i.e., S-nitrosothiols and ATP) (Ross et al., 1962; Frandsenn et al., 2001; Doctor and Stamler, 2011), and biophysical effects, via the influence of RBCs on blood rheology (determined by RBC deformability), aggregation (with each other), and adhesion (to endothelium). Together, these functions place RBCs at the center of O_2 homeostasis regulation.

The highly infectious coronavirus 2019 disease (COVID-19) caused by severe acute respiratory coronavirus 2 (SARS-CoV-2) (Zhu et al., 2020) is characterized by impaired O_2 delivery homeostasis. The COVID-19 virus S1 spike protein is postulated to interact with RBCs via RBC CD147 (Wang et al., 2020), evidenced by the detection of RBC surface viral spike protein and complement activation products (Lam et al., 2020; Bouchla et al., 2021). Additionally, COVID-19 spike protein glycans may also bind to glycoconjugates on the surface of red blood cells (Boschi et al., 2022). These interactions, in addition to the acute inflammation, which is a feature of COVID-19 (Wong, 2021) [and already known to affect RBC rheological properties (Pretorius, 2018)], likely affect RBC surface chemistry and rheology, which are proposed to result in intravascular thrombosis (Weisel and Litvinov, 2019), associated lung injury (Lam et al., 2021), and hypoxemia (Montenegro et al., 2021). Additionally, COVID-19 subjects often present with anemia, the severity of which appears greatest in those most critically ill (Chen et al., 2021), although it is not clear if this effect arises from increased RBC hemolysis and/or clearance, reduced hematopoiesis, or a combination of these factors. Unless compensated through homeostatic adaptation of blood flow and/or Hb–O_2 affinity, reduced O_2-carrying capacity diminishes O_2 capacitance (i.e., the amount of O_2 released across any given arteriovenous pO_2 difference) (Mairbaurl and Weber, 2012), thereby loading and placing undue strain on the cardiovascular system to compensate for reduced O_2 delivered per mL blood, which requires work to increase cardiac output in the setting of reduced capacity for myocardial O_2 delivery, potentially contributing to disease pathogenesis.

Despite the fundamental RBC role in O_2 homeostasis and the known impact of COVID-19 on O_2 delivery homeostasis, the effect of COVID-19 on RBC properties and physiology is not well described nor quantified. The aim of this study was to determine whether RBCs from hospitalized COVID-19 subjects demonstrated altered features (or impaired compensation) relevant to O_2 homeostasis, i.e., hematological parameters, altered O_2 transport characteristics (i.e., Hb–O_2 affinity/cooperativity), impaired rheology, and/or altered release of vasoactive compounds, i.e., a diminished hypoxic vasodilatory reflex. Additionally, given the ABO blood-type dependence on susceptibility to COVID-19 infection and spike protein–RBC interaction (Barnkob et al., 2020; Severe Covid et al., 2020; Wu et al., 2023), we assessed whether changes observed in features relevant to O_2 homeostasis were associated with blood type.

Materials and methods

Subjects

This study was approved by the UMB Human Research Ethics Committee, and written informed consent was obtained from all participants in accordance with the Declaration of Helsinki. We studied 18 COVID-19 subjects who were hospitalized at the University of Maryland Medical Center (Baltimore, United States) between September 2020 and January 2022 and 20 non-hospitalized healthy control individuals. SARS-CoV-2 infection was confirmed in all subjects by polymerase chain reaction (PCR) performed on material collected using the nasopharyngeal swab. Medical records were reviewed to collect demographic and general clinical data.

Blood sampling and processing

Venous blood was drawn into EDTA or heparin vacutainers and immediately placed on ice until analysis, which was performed within 24 h of collection. For complete blood count (CBC), oxygen dissociation curve (ODC—Hemox), and ektacytometry (LORRCA) analyses, whole blood was used, so no further processing was performed. RBC counts (CBC HORIBA) were adjusted for each assay platform (following the addition of whole blood to assay buffer) according to assay specifications. For hypoxic vasodilation (HVD), RBCs were separated from whole blood and washed three times (2,000 g, 10 min, 4°C, PBS) prior to analysis. Blood samples were equilibrated at the appropriate assay temperature prior to measurement.

Materials and reagents

Unless stated, reagents were purchased from Sigma-Aldrich Inc. (St. Louis, United States).

Hematological parameters and oximetry

Standard hematological parameters were measured in the clinic or research laboratory using conventional complete blood count analyzers (HORIBA, Kisshoin, Japan).

TABLE 1 Healthy control and COVID-19 subject demographics.

		Healthy			COVID-19		
		Male	Female	Total	Male	Female	Total
Demographics	N	9	11	20	9	9	18
	Age (mean)	45.4 ± 9.8	46.5 ± 9.6	46.1 ± 9.4	50.8 ± 15.4	54.4 ± 9.2	52.6 ± 12.5
	Age [median (25th and 75th percentile)]	44 [41; 52]	54 [35; 54]	44 [39; 54]	55 [35; 64]	58 [45; 62]	58 [42; 62]
Comorbidities	Obesity	—	—	—	5 (56%)	7 (78%)	12 (67%)
	Hypertension	—	—	—	6 (67%)	6 (67%)	12 (67%)
	Diabetes	—	—	—	1 (11%)	8 (89%)	9 (50%)
	Heart failure	—	—	—	3 (33%)	3 (33%)	6 (33%)
	Hyperlipidemia	—	—	—	0 (0%)	5 (56%)	5 (28%)
	Chronic kidney disease (CKD)	—	—	—	4 (44%)	1 (11%)	5 (28%)
	Sample collection (days from symptom onset)	—	—	—	13.4 ± 10.3	11.3 ± 6.4	12 (67%)
Severity	SAPS II score	—	—	—	27.3 ± 13.1	23.0 ± 9.5	25.6 ± 11.6
Outcome	Death (%)	0	0	0	2 (22%)	1 (11%)	3 (17%)

Hemorheological parameters

RBC osmotic fragility, deformability, and aggregation were measured through ektacytometry using LORRCA (RR Mechatronics, Hoorn, Netherlands). This assay quantifies cell deformability as an elongation index [i.e., a ratio in the difference between the major and minor axes in cellular diffraction patterns over their sum (Lazarova et al., 2017; Gutierrez et al., 2021)], whilst cells are under constant shear. Three different measurements were performed: 1) osmoscan, yielding a set of elongation indices measured at 37°C and a single shear (30 Pa), across a wide osmotic gradient (~80–700 mOsm); 2) deformability scan, yielding a set of elongation indices at 37°C and a fixed physiologic osmolality, across a shear range (0.3–30 Pascal); and 3) aggregation scan, i.e., a syllectogram, a time-dependent intensity plot of backscattered light generated when RBCs, initially subjected to shear (to fully induce disaggregation), are allowed to return to their original randomly oriented biconcave shape, lose alignment, and aggregate (as the shear is stopped) (Dobbe et al., 2003). Measurement outputs of aggregation included aggregation index (see Figure 4A) calculated as area A (the area within the rectangle above the syllectogram curve) divided by area A plus area B (the area within the rectangle below the syllectogram curve) multiplied by 100, the amplitude of aggregation, and $t_{1/2}$. Whole blood was used (aggregation) or added and thoroughly mixed in an iso-osmolar polyvinylpyrrolidone (EIon ISO solution for osmoscan and deformability measurements—5 mL; RR Mechatronics, Hoorn, Netherlands; mean viscosity ~29.8 mPa*s, osmolality ~285 mOsm, pH ~7.4), allowing normalization of the RBC count for each specific assay platform (as outlined by the manufacturer).

O_2 transport parameters

O_2–hemoglobin dissociation curves were composed from the simultaneous direct *in vitro* measurement of O_2 partial pressure (pO_2) and hemoglobin O_2 saturation ($HbSO_2$) during controlled hemoglobin deoxygenation (O_2 unloading) and re-oxygenation (O_2 loading) (Guarnone et al., 1995) (Hemox-Analyzer, TSC Scientific Corporation, New Hope, PA, United States). Whole blood (25 µL was diluted in 3 mL 50 mM BIS-Tris, and 100 mM NaCl buffered to either pH 7.2, 7.4, or 7.6) (Benesch et al., 1969) with the addition of bovine serum albumin (BSA) (12 µL) and an antifoaming agent (6 µL), both supplied by the manufacturer. Samples were equilibrated (37°C) while bubbled with air and then subsequently deoxygenated, with exposure to N_2. The Hb p50 value (pO_2 at which $HbSO_2$ is 50%) was extrapolated from the plotted relationship of the above two variables (oxy-hemoglobin desaturation curve; ODC). In addition, the Hill coefficient was calculated (TCS Hemox Data Acquisition System, TCS Scientific Corp, New Hope, PA, United States), providing an index of cooperativity, and the Bohr plot was determined (Guarnone et al., 1995). Additional analyses were performed from ODC data, including the calculation of blood O_2 content from the O_2 unloading arm of the Hemox ODC curves; SO_2 was converted to blood O_2 content assuming that 1 g Hb binds to 1.34 mL O_2 and multiplying this by the subjects [Hb]. Blood O_2 capacitance was also calculated from the ODC, using the calculation of Mairbaurl and Weber (2012).

RBC vasoactivity (hypoxic vasodilation)

Male New Zealand white rabbits (1.8–2 Kg) were euthanized by intravenous injection of sodium pentobarbital. The aorta was harvested, and endothelium-intact rings were prepared for isometric tension recordings by mounting on a Radnoti vascular ring array (Harvard Apparatus, Holliston, MA, United States): 2 g resting tension, 37°C, and Krebs (NaCl 118 mM, KCl 4.8 mM, KH_2PO_4 1.2 mM, $MgSO_4$ 1.2 mM, $NaHCO_3$ 24 mM, glucose 11.0 mM, $CaCl_2$ 2.5 mM, and disodium EDTA 0.03 mM); bath pO_2 was controlled by bubbling appropriate gas mixtures, as described (Pinder et al.,

10.3389/fphys.2023.1320697

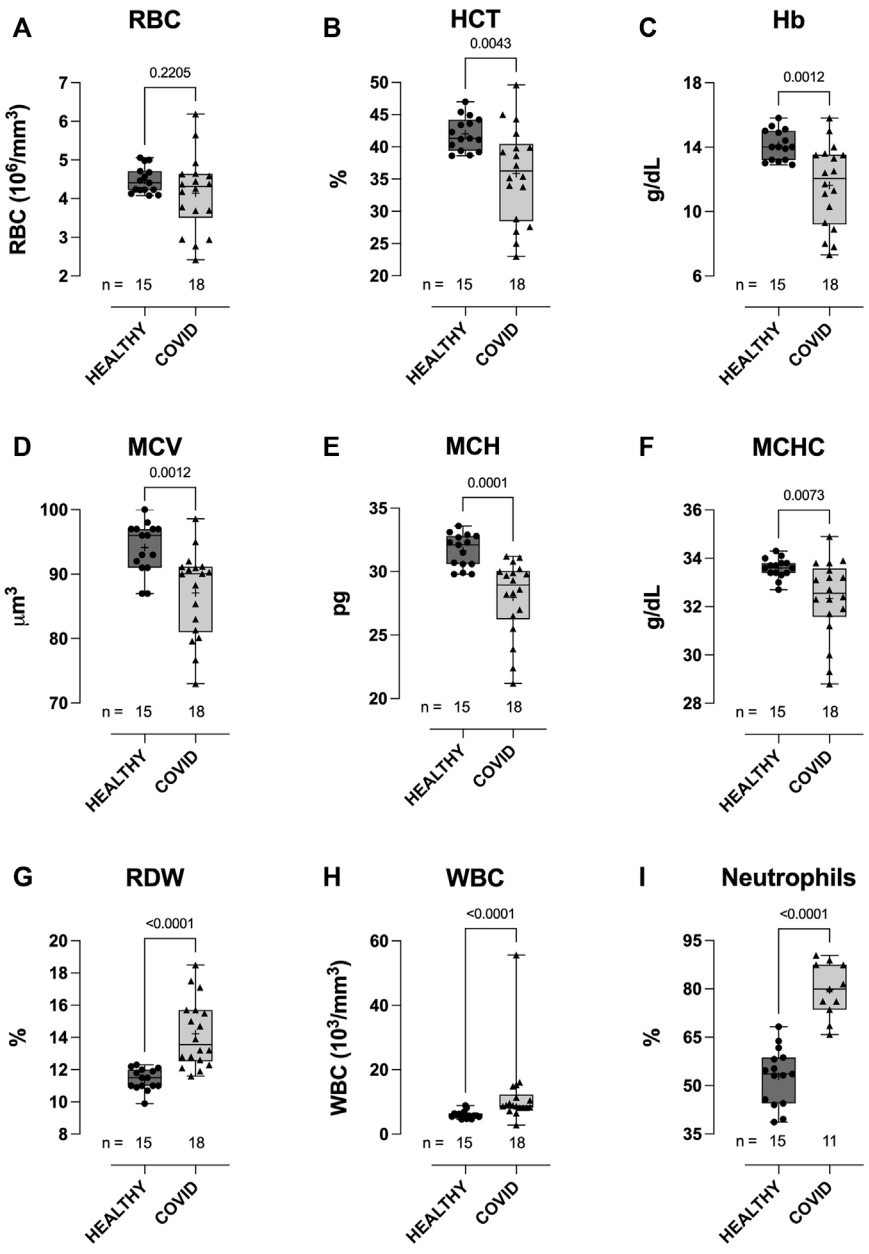

FIGURE 1
Clinical hematological parameters of healthy control and hospitalized COVID-19 subjects. Compared to healthy controls, blood samples from COVID-19 subjects demonstrated higher white blood cell (WBC) counts **(H)**, with a higher percentage of neutrophils **(I)**. No difference between groups was observed in red blood cell (RBC) counts **(A)**. COVID-19 subjects also demonstrated lower hematocrits (HCT) **(B)**, hemoglobin concentration [Hb] **(C)**, mean corpuscular volume (MCV) **(D)**, mean corpuscular hemoglobin **(E)**, mean corpuscular hemoglobin concentration (MCHC) **(F)**, and higher red cell distribution width (RDW) **(G)**. Data are presented as the box and whisker plot. The median is indicated by a solid line, and the mean is represented by +. Notably, a subset of controls (n = 5) did not have CBC measures performed. In addition, neutrophil counts were not available for some of the COVID-19 subjects.

2009). Isometric tension was recorded continuously by transducers linked to a PowerLab 8SP/octal bridge (AD Instruments, Colorado Springs, CO, United States) connected to a PC running LabChart 7 (AD Instruments, Colorado Springs, CO, United States). Rings were pre-conditioned at 95% O_2, 5% CO_2, with 10^{-6} mol/L phenylephrine (PE) and 10^{-5} mol/L acetylcholine (ACh); then, under hypoxia (95% N_2, 5% CO_2; ~1% O_2), PE (5×10^{-6} mol/L) was used to increase baseline tension, before 30 µL of pelleted RBCs were injected into each bath, and the data were analyzed, as outlined previously (James et al., 2004). In brief, endothelium-intact rings were identified as those producing an ACh relaxation response during preconditioning that was >60% of the maximal induced tension (by PE); rings that did not produce this amount of relaxation were excluded. For each experiment, eight ring preparations were run in parallel, n = 1 represents data averaged from all endothelium-intact rings (possibly 8 in total) that were treated identically; the % relaxation was calculated as the RBC-induced decrease in tension as a percentage of the preceding

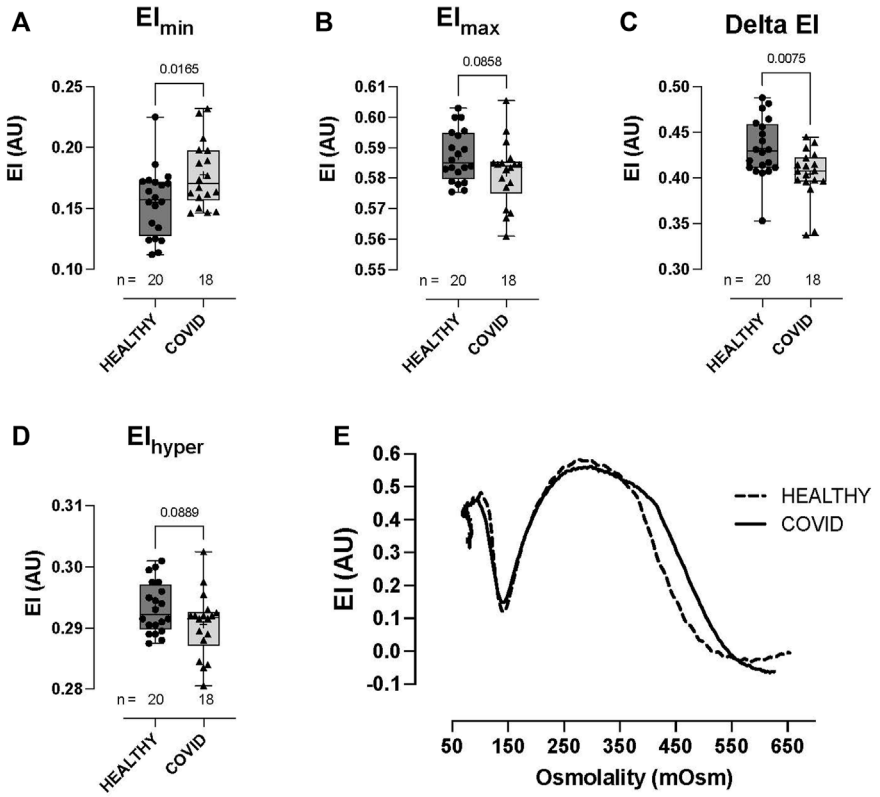

FIGURE 2
Shear-induced RBC osmotic fragility in healthy controls and hospitalized COVID-19 subjects measured using LORRCA. Compared to healthy control RBCs, COVID-19 RBCs demonstrated significant impairment in cell volume regulation, with higher elongation index minimum, EImin **(A)**, lower elongation index maximum, EImax **(B)**, lower delta elongation index **(C)**, and elongation index hyper **(D)**. No differences were observed in buffer osmolality at EImin (Omin), EImax (OEImax), the delta osmolality, or hyperosmolality (Ohyper). Representative traces from healthy controls and COVID-19 subjects **(E)**. Data are presented as the box and whisker plot. The median is indicated by a solid line, and the mean is represented by +.

baseline plateau tension (both under the above hypoxic bath conditions) (James et al., 2004).

Statistical analyses

Results are presented as the mean ± standard deviation (SD) (or SEM where indicated). Column statistics were performed, and a normality/lognormality test (Shapiro–Wilk test) was undertaken to confirm normal data distribution. Data were plotted as box and whisker plots with each data point shown (box extending from the 25th to 75th percentile) and the whiskers representing minimum and maximum points. For parametric data, group comparisons of means were analyzed using the *t*-test (Student's). For non-parametric data, group comparisons of mean ranks were analyzed using Mann–Whitney *U*-test (Prism, GraphPad Inc.; La Jolla, CA). Curves (Figures 3E, 5F, 8E) were compared via two-way ANOVA (mixed-effects analysis), and comparison of means at each shear (3E, 8E) or each lung-to-tissue O_2 flux (5F) between groups were performed. Pearson's product moment correlation coefficient was computed to assess the relationship between mean corpuscular hemoglobin concentration (MCHC)/mean corpuscular volume (MCV) and RBC deformability (Figure 3H). A *p*-value <0.05 was considered significant. For original data please contact Allan Doctor at ADoctor@som.umaryland.edu.

Results

Patient demographics and clinical presentation

Healthy age/sex-matched controls were compared with COVID-19 subjects (sex distribution; chi-squared test (X^2 1, N = 38) = 0.095, $p = 0.758$; mean age; COVID-19: 52.6 ± 12.5 years vs healthy control 46.1 ± 9.4 years, $p = 0.074$) (Table 1). As is typical of hospitalized subjects in intensive care, COVID-19 subjects presented with multiple comorbidities (Table 1). As a gauge of COVID-19 severity, we report the mean Simplified Acute Physiology Scores (SAPS II) (25.6 ± 11.6 AU), in addition to the fact that 3 of the 18 COVID-19 subjects (17%) died during their hospitalization stay (Table 1).

Clinical hematologic parameters—healthy controls vs COVID-19 subjects

The WBC count was higher in hospitalized COVID-19 subjects than in healthy controls (12.1 ± 11.32 vs 6.1 ± 1.2: 103/mm^3, $p <$ 0.0001; Figure 1H), and WBC counts from the COVID-19 subjects comprised a significantly higher percentage of neutrophils than

10.3389/fphys.2023.1320697

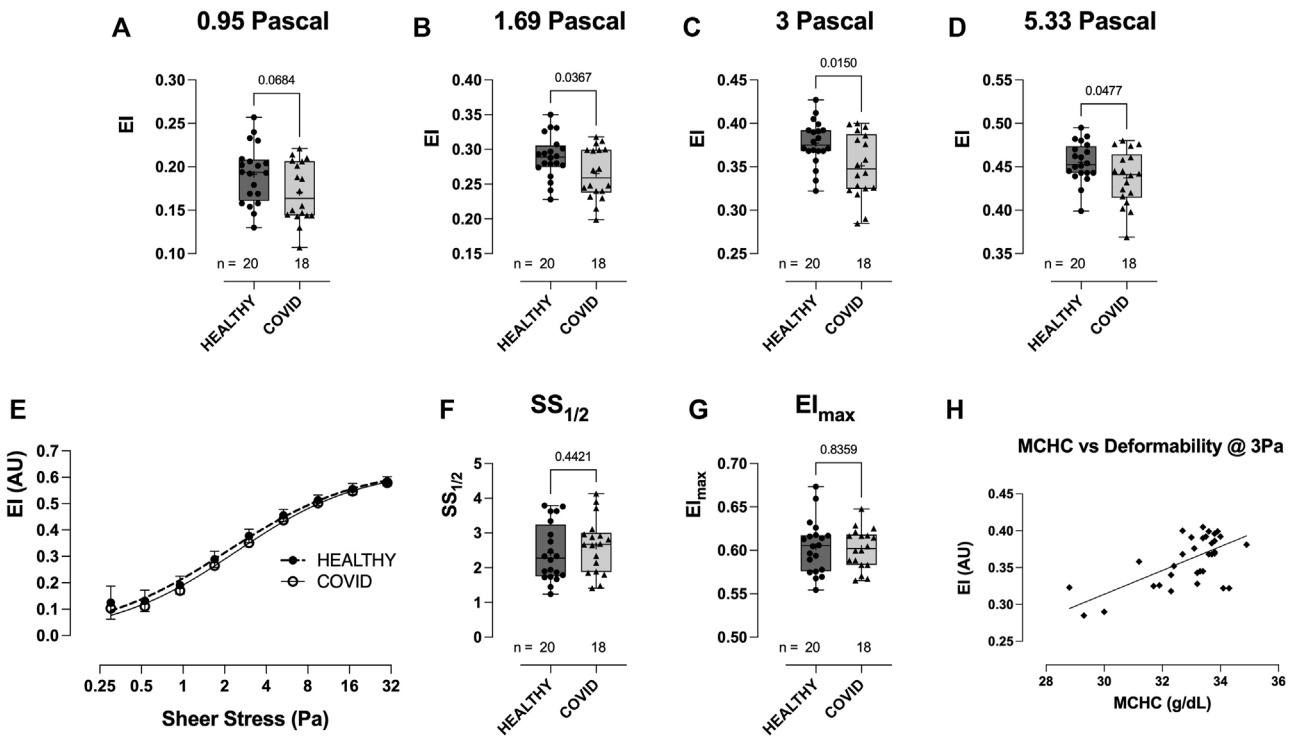

FIGURE 3
Shear-induced RBC deformability in healthy controls and hospitalized COVID-19 subjects, measured using LORRCA. Compared to healthy controls, RBC deformability was significantly reduced in hospitalized COVID-19 subjects across a range of shears: 0.95 **(A)**, 1.69 **(B)**, 3 **(C)**, and 5.33 Pa **(D)**. Deformability curve **(E)** and the calculated values from the deformability curves plotted, including SS1/2 **(F)** and EImax **(G)**. Correlation between MCHC and RBC deformability (at 3 Pa) plotted to show the relationship between these variables **(H)**. Data are presented as the box and whisker plot. The median is indicated by a solid line, and the mean is represented by +.

those from healthy controls (79.6 ± 8.4 vs 52.9 ± 8.8: %, $p < 0.0001$; Figure 1I). RBC counts did not differ between groups (Figure 1A). Compared to healthy controls, hematocrit (35.9 ± 7.38 vs 42.0 ± 2.62: %, $p = 0.0043$; Figure 1B), Hb concentration (11.6 ± 2.42 vs 14.1 ± 0.93: g/dL, $p = 0.0012$; Figure 1C), MCV (87.1 ± 6.75 vs 94.1 ± 3.94: μm^3, $p = 0.0012$; Figure 1D), mean corpuscular hemoglobin (MCH; 28.0 ± 2.99 vs 31.7 ± 1.31: pg, $p = 0.0001$; Figure 1E), and MCHC (32.3 ± 1.64 vs 33.6 ± 0.41: g/dL, $p = 0.0073$; Figure 1F) were all lower in COVID-19 subjects, whilst RBC distribution width was higher (14.2 ± 2.08 vs 11.4 ± 0.67: %, $p < 0.0001$; Figure 1G).

Hemorheological parameters—healthy controls vs COVID-19 subjects

RBCs from COVID-19 subjects demonstrated altered ability to control the cell volume across an osmotic gradient (~100–500 mOsm) under shear (30 Pa). At low osmolality (~140 mOsm—at EImin), COVID-19 RBCs showed higher EI than healthy control RBCs (0.177 ± 0.027 vs 0.155 ± 0.028, respectively: EImin, $p = 0.0165$; Figure 2A). This hypotonic osmolality coincides with the osmolality at which 50% of the cells would hemolyze in an osmotic fragility assay (Clark et al., 1983), suggesting a lower surface area-to-volume ratio of the COVID-19 cells compared to the healthy controls and/or a loss of cell volume regulation. At physiologic and hyper-osmolality, RBC deformability in the COVID-19 subjects trended lower than that in healthy controls, although this difference was not statistically significant (EImax $p = 0.0858$ and EIhyper $p = 0.0889$; Figures 2B, D). The dynamic range in deformability across the measured osmotic gradient (deltaEI) was significantly lower in RBCs from COVID-19 subjects than those from controls (0.404 ± 0.028 vs 0.433 ± 0.032, respectively: deltaEI, $p = 0.0075$; Figure 2C). Buffer osmolalities at EImin, EImax, deltaEI, and EIhyper were not significantly different between the two groups (Figure 2E—representative osmoscans).

RBC deformability at fixed osmolality (~285 mOsm) across a range of shears (0.3–30 Pascal; Pa) was significantly lower in the hospitalized COVID-19 subjects than in healthy controls (Figure 3). Importantly, this difference between groups was observed in the physiologic shear range (i.e., 1.69 Pa, $p = 0.0367$; 3 Pa, $p = 0.0150$; 5.33 Pa, $p = 0.0477$; Figures 3A–D). No difference was observed in the deformability curves between the healthy controls and COVID-19 subjects (Figure 3E), as confirmed in the analysis of SS1/2 (Figure 3F) and the calculated EImax (Figure 3G). Given that cell geometry dictates that MCHC (and MCV) are linked to the ability of RBCs to deform, we assessed the relationship between MCHC/MCV and deformability (at 3 Pa) and observed an expected significant correlation between these parameters (MCHC vs deformability = r (31) = 0.453, $p < 0.0001$; Figure 3H; MCV vs. deformability = r (31) = 0.17, $p = 0.0172$; data not shown).

Whilst the extent of RBC aggregation (Amplitude, AMP; AU) was not significantly different between the healthy controls and COVID-19 subjects (Figures 4A–C), RBC aggregation kinetics were significantly accelerated in the hospitalized COVID-19

10.3389/fphys.2023.1320697

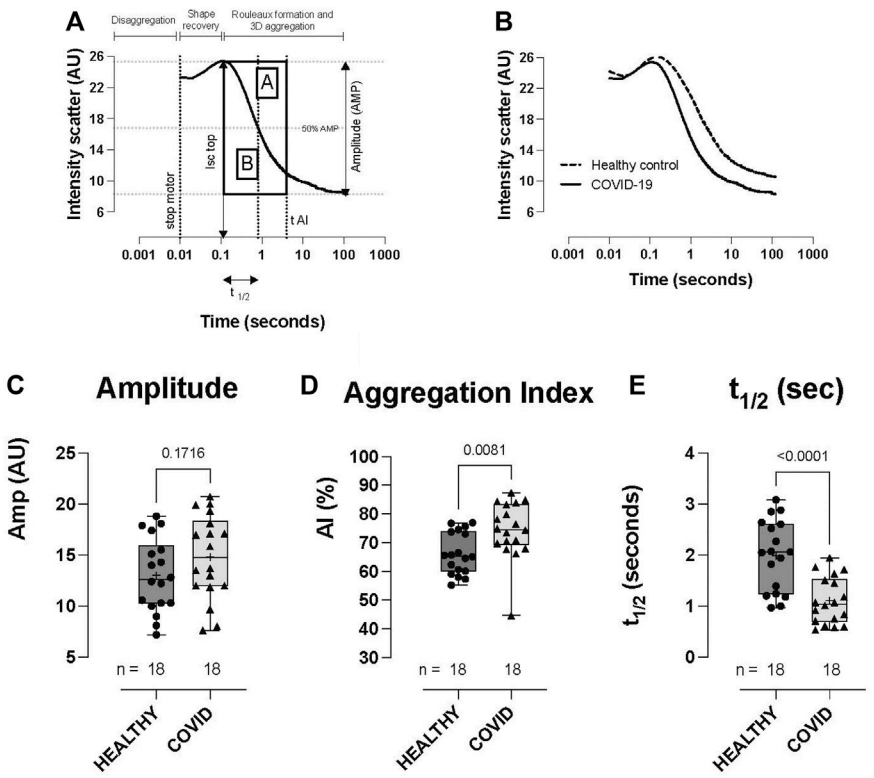

FIGURE 4
RBC aggregation (syllectogram) in healthy controls and hospitalized COVID-19 subjects, measured using LORRCA. Syllectogram of RBC aggregation plotted on a logarithmic timescale demonstrating the indices plotted **(A)**. Representative syllectogram traces from healthy controls and COVID-19 subjects **(B)**. No difference was observed in the total aggregation response between healthy controls and COVID-19 subjects (amplitude) **(C)**. Aggregation profile (aggregation index) **(D)** and the kinetics of aggregation (t1/2) **(E)** were significantly different between the groups, with COVID-19 subjects demonstrating higher AI% and a shorter time to reach half-maximal aggregation (t1/2). Data are presented as the box and whisker plot. The median is indicated by a solid line, and the mean is represented by +. Notably, two control subjects did not have aggregation measurements performed.

subjects compared to healthy controls, as defined by the aggregation index (74.3 ± 9.96 vs 66.2 ± 7.27: AI%, p = 0.0081; COVID-19 vs healthy control) and t1/2 (1.10 ± 0.457 vs 1.99 ± 0.69: t1/2 s, $p < 0.0001$; COVID-19 vs healthy control; Figures 4A, B, D, E).

RBC O_2 transport parameters—healthy controls vs COVID-19 subjects

No significant difference was observed in RBC–O_2 affinity (i.e., p50) between the healthy control and COVID-19 subjects across three pH measurements (pH 7.2: 28.77 ± 1.87 vs 29.83 ± 2.31, p = 0.2198; pH 7.4: 23.06 ± 1.69 vs 24.3 ± 2.25, p = 0.124; and pH 7.6: 18.69 ± 1.67 vs 19.59 ± 1.72, p = 0.1929, healthy control vs. COVID-19, respectively; Figure 5A). Hb–O_2 cooperativity was not significantly different between the healthy controls or COVID-19 subjects (pH 7.2: 2.68 ± 0.20 vs 2.57 ± 0.11, p = 0.1433; pH 7.4: 2.65 ± 0.21 vs 2.56 ± 0.12, p = 0.1826; and pH 7.6: 2.66 ± 0.28 vs 2.51 ± 0.14, p = 0.0968, healthy control vs COVID-19, respectively; Figure 5B). The Bohr effect (i.e., the shift in the ODC in response to pH change), tested by running ODCs at three fixed pH levels, was not different between the healthy control and COVID-19 groups (Figure 5C). We calculated the mean total blood O_2 content as a function of blood pO_2 for each pH, per gram Hb (Figure 5D) and per Liter blood (Figure 5E) after calculating blood O_2 content from acquired data [i.e., for per gram Hb calculation, SO_2 was converted to blood O_2 content given that 1 g hemoglobin binds to 1.34 mL O_2, for per Liter blood calculation, SO_2 was converted to blood O_2 content per gram Hb and then multiplied by each subject's [Hb]; (Figure 5D); this analysis demonstrates the significant reduction in blood O_2 content between the COVID-19 subjects and healthy controls for similar O_2 tensions. Next, we calculated O_2 capacitance [absolute amount of O_2 released by RBCs upon transit across a given physiologic O_2 gradient (lung → tissue)] (Mairbaurl and Weber, 2012) from the Hb–O_2 saturation at 100 mmHg, using an O_2 loading curve at pH 7.4 (representing RBC O_2 content in pulmonary veins) and the Hb–O_2 saturation at various pO_2 values on the O_2 dissociation curve measured at pH 7.2 (representing RBC O_2 content in perfused tissue). These data, which integrate both O_2-carrying capacity and Hb–O_2 affinity, quantify the amount of O_2 unloaded across the physiologic range of arterio-venous (A-V) pO_2 differences encountered during circulatory transit. We observed a significant, progressive reduction in O_2 capacitance in COVID-19 subjects for A-V O_2 gradients >70 mmHg (i.e., equivalent to tissue pO_2 < 30 mmHg, $p < 0.05$; Figure 5F), with RBCs from COVID-19

10.3389/fphys.2023.1320697

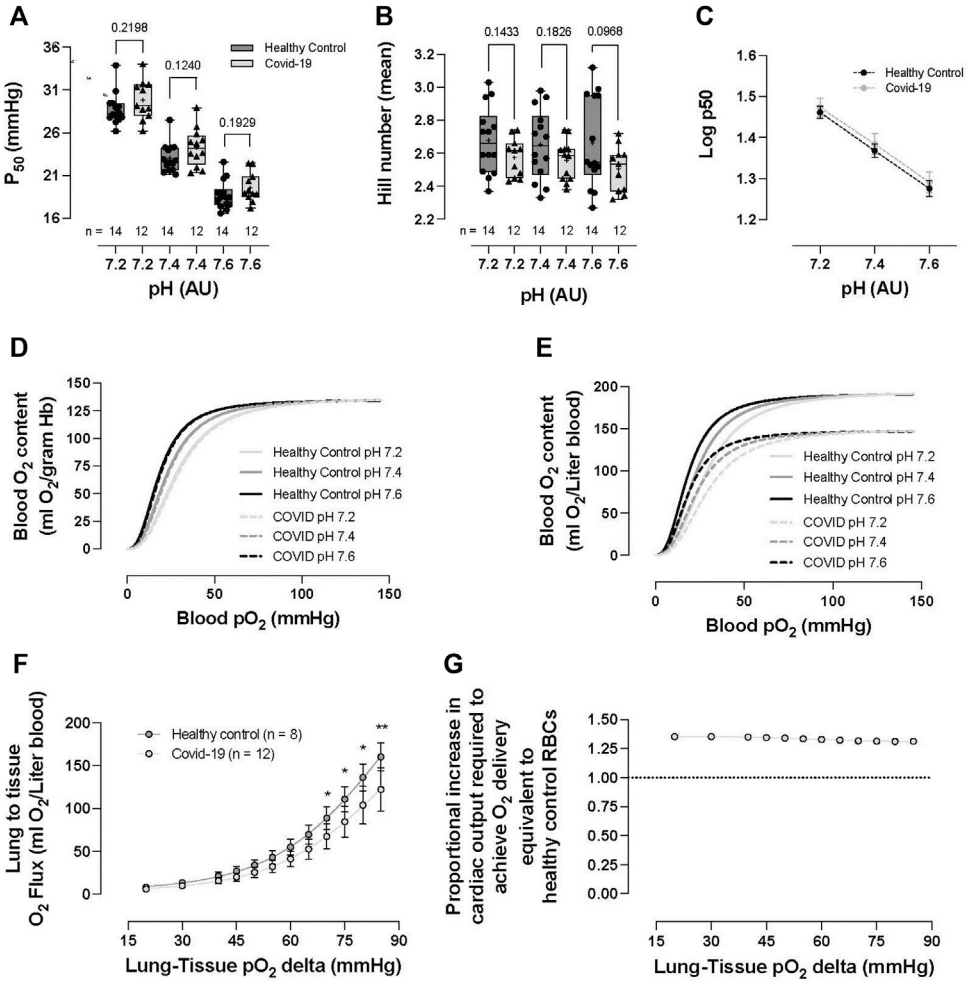

FIGURE 5
RBC O_2 transport parameters of healthy controls and hospitalized COVID-19 subjects. No significant differences were observed between healthy controls or COVID-19 subjects in p50 (i.e., partial pressure of O_2 that hemoglobin within RBCs 50% saturated with O_2) **(A)**, Hb cooperativity as determined by the Hill number (mean) **(B)**, or Bohr effect **(C)**. No significant differences were observed in blood O_2 content per gram Hb (calculated from Hemox ODCs) between healthy controls and COVID-19 RBCs **(D)**. Impact of anemia on O_2 delivery evaluated via the calculation of O_2 content per liter of blood (from ODC and CBC analyses). COVID-19 subjects demonstrated significantly reduced blood O_2 content (ml O_2/L) **(E)**. The reduction in blood O_2 content was explored following the calculation of O_2 capacitance (quantifying the amount of O_2 unloaded for a given A-V pO_2 difference). COVID-19 subjects presented with significantly reduced O_2 capacitance, calculated from the Hb–O_2 saturation at 100 mmHg, taken from the O_2 loading curve measured at pH 7.4 (reflecting O_2 uptake conditions in the lung) and the corresponding Hb–O_2 saturations at various pO_2 values taken from the O_2 unloading curve measured at pH 7.2 (reflecting O_2 unloading from RBCs at the tissue level) (Mairbaurl and Weber, 2012) **(F)**. To overcome the O_2 deficit, the proportional increase in cardiac output necessary to achieve O_2 delivery equivalence to healthy control RBCs was calculated (need in COVID-19 subjects was ~1.3–1.4 times that of healthy control individuals) **(G)**. Data are presented as the box and whisker plots. The median is indicated by a solid line, and the mean is represented by + **(A,B)**. Data plotted as the XY plot ± SD **(C)**, **(G)** plotted without error bars, **(D–E)** plotted as mean ± SD, **(F)** plotted as the proportion between healthy controls and COVID-19 subjects. Notably, Hemox analysis was not performed on all subjects, and some subjects did not undergo CBC analysis, allowing the calculation of blood O_2 content or O_2 capacitance.

subjects demonstrating capacity for only ~70–75% of the calculated lung-to-tissue O_2 flux (mL) across the physiologic O_2 gradient compared to that for healthy controls (Figure 5F).

RBC vasoactivity (HVD response)—healthy controls vs COVID-19 subjects

No difference was observed in the hypoxic vasodilatory response of RBCs from healthy controls vs COVID-19 subjects, normalized to the maximal PE constriction of the respective vascular rings (8.67% ± 1.9% vs 9.4% ± 2.3%, p = 0.413, control vs COVID-19, respectively—data not shown).

RBC properties COVID-19 blood type

Analysis was performed to assess whether blood type influenced RBC properties in the hospitalized COVID-19 subjects. Patient numbers and demographics between the two majority blood-type groups in our cohort (i.e., A and O; sex distribution, age, and sample collection time from disease onset) were not significantly different (p > .05–Table 2).

TABLE 2 COVID-19 subject demographics by blood type.

		Blood type A	Blood type O
Demographics	Age (mean)	52.6 ± 13.2	57.2 ± 8.6
	Age [median (25th and 75th percentile)]	59 [47; 61]	58 [52; 64]
	Subject number	7	6
	Sex (M/F)	3/4	3/3
	Obesity	5 (71%)	3 (50%)
	Hypertension	4 (57%)	5 (83%)
	Diabetes	5 (71%)	3 (50%)
	Heart failure	4 (57%)	2 (33%)
	Hyperlipidemia	3 (43%)	1 (17%)
	Chronic kidney disease (CKD)	2 (29%)	2 (33%)
	Sample collection (days from symptom onset)	10.3 ± 7.8	14.7 ± 11.7
Severity	SAPS II score	26.6 ± 8.8	30.0 ± 14.0
Outcome	Death (%)	2 (29%)	1 (17%)

Clinical hematologic parameters—COVID-19 blood type

Hospitalized COVID-19 subjects with blood-type A or O showed similar hematological values (no difference between groups in RBC count, HCT, Hb concentration, MCV, RDW, WBC count, or neutrophil %) (Figures 6A–D, G–I). However, MCH (25.8 ± 3.72 vs 29.5 ± 1.58, p = 0.0348; Figure 6E) and MCHC were significantly lower in the blood-type O group than in the blood-type A group (33.2 ± 0.56 vs 30.6 ± 1.42, p = 0.0008; Figure 6F).

Hemorheological parameters—COVID-19 blood type

Hospitalized COVID-19 subjects with blood type O demonstrated significant impairment in the ability to regulate cell volume during osmotic stress. At low osmolality (~140 mOsm), RBC deformability in the blood-type O COVID-19 patient group was significantly higher than that in the blood-type A group (0.200 ± 0.026 vs 0.162 ± 0.021, respectively: EImin p = 0.0148; Figure 7A). Once again, this hypotonic osmolality coincides with the osmolality at which 50% of the cells would hemolyze in an osmotic fragility assay (Clark et al., 1983), suggesting a lower surface area-to-volume ratio of the blood type-A COVID-19 cells compared to the blood-type O and/or a loss of cell volume regulation. At physiologic and hyperosmolality, RBC deformability was not different between the two groups (Figures 7B, D, respectively). The dynamic range for deformability across the osmotic gradient (deltaEI) was significantly lower in the blood-type O COVID-19 group than in the blood-type A group (0.381 ± 0.033 vs 0.421 ± 0.016, respectively: deltaEI p = 0.0156; Figure 7C). Furthermore, buffer osmolalities at EImin (i.e., Omin) and EImax (i.e., OEImax) were significantly lower in the blood-type O COVID-19 group than in the blood-type A group (Figures 7E, F, respectively) but not the DeltaO or Ohyper (Figures 7G, H, respectively).

Across a range of physiological shear stress (from 0.95 to 5.33 Pa), RBC deformability in the blood-type O hospitalized COVID-19 patient group was significantly lower than that in the blood-type A group (Figures 8A–E). Whilst no significant difference was observed in the deformability curves between blood-types O and A (Figure 8E), blood-type A subjects demonstrated a significantly reduced SS1/2 (3.34 ± 0.65 vs 2.14 ± 0.66, respectively: p = 0.0072; Figure 8F) and higher calculated EImax (0.58 ± 0.02 vs 0.61 ± 0.03, respectively: p = 0.0527; Figure 8G).

The total extent of RBC aggregation (AMP, AU) was significantly lower in the blood-type O COVID-19 group than in the blood-type A group (10.36 ± 2.48 vs 16.76 ± 2.89: AMP AU, p = 0.0025; Figure 9A). Additionally, the kinetics of RBC aggregation were significantly different between groups, with RBCs from hospitalized COVID-19 subjects with blood-type O aggregating faster than those with blood-type A (79.0 ± 7.5 vs 71.0 ± 4.7: aggregation index;, p = 0.0471; Figure 9B; 0.92 ± 0.46 vs 1.48 ± 0.34: t1/2 s, p = 0.0471; Figure 9C).

Discussion

We quantified RBC features relevant to O_2 delivery homeostasis in hospitalized COVID-19 subjects and observed 1) an altered hematological profile, with significantly elevated WBC counts, higher neutrophil levels, marked anemia (HCT and Hb), reduced RBC volume (MCV) and RBC [Hb] (MCH and MCHC), and increased RDW; 2) diminished O_2-carrying capacity and O_2 capacitance [integrated effect of lower (Hb) and lower O_2 delivery per gram Hb across the physiologic O_2 gradient]; and 3) impaired hemorheology, distinguished by (a) loss of cell volume regulation, (b) reduced RBC deformability, and (c) accelerated RBC aggregation kinetics, but 4) without change in the hypoxic vasodilatory reflex of RBCs. These COVID-19 disease RBC

10.3389/fphys.2023.1320697

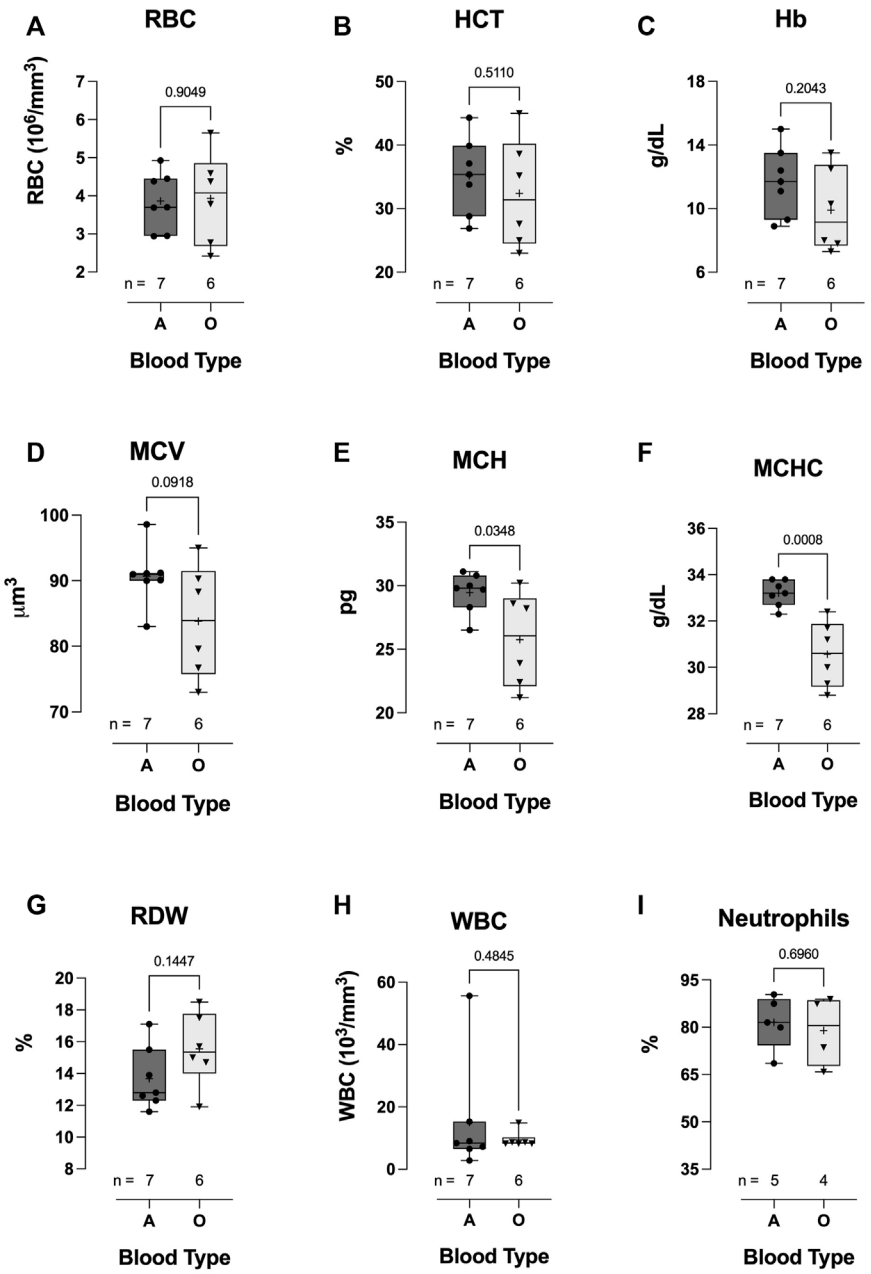

FIGURE 6
Effect of blood-types A and O on COVID-19 clinical hematological parameters. No significant differences were observed in WBC count **(H)**, neutrophil % **(I)**, RBC count **(A)**, HCT **(B)**, Hb concentration **(C)**, MCV **(D)**, or RDW **(G)**. However, MCH **(E)** and MCHC **(F)** were significantly lower in blood-type O COVID-19 subjects than in blood-type A patients. Data are presented as the box and whiskers plot. The median is indicated by a solid line, and the mean is represented by +.

features were found to be exaggerated in hospitalized COVID-19 subjects with blood-type O compared to those with blood-type A.

Others have observed that hospitalized COVID-19 subjects present with anemia (i.e., RBC lack or diminished hemoglobin concentration) (Taneri et al., 2020; Bergamaschi et al., 2021) and hypoxemia (Montenegro et al., 2021). Blood O_2-carrying capacity (i.e., blood O_2 content) is essential to maintain O_2 delivery homeostasis and is determined by both hemoglobin concentration and O_2 affinity. Reduced blood O_2-carrying capacity has obvious implications for tissue O_2 delivery and potential O_2 supply/demand gap, which is a risk factor for organ injury (Bergamaschi et al., 2021). Herein, we report reduced Hb concentration, hematocrit, MCV, MCH, and MCHC in our COVID-19 subjects, without a change in RBC count. The RBC count trended lower in the COVID-19 subjects than in healthy controls; however, the large variation in this measurement might explain the non-significant finding. These changes in RBC size, in addition to RBC [Hb], are indicative of microcytic hypochromic anemia, which has previously been observed in COVID-19 subjects (Elemam et al., 2022). However, we caution that some of these

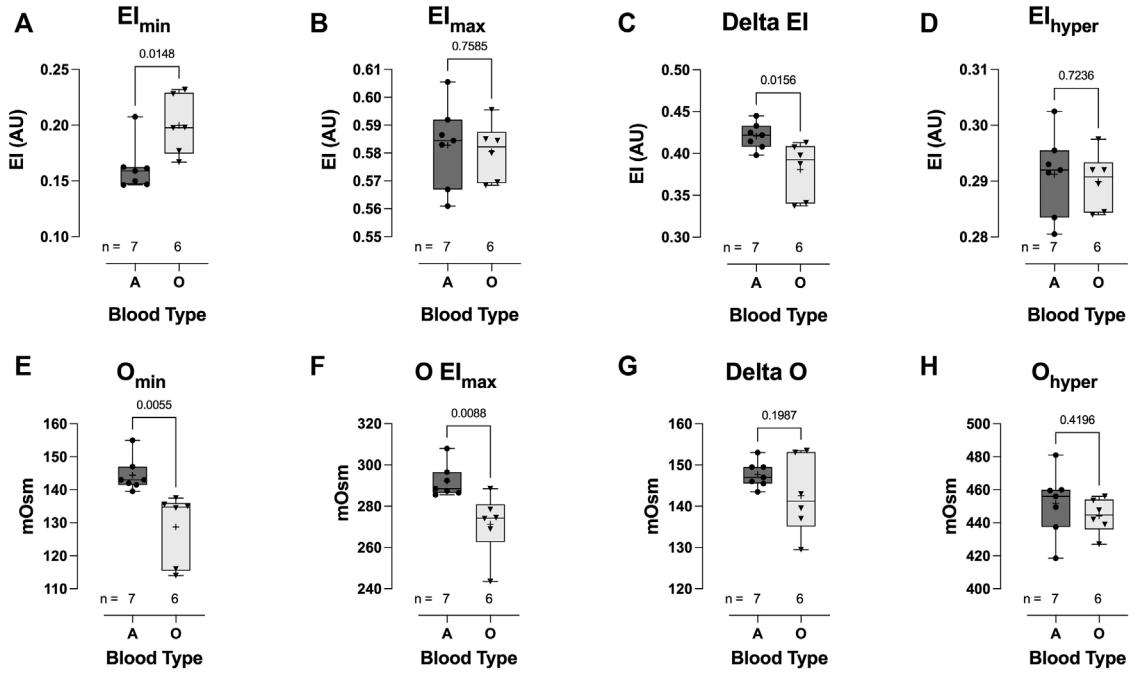

FIGURE 7
Effect of blood-types A and O on COVID-19 shear-induced RBC osmotic fragility. RBCs from COVID-19 subjects with blood-type O demonstrated significant impairment in cell volume regulation, with higher elongation index minimum (EImin) **(A)**, compared to those with blood-type A. No difference between blood types was observed in the elongation index maximum (EImax) **(B)**. Consequently, COVID-19 subjects with blood-type O demonstrated a significantly reduced delta elongation index **(C)** compared with subjects with blood-type A. No difference between blood types was observed in elongation index hyper **(D)**. The buffer osmolality at EImin (Omin) **(E)** and EImax (OEImax) **(F)** was significantly lower in blood-type O than in blood-type A subjects. However, the delta osmolality **(G)** and hyperosmolality (Ohyper) **(H)** were not different between blood types. Data are presented as the box and whiskers plot. The median is indicated by a solid line, and the mean is represented by +.

findings might partially be explained by comorbidity differences between the COVID-19 and healthy control populations.

Non-hemodynamic homeostatic adaptations counter the effect of anemia, increasing erythropoietin (EPO) (stimulating RBC production) and 2,3 DPG (right-shifting the ODC, aiding HbO_2 offloading) and altering the intra-erythrocytic milieu (i.e., affecting pH). These adaptations can be quantified by measuring [Hb], reticulocyte count (RBC production), and the O_2 dissociation curve (2,3 DPG and intra-RBC milieu changes), on which the p50 point is defined by the pO_2 at which $HbSO_2$ is 50%. In line with multiple other studies, we show no difference in the standard p50 between acute COVID-19 subjects and controls (Daniel et al., 2020; DeMartino et al., 2020; Renoux et al., 2021). However, we observed a non-significant trend toward higher p50 in the COVID-19 subjects across all three pH measurements. Considering that the reported effect of anemia typically elicits a p50 increase of ~4 mmHg (~26.7–~30.7 mmHg; pH 7.4, 37°C), following a ~50% reduction in [Hb] (resulting from reduced RBC production or loss of RBCs; ~14.8 g/dL to ~7.5 g/dL), with compensation provided by increased 2,3 DPG (~12.7 μmol/gHb to ~18.7 μmol/gHb) (Boning and Enciso, 1987); the variance in our data and lack of a statistically significant change in p50 might simply reflect the moderate degree of anemia in our COVID-19 population [(Hb) 11.6 ± 2.42 vs 14.1 ± 0.93: g/dL, $p = 0.0012$; Figure 1E]. Unfortunately, we did not measure 2,3 DPG in this study, which has been an issue with many COVID-19 studies, due to the lack of availability of test kits (Boning et al., 2021). Only one study to date reports on 2,3 DPG in COVID-19, showing a significant increase with moderate anemia compared to non-COVID subjects (measurement technique only reported arbitrary units) (Thomas et al., 2020).

O_2 delivery homeostasis is not only a function of blood O_2 content but also blood flow. In fact, the latter is the more important determinant, specifically because the dynamic range in O_2 content is limited [varying linearly with (Hb) and percentage O_2 saturation], whereas regional blood flow (a function of vessel radius to the fourth power) may be increased or decreased by several orders of magnitude. Consequently, it is the volume and distribution of blood flow that are modulated by physiologic reflexes that maintain dynamic coupling between O_2 delivery and metabolic demand (Ross et al., 1962; Frandsenn et al., 2001). For the COVID-19 subjects to offset the reduction in blood O_2-carrying capacity resulting from anemia (shown in Figure 5E), we would have expected a larger adaptive increase in p50 (Figure 5A) and a resulting greater difference between the healthy control and COVID-19 subjects in terms of blood O_2 content per gram Hb (Figure 5D). Conversely, we observed diminished O_2 capacitance (accounting for both the effect of anemia and lack of adaptation in HbO_2 affinity, i.e., calculated as the amount of O_2 unloaded for a given A-V pO_2 difference from ODCs 16; Figure 5F). This finding quantifies the burden of increased cardiac output required to compensate for impaired blood O_2 transport capacitance in COVID-19 subjects, which

10.3389/fphys.2023.1320697

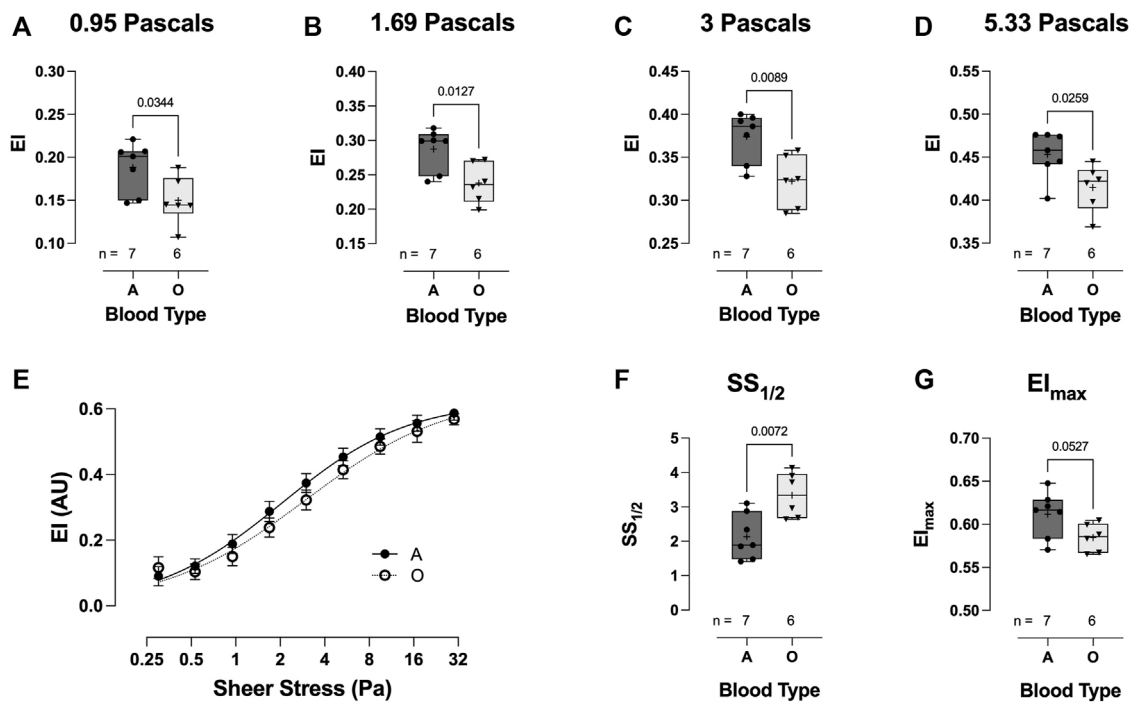

FIGURE 8
Effect of blood-types A and O on COVID-19 shear-induced RBC deformability. RBCs from COVID-19 subjects with blood-type A demonstrated significantly greater deformability at 0.95 **(A)**, 1.69 **(B)**, 3 **(C)**, and 5.33 Pa **(D)** than those from individuals with blood-type O. No differences were observed in the plotted deformability curves **(E)**; however, SS1/2 was significantly reduced in blood-type A than in blood-type O **(F)**, whilst calculated Elmax was higher **(G)**. Data are presented as the box and whiskers plot. The median is indicated by a solid line, and the mean is represented by +.

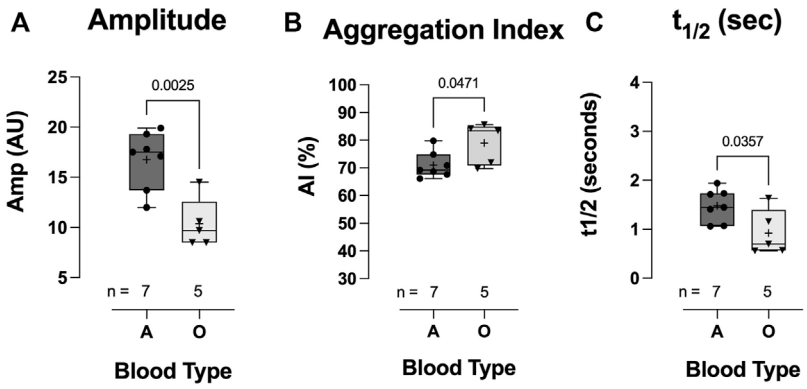

FIGURE 9
Effect of blood-types A and O on COVID-19 RBC aggregation. Individuals with blood-type A demonstrated significantly greater total aggregation (amplitude) **(A)** but a slower aggregation response, i.e., lower aggregation index **(B)** and longer t1/2 **(C)**. Data are presented as the box and whisker plot. The median is indicated by a solid line, and the mean is represented by +. Notably, one blood-type O individual did not have enough blood for aggregation measurement.

requires an increase of 130%–140% in cardiac output relative to that in healthy control individuals (Figure 5G, calculated from Figure 5F, i.e., the fold difference in O_2 capacitance between COVID-19 subjects and healthy controls). This is particularly problematic since the demand for increased cardiac output burdens the myocardium with increased work despite concurrent diminished myocardial O_2 delivery.

Numerous physical (i.e., deformability) and biochemical (i.e., factors which modulate vascular smooth muscle contractility) properties of RBCs play an essential role in determining microcirculatory flow (Lanotte et al., 2016) and as such play a significant role in maintaining O_2 homeostasis. RBC biomechanical properties have been previously demonstrated to be altered in COVID-19 subjects

(Kubankova et al., 2021; Grau et al., 2022), with RBCs exhibiting structural protein damage and membrane lipid remodeling (Thomas et al., 2020). We likewise demonstrate a significant reduction in RBC deformability across an isotonic shear stress gradient—LORRCA, RR Mechatronics 0.53–30 Pa (Figure 3). Deformability was also measured across an osmotic gradient (osmotic fragility—LORRCA Osmoscan), wherein we observed greater RBC deformability in RBCs from COVID-19 subjects than in those from healthy controls at low osmolality (i.e., higher EImin) in combination with a lower dynamic range in deformability across the osmotic gradient (i.e., lower deltaEI), suggestive of a lower surface area-to-volume ratio of the COVID-19 RBCs compared to the healthy controls, and/or a loss in the ability to regulate cell volume. A decrease in the surface area-to-volume ratio could be explained by increased blebbing and loss of damaged membrane from the COVID-19 RBCs, whilst loss of the ability to regulate cell volume might result from impaired RBC energetics, with reduced ATP for ion channel function, although the lack of change in p50 values between groups is suggestive of no critical change in ATP content. Furthermore, we also observed significant differences in RBC aggregation kinetics between the hospitalized COVID-19 subjects and controls, with COVID-19 enhancing aggregation, as shown by others (Nader et al., 2021; Renoux et al., 2021). In combination, these changes observed for RBCs from hospitalized COVID-19 subjects indicate rheological impairment that would be expected to significantly impair blood flow and contribute to dysregulation of O_2 delivery homeostasis.

RBCs themselves also play an essential role in matching perfusion sufficiency to O_2 demand via the release or scavenging of vasoactive signaling molecules (NO, NO+, and ATP). One such reflex is the regulation of hypoxic vasodilation (Ross et al., 1962; McMahon et al., 2000; Pawloski et al., 2001; McMahon et al., 2002; Buehler and Alayash, 2004; Singel and Stamler, 2005) through a series of O_2-responsive, thiol-based transfers of NO groups to the endothelium (McMahon et al., 2002; Doctor et al., 2005; Palmer et al., 2007). We assessed the ability of RBCs to elicit the HVD response in the aortic tissue ring bath. Interestingly, we observed no difference in the HVD response between RBCs from hospitalized COVID-19 subjects and healthy controls. This was somewhat surprising, given the fact that others have shown higher levels of NO inside RBCs from COVID-19 hypoxemic subjects (Mortaz et al., 2020). Whilst the mechanism(s) causing the accumulation of intracellular NO in RBCs of COVID-19 subjects is still unclear, it appears that the higher NO content is not associated with an increase in vasoactive NO species release under hypoxic conditions, and thus, the physiologic relevance of this increased NO remains undefined.

Several recent studies have investigated the association between blood type and COVID-19 infection (Kim et al., 2021). Whilst it has been reported that blood-type A might be predisposed to increased susceptibility of infection with SARS-CoV-2 and type O and Rh-negative blood groups might be protective, no clear relationship appears to exist between blood type and COVID-19-related severity of illness or mortality. We looked to identify whether any relationship existed between blood type and RBC features related to maintenance of O_2 homeostasis. In a limited subset of individuals, we compared RBCs of hospitalized COVID-19 subjects with blood type A or O. Somewhat surprisingly, we observed that the abnormal RBC properties associated with hospitalized COVID-19 subjects appeared exaggerated in blood-type O hospitalized COVID-19 subjects compared to blood type A. This is contrary to a reported putative protective role of blood-type O in terms of severity of illness and mortality.

We are aware of the limitations of our study. First, we acknowledge the small subject size, in addition to the fact that the hospitalized COVID-19 subjects 1) present with numerous comorbidities, which might also be expected to influence RBC physiology, in addition to 2) being given medications that might potentially have impacted the measurements herein (i.e., O_2 affinity and NO metabolism). It is also likely that even though all subjects studied were hospitalized, which itself is an indication of disease severity, individuals studied had wide-ranging morbidity; thus, the variance in the data from COVID-19 subjects likely reflect wide-ranging subject morbidity. We also wish to highlight that acute inflammation itself is known to affect RBC rheological properties (Pretorius, 2018). Consequently, we cannot rule out that altered RBC features observed in hospitalized COVID-19 subjects may have resulted from the inflammatory response induced by COVID-19 and not directly from COVID-19 virus interaction with RBCs. Rheological studies have previously demonstrated blood sensitivity to anti-coagulant, short-term storage, and cold shock (Baskurt et al., 2009). We consequently wish to highlight that a subset of the healthy controls (n = 6) was collected in EDTA (all remaining samples were collected in heparin). Furthermore, this small subset of controls was analyzed within 24 h of collection, while all other samples were analyzed within 6 h of collection (no significant differences in any of the measurements were observed between this subset and the other controls). To put into context the impairment in blood oxygen transport capacitance observed in COVID-19 subjects, we calculated the increase in cardiac output necessary to compensate for this. We would like to highlight that cardiac output was not measured in this study. In addition, we did not collect data on mechanical ventilation, which would increase pulmonary vascular resistance, due to inflation in lung volume, and would affect the cardiac output. Finally, the samples for aggregation studies were not normalized for hematocrit. Despite these limitations, our observations highlight that multiple RBC features essential for the maintenance of O_2 delivery homeostasis and the matching of perfusion sufficiency to O_2 demand are disrupted in hospitalized COVID-19 subjects and that the surface chemistry of the RBC may play a role in COVID-19-related RBC impairment. This could explain the enhanced risk for thromboembolic events observed in COVID-19 subjects as well as impairment to microvascular blood flow. Whilst these findings demonstrate altered RBC properties in the acute phase of infection, it would be interesting to further study and follow on hospital release to assess whether these features are prolonged for the lifespan of RBCs (i.e. 120 days) and/or play a role in long-term COVID-19.

Data availability statement

The raw data supporting the conclusion of this article will be made available by the authors, without undue reservation.

Ethics statement

The studies involving humans were approved by the University of Maryland CICERO Institutional Review Board (IRB). The studies were conducted in accordance with the local legislation and institutional requirements. The participants provided their written informed consent to participate in this study. The animal study was approved by the University of Maryland Institutional Animal Care and Use Committee (IACUC). The study was conducted in accordance with the local legislation and institutional requirements.

Author contributions

SR: conceptualization, data curation, formal analysis, investigation, methodology, project administration, supervision, writing–original draft, and writing–review and editing. MB: data curation, investigation, methodology, project administration, supervision, and writing–review and editing. ZS: data curation, investigation, methodology, and writing–review and editing. QW: investigation, project administration, supervision, and writing–review and editing. TR: investigation, project administration, and writing–review and editing. TB: investigation, project administration, and writing–review and editing. AD: conceptualization, data curation, formal analysis, funding acquisition, project administration, resources, supervision, writing–original draft, and writing–review and editing.

Funding

The author(s) declare that financial support was received for the research, authorship, and/or publication of this article. The study was supported by Research Support R01GM113838 and R01HL161071.

Conflict of interest

The authors declare that the research was conducted in the absence of any commercial or financial relationships that could be construed as a potential conflict of interest.

Publisher's note

All claims expressed in this article are solely those of the authors and do not necessarily represent those of their affiliated organizations, or those of the publisher, the editors, and the reviewers. Any product that may be evaluated in this article, or claim that may be made by its manufacturer, is not guaranteed or endorsed by the publisher.

References

Barnkob, M. B., Pottegard, A., Stovring, H., Haunstrup, T. M., Homburg, K., Larsen, R., et al. (2020). Reduced prevalence of SARS-CoV-2 infection in ABO blood group O. *Blood Adv.* 4 (20), 4990–4993. doi:10.1182/bloodadvances.2020002657

Baskurt, O. K., Boynard, M., Cokelet, G. C., Connes, P., Cooke, B. M., Forconi, S., et al. (2009). New guidelines for hemorheological laboratory techniques. *Clin. Hemorheol. Microcirc.* 42 (2), 75–97. doi:10.3233/CH-2009-1202

Benesch, R. E., Benesch, R., and Yu, C. I. (1969). The oxygenation of hemoglobin in the presence of 2,3-diphosphoglycerate. Effect of temperature, pH, ionic strength, and hemoglobin concentration. *Biochemistry.* 8 (6), 2567–2571. doi:10.1021/bi00834a046

Bergamaschi, G., Borrelli de Andreis, F., Aronico, N., Lenti, M. V., Barteselli, C., Merli, S., et al. (2021). Anemia in patients with Covid-19: pathogenesis and clinical significance. *Clin. Exp. Med.* 21 (2), 239–246. doi:10.1007/s10238-020-00679-4

Boning, D., and Enciso, G. (1987). Hemoglobin-oxygen affinity in anemia. *Blut.* 54 (6), 361–368. doi:10.1007/BF00626019

Boning, D., Kuebler, W. M., and Bloch, W. (2021). The oxygen dissociation curve of blood in COVID-19. *Am. J. Physiol. Lung Cell Mol. Physiol.* 321 (2), L349–L357. doi:10.1152/ajplung.00079.2021

Boschi, C., Scheim, D. E., Bancod, A., Militello, M., Bideau, M. L., Colson, P., et al. (2022). SARS-CoV-2 spike protein induces hemagglutination: implications for COVID-19 morbidities and therapeutics and for vaccine adverse effects. *Int. J. Mol. Sci.* 23 (24), 15480. doi:10.3390/ijms232415480

Bouchla, A., Kriebardis, A. G., Georgatzakou, H. T., Fortis, S. P., Thomopoulos, T. P., Lekkakou, L., et al. (2021). Red blood cell abnormalities as the mirror of SARS-CoV-2 disease severity: a pilot study. *Front. physiology* 12, 825055. doi:10.3389/fphys.2021.825055

Buehler, P. W., and Alayash, A. I. (2004). Oxygen sensing in the circulation: "cross talk" between red blood cells and the vasculature. *Antioxidants redox Signal.* 6 (6), 1000–1010. doi:10.1089/ars.2004.6.1000

Chen, C., Zhou, W., Fan, W., Ning, X., Yang, S., Lei, Z., et al. (2021). Association of anemia and COVID-19 in hospitalized patients. *Future Virol.* 16, 459–466. doi:10.2217/fvl-2021-0044

Clark, M. R., Mohandas, N., and Shohet, S. B. (1983). Osmotic gradient ektacytometry: comprehensive characterization of red cell volume and surface maintenance. *Blood.* 61 (5), 899–910. doi:10.1182/blood.v61.5.899.bloodjournal615899

Daniel, Y., Hunt, B. J., Retter, A., Henderson, K., Wilson, S., Sharpe, C. C., et al. (2020). Haemoglobin oxygen affinity in patients with severe COVID-19 infection. *Br. J. Haematol.* 190 (3), e126–e127. doi:10.1111/bjh.16888

DeMartino, A. W., Rose, J. J., Amdahl, M. B., Dent, M. R., Shah, F. A., Bain, W., et al. (2020). No evidence of hemoglobin damage by SARS-CoV-2 infection. *Haematologica* 105 (12), 2769–2773. doi:10.3324/haematol.2020.264267

Dobbe, J. G., Streekstra, G. J., Strackee, J., Rutten, M. C., Stijnen, J. M., and Grimbergen, C. A. (2003). Syllectometry: the effect of aggregometer geometry in the assessment of red blood cell shape recovery and aggregation. *IEEE Trans. Biomed. Eng.* 50 (1), 97–106. doi:10.1109/TBME.2002.807319

Doctor, A., Platt, R., Sheram, M. L., Eischeid, A., McMahon, T., Maxey, T., et al. (2005). Hemoglobin conformation couples erythrocyte S-nitrosothiol content to O2 gradients. *Proc. Natl. Acad. Sci. U. S. A.* 102 (16), 5709–5714. doi:10.1073/pnas.0407490102

Doctor, A., and Stamler, J. S. (2011). Nitric oxide transport in blood: a third gas in the respiratory cycle. *Compr. Physiol.*, 12011. doi:10.1002/cphy.c090009

Elemam, N. M., Talaat, I. M., Bayoumi, F. A., Zein, D., Georgy, R., Altamimi, A., et al. (2022). Peripheral blood cell anomalies in COVID-19 patients in the United Arab Emirates: a single-centered study. *Front. Med. (Lausanne)* 9, 1072427. doi:10.3389/fmed.2022.1072427

Frandsenn, U., Bangsbo, J., Sander, M., Höffner, L., Betak, A., Saltin, B., et al. (2001). Exercise-induced hyperaemia and leg oxygen uptake are not altered during effective inhibition of nitric oxide synthase with N(G)-nitro-L-arginine methyl ester in humans. *J. Physiol.* 531 (Pt 1), 257–264. doi:10.1111/j.1469-7793.2001.0257j.x

Grau, M., Ibershoff, L., Zacher, J., Bros, J., Tomschi, F., Diebold, K. F., et al. (2022). Even patients with mild COVID-19 symptoms after SARS-CoV-2 infection show prolonged altered red blood cell morphology and rheological parameters. *J. Cell Mol. Med.* 26 (10), 3022–3030. doi:10.1111/jcmm.17320

Guarnone, R., Centenara, E., and Barosi, G. (1995). Performance characteristics of Hemox-Analyzer for assessment of the hemoglobin dissociation curve. *Haematologica* 80 (5), 426–430.

Gutierrez, M., Shamoun, M., Seu, K. G., Tanski, T., Kalfa, T. A., and Eniola-Adefeso, O. (2021). Characterizing bulk rigidity of rigid red blood cell populations in sickle-cell disease patients. *Sci. Rep.* 11 (1), 7909. doi:10.1038/s41598-021-86582-8

James, P. E., Lang, D., Tufnell-Barret, T., Milsom, A. B., and Frenneaux, M. P. (2004). Vasorelaxation by red blood cells and impairment in diabetes: reduced nitric oxide and oxygen delivery by glycated hemoglobin. *Circulation Res.* 94 (7), 976–983. doi:10.1161/01.RES.0000122044.21787.01

Kim, Y., Latz, C. A., DeCarlo, C. S., Lee, S., Png, C. Y. M., Kibrik, P., et al. (2021). Relationship between blood type and outcomes following COVID-19 infection. *Semin. Vasc. Surg.* 34 (3), 125–131. doi:10.1053/j.semvascsurg.2021.05.005

Kubankova, M., Hohberger, B., Hoffmanns, J., Fürst, J., Herrmann, M., Guck, J., et al. (2021). Physical phenotype of blood cells is altered in COVID-19. *Biophysical J.* 120 (14), 2838–2847. doi:10.1016/j.bpj.2021.05.025

Lam, L. K. M., Reilly, J. P., Rux, A. H., Murphy, S. J., Kuri-Cervantes, L., Weisman, A. R., et al. (2021). Erythrocytes identify complement activation in patients with COVID-19. *Am. J. Physiol. Lung Cell Mol. Physiol.* 321 (2), L485–L489. doi:10.1152/ajplung.00231.2021

Lam, L. M., Murphy, S. J., Kuri-Cervantes, L., Weisman, A. R., Ittner, A. C., Reily, J. P. R., et al. (2020). *Erythrocytes reveal complement activation in patients with COVID-19*. medRxiv.

Lanotte, L., Mauer, J., Mendez, S., Fedosov, D. A., Fromental, J. M., Claveria, V., et al. (2016). Red cells' dynamic morphologies govern blood shear thinning under microcirculatory flow conditions. *Proc. Natl. Acad. Sci. U. S. A.* 113 (47), 13289–13294. doi:10.1073/pnas.1608074113

Lazarova, E., Gulbis, B., Oirschot, B. V., and van Wijk, R. (2017). Next-generation osmotic gradient ektacytometry for the diagnosis of hereditary spherocytosis: interlaboratory method validation and experience. *Clin. Chem. Lab. Med.* 55 (3), 394–402. doi:10.1515/cclm-2016-0290

Mairbaurl, H., and Weber, R. E. (2012). Oxygen transport by hemoglobin. *Compr. Physiol.* 2 (2), 1463–1489. doi:10.1002/cphy.c080113

McMahon, T. J., Exton Stone, A., Bonaventura, J., Singel, D. J., and Solomon Stamler, J. (2000). Functional coupling of oxygen binding and vasoactivity in S-nitrosohemoglobin. *J. Biol. Chem.* 275 (22), 16738–16745. doi:10.1074/jbc.M000532200

McMahon, T. J., Moon, R. E., Luschinger, B. P., Carraway, M. S., Stone, A. E., Stolp, B. W., et al. (2002). Nitric oxide in the human respiratory cycle. *Nat. Med.* 8 (7), 711–717. doi:10.1038/nm718

Montenegro, F., Unigarro, L., Paredes, G., Moya, T., Romero, A., Torres, L., et al. (2021). Acute respiratory distress syndrome (ARDS) caused by the novel coronavirus disease (COVID-19): a practical comprehensive literature review. *Expert Rev. Respir. Med.* 15 (2), 183–195. doi:10.1080/17476348.2020.1820329

Mortaz, E., Malkmohammad, M., Jamaati, H., Naghan, P. A., Hashemian, S. M., Tabarsi, P., et al. (2020). Silent hypoxia: higher NO in red blood cells of COVID-19 patients. *BMC Pulm. Med.* 20 (1), 269. doi:10.1186/s12890-020-01310-8

Nader, E., Nougier, C., Boisson, C., Poutrel, S., Catella, J., Martin, F., et al. (2021). Increased blood viscosity and red blood cell aggregation in patients with COVID-19. *Am. J. Hematol.* 97, 283–292. doi:10.1002/ajh.26440

Palmer, L. A., Doctor, A., Chhabra, P., Sheram, M. L., Laubach, V. E., Karlinsey, M. Z., et al. (2007). S-nitrosothiols signal hypoxia-mimetic vascular pathology. *J. Clin. investigation* 117 (9), 2592–2601. doi:10.1172/JCI29444

Pawloski, J. R., Hess, D. T., and Stamler, J. S. (2001). Export by red blood cells of nitric oxide bioactivity. *Nature* 409 (6820), 622–626. doi:10.1038/35054560

Pinder, A. G., Rogers, S. C., Morris, K., and James, P. E. (2009). Haemoglobin saturation controls the red blood cell mediated hypoxic vasorelaxation. *Adv. Exp. Med. Biol.* 645, 13–20. doi:10.1007/978-0-387-85998-9_3

Pretorius, E. (2018). Erythrocyte deformability and eryptosis during inflammation, and impaired blood rheology. *Clin. Hemorheol. Microcirc.* 69 (4), 545–550. doi:10.3233/CH-189205

Renoux, C., Fort, R., Nader, E., Boisson, C., Joly, P., Stauffer, E., et al. (2021). Impact of COVID-19 on red blood cell rheology. *Br. J. Haematol.* 192 (4), e108–e111. doi:10.1111/bjh.17306

Ross, J. M., Fairchild, H. M., Weldy, J., and Guyton, A. C. (1962). Autoregulation of blood flow by oxygen lack. *Am. J. Physiol.* 202, 21–24. doi:10.1152/ajplegacy.1962.202.1.21

Sender, R., Fuchs, S., and Milo, R. (2016). Revised estimates for the number of human and bacteria cells in the body. *PLoS Biol.* 14 (8), e1002533. doi:10.1371/journal.pbio.1002533

Severe Covid, G. G., Ellinghaus, D., Degenhardt, F., Bujanda, L., Buti, M., Albillos, A., et al. (2020). Genomewide association study of severe covid-19 with respiratory failure. *N. Engl. J. Med.* 383 (16), 1522–1534. doi:10.1056/NEJMoa2020283

Singel, D. J., and Stamler, J. S. (2005). Chemical physiology of blood flow regulation by red blood cells: the role of nitric oxide and S-nitrosohemoglobin. *Annu. Rev. physiology* 67, 99–145. doi:10.1146/annurev.physiol.67.060603.090918

Taneri, P. E., Gomez-Ochoa, S. A., Llanaj, E., Raguindin, P. F., Rojas, L. Z., Roa-Díaz, Z. M., et al. (2020). Anemia and iron metabolism in COVID-19: a systematic review and meta-analysis. *Eur. J. Epidemiol.* 35 (8), 763–773. doi:10.1007/s10654-020-00678-5

Thomas, T., Stefanoni, D., Dzieciatkowska, M., Issaian, A., Nemkov, T., Hill, R. C., et al. (2020). Evidence of structural protein damage and membrane lipid remodeling in red blood cells from COVID-19 patients. *J. proteome Res.* 19 (11), 4455–4469. doi:10.1021/acs.jproteome.0c00606

Wang, K., Chen, W., Zhang, Z., Deng, Y., Lian, J. Q., Du, P., et al. (2020). CD147-spike protein is a novel route for SARS-CoV-2 infection to host cells. *Signal Transduct. Target Ther.* 5 (1), 283. doi:10.1038/s41392-020-00426-x

Weisel, J. W., and Litvinov, R. I. (2019). Red blood cells: the forgotten player in hemostasis and thrombosis. *J. Thromb. Haemost.* 17 (2), 271–282. doi:10.1111/jth.14360

Wong, R. S. Y. (2021). Inflammation in COVID-19: from pathogenesis to treatment. *Int. J. Clin. Exp. Pathol.* 14 (7), 831–844.

Wu, S. C., Arthur, C. M., Jan, H. M., Garcia-Beltran, W. F., Patel, K. R., Rathgeber, M. F., et al. (2023). Blood group A enhances SARS-CoV-2 infection. *Blood* 142 (8), 742–747. doi:10.1182/blood.2022018903

Zhu, N., Zhang, D., Wang, W., Li, X., Yang, B., Song, J., et al. (2020). A novel coronavirus from patients with pneumonia in China. *N. Engl. J. Med.* 382 (8), 727–733. doi:10.1056/NEJMoa2001017

frontiers | Frontiers in Physiology

TYPE Perspective
PUBLISHED 10 April 2024
DOI 10.3389/fphys.2024.1363987

OPEN ACCESS

EDITED BY
Lars Kaestner,
Saarland University, Germany

REVIEWED BY
Vassilis L. Tzounakas,
University of Patras, Greece

*CORRESPONDENCE
Kate Hsu,
khsu1@mmh.org.tw

RECEIVED 31 December 2023
ACCEPTED 21 March 2024
PUBLISHED 10 April 2024

CITATION
Hsu K (2024), Erythroid anion transport, nitric oxide, and blood pressure.
Front. Physiol. 15:1363987.
doi: 10.3389/fphys.2024.1363987

Erythroid anion transport, nitric oxide, and blood pressure

Kate Hsu [1,2,3]*

[1]The Laboratory of Immunogenetics, Department of Medical Research, MacKay Memorial Hospital, New Taipei City, Taiwan, [2]MacKay Junior College of Medicine, Nursing, and Management, New Taipei City, Taiwan, [3]Institute of Biomedical Sciences, MacKay Medical College, New Taipei City, Taiwan

Glycophorin A and glycophorin B are structural membrane glycoproteins bound in the band 3 multiprotein complexes on human red blood cells (RBCs). Band 3 is an erythroid-specific anion exchanger (AE1). AE1-mediated HCO_3^- transport provides the substrate for the enzyme-catalyzed conversion $HCO_{3\,(aq)}^- \rightleftharpoons CO_{2(g)}$, which takes place inside the RBCs. Bicarbonate transport via AE1 supports intravascular acid–base homeostasis and respiratory excretion of CO_2. In the past decade, we conducted several comparative physiology studies on Taiwanese people having the glycophorin variant GPMur RBC type (which accompanies greater AE1 expression). We found that increased anion transport across the erythrocyte membrane not only enhances gas exchange and lung functions but also elevates blood pressure (BP) and reduces nitric oxide (NO)-dependent vasodilation and exhaled NO fraction (FeNO) in healthy individuals with GP.Mur. Notably, in people carrying the GPMur blood type, the BP and NO-dependent, flow-mediated vasodilation (FMD) are both more strongly correlated with individual hemoglobin (Hb) levels. As blood NO and nitrite (NO_2^-) are predominantly scavenged by intraerythrocytic Hb, and NO_2^- primarily enters RBCs via AE1, could a more monoanion-permeable RBC membrane (i.e., GPMur/increased AE1) enhance NO_2^-/NO_3^- permeability and Hb scavenging of NO_2^- and NO to affect blood pressure? In this perspective, a working model is proposed for the potential role of AE1 in intravascular NO availability, blood pressure, and clinical relevance.

KEYWORDS

band 3 (anion exchanger-1, AE1), GP.Mur (Miltenberger subtype III, Mi.III), nitric oxide, blood pressure, vasodilation, dipyridamole, glycophorin, erythrocyte

Introduction

Hemoglobin (Hb) is the main scavenger of NO species in the mammalian vasculature (Lancaster, 1994; Patel et al., 2011). Band 3, an anion transporter with ~ a million protein copies per human RBC, has been postulated to play a critical role in erythrocyte processing of NO species since late 1990s (Vaughn et al., 2000; Huang et al., 2001; Pawloski et al., 2001; Han et al., 2003; Kim-Shapiro et al., 2006; Jana et al., 2018; Premont et al., 2020). We came across this perplexing topic of research when we were conducting human exercise tests that examined the impacts of GP.Mur on respiration and unexpectedly found a significant association between GP.Mur and higher blood pressure. GP.Mur (a glycophorin B-A-B variant exclusively expressed on human RBCs) is a blood type unique to Southeast Asian (SEA) populations, with ~4.7% prevalence in Taiwan and 2–23% in many areas of SEA, and is rare among non-SEA ethnic populations (e.g., Japanese and other ethnic groups of the Northeastern Asian origins) (Prathiba et al., 2002; Hsu et al., 2013; Wei et al., 2016; Jongruamklang et al., 2020; Yang et al., 2021; Kaito et al., 2022). The main molecular

function of GP.Mur is to enhance AE1 protein expression on the RBC membrane (Hsu et al., 2009). Since the cytoplasmic domain of AE1 binds hemoglobin (preferentially deoxyHb) in the submembranous interface and deoxyHb also functions as a nitrite reductase that produces nitric oxide (Walder et al., 1984; Gladwin et al., 2009), we hypothesized that AE1 might be involved in regulation of blood pressure through intraerythrocytic Hb–NOx reactions.

Blood pressure and NO-dependent vasodilation are affected by GP.Mur/increased AE1

From the respiratory/exercise physiology studies conducted on healthy adults and professional athletes, we repeatedly observed a slightly but statistically significant higher systolic blood pressure (SBP) among those carrying the GP.Mur blood type (Hsu et al., 2015; Chen et al., 2022; Hsu et al., 2023). For verification, we collaborated with one of our health check-up centers located in Eastern Taiwan, where the GP.Mur+ population is four times higher than that in other regions of Taiwan (Chen et al., 2022). We selected 989 Eastern Taiwanese residents under 55 years of age (one-fifth of them were GP.Mur+) whose clinical laboratory data from the annual health check-up were within the normal ranges and who were not on any drug treatments, including antihypertensives. Among them, the non-diseased men and women with GP.Mur indeed presented 3–5 mmHg higher systolic blood pressure (SBP) than the negative control people (Chen et al., 2022). Intriguingly, in this study, the incidence of early-onset hypertension (BP > 130/80 mmHg in those ≤45 years old) is significantly higher among GP.Mur+ carriers. Young men and women under 45 years of age are 1.6-fold and 3.4-fold more likely to present hypertension than age-matched controls living in the same area. As early-onset hypertension is largely hereditary (Suvila et al., 2020), this type of early-onset hypertension found among GP.Mur+ carriers is unlikely to be mainly due to unhealthy lifestyles ("GP.Mur-unique hypertension").

To test our hypothesis that AE1-Hb could contribute to "GP.Mur-unique hypertension" via AE1–Hb–NO reactions in RBCs, we examined the impacts of GP.Mur/more AE1 on NO-dependent vasodilation in male college athletes. We measured their flow-mediated vasodilation (FMD, reflecting NO-mediated vasodilation (Green et al., 2014)) and nitroglycerin-induced, NO-independent vasodilation (NID) in this homogeneous population. Ultrasound was used to track vasodilation or the degree of increase in the brachial arterial diameter of each subject during a period of stimulation and recovery (FMD was stimulated by 5-minute vasoconstriction and NID by sublingual nitroglycerin). While NID in GP.Mur+ and the control athletes was not different, FMD measured in the GP.Mur+ athletes was significantly lower than FMD measured in the control athletes (4.6% ± 2.3% [GP.Mur] versus 6.3% ± 2.4% [control]) (Hsu et al., 2021).

Stronger dependence of FMD and BP on Hb levels in GP.Mur+ people

From a seminal study on Andean high-altitude dwellers with excessive erythrocytosis (EE), a significantly inverse correlation was found between Hb and NO-dependent vasodilation (%FMD) in EE patients (Tremblay et al., 2019). In these GP.Mur+ athletes, we also observed a significantly inverse correlation between Hb and %FMD (Figure 1B: the correlation is shown as the solid line); this correlation was not found in the control athletes (Figure 1B: shown as a dotted line as the correlation was not statistically significant) (Hsu et al., 2021). A closer comparison between Tremblay's and our data revealed a key difference: Hb in the highlanders with EE was abnormally high (20–27 g/dL), and that for the male college athletes in this study with or without GP.Mur was all within the normal range for men (12.5–17 g/dL). The inverse correlation of Hb-FMD was not found in our GPMur-negative control athletes or in the Andean non-patient highlander subjects whose Hb levels were below 21 g/dL (Tremblay et al., 2019). Hb is a major NO scavenger, and abnormally high Hb concentrations (accompanied with an abnormally higher RBC count) undoubtedly scavenge more NO in the vasculature and result in lower FMD (as in the EE cases). In contrast, the significant Hb–FMD inverse correlation found within the normal range of Hb in the GP.Mur+ subjects indicates that their NO-dependent vasodilation is more sensitive to intravascular Hb concentrations (Figure 1B).

Hb and blood pressure are weakly but directly correlated. The direct correlation of Hb and BP was first identified in half a million Dutch blood donors at Sanquin: an increase of 1 g/dL Hb accompanies an increase of ~0.81 mmHg SBP among Dutch men (Atsma et al., 2012). The degrees of the Hb–BP correlation vary slightly between men and women or among different ethnic populations (Gobel et al., 1991; Kawamoto et al., 2012; Lee et al., 2015; Xuan et al., 2019; Abumohsen et al., 2021).

In our population study conducted at the health check-up center in Eastern Taiwan, an increase of 1 g/dL Hb accompanies a ~2.9 mmHg increase of SBP in GP.Mur+ men, compared to an ~1.8 mmHg increase of SBP in the control (GP.Mur-negative) men, after controlled for age and BMI by multivariate regression (Figure 1C) (Chen et al., 2022). Compared to the controls, the blood pressure in the GP.Mur+ men was ~60% more dependent on individual Hb levels. The positive correlation between Hb and BP could be caused by the following: (1) more circulating RBCs (as shown with an abnormally higher RBC count and Hb concentrations in high-altitude EE) increase blood viscosity and intravascular pressure (Tremblay et al., 2019), and (2) Hb scavenges intravascular NO species more effectively (as shown with a stronger Hb–FMD correlation and stronger Hb–BP correlation found in GP.Mur+ carriers) (Figure 1B, C) (Hsu et al., 2021; Chen et al., 2022). Since Hb is enclosed inside the RBC membrane, the second scenario points to the fact that GP.Mur/increased AE1 activities on the RBC membrane could promote Hb scavenging of NO species during blood circulation.

Toward developing a hypothesis that increased AE1 expression could reduce systemic NO

A higher monoanion permeability of the GP.Mur+ RBC membrane enhances the NO_2^-/NO_3^- flux across the RBC membrane and intraerythrocytic processing of NO species (Figure 1A, D). NO_2^- and NO_3^- (nitrate) are the major

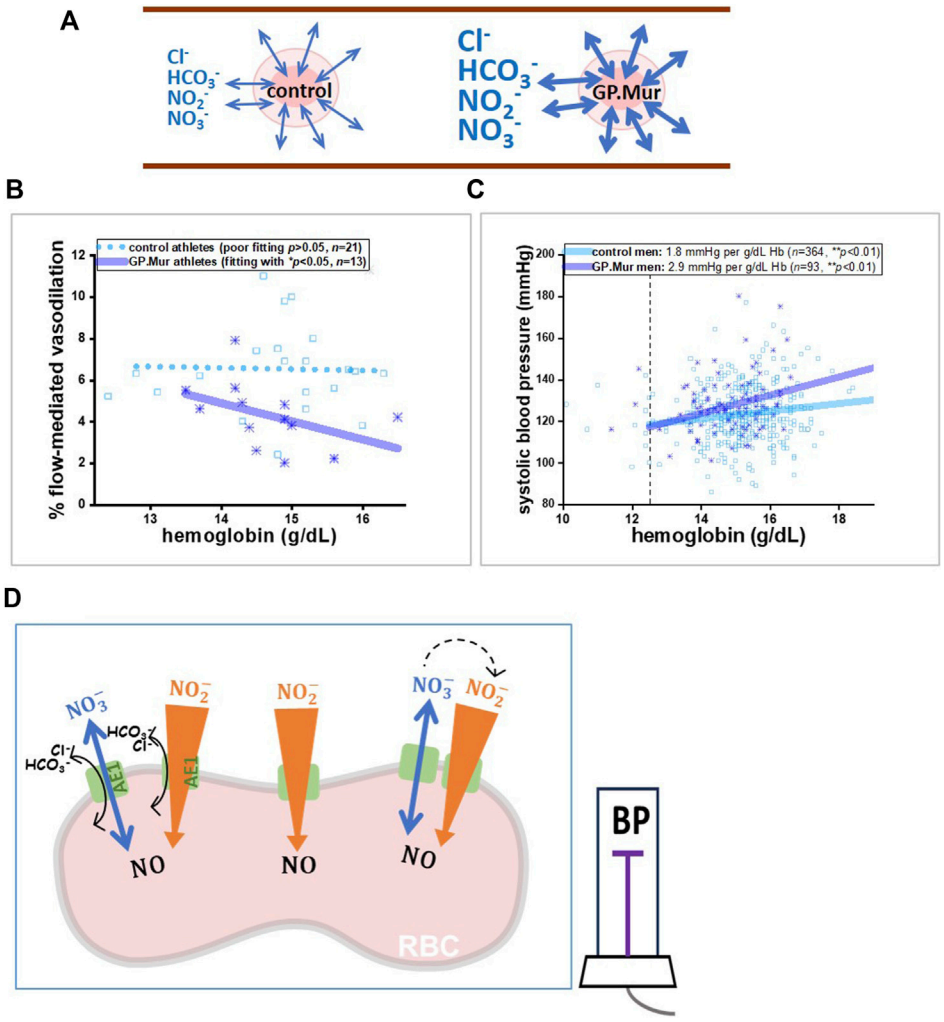

FIGURE 1
A model illustrating that GP.Mur/higher AE1 expression could increase NOx metabolic cycling and NO scavenging by intraerythrocytic Hb. **(A)** The bidirectional arrows indicate anion fluxes (mostly HCO_3^-, Cl^-, NO_2^-, and NO_3^-) via AE1 (Jennings, 2021). The GP.Mur+ RBC membrane is more permeable to these monoanions (shown as thicker bidirectional arrows). **(B, C)** Previous studies on healthy people showed that GPMur/increased AE1 imposes higher sensitivities of FMD and SBP to Hb levels. **(B)** The Hb–FMD correlation for GP.Mur+ male athletes (R ~ 0.53) was replotted using the published data (Hsu et al., 2021). **(C)** The Hb–SBP correlations for GP.Mur+ men (R ~ 0.44) and for control men (R ~ 0.37) were replotted using the published data collected at the MMH health check-up center in Eastern Taiwan (Chen et al., 2022). These GP.Mur comparative human studies revealed that GP.Mur/higher AE1 expression reduces NO-dependent FMD and increases blood pressure. **(D)** In the proposed model, AE1 (green gate) transports nitrite (orange-colored arrow) and nitrate (blue arrow) across the red cell membrane. Nitrite influx is followed by rapid and complex redox reactions catalyzed by Hb inside the RBCs, and thus the large concentration gradient of nitrite across the RBC membrane should favor nitrite influx (Chen et al., 2024). Nitrate is generally synthesized from excessive NO by oxyHb and is a stable reservoir of NO that permeates in or out of the RBCs via AE1 following its concentration gradient (bidirectional flux of nitrate). If depletion of plasma nitrite could accelerate the enzymatic conversion of extracellular nitrate to nitrite by nitrate reductase and xanthine oxidoreductase (dotted arrows), this may help explain how GP.Mur/higher AE1 lowers systemic NO and triggers high BP.

constituents of the intravascular NO reservoir. Excessive NO in the vasculature is mainly converted to nitrate by oxygenated Hb (NO + oxyHb → NO_3^- + metHb). Compared to nitrite, nitrate is a more stable and much less reactive NO metabolite. Both NO_2^- and NO_3^- freely permeate across the RBC membrane through AE1 (Jennings, 2021; Chen et al., 2024). The more reactive nitrite (half-life ~0.5 h compared to 5–8 h of nitrate) tends to be converted to NO in a less oxygenated environment, e.g., arterioles. This reaction stimulated by hypoxia (NO_2^- + deoxyHb → NO + metHb) facilitates vasodilation and blood flow (Cosby et al., 2003; Dejam et al., 2005). In the case of GP.Mur, enhanced nitrite flux helps facilitate deoxyHb-catalyzed reduction of nitrite to NO gas. NO, with a half-life of ~2 msec, dissipates extremely rapidly. Faster erythrocyte processing of NO conceivably may reduce systemic NO (Figure 1D).

However, from the previous study, we did not find blood plasma levels of NO_2^- and NO_3^- to be significantly different between GP.Mur+ and GP.Mur-negative athletes (Hsu et al., 2021), although we also did not ask the study participants to have the same diet. Various factors, including individual diet preferences, could dynamically affect their blood NOx levels (NO_2^- + NO_3^-). NO bioavailability can be increased in our body with consumption of more leafy green vegetables and beetroot (and even more nitrate-cured meats) in the diet.

On the other hand, fractional exhaled NO (FeNO) was affected by GP.Mur. FeNO was measured using NIOX, a clinical instrument

TABLE 1 FeNO from GP.Mur+ versus non-GP.Mur college athletes before and after an exhaustive running test. Minute ventilation (V_E) was measured by cardiopulmonary exercise testing (CPET), which was immediately followed by FeNO measurement within a minute post-run. Statistical testing was performed by unpaired *t*-test. *n.s.*, not significant. The study was approved by the MMH Institutional Review Board (MMH-IRB registration: 19MMHIS081e).

Group (N)	Non-GP.Mur (36)	GP.Mur (15)	*p*-value
Pre-run FeNO (ppb)	31.3 ± 22.4	21.3 ± 14.8	*n.s.*
1 min post-run FeNO (ppb)	25.5 ± 17.1	15.7 ± 10.7	$^*p < 0.05$
4 min post-run FeNO (ppb)	26.5 ± 16.8	17.9 ± 11.8	*n.s.*
Pre-run V_E (L/min)	13.5 ± 3.1	16.9 ± 4.8	$p < 0.05$
0–1 min post-run V_E (L/min)	132.3 ± 24.3	145.5 ± 17.1	$P \sim 0.06$
Pre-run VNO (nL/min)	339.0 ± 242.7	274.0 ± 171.0	*n.s.*
0–1 min post-run VNO (nL/min)	2771.3 ± 1983.1	1847.0 ± 1134.3	$^*p < 0.05$

that is intended to measure NO generated from Th2-driven inflammatory iNOS activities for the diagnosis of asthma (Menzies-Gow et al., 2020). We challenged the college athletes with an exhaustive running test protocol and measured their FeNO before the run and at the first and the fourth minute post-run. Their FeNO values decreased substantially from the exhaustive run and then rebounded gradually during the recovery phase, indicating a greater need for NO for vasodilation as intense exercise increased blood flow and gas exchange (Table 1: nearly 10-fold increases in minute ventilation [V_E]). Both FeNO and the minute volume of exhaled NO (VNO = V_E * FeNO) were generally lower in GP.Mur+ than GP.Mur-negative athletes, and the differences reached statistical significance immediately after exercise (Table 1: 1-min post-run measurements). iNOS-associated type II airway inflammation was not involved, and clinical asthma was not found in these athletes since none of them showed >50 ppb FeNO. Thus, GP.Mur/increased AE1 affected exhaled NO (FeNO), which reflects lower NO in the pulmonary vasculature, especially during exercise-expanded pulmonary circulation (Table 1).

Although the levels of blood plasma NO metabolites were not different between GP.Mur and non-GP.Mur college athletes (Hsu et al., 2021), in our recently developed *GYP.Mur* knock-in (GPMur KI) B6J mice, significantly reduced NO bioavailability and early-onset hypertension were observed (unpublished data). Unlike the human study (Hsu et al., 2021), GPMur KI and the wildtype B6J mice are all bred under the same condition and fed with the same chow. The new murine data support the hypothesis that GP.Mur/more AE1 could contribute to reduced NO bioavailability. Perhaps by means of reduction of blood NO bioavailability (e.g., nitrate), the individual blood pressure setting could be elevated. The eNOS knock-out mice also show similar phenotypes—reduced blood NO bioavailability and hypertension (Wood et al., 2013).

AE1 transports NO_2^-/NO_3^- for erythrocyte processing of NO

To examine the effects of AE1-mediated NO_2^-/NO_3^- transport on intraerythrocytic processing of NO species, we treated human whole blood samples (containing plasma and blood cells) with excessive nitrite (1 mM, compared to the generally submicromolar nitrite in human blood). The excessively added nitrite in the whole blood sample decreased from 1 mM to 10 μM within 20 min, indicating a rapid scavenging and metabolism of NO_2^- by Hb. Using live-cell image recording with NO-sensitive fluorophore DAF, a surge of DAF fluorescence inside the RBCs appeared visibly within 1–2 min after adding excessive NO_2^- in the milieu (Chen et al., 2024). If erythroid anion transport was first blocked by AE1-targeting antibodies or was delayed by replacing Cl^- (the counter-ion of AE1-mediated transport) with AE1-impermeant gluconate monoanion in the milieu, excessively added nitrite could remain imperishable in the blood plasma for a very long time. These demonstrate that inhibition of erythroid anion transport substantially reduces the rates of NO_2^-/NO scavenging and metabolism catalyzed by intraerythrocytic Hb (Chen et al., 2024).

Discussion

From our human studies conducted in 2017–2022, we found that GP.Mur/increased AE1 is associated with early-onset hypertension. Non-diseased people with the GP.Mur blood type generally have slightly higher blood pressure, lower NO-dependent vasodilation, and lower fraction of exhaled nitric oxide (Table 1; Figure 1B, C) (Hsu et al., 2021; Chen et al., 2022). It has been a general impression among health workers in Eastern Taiwan that the local populations with higher percentages of GP.Mur are more susceptible to stroke and type II diabetes (T2D), though rigorous epidemiologic surveys have not been reported. Notably, hypertension is the major risk factor for both stroke and T2D.

To understand how the expression of glycophorin B-A-B variant GP.Mur on RBCs leads to higher blood pressure, we began to formulate a working model with the basic science that it is thermodynamically unfavorable for charged ions to permeate through the lipid bilayer (Figure 1A, D). More AE1 embedded in the RBC membrane makes the cells more permeable to monoanions and expedites NO_2^-/NO_3^- membrane transport. NO_2^- influx is particularly affected, as its concentration gradient across the red cell membrane is presumably much bigger due to deoxyHb-mediated NO_2^- reduction to NO gas, which takes place inside the RBCs. When NO_2^- enters an erythrocyte, NO_2^- is also converted to N_2O_3, GSNO, and other NO species catalyzed by

the Hb of different oxidation states (Patel et al., 2011). Thus, higher AE1 expression accelerates intraerythrocytic NO_2^-/NO metabolism, driving the conversion of NO_3^- to NO_2^- by microbiota nitrate reductases and xanthine oxidoreductase (Kapil et al., 2013); this conceivably also lowers plasma nitrate.

Since GP.Mur/increased AE1 is associated with blood NOx reduction, could blockade of AE1 instead help maintain NO bioavailability? Dipyridamole is an old anti-thrombotic and antianginal drug that blocks erythroid AE1 (Allahham et al., 2022). Dipyridamole reduces platelet aggregation and potentiates vasodilation with multiple mechanisms; its most well-studied mechanism for vasodilation is inhibition of adenosine receptors (Gamboa et al., 2005; Allahham et al., 2022). Whether dipyridamole as an AE1 inhibitor could also potentiate vasodilation has not been investigated because the link between AE1 and NO has been unclear for a long time. Dipyridamole, as a blocker of adenosine receptors, reduces the cellular uptake of adenosine and increases extracellular adenosine concentrations, which stimulates the activities of adenosine cyclase to generate more cAMP to potentiate eNOS activities and prostacyclin production (Gamboa et al., 2005; Allahham et al., 2022). Nonetheless, the transcript level of AE1 in human whole blood is 3-fold or higher than that of adenosine receptors (78.9 transcripts per million or TPM [AE1] versus 24.3 TPM [ADORA2A] from the human GTEx consortium) (Consortium et al., 2017). With our recent findings (Hsu et al., 2021; Chen et al., 2022; Chen et al., 2024), it is thus possible that dipyridamole-induced vasodilation could also be due to inhibition of erythroid AE1.

Dipyridamole binds to the AE1 dimer in a 1:1 stoichiometry and with a high affinity (K_d ~1.2 μM) (Falke and Chan, 1986). As a secondary effect of AE1 inhibition, dipyridamole indirectly reduces K+ efflux from RBCs. Clinically, this function of dipyridamole protects sickle RBCs from excessive cation efflux and consequent dehydration (Joiner et al., 2001). Through the same mechanism, dipyridamole also protects RBC concentrates (i.e., as a transfusion product) from K+ leakage caused by virus-inactivating photosensitizer treatments (vanSteveninck et al., 2000). In the latter example, AE1–dipyridamole binding not only protects RBCs from K+ leak-associated hemolysis but also from peroxidative damage (Nepomuceno et al., 1997; van; Steveninck et al., 2000). Since AE1 is functionally versatile, without a doubt, our current model of AE1 in blood NO processing and vasodilation (Figure 1D) is far from complete.

Similar to the finding that GP.Mur increases erythroid HCO_3^- permeability and respiratory excretion of CO_2 (Hsu et al., 2009; Hsu et al., 2015; Hsu et al., 2023), here, we proposed that GP.Mur also increases erythroid NO_3^-/NO_2^- permeability to accelerate erythrocyte processing of NO metabolites, which affects blood pressure (Patel et al., 2011) (Figure 1D). Could the two distinct anion transport modes of AE1 be coupled and AE1 serve as a coordinator for the seemingly separate physiological processes? A recently emerged clue is that GP.Mur+ carriers tend to rely more on aerobic respiration during intense exercise (Hsu et al., 2023). As intense physical activities demand more O_2 delivery and blood flow, conceivably intravascular NO is metabolized and dissipated faster. With the new GPMur KI mouse model that recapitulates the hypertensive phenotype of GP.Mur+ people, we hope to uncover these physiologic interplays and health relevance stemming from the AE1-mediated transport of HCO_3^-/Cl^- and NO_3^-/NO_2^- in the future.

Data availability statement

The raw data supporting the conclusion of this article will be made available by the authors, without undue reservation.

Ethics statement

The studies involving humans were approved by the MacKay Memorial Hospital Institutional Review Board. The studies were conducted in accordance with the local legislation and institutional requirements. The participants provided their written informed consent to participate in this study.

Author contributions

KH: writing–review and editing and writing–original draft.

Funding

The author(s) declare that financial support was received for the research, authorship, and/or publication of this article. This work was supported by grants from the Taiwan Ministry of Science and Technology (MOST 108-2628-B-195-001; 109-2628-B-195-001; 110-2628-B-195-001) and from MacKay Memorial Hospital to KH(MMH 111-26; 112-63; MMH 111-38; MMH 112-128; MMH 113-67).

Acknowledgments

We thank Hui-Ju Lin (MMH) and the students and faculty members of the University of Taipei for supporting and participating in the FeNO study and Prof. Yenta Lu (MMH Pulmonary medicine) for NIOX.

Conflict of interest

The author declares that the research was conducted in the absence of any commercial or financial relationships that could be construed as a potential conflict of interest.

Publisher's note

References

Abumohsen, H., Bustami, B., Almusleh, A., Yasin, O., Farhoud, A., Safarini, O., et al. (2021). The association between high hemoglobin levels and pregnancy complications, gestational diabetes and hypertension, among Palestinian women. *Cureus* 13, e18840. doi:10.7759/cureus.18840

Allahham, M., Lerman, A., Atar, D., and Birnbaum, Y. (2022). Why not dipyridamole: a review of current guidelines and Re-evaluation of utility in the modern era. *Cardiovasc Drugs Ther.* 36, 525–532. doi:10.1007/s10557-021-07224-9

Atsma, F., Veldhuizen, I., De Kort, W., Van Kraaij, M., Pasker-De Jong, P., and Deinum, J. (2012). Hemoglobin level is positively associated with blood pressure in a large cohort of healthy individuals. *Hypertension* 60, 936–941. doi:10.1161/HYPERTENSIONAHA.112.193565

Chen, P. L., Huang, K. T., Chen, L. Y., and Hsu, K. (2024). Erythroid anion Exchanger-1 (band 3) transports nitrite for nitric oxide metabolism. *Free Radic. Biol. Med.* 210, 237–245. doi:10.1016/j.freeradbiomed.2023.11.028

Chen, Y. C., Hsu, K. N., Lai, J. C., Chen, L. Y., Kuo, M. S., Liao, C. C., et al. (2022). Influence of hemoglobin on blood pressure among people with GP.Mur blood type(☆). *J. Formos. Med. Assoc.* 121, 1721–1727. doi:10.1016/j.jfma.2021.12.014

Consortium, G., Laboratory, D. A., Enhancing, G. G., Fund, N. I. H. C., Source Site, N., Biospecimen Collection Source Site, R., et al. (2017). Genetic effects on gene expression across human tissues. *Nature* 550, 204–213. doi:10.1038/nature24277

Cosby, K., Partovi, K. S., Crawford, J. H., Patel, R. P., Reiter, C. D., Martyr, S., et al. (2003). Nitrite reduction to nitric oxide by deoxyhemoglobin vasodilates the human circulation. *Nat. Med.* 9, 1498–1505. doi:10.1038/nm954

Dejam, A., Hunter, C. J., Pelletier, M. M., Hsu, L. L., Machado, R. F., Shiva, S., et al. (2005). Erythrocytes are the major intravascular storage sites of nitrite in human blood. *Blood* 106, 734–739. doi:10.1182/blood-2005-02-0567

Falke, J. J., and Chan, S. I. (1986). Molecular mechanisms of band 3 inhibitors. 2. Channel blockers. *Biochemistry* 25, 7895–7898. doi:10.1021/bi00372a016

Gamboa, A., Abraham, R., Diedrich, A., Shibao, C., Paranjape, S. Y., Farley, G., et al. (2005). Role of adenosine and nitric oxide on the mechanisms of action of dipyridamole. *Stroke* 36, 2170–2175. doi:10.1161/01.STR.0000179044.37760.9d

Gladwin, M. T., Grubina, R., and Doyle, M. P. (2009). The new chemical biology of nitrite reactions with hemoglobin: R-state catalysis, oxidative denitrosylation, and nitrite reductase/anhydrase. *Acc. Chem. Res.* 42, 157–167. doi:10.1021/ar800089j

Gobel, B. O., Schulte-Gobel, A., Weisser, B., Glanzer, K., Vetter, H., and Dusing, R. (1991). Arterial blood pressure. *Am. J. Hypertens.* 4, 14–19. doi:10.1093/ajh/4.1.14

Green, D. J., Dawson, E. A., Groenewoud, H. M., Jones, H., and Thijssen, D. H. (2014). Is flow-mediated dilation nitric oxide mediated? a meta-analysis. *Hypertension* 63, 376–382. doi:10.1161/HYPERTENSIONAHA.113.02044

Han, T. H., Qamirani, E., Nelson, A. G., Hyduke, D. R., Chaudhuri, G., Kuo, L., et al. (2003). Regulation of nitric oxide consumption by hypoxic red blood cells. *Proc. Natl. Acad. Sci. U. S. A.* 100, 12504–12509. doi:10.1073/pnas.2133409100

Hsu, K., Chi, N., Gucek, M., Van Eyk, J. E., Cole, R. N., Lin, M., et al. (2009). Miltenberger blood group antigen type III (Mi.III) enhances the expression of band 3. *Blood* 114, 1919–1928. doi:10.1182/blood-2008-12-195180

Hsu, K., Kuo, M. S., Yao, C. C., Lee, T. Y., Chen, Y. C., Cheng, H. C., et al. (2015). Expedited CO2 respiration in people with Miltenberger erythrocyte phenotype GP.Mur. *Sci. Rep.* 5, 10327. doi:10.1038/srep10327

Hsu, K., Lin, Y. C., Chao, H. P., Lee, T. Y., Lin, M., and Chan, Y. S. (2013). Assessing the frequencies of GP.Mur (mi.III) in several Southeast Asian populations by PCR typing. *Transfus. Apher. Sci.* 49, 370–371. doi:10.1016/j.transci.2013.05.011

Hsu, K., Liu, Y., Tseng, W., Huang, K., Liu, C., Chen, L., et al. (2021). Comodulation of NO-dependent vasodilation by erythroid band 3 and hemoglobin: a GP.Mur athlete study. *Front. Cardiovasc. Med.* 8, 740100. doi:10.3389/fcvm.2021.740100

Hsu, K., Tseng, W. C., Chen, L. Y., Chen, P. L., Lu, Y. X., Chen, Y. S., et al. (2023). Effects of greater erythroid Cl(-)/HCO(3)(-) transporter (band 3) expression on ventilation and gas exchange during exhaustive exercise. *Am. J. Physiol. Lung Cell Mol. Physiol.* 324, L825–L835. doi:10.1152/ajplung.00036.2022

Huang, K. T., Han, T. H., Hyduke, D. R., Vaughn, M. W., Van Herle, H., Hein, T. W., et al. (2001). Modulation of nitric oxide bioavailability by erythrocytes. *Proc. Natl. Acad. Sci. U. S. A.* 98, 11771–11776. doi:10.1073/pnas.201276698

Jana, S., Strader, M. B., Meng, F., Hicks, W., Kassa, T., Tarandovskiy, I., et al. (2018). Hemoglobin oxidation-dependent reactions promote interactions with band 3 and oxidative changes in sickle cell-derived microparticles. *JCI Insight* 3, e120451. doi:10.1172/jci.insight.120451

Jennings, M. L. (2021). Cell physiology and molecular mechanism of anion transport by erythrocyte band 3/AE1. *Am. J. Physiol. Cell Physiol.* 321, C1028–C1059. doi:10.1152/ajpcell.00275.2021

Joiner, C. H., Jiang, M., Claussen, W. J., Roszell, N. J., Yasin, Z., and Franco, R. S. (2001). Dipyridamole inhibits sickling-induced cation fluxes in sickle red blood cells. *Blood* 97, 3976–3983. doi:10.1182/blood.v97.12.3976

Jongruamklang, P., Grimsley, S., Thornton, N., Robb, J., Olsson, M. L., and Storry, J. R. (2020). Characterization of GYP*Mur and novel GYP*Bun-like hybrids in Thai blood donors reveals a qualitatively altered s antigen. *Vox Sang.* 115, 472–477. doi:10.1111/vox.12909

Kaito, S., Suzuki, Y., Masuno, A., Isa, K., Toyoda, C., Onodera, T., et al. (2022). Frequencies of glycophorin variants and alloantibodies against Hil and MINY antigens in Japanese. *Vox Sang.* 117, 94–98. doi:10.1111/vox.13121

Kapil, V., Haydar, S. M., Pearl, V., Lundberg, J. O., Weitzberg, E., and Ahluwalia, A. (2013). Physiological role for nitrate-reducing oral bacteria in blood pressure control. *Free Radic. Biol. Med.* 55, 93–100. doi:10.1016/j.freeradbiomed.2012.11.013

Kawamoto, R., Tabara, Y., Kohara, K., Miki, T., Kusunoki, T., Katoh, T., et al. (2012). A slightly low hemoglobin level is beneficially associated with arterial stiffness in Japanese community-dwelling women. *Clin. Exp. Hypertens.* 34, 92–98. doi:10.3109/10641963.2011.618202

Kim-Shapiro, D. B., Schechter, A. N., and Gladwin, M. T. (2006). Unraveling the reactions of nitric oxide, nitrite, and hemoglobin in physiology and therapeutics. *Arterioscler. Thromb. Vasc. Biol.* 26, 697–705. doi:10.1161/01.ATV.0000204350.44226.9a

Lancaster, J. R., Jr. (1994). Simulation of the diffusion and reaction of endogenously produced nitric oxide. *Proc. Natl. Acad. Sci. U. S. A.* 91, 8137–8141. doi:10.1073/pnas.91.17.8137

Lee, S. G., Rim, J. H., and Kim, J. H. (2015). Association of hemoglobin levels with blood pressure and hypertension in a large population-based study: the Korea National Health and Nutrition Examination Surveys 2008-2011. *Clin. Chim. Acta* 438, 12–18. doi:10.1016/j.cca.2014.07.041

Menzies-Gow, A., Mansur, A. H., and Brightling, C. E. (2020). Clinical utility of fractional exhaled nitric oxide in severe asthma management. *Eur. Respir. J.* 55, 1901633. doi:10.1183/13993003.01633-2019

Nepomuceno, M. F., Alonso, A., Pereira-Da-Silva, L., and Tabak, M. (1997). Inhibitory effect of dipyridamole and its derivatives on lipid peroxidation in mitochondria. *Free Radic. Biol. Med.* 23, 1046–1054. doi:10.1016/s0891-5849(97)00135-4

Patel, R. P., Hogg, N., and Kim-Shapiro, D. B. (2011). The potential role of the red blood cell in nitrite-dependent regulation of blood flow. *Cardiovasc Res.* 89, 507–515. doi:10.1093/cvr/cvq323

Pawloski, J. R., Hess, D. T., and Stamler, J. S. (2001). Export by red blood cells of nitric oxide bioactivity. *Nature* 409, 622–626. doi:10.1038/35054560

Prathiba, R., Lopez, C. G., and Usin, F. M. (2002). The prevalence of GP.Mur and anti-"Mia" in a tertiary hospital in Peninsula Malaysia. *Malays J. Pathol.* 24, 95–98.

Premont, R. T., Reynolds, J. D., Zhang, R., and Stamler, J. S. (2020). Role of nitric oxide carried by hemoglobin in cardiovascular physiology: developments on a three-gas respiratory cycle. *Circ. Res.* 126, 129–158. doi:10.1161/CIRCRESAHA.119.315626

Steveninck, J., Trannoy, L. L., Besselink, G. A., Dubbelman, T. M., Brand, A., De Korte, D., et al. (2000). Selective protection of RBCs against photodynamic damage by the band 3 ligand dipyridamole. *Transfusion* 40, 1330–1336. doi:10.1046/j.1537-2995.2000.40111330.x

Suvila, K., Langen, V., Cheng, S., and Niiranen, T. J. (2020). Age of hypertension onset: overview of research and how to apply in practice. *Curr. Hypertens. Rep.* 22, 68. doi:10.1007/s11906-020-01071-z

Tremblay, J. C., Hoiland, R. L., Howe, C. A., Coombs, G. B., Vizcardo-Galindo, G. A., Figueroa-Mujica, R. J., et al. (2019). Global REACH 2018: high blood viscosity and hemoglobin concentration contribute to reduced flow-mediated dilation in high-altitude excessive erythrocytosis. *Hypertension* 73, 1327–1335. doi:10.1161/HYPERTENSIONAHA.119.12780

Vaughn, M. W., Huang, K. T., Kuo, L., and Liao, J. C. (2000). Erythrocytes possess an intrinsic barrier to nitric oxide consumption. *J. Biol. Chem.* 275, 2342–2348. doi:10.1074/jbc.275.4.2342

Walder, J. A., Chatterjee, R., Steck, T. L., Low, P. S., Musso, G. F., Kaiser, E. T., et al. (1984). The interaction of hemoglobin with the cytoplasmic domain of band 3 of the human erythrocyte membrane. *J. Biol. Chem.* 259, 10238–10246. doi:10.1016/s0021-9258(18)90956-7

Wei, L., Shan, Z. G., Flower, R. L., Wang, Z., Wen, J. Z., Luo, G. P., et al. (2016). The distribution of MNS hybrid glycophorins with Mur antigen expression in Chinese donors including identification of a novel GYP.Bun allele. *Vox Sang.* 111, 308–314. doi:10.1111/vox.12421

Wood, K. C., Cortese-Krott, M. M., Kovacic, J. C., Noguchi, A., Liu, V. B., Wang, X., et al. (2013). Circulating blood endothelial nitric oxide synthase contributes to the regulation of systemic blood pressure and nitrite homeostasis. *Arterioscler. Thromb. Vasc. Biol.* 33, 1861–1871. doi:10.1161/ATVBAHA.112.301068

Xuan, Y., Zuo, J., Zheng, S., Ji, J., and Qian, Y. (2019). Association of hemoglobin and blood pressure in a Chinese community-dwelling population. *Pulse (Basel)* 6, 154–160. doi:10.1159/000494735

Yang, M. H., Chen, J. W., Sayaka, K., Uchikawa, M., Tsuno, N. H., Wei, S. T., et al. (2021). Universal detection of mi(a) antigen and frequencies of glycophorin hybrids among blood donors in taiwan by human monoclonal antibodies against mi(a) (MNS7), mur (MNS10), and MUT (MNS35) antigens. *Diagn. (Basel)* 11, 806. doi:10.3390/diagnostics11050806

frontiers | Frontiers in Physiology

TYPE Review
PUBLISHED 10 June 2024
DOI 10.3389/fphys.2024.1394650

OPEN ACCESS

EDITED BY
Lars Kaestner,
Saarland University, Germany

REVIEWED BY
Vassilis L. Tzounakas,
University of Patras, Greece
John Stanley Gibson,
University of Cambridge, United Kingdom

*CORRESPONDENCE
Tim J. McMahon,
tim.mcmahon@duke.edu

RECEIVED 01 March 2024
ACCEPTED 24 April 2024
PUBLISHED 10 June 2024

CITATION
Wise TJ, Ott ME, Joseph MS, Welsby IJ, Darrow CC and McMahon TJ (2024), Modulation of the allosteric and vasoregulatory arms of erythrocytic oxygen transport. *Front. Physiol.* 15:1394650. doi: 10.3389/fphys.2024.1394650

Modulation of the allosteric and vasoregulatory arms of erythrocytic oxygen transport

Thomas J. Wise[1], Maura E. Ott[1], Mahalah S. Joseph[1,2], Ian J. Welsby[1], Cole C. Darrow[1] and Tim J. McMahon[1,3]*

[1]Duke University School of Medicine, Durham, NC, United States, [2]Florida International University School of Medicine, Miami, FL, United States, [3]Durham VA Health Care System, Durham, NC, United States

Efficient distribution of oxygen (O_2) to the tissues in mammals depends on the evolved ability of red blood cell (RBC) hemoglobin (Hb) to sense not only O_2 levels, but metabolic cues such as pH, PCO_2, and organic phosphates, and then dispense or take up oxygen accordingly. O_2 delivery is the product of not only oxygen release from RBCs, but also blood flow, which itself is also governed by vasoactive molecular mediators exported by RBCs. These vascular signals, including ATP and S-nitrosothiols (SNOs) are produced and exported as a function of the oxygen and metabolic milieu, and then fine-tune peripheral metabolism through context-sensitive vasoregulation. Emerging and repurposed RBC-oriented therapeutics can modulate either or both of these allosteric and vasoregulatory activities, with a single molecule or other intervention influencing both arms of O_2 transport in some cases. For example, organic phosphate repletion of stored RBCs boosts the negative allosteric effector 2,3 biphosphoglycerate (BPG) as well as the anti-adhesive molecule ATP. In sickle cell disease, aromatic aldehydes such as voxelotor can disfavor sickling by increasing O_2 affinity, and in newer generations, these molecules have been coupled to vasoactive nitric oxide (NO)-releasing adducts. Activation of RBC pyruvate kinase also promotes a left shift in oxygen binding by consuming and lowering BPG, while increasing the ATP available for cell health and export on demand. Further translational and clinical investigation of these novel allosteric and/or vasoregulatory approaches to modulating O_2 transport are expected to yield new insights and improve the ability to correct or compensate for anemia and other O_2 delivery deficits.

KEYWORDS

S-nitrosothiols, ATP, transfusion, sepsis, sickle cell disease, hypoxia, endothelium

Background

Coupling of O_2 sensing and O_2 release in red blood cell hemoglobin

Red blood cells (RBCs) operate on several levels to sense and regulate the flux of O_2 from lung air to tissues and the removal of CO_2 and other waste products from tissues to lung air. Specifically, RBC hemoglobin (Hb) senses O_2 tension and adopts an O_2-binding (in the lungs) or O_2-releasing (when perfusing the tissues) posture according to host needs and the environment. This tight coupling of O_2 sensing and demand is fine-tuned and made to fit the metabolic context through relevant allosteric effectors of Hb

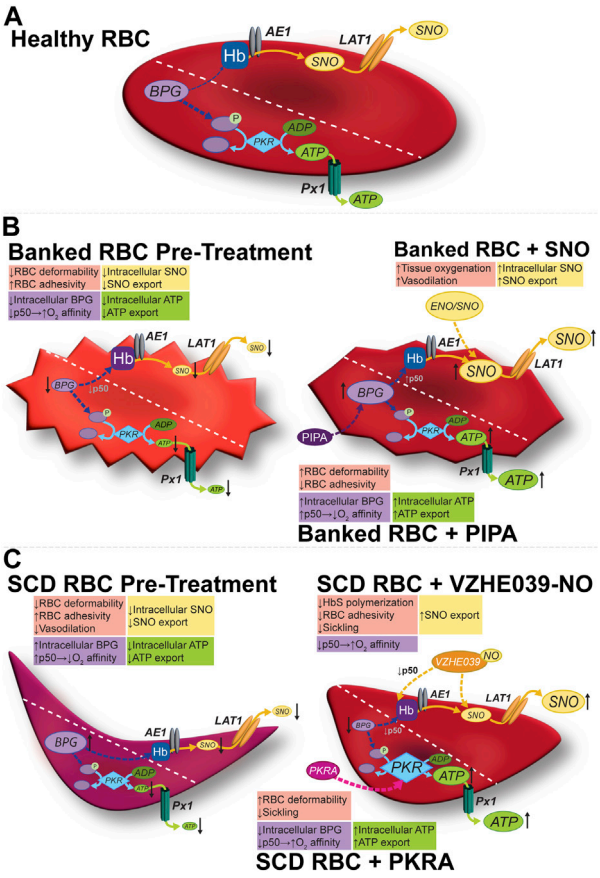

FIGURE 1
Modulation of the allosteric and vasoregulatory arms of erythrocytic O_2 transport. **(A)** Glycolysis in healthy RBCs generates the allosteric effector BPG and the ATP vital for cell-intrinsic (e.g., integrity, deformability) and cell-extrinsic (antiadhesive) functions. RBCs export vasoregulatory ATP via Px1 (pannexin 1). SNO is formed on RBC Hb, and can exit via membrane LAT1, possibly after being relayed by AE1. **(B)** In banked RBCs, SNOs and vasoactivity are depressed early (hours) and BPG and ATP are depressed later (weeks). Impaired vasoactivity, heightened O_2 affinity (lower P_{50}), and a proadhesive phenotype (among others) result. The respective mediator and functional changes can be rescued by preserving (e.g., using hypoxic RBC storage) or repleting the precursors (e.g., with PIPA) of organic phosphates or by using a SNO donor such as ENO (ethyl nitrite). **(C)** In sickle RBCs, both SNO and ATP are depressed, in turn depressing vasoactivity. BPG is elevated, shifting O_2 affinity "rightward (P_{50} is up)" to favor deoxygenation and thus sickling. Activating PKR increases ATP at the expense of BPG (upstream in glycolysis), resulting in resistance to hemolysis and potentially improving ATP export, and disfavoring sickling, respectively. VZHE039-NO stabilizes oxygenated Hb (i.e., lowers P_{50}), directly inhibits Hb polymerization (thus preventing sickling two ways), and donates antiadhesive (S)NO. Diagonal dashed lines segregate the BPG/ATP/glycolysis and Hb/SNO/AE1/LAT1 axes for illustration, but these cascades do interact (e.g., BPG and Hb; SNO and GAPDH).

function such as pH, temperature and CO_2 tension. Longer-term adjustment of the balance between O_2 binding and release is accomplished through the generation in RBCs of BPG, which favors O_2 offloading, for example, in chronic anemia. Additional layers of adaptation recruit increased RBC numbers, for example, via erythropoietin's coupling of new RBC production to the sensing of hypoxia via hypoxia-inducible factor (HIF) and other regulators.

Coupling of O_2 sensing and vascular mediator release by RBCs (and Hb)

More recently recognized is the ability of the RBC to generate and export vasoregulatory mediators as a function of the metabolic context, a "second arm" of the coupled O_2 sensing and delivery function of the RBC. For example, an S-nitrosothiol (SNO) group formed on Hb from precursor NO can be relayed to the RBC membrane and subsequently exported to effect hypoxic vasodilation, an allosterically governed fundamental vascular reflex dependent on RBCs (Figure 1). This O_2-sensitive, allosterically governed blood flow regulation by S-nitrosohemoglobin (SNO-Hb) ensures efficient and well-distributed tissue oxygenation. RBCs also generate and export vasoregulatory and antiadhesive ATP (Figure 1) preferentially in hypoxia, because the docking of deoxygenated Hb at the cytoplasmic domain of the protein band 3 (cdB3) in the RBC membrane allows the cytosolic re-assembly of the glycolytic enzyme complex (which is sequestered on cdB3 when Hb is oxygenated and thus unable to effect glycolysis). Dysregulation of these vasoregulatory activities of the RBC characterize both RBC-intrinsic (e.g., sickle cell disease, malaria, or blood storage) and RBC-extrinsic (e.g., sepsis, diabetes mellitus) diseases. In RBCs, ATP and (S)NO are also critical in cell health, including the maintenance of RBC deformability necessary for its efficient transit through narrow capillaries (Ramdani and Langsley, 2014). In turn, mechanical deformation also triggers ATP release from RBCs and can stimulate endothelial nitric oxide (NO) synthesis, in turn regulating blood flow and the delivery of oxygen (O_2) to tissues (Ramdani and Langsley, 2014).

Emerging and existing or repurposed RBC therapeutics can modulate the setpoints and gain for O_2 binding and release, the vasoregulatory mediators harnessed by RBCs for O_2 delivery, or even both of these two arms of the RBC's control of O_2 delivery. In some cases, a single molecule or therapeutic can modulate both RBC arms of O_2 delivery. Interactions between the former (allosteric effectors) and the latter (vasoregulatory factors) can at least in theory have net additive, neutral, or even inhibitory effects on O_2 delivery or uptake. Here we review newer therapeutic approaches to restoring RBC function when deficient, as well as mechanistically novel applications of existing molecules. We describe these approaches to modulating RBC function in healthy RBCs and in the context of disease states.

Red blood cell storage

RBC storage lesions

RBC storage lesions affect RBC quality and transfusion outcomes

While lifesaving for treatment of anemia in selected patients, transfusion of RBCs is neither entirely benign nor frequently beneficial. The process of RBC storage for later transfusion alters the RBC in multiple ways, collectively known as "storage lesions" (Bennett-Guerrero et al., 2007). These storage lesions include changes in RBC structure, composition, and function including decreased BPG, ATP, and SNO levels (Yoshida et al., 2019). These changes contribute to progressive increases in hemolysis,

decreasing RBC membrane integrity, and depressed vasoactivity, and may contribute to the well documented lack of benefit (or even harm) of RBC transfusion for many patients with mild to moderate anemia (Hebert et al., 1999; Lacroix et al., 2007; Koch et al., 2008; Wang et al., 2012; Holst et al., 2014).

Variability in donor RBC metabolism and function

Variability in RBC behavior and underlying mediators even among healthy donors

Variation in RBC metabolic activity is not limited to disease states such as PKD, G6PD deficiency, or sickle cell disease, and the inter-donor variability in rates of RBC lysis with cold storage has long suggested metabolic polymorphism. The functional significance of varying RBC ATP was illustrated in a large study of healthy blood donors, along with new genetic insights into its control. Nemkov et al. demonstrated that even after accounting for age, sex and ethnicity, genetic polymorphisms in phosphofructokinase 1 (PFKP), hexokinase 1 (HK1) and the ADP-ribosyl cyclase CD38 accounted for variability in glycolysis in healthy blood. ATP (and other indices of glycolytic activity such as lactate and hypoxanthine) in turn associated significantly with hemolytic propensity *ex vivo* and after RBC transfusion in critically ill patients. *PKLR* (encoding PK in the liver and RBCs) was among the genes for which metabolite quantitative trait loci associated significantly with glycolysis, suggesting a druggable target for potential intervention (Nemkov et al., 2024).

RBC transfusion and metabolomics

Large studies of the degree of post-transfusion recovery of RBCs in recipients have revealed substantial variability from donor to donor, and high reproducibility of post-transfusion recovery (PTR) of RBCs from a given donor, consistent with the importance of heritable traits governing this essential measure of transfusion effectiveness. The variability in PTR is clearly linked to variable donor genetics and metabolomes (Nemkov et al., 2024).

Altered RBC storage quality secondary to specific donor characteristics

Specific characteristics in donors affect the quality and longevity of stored RBC units derived from their donated blood. Donor obesity, sex, and HbA1c level correlate with stored RBC quality (Hazegh et al., 2021; Tzounakas et al., 2021; Li et al., 2022). The underlying variability has led researchers and clinicians to assert that storage time alone is insufficient to assess quality of stored RBCs (Barshtein et al., 2020). Researchers have explored more accurate methods to non-invasively measure unit hemolysis and quality including sphingomyelinase activity and using spectroscopy (Melzak et al., 2020; Vardaki et al., 2021).

Inter-individual variability of RBC O_2 affinity/P_{50}

In general, an individual's O_2 carrying capacity can be estimated in part by the hemoglobin (Hb) concentration and the Hb O_2 saturation (measured, for example, by pulse oximetry). These are important indicators but do not take into account the hemoglobin O_2 affinity, which plays a key role in O_2 delivery to tissues. Recent research has shown variation in a patient Hb O_2 affinity and established that patient-specific normal variants may affect oxygen delivery. While O_2 dissociation curves are necessary to accurately determine the P_{50}, and the hemoglobin O_2 affinity, estimates in real time of a patient's (or a donor's) P_{50} and other indices of O_2-binding properties from blood gas samples could guide RBC transfusion decision-making more precisely (Lilly et al., 2013; Balcerek et al., 2020).

Individualized assessment of RBC qualities and directed use of RBC additives

The study of RBC-omics, a global detailed analysis of all molecules involved in RBC processes, has led to a richer understanding of the complexity of RBC metabolism and signaling. Some omics experts, including D'Alessandro, view the results as indicating that RBCs are not a mere vehicle for oxygen delivery, but also an organ complex interacting bidirectionally with its microenvironment via molecular mediators. This reframing aligns with newly recognized RBC functions (e.g., vasoregulation) and arrives in an era of new technologies in anemia management, such as new additives, evolving medical indications for treatment, and new blood preservation techniques. This new landscape demands the investigation of when, how, and with whom these technologies should be used to mitigate and treat the burden of anemia. RBC omics are helping to answer these questions when paired with new high-throughput devices and machine learning programs (D'Alessandro, 2023).

RBC unit selection for transfusion, D'Alessandro et al. (2023) argue, could be informed by omics and machine learning to personalize decision-making. Current strategies consist of weighing consideration for maximizing inventory usage (first in–first out) with prioritizing fresh units (last in–first out). Detailed study of the units themselves will give physicians more tools to assess the units. Merely using storage duration assumes a direct and proportional correlation between storage duration and storage lesions. This heuristic, while inexpensive and convenient, may not provide the best possible match of patient to blood product. Significant diversity and variation were evident in the genomics of RBC samples, with almost 900,000 polymorphisms found from 13,000 different donors. This variation corresponded with a wide variation in the propensity of blood to hemolyze. In addition to these genomic variations, many medications (acetaminophen, antidepressants, and others) and molecules from donor diets present in donated blood may affect their storage (D'Alessandro et al., 2023).

Some have discussed recent large randomized clinical trials (RCTs) and concluded that adverse events from blood transfusion are not correlated with the storage duration of blood products (Donovan et al., 2022). RBC omics and more precise RBC measurements may offer new insights. RBC gas exchange in the capillaries occurs in seconds in concert with several molecular mediators. Omics may illuminate differences in the patient and blood product that also play a role in the exchange, not controlled for in previous studies. The trials discussed mainly included patients with stable anemia. Excluded, therefore, were populations most affected by the known storage lesions, i.e. those requiring massive

transfusions, those with reduced cardiac output, and those at risk for decreased organ perfusion (Donovan et al., 2022). Additionally, "negative" RCTs comparing outcomes after transfusion of RBCs stored "shorter vs longer" would not be expected to reflect the consequences of the set of changes that we and others have demonstrated early in storage (days 0–7) (Bennett-Guerrero et al., 2007).

"Lab-on-a-chip" technology can evaluate in real time individual RBC units for quality and compatibility with recipient patients. This could allow for more specific matching of blood products to patients and would bring blood transfusion into the century of "personalized medicine" (Isiksacan et al., 2023). Nemkov et al. established a high-throughput platform with the ability to inform the development and approval of novel additives to stored RBC. Previously, the process of testing new possible additives has been bottlenecked by a lack of expeditious and efficient evaluation techniques and platforms. Modern platforms could accelerate the process and identify novel candidates for research. Their platform was validated against well-established previous studies (Nemkov et al., 2022).

Oxygen delivery

Disconnect between O_2 delivery and changes in tissue PO_2

In hamsters made anemic by isovolemic hemodilution, Cabrales et al. compared the microvascular and systemic effects of transfusion with RBCs of either higher or lower O_2 affinity than native RBCs, using allosteric effectors electroporated into the cells. In animals receiving high-affinity RBCs, systemic hemodynamics and O_2 delivery were maintained stable, while tissue PO_2 decreased (contributing to a steep O_2 gradient driving O_2 diffusion to tissues) (Cabrales et al., 2008). In contrast, RBCs with moderately low affinity induced microvascular vasoconstriction, decreased O_2 delivery and O_2 extraction, and raised tissue PO_2. Taken together, these findings point to a disconnect between tissue PO_2 changes on the one hand, vs changes in O_2 delivery and O_2 extraction by tissues on the other, in the face of allosteric modulation in the setting of anemia. The relationship of these observations to physiological benefit or harm has not yet been elucidated.

Hypoxic blood storage

Hypoxic RBC storage

As an alternative to repleting deficient factors lost during blood banking as discussed above, one may modify storage conditions driving these losses to proactively avoid lesion development. One common lesion, oxidative damage, is caused by the buildup of oxidative species secondary to storage in the face of high levels of O_2. Pittman et al. (2022) discussed how RBCs stored in hypoxemic environments could mitigate this while having no effect on the efficacy of the RBC transfusion. The authors argue that these hypoxically stored RBCs endure exposure to fewer oxidative insults and thus less exposure to the downstream harmful lipid oxidation products following the oxidation of hemoglobin to methemoglobin. These oxidative products may disrupt the normal physiologic functioning of the RBC as well as have inflammatory effects on the patient following transfusion. Yoshida et al. developed and described a method of hypoxic RBC storage, in which the oxygen content in RBC units is lowered before refrigeration and maintained at low levels throughout cold storage. This alternative storage method, now known by the trade name Hemanext, mitigates oxidative stress (driven by abundant O_2) and thus storage lesion development, and preserves BPG and to some extent ATP, suggesting potential advantages for critically ill and other anemic patients needing RBC transfusion for anemia. Interestingly, while the finding that RBCs stored conventionally become progressively more fully saturated with O_2 over the typical 6 weeks of storage is generally universal, Yoshida et al. (2017) demonstrated a surprising variability in RBC HbO_2 saturation levels, even when comparing at the beginning of storage. Accordingly, hypoxic RBC storage could potentially increase the degree of consistency of post-storage (and post-transfusion) RBC functions. More broadly, multiple investigators have highlighted the fact that inter-donor variability in RBC function and metabolic profile is high, and that stored RBC behavior is poorly described in terms of the storage time alone (Dumbill et al., 2023).

Advantage of hypoxically stored RBC in hemorrhagic shock

Williams and their team used mouse models of hemorrhagic shock to investigate whether the anaerobic storage of RBC could confer better outcomes than traditionally stored RBC through the reduction of oxidative damage to RBC while not depleting patient oxygen levels. Their model demonstrated that the deoxygenated blood quickly returns to physiologic levels of oxygenation following transfusion and mixing with patient blood in circulation. This, in concert with previous studies validating that anaerobically stored RBCs undergo decreased oxidative damage, advances this storage medium as a promising avenue for further research. In a rat model, resuscitation using hypoxically stored RBCs for transfusion reduce RBC transfusion volumes needed in hemorrhagic shock (Williams et al., 2020).

Stored RBC senescence markers modified by hypoxic RBC storage

Bencheikh et al. (2022) demonstrated a protective influence of hypoxic RBC storage (using Hemanext technology) on the appearance of RBC senescence markers (ROS increases, phosphatidylserine (PS) exposure, and calcium entry as assessed by flow cytometry), particularly at 21 and 42 days of otherwise conventional storage. Adhesivity of hypoxically stored RBCs in healthy plasma or in plasma from SCD (at rest or obtained during acute chest syndrome crisis) to thrombospondin (TSP)-1 was significantly attenuated on Day 0, with trends for a beneficial effect of hypoxic storage seen at the longer timepoints (21 and 42 days). The effects of the hypoxic storage of RBCs used to condition subsequent adhesion responses of SCD RBCs to endothelial cells was significant only for 42-day RBCs, and only when a 10% hemolysate was also included in the preconditioning medium. In summary, these findings point to storage-time-dependent beneficial effects of hypoxic RBC storage on indices reflecting senescence changes and adhesivity of sickle RBCs in cell culture models.

Metabolic modulation for pRBC oxidative stress due to irradiation

When immunocompromised patients need RBC transfusion, the units are first irradiated to lower the risk of transfusion-associated graft-vs.-host disease. The gamma-(γ-)irradiation used can accelerate the storage-induced adverse changes in RBCs, largely by promoting the storage-associated oxidative changes. The oxidative changes stem in part from the increasing O_2 levels in the RBC unit. Bardyn et al. (2021) demonstrated that RBC unit storage under conditions of low (and falling) O_2 and CO_2 protects against storage-induced deterioration in RBC deformability and the progressive RBC lysis and formation of abnormal spherocytes. The authors consider the possibility that the *in vitro* benefits are secondary to preserved RBC glycolysis and, in fact ATP and BPG levels are better preserved after hypoxic (vs conventional) storage in γ-irradiated RBC units. Consistent with the prediction that preserved BPG stability can promote the ability of stored RBCs to offload O_2 Rabcuka et al. (2022), Rabcuka et al. demonstrated in Hemanext RBCs superior O_2 offloading kinetics and a distinct metabolic signature characterized by preserved pyruvate consistent with protection of glycolysis.

Normoglycemic RBC storage

Normoglycemic RBC storage preserves RBC ATP content and export and RBC deformability

Just as functional excess of O_2 may drive RBC storage lesions, excessive glucose may also be harmful to optimal RBC function. Typical additive solutions contain glucose at >30 mM (five-fold or more over normal blood glucose). Wang et al. (2014) and Liu et al. (2022) demonstrated storing RBCs in normoglycemic conditions may mitigate storage lesions when compared to the current accepted practice of storage under hyperglycemic conditions. Using a 3D-printed transfusion-on-a-chip platform Liu et al. and Spence et al. observed erythrocytes under both storage conditions and in a model of post-transfusion conditions. They found that use of the conventional additive solution AS-1, a hyperglycemic mediums led to a decrease in ATP release and a change in the deformability of the RBC membrane which is reversible upon introduction into their *in vitro* model of transfusion only up to 14 days of storage. Normoglycemic storage medium ("AS-1N") allowed for RBCs to maintain deformability and release ATP at normal levels for up to 5 weeks, and these "AS-1N" RBCs also responded to stimulation with Zn (zinc) and C-peptide by releasing ATP and deforming maximally. A reduction in storage lesions could decrease the volume of RBC units necessary for resuscitation as well as reduce the adverse effects of transfusion overall. More studies into the storage medium and its role in storage lesions could benefit future anemic patients (Liu et al., 2022). Co-development of technology supporting sustained normoglycemia adds to the translational promise of this improved approach to optimizing RBC function during storage (Soule et al., 2024).

Rejuvenated stored RBCs (organic phosphate repletion), and roles of other phosphates

PIPA (Rejuvesol) and "rejuvenation" of stored RBCs

Depletion of BPG, the negative allosteric effector of O_2 binding activity of Hb (Figure 1; Table 1) begins to occur during the first week of RBC storage and is effectively complete by the second week. The BPG depletion raises the O_2 affinity in banked blood, which could limit facile O_2 delivery to tissues after RBC transfusion and thus be detrimental in certain anemic populations. Secondary additive solutions such as PIPA solutions (containing pyruvate, inosine, phosphate, and adenine; known commercially as Rejuvesol®) can be added to RBC units to mitigate this effect as well as related ATP storage lesions and storage-dependent morphological deterioration of the RBC. Such "rejuvenation" was originally performed in the last few days of the typical 6-week storage period but can restore ATP and BPG levels after 2 weeks of storage. In addition to restoring BPG, PIPA treatment of stored RBCs does restore the ability to export ATP upon demand, in turn promoting salutary RBC vasoactivity including the ability to resist adhesion to the endothelium (Kirby et al., 2014).

In practice, however, and despite FDA approval, PIPA is seldom used outside of its application in the cryopreservation of rare blood types. Gehrke et al. and Evans et al. tested the effects of an approach that makes PIPA incubation (aka "rejuvenation") more practical: the addition of PIPA at Day 3 of cold storage. This avoids the conventional (but cumbersome) one-hour, 37°C incubation of the RBC unit with PIPA (conditions linked to its FDA-approved clinical use) (Gehrke et al., 2018; Gehrke et al., 2019). Cold PIPA incubation, like conventional PIPA use, increased ATP and BPG levels (Figure 1, middle panels) to just above the upper limit of normal and mitigated the storage-induced increase in O_2 affinity, without engendering additional RBC lysis or vulnerability to lysis of the RBCs in a benchtop model of a cardiopulmonary bypass circuit. This approach could improve post-storage RBC function not only via maintenance of the P_{50} at near-normal values, but also via the increased erythrocytic ATP, which is necessary for enzymes functioning to defend RBC integrity and for blood flow-regulating vasoactivity that fine-tunes O_2 delivery. Indeed, cold "rejuvenation/PIPA treatment" attenuated storage-induced declines in deformability and the progressive increases in mechanical fragility and RBC lysis (Evans et al., 2020). Among other potential downstream mechanisms of the benefits of preserving these critical organic phosphates, they may inhibit fatty acid desaturases, in turn limiting fatty acid accumulation (Thomas et al., 2021). When the ability of Rejuvesol to restore metabolites in RBCs stored over an extended period was studied, it was found to be effective in restoring BPG and ATP levels in RBCs stored in multiple mediums for up to 120 days. While the stored cells responded to "rejuvenation" less over time, when rejuvenated their BPG and ATP levels exceeded those in fresh blood for 72- and 96-hours post-treatment, respectively (Meyer et al., 2011; Smethurst et al., 2019). Notably, following transfusion, BPG is gradually regenerated in the transfused RBCs, with levels ultimately matching those of the recipient by 72 h (Valeri and Hirsch, 1969; Heaton et al., 1989).

TABLE 1 Changes in erythrocytic allosteric function and vasoregulation in selected diseases or conditions, and effects following some relevant modulatory interventions.

Disease or condition		Intervention		References
RBC storage lesion	Effect on RBC allosteric mediators	Allosteric modulator		
		Name and mechanism	Effect	
	↓ATP export, late ↓ ATP content; ↓BPG, ↑Oxygen affinity; ↓S1P; ↓SNO	PIPA—Rejuvesol: RBC rejuvenation using a solution of pyruvate, inosine, phosphate and adenine	↑ATP content and export; ↑BPG, ↓Oxygen affinity; ↑RBC deformability, adhesivity, and oxygen delivery	Kirby et al. (2014), Srinivasan et at. (2018), Rabcuka et al. (2022)
		Hypoxic RBC storage—Hemanext: Decreases oxidative stress inherent to conventional storage	↑ATP content and export; ↑BPG, ↓Oxygen affinity; ↓Post-transfusion inflammation; reduces RBC volume needed to resuscitate after hemorrhage	Yoshida et al. (2017), Nazeman et al. (2022), Pittman et al. (2022), Williams et al. (2020)
		Normoglycemic storage: Prevents lesions secondary to conventional storage at more than 5× normal glucose levels	↑ATP export; ↑RBC deformability	Wang et al. (2014), Liu et al. (2022), Soule et al. (2024)
	Effect on RBC function and vasoregulation	Vasoregulatory modulator		
		Name and mechanism	Effect	
	↓RBC deformability; ↑RBC adhesivity; ↓Vasoactivity; ↓Survival; ↓Oxygen delivery	S1P supplementation: Promotes RBC glycolysis by mediating the binding of hemoglobin to the N-terminus of the RBC membrane anion transporter Band 3	↑ATP content and export; ↑BPG, ↓Oxygen affinity; ↑RBC deformability, adhesivity, and oxygen delivery; ↓ NADPH	Hay et al. (2023)
		Ethyl nitrite (ENO): SNO donor repletes pathologically deficient level in recipient	↑RBC SNO, ↓RBC adhesivity, ↑RBC deformability, ↑Hypoxia-induced vasodilation	Riccio et al. (2015), Reynolds et al. (2007)
Sickle cell disease (SCD)	Effect on RBC allosteric mediators	Allosteric modulator		
		Name and mechanism	Effect	
	↓ATP content and export; ↑BPG, ↓Oxygen affinity	PIPA—Rejuvesol	↓BPG, ↑Oxygen Affinity, ↓RBC transfusion dependence	Lopez Domowicz et al. (2020)
		Polymerization inhibitor—Voxeletor: Increases Hb oxygen affinity, favoring oxyHb state	↓BPG, ↑Oxygen Affinity, ↓RBC sickling and polymerization; ↑Hb levels; ↓Hemolysis	Suhail (2024), Howard et al. (2021), Shah et al. (2022)
		Polymerization inhibitor/NO donor—VZHE-039-NO: Increases Hb oxygen affinity AS WELL AS directly interrupts polymerization and donates vasoactive NO	↓BPG, ↑Oxygen affinity, ↓RBC sickling and polymerization; ↑Hb levels; ↓Hemolysis; ↓RBC adhesivity	Huang et al., 2022; Abdulmalik et al.,
	Effect on RBC function and vasoregulation	Vasoregulatory modulator		
		Name and mechanism	Effect	
	Decreased deformability; increased adhesivity; decreased vasoactivity; increased RBC polymerization; ↓SNO	RBC-specific pyruvate kinase activator (PKRA)—Mitapivat, Etavopivat: Activation of pyruvate kinase R increases production of ATP through RBC glycolysis; lowers BPG	↑RBC ATP content and export; ↓BPG, ↑Oxygen affinity; ↑RBC Deformability, ↓RBC Sickling; ↓Hemolysis	Quezado et al. (2022)
		ENO	↑RBC SNO, ↓RBC adhesivity, ↑RBC deformability, ↑Hypoxia-induced vasodilation	Reynolds et al. (2023), Pawloski et al. (2005)
Malaria	Effect on RBC allosteric mediators			
	↑ATP export → ↑Parasitemia			
	Effect on RBC function and vasoregulation	Vasoregulatory modulator		
		Name & mechanism	Effect	
	↓RBC deformability, ↑Hemolysis	Purinergic P2Y receptor inhibitor —KN-62, Ip5I: Inhibition of Pxn 1 channels; decreases RBC ATP export and extracellular ATP	↓ATP export → ↓Parasitemia	Tanneur et al. (2006); Levano-Garcia et al. (2010); Alvarez et al. (2014)

(Continued on following page)

TABLE 1 (*Continued*) Changes in erythrocytic allosteric function and vasoregulation in selected diseases or conditions, and effects following some relevant modulatory interventions.

Disease or condition		Intervention		References
		E-NTPDase inhibitor: Inhibition of this P. falciparum specific ectonucleotidase decreases the hydrolysis of ATP to AMP, thus decreasing RBC cAMP levels	↓RBC cAMP, ↓ATP export, ↑RBC deformability → ↓Parasitemia	Borges-Pereira et al. (2017), Paul et al. (2019)
Pyruvate kinase deficiency (PKD)	Effect on RBC allosteric mediators			
	↓ATP content and export; ↑BPG, ↓Oxygen affinity			
	Effect on RBC function and vasoregulation	Vasoregulatory modulator		
		Name & mechanism	Effect	
	Hemolysis	PKRA	↑PK enzymatic activity, ↑RBC Glycolysis, ↑ATP content and export	Ayi et al. (2008); Al-Samkari et al. (2022)
β-Thalassemia	Effect on RBC allosteric mediators			
	↓ATP content and export; ↑BPG, ↓Oxygen affinity			
	Effect on RBC function and vasoregulation	Vasoregulatory modulator		
		Name and mechanism	Effect	
	Hemolysis	PKRA	↑ATP export; ↑Erythropoiesis; ↓Oxidative stress; ↑Mitochondrial function	Al-Samkari et al. (2022); Matte et al. (2021)
Pulmonary arterial hypertension	Effect on RBC function and vasoregulation	Vasoregulatory modulator		
		Name and mechanism	Effect	
	↓SNO; Decreased vasoactivity	ENO	↑RBC SNO, ↑RBC vasoactivity, Improved pulmonary hemodynamics	McMahon et al. (2005), Moya et al. (2001), Moya et al. (2002)

Transfusion with "rejuvenated" blood (PIPA RBCs) could increase tissue O_2 delivery

As stated previously, RBC storage results in an increase in hemoglobin oxygen affinity (decreased P_{50}), in part due to depletion of BPG. This increase in oxygen affinity may have particularly deleterious effects in anemic patients undergoing cardiac surgery or massive hemorrhage. These populations are particularly susceptible due to limited cardiac reserve and risk of decreased organ perfusion. Srinivasan et al. asked the question "Could one unit of low oxygen affinity blood offer the same benefits of two units of standard blood?" They created and utilized an *in vitro* model of transfusion to assess this question. Their simulated model demonstrated that 'rejuvenated' units could incrementally decrease hemoglobin oxygen affinity (increase P_{50}) following transfusion with 1, 2 and 3 units compared to standard stored RBC units. While standard RBC transfusion increased oxygen delivery, rejuvenated units were calculated to increase oxygen utilization in the tissues based on calculations of arteriovenous oxygen content difference. For patients with robust reserve of cardiac output, standard RBC transfusion may not confer negative outcomes secondary to its increased hemoglobin oxygen affinity, but in patients with reduced cardiac reserve, treatment of perioperative anemia with rejuvenated RBC units may promote improved outcomes (Srinivasan et al., 2018). This assertion is also supported by evidence of better metabolic resuscitation in an animal hemorrhage model using blood with preserved BPG and ATP versus standard storage (Williams et al., 2020)*, as discussed later in the section on hypoxic blood storage methods. While clinical studies comparing outcomes after rejuvenated versus standard RBC treatment, are lacking it has been demonstrated that P_{50} does decrease *in vivo* after large volume transfusions, and this decrease can be ameliorated by transfusing rejuvenated/PIPA treated RBCs. In a pilot study in sickle cell disease (SCD) patients undergoing red blood cell exchange (RCE) transfusion therapy, standard RCE was compared with RCE using the last 4 RBC units treated with PIPA. The findings indicated that PIPA-treated RCE maintained RBC oxygen affinity (consistent with the preservation of BPG), and more generally identified favorable or neutral effects on key metabolic and vascular biomarkers in chronically transfused SCD patients (Lopez Domowicz et al., 2020).

PIPA, BPG, and O_2 offloading kinetics *in vitro*

Efficient and responsive offloading of O_2 is an essential function of RBCs. Although the O_2-binding characteristics of Hb and RBCs are widely understood through O_2 equilibrium curves, the kinetics of O_2 fluxes is also critical. Using a microfluidic chamber designed to rapidly switch between oxygenated and hypoxic perfusate and fluorescent probes reading hemoglobin O_2 saturation, Rabcuka et al. (2022) demonstrated in banked RBCs that single-cell O_2 desaturation kinetics in hypoxia are superior after hypoxic

storage (Hemanext™ storage system) or after mid-storage PIPA loading ("rejuvenation") as compared to those after conventional RBC storage. The benefits of hypoxic RBC storage persisted until about 35 days of storage. Metabolomic signatures common to the benefits of rejuvenation and hypoxic RBC storage were identified, as were signatures unique to each. In contrast, only a few proteins were significantly protected from oxidation by hypoxic storage, and no distinguishing lipidomic signature was identified.

Diffusion-limited state and the effects of PIPA/BPG in perfused kidneys

The clinical significance of changes in the kinetics of O_2 binding and release, or in the position and shape of the O_2 dissociation curve in general, has been debated. In banked RBCs, for example, the leftward shift driven in part by depletion of BPG has been viewed as only a minor concern. One argument holds that PO_2 in blood will equilibrate with that of the tissues during the time it takes the RBC to traverse the capillary; higher-affinity RBCs may take longer (the argument goes) but offloading ultimately does take place during transit. This condition in O_2 delivery is sometimes referred to as a "perfusion-limited" state. Dumbill et al. (2023) recently published elegant new findings challenging this contention. In explanted human kidneys considered for transplantation, they demonstrated that perfusion with PIPA-treated RBC transfusates, which returns the P_{50} and O_2-offloading time constant toward that of fresh RBCs, resulted in 60% higher renal cortical PO_2 as compared to perfusion with control stored RBCs from the same donor. These findings support a "diffusion-limited" model of O_2 delivery, in which the O_2-offloading kinetic properties of the perfusing RBCs play an important role in O_2 transfer. The diffusion-limited model may be particularly relevant in organs with higher O_2 needs, including the brain, skeletal muscle, and the heart; when regional blood flow is elevated (shortening RBC transit time), and when anemia is present.

Should microcirculatory indices be investigated to inform decision-making for RBC transfusion?

Microcirculatory functions that govern tissue perfusion are logical indices to guide medical decision-making and act as therapeutic targets, but progress has been limited by a paucity of evidence of their incremental value beyond standard parameters (macrohemodynamic indices like blood pressure, cardiac output, and pulse oximetry) and by uncertainty over the relevance of microcirculatory data from accessible circulatory beds (e.g., the sublingual microvasculature). In critically ill adults, Van Manen et al. (2020) identified significant differences in the RBC-transfusion-induced change in microcirculatory indices (proportion of perfused vessels and microvascular flow index) in patients with greater illness severity as compared to those with moderately severe illness, as defined by SOFA (sequential organ failure assessment) scores. The results suggest that the addition of a microcirculatory index in decision-making over about RBC transfusion is worthy of study. Given the emergence of clinically accessible modulators of both arms (O_2 kinetics and vasoregulation) of the control of O_2 delivery by RBCs, it is also tempting to speculate that integration of a microcirculatory endpoint in decision algorithms could identify critically ill patient endotypes (subsets of patients) who may benefit from transfusion with modified units of RBCs that are (for example) poised to offload O_2 more efficiently, poised to vasodilate more readily, or both (or neither). Alternatively, differential (or mutual) regulation of these RBC O_2-delivery functions could be influenced independent of the need for RBC transfusion by systemic (oral) administration of agents in these therapeutic classes.

Metabolic effects of S1P in the RBC

Multiple approaches to augmenting organic phosphates (ATP and/or BPG particularly) in either native or transfused (stored) RBCs have been demonstrated. In contrast to the PIPA approach which depends upon boosting substrate/precursors, agents that promote glycolysis enzymatically or via competition (described below) are also effective but may have different advantage/disadvantage profiles. Sphingosine-1-phosphate (S1P) promotes RBC glycolysis by mediating the binding of hemoglobin to the N-terminus (cytoplasmic tail) of the RBC membrane anion transporter Band 3 (also termed anion exchanger 1 (AE1)). This drives glycolysis by freeing up the complex of glycolytic enzymes that otherwise remain inactivated by assembling on the cytoplasmic domain of Band 3 (cdB3). Because RBC storage leads to loss of S1P, supplementing S1P is logical. Hay et al. demonstrated the ability of exogenous S1P ("dosed" so as to restore pre-storage levels) boosted RBC ATP and BPG levels. However, this came at the expense of generation of NADPH, a reductant generated via the pentose phosphate pathway (PPP), whose activity is blunted when glycolysis accelerates due to substrate competition. While the immediate result may be disappointing, there is reason to reconsider the S1P approach, for example, in combination with provision of additional substrate and/or under conditions (such as *in vivo*) where RBCs are cycling normally between oxygenated (promoting PPP activity and NADPH generation) and deoxygenated (promoting glycolysis and thus ATP and BPG synthesis) states (D'Alessandro et al., 2023; Donovan et al., 2022; Isiksacan et al., 2023; Nemkov et al., 2022; Nielsen et al., 2017).

Red blood cells in disease states

PKD and thalassemia

Pyruvate kinase, ATP, and hemolytic anemias

The sole pathway for the generation of ATP in red blood cells is glycolysis, with pyruvate kinase generating ATP from ADP late in glycolysis. Persons with PK deficiency (PKD) are susceptible to hemolytic anemia. PKD patients are relatively protected from infection with malaria, an effect that may have driven the high frequency of the *PKLR* genetic variants in the sub-Saharan African population (Ayi et al., 2008). This paradoxical protective effect is reminiscent of the protective effect of HbS against malarial infection. Conversely, when heterozygous HbS ("sickle trait") and PKD coincide, an SCD phenotype emerges. In two independent cohorts of child and adult patients with HbSS or HbSβo (beta-thalassemia) SCD, certain *PKLR* variants were demonstrated to associate with the frequency of acute pain episodes requiring hospitalization (Wang et al., 2022). These findings underscore a modulatory role for RBC PK (PKR) in SCD outcomes and symptoms and are supportive of investigation of the use of PKR

activators in reducing the frequency of such acute pain episodes and other pathophysiology, especially in individuals with such *PKLR* variants (Wang et al., 2022). PKD is characterized by chronic hemolytic anemia and iron overload. The benefits of pyruvate kinase activation are several: improvements are seen in erythropoiesis and iron homeostasis. Recent clinical reports have indicated that the PKR activators etavopivat and mitapivat have beneficial effects in other etiologies of anemia beyond PKD, including beta-thalassemia.

PKR activation in PKD and thalassemia

The pyruvate kinase (PK) activators AG-348 (mitapivat, by Agios Pharmaceuticals) and FT-4202 (known as etavopivat, originally by Forma now Novo Nordisk), have shown early promise in addressing various hereditary hemolytic anemias, in PK deficiency (PKD) and beyond. In a study investigating PKD, a rare hereditary condition affecting red blood cell (RBC) glycolytic metabolism, AG-348 effectively increased PK enzymatic activity and stability in PK-deficient RBCs, apparently restoring glycolytic pathway activity (Rab et al., 2021). In phase III clinical trials for PK deficiency, mitapivat was shown to be safe and efficacious, with results suggesting its potential as a disease-modifying therapy for hereditary hemolytic anemias (Al-Samkari and van Beers, 2021). Mitapivat also showed promise in treating β-thalassemia-related anemia by improving erythropoiesis, reducing oxidative stress, and enhancing mitochondrial function (Matte et al., 2021). Additionally, mitapivat demonstrates potential beyond these disorders, showing efficacy in hereditary spherocytosis according to preclinical studies (Matte et al., 2021). Clinical trials focusing on PK deficiency patients reveal mitapivat's capacity to improve markers of ineffective erythropoiesis and iron homeostasis, offering a potential reduction in iron overload. With convenient oral administration and a safety profile comparable to placebo in adults with PK deficiency, mitapivat and etavopivat have emerged as promising new therapeutic options for various hereditary hemolytic anemias, including those lacking currently approved drug therapies (Schroeder et al., 2022; Shrestha et al., 2021). The results suggest that PKRAs have the potential to be effective and disease-modifying therapies for PK deficiency, offering early and robust Hb responses and the normalization of Hb levels in a significant proportion of patients.

Sickle cell disease

Allosteric modulation using voxelotor in SCD

The hallmark transformation to sickle (crescent)-shaped cells in sickle cell disease (SCD) takes place upon SCD RBC deoxygenation as HbS gains the ability polymerize when in its deoxygenated, but not in the oxygenated, state. Polymerization leads to the formation of long, insoluble fibers that stretch and distort the RBC, ultimately forcing the sickle shape. The polymerization of sickled HbS leads to vaso-occlusive crises (VOCs) in patients, and the number of sickled RBCs has been shown to rise one to three days before the clinical presentation of VOC (Table 1). Polymerized sickled RBCs have decreased deformability, obstruct the microvasculature, and promote end-organ damage, as well as intense pain for the patient. VOCs drive much of the morbidity and mortality in SCD with hospitalization necessary for 95% of VOC presentations (Darbari et al., 2020; Suhail, 2024). Metcalf et al. (2017) investigated the use of positive allosteric RBC modulators (that can increase the oxygen affinity of hemoglobin) to increase the proportion of HbS in the oxy-HbS state. The aim was to assess whether stabilizing HbS in the oxygenated state could prevent polymerization. They found success with a compound, then called GBT440, which through reversible and covalent binding to hemoglobin, stabilized the oxygenated state and limited polymerization. Advantageously, it was also found to be orally bioavailable and partitioned to RBC at an RBC/plasma ratio of 150, allowing for low systemic concentrations while still having a therapeutic effect. A large phase III randomized trial, the Hemoglobin Oxygen Affinity Modulation to Inhibit HbS Polymerization (HOPE) Trial, showed this molecule, now known as voxelotor, to be safe and effective and led to its FDA approval for treatment of sickle cell disease (Vichinsky et al., 2019; Howard et al., 2021). In these trials, voxelotor increased hemoglobin levels, decreased the incidence of anemia, and decreased hemolysis. However, treatment was not associated with any change in frequency of VOCs. Since its approval, voxelotor has been associated with lower transfusion requirements, fewer prescribed opiates, and an increase in mean Hb as compared to standard therapy (Shah et al., 2022). Overall, voxelotor has been a proof of concept for the therapeutic power and clinical impact of the altering Hb O_2 affinity.

With multiple new interventions including voxelotor and PKR activators (acting to suppress BPG) such as etavopivat, there is now a need to compare therapies. Moody et al. (2024) created a quantitative model allowing comparison of each intervention with an effective dose of hydroxyurea (induction of endogenous HbF to 30%) and modeling how the two medications might work together (which can also reduce the required dosing of each agent). This clinical tool, and others like it, could, if validated, guide providers in their choice of therapy and dosage for treatment of SCD. Investigating other potential benefits of voxelotor in SCD patients, Mendelson et al. (2024) used a mouse model to show that of voxelotor could replace the several months of RBC transfusion currently required prior to gene therapy for SCD. New assays will allow the future identification of novel anti-sickling compounds (Nakagawa et al., 2022). These new roles for voxelotor, as well as the discovery of novel compounds, could increase the overall availability and use of disease-modifying therapy (DMT) for SCD, as rates of DMT use remain low even with the introduction of newer therapies (Newman et al., 2023).

Voxelotor in acute lung injury and hypoxemia

The ability to manipulate the oxygen affinity of hemoglobin may also be leveraged in situations of hypoxia outside of SCD. There is a theoretical advantage to left-shifting the oxygen dissociation curve, and thus increasing the oxygen affinity for Hb, in hypoxemia. This intervention allows for increased oxygen binding at a given PO_2, which could increase the uptake of oxygen in the lungs in critically ill patients including those with acute lung injury. While voxelotor is only FDA-approved at this time for use in sickle cell disease, recent studies explored its usage in other settings. Vlahakis et al. (2019) showed the promise of this therapy in idiopathic pulmonary fibrosis (IPF) patients, showing that voxelotor decreased exercise-induced hypoxemia in a small cohort of IPF patients. Stewart et al. (2020) showed voxelotor could increase arterial oxygen saturation in healthy patients during hypoxia and submaximal exercise. With the goal of reducing hypoxemia by means other than via supplemental oxygen delivery (which can itself be toxic), improving ventilation/perfusion (V/Q)

mismatch, and limiting RBC transfusion, centers have begun to trial voxelotor with patients receiving intensive care. Two such cases in critically ill patients experiencing hypoxemia were treated with voxelotor at Duke University by one of the authors. While clinical benefit cannot be established by case reports, no adverse effects from the trial were noted and the tolerability of the therapy was demonstrated (Al-Qudsi et al., 2023). More robust testing with large RCTs is necessary to further assess the efficacies and roles of these interventions.

Voxelotor has been successful in increasing Hb levels in patients but relying on this singular metric as a heuristic for oxygen supply to tissues could lead to misunderstanding and even patient harm. The oxygen carrying capacity of Hb as well as its ability to offload oxygen are also important factors in transferring oxygen from the lungs to tissues. Increasing the oxygen affinity of hemoglobin allows for increased onloading of oxygen in the lungs, but, conversely, may disfavor or decrease unloading of oxygen to the tissues. This fact has led to concern around the possibility that these DMTs that increase O_2 affinity of Hb could have the negative effect of decreased tissue O_2 delivery. Longer-term follow-up of participants in the HOPE trial has shown no end-organ perfusion related damage secondary to voxelotor treatment, although these studies might lack the power needed to find such changes (Howard et al., 2021). Alternatively, the lack of net harm (via impaired O_2 offloading in the tissues), if confirmed, could reflect compensatorily increased activity of local microcirculatory regulators including ATP and SNO.

O_2 affinity in SCD and the rationale(s) for PKR activation

PKR activation is rational in SCD not only because boosting RBC ATP may be beneficial, but also by lowering BPG levels resulting in a favorable change in O_2 affinity (Figure 1; Table 1). O_2 affinity and dissociation behavior in SCD blood differ from that of healthy blood in several respects. BPG levels are increased in SCD, but the degree of change varies (Table 1; Figure 1). Overall, the resulting "rightward shift" in the O_2 binding curve is small, and depressed O_2 saturation of HbS arises more from increases in CO-Hb (carbonmonoxyHb; CO is generated endogenously as a byproduct of heme turnover following hemolysis) and in oxidized metHb (Needleman et al., 1999). Variable compensatory upregulation of production of fetal Hb moves O_2 affinity in the opposite direction (higher). Finally, once polymerized (as during SCD crisis), functional HbS affinity is lower. Pulse oximetric readings of Hb O_2 saturation may be misleading for two major reasons: first, there is a now well-recognized algorithmic bias in pulse oximetry based SpO_2 readings owing to subject skin color (pigment), with major implications in patients of African descent (Wong et al., 2021). Secondly, the SpO_2 values are skewed by the presence of CO-Hb and metHb as noted.

The investigational erythrocyte pyruvate kinase (PKR) activator etavopivat was also studied in clinical trials (Xu et al., 2022) focused on sickle cell disease (SCD) patients (Figure 1). These trials aimed to identify the maximum dose with an acceptable safety profile. Cohorts of patients with SCD treated were with varying doses of etavopivat for 2 weeks; improvements were seen in various markers and the drug was well-tolerated according to safety profiles (Forsyth et al., 2022). In an open-label study of patients treated with etavopivat for 12 weeks, similarly reassuring results were demonstrated in terms of safety, along with improved markers of anemia and hemolysis (Saraf et al., 2024). These findings suggest that etavopivat could be an effective treatment for SCD patients, potentially reducing the risk of vaso-occlusive crises and end-organ damage. Etavopivat may hold promise for the treatment of sickle cell disease and other hemoglobin disorders by targeting some of the underlying pathophysiology. Interestingly, the benefits in SCD may reflect not only the increased RBC ATP levels, but also decreased BPG, as described below.

PKR activation in a mouse model of SCD

In sickle cell disease, RBC sickling and its downstream consequences depend on HbS (sickle hemoglobin) deoxygenation. In the SCD RBC, deoxygenation is favored due to elevated levels of BPG. Treatments that lower the BPG concentration and thereby raise O_2 affinity (lower P_{50}) are therefore predicted to have therapeutic benefit (Table 1). Indeed, indirect (e.g., hydroxyurea, which stimulates production of high-O_2-affinity fetal hemoglobin, HbF) and direct (voxelotor) approaches to increase O_2 affinity have demonstrated benefits in SCD. RBCs from persons with SCD contain and export lower amounts of vasoregulatory ATP, which may contribute to the dysregulation of the microcirculation in this disease, as manifested acutely by vasoocclusion and chronically by increased susceptibility to ischemic strokes. Activation of PKR in SCD is therefore therapeutically attractive for at least two effects: it can raise intra-RBC ATP, which is important for both numerous cell-intrinsic functions such as preserving cell integrity and minimizing hemolysis and for extrinsic RBC actions such as vasoregulatory effects of ATP. Additionally of benefit in SCD is that PKR activation can lower BPG. In both human SCD and the Berkeley SCD mouse model, BPG levels are elevated, and ATP is depressed as compared to controls (Jensen et al., 1973; Zhang et al., 2011; Shrestha et al., 2021; Forsyth et al., 2022; Schroeder et al., 2022). In contrast, the Townes SCD mouse model is characterized by upregulated PKR protein, elevated ATP, and decreased BPG (Quezado et al., 2022). Nevertheless, the PKR activator mitapivat increased RBC ATP values further while having no effect on BPG levels in Townes mice. In parallel, the PKRA induced favorable changes in RBC mitochondrial retention, RBC oxidative tone, and leukocytosis but no significant attenuation of sickling threshold. These findings suggest that increases in RBC ATP alone may be beneficial in SCD, even when baseline ATP values are near normal. In sickle cell disease, mitapivat's ability to increase ATP levels and reduce complications in a mouse model underscores its potential therapeutic effects, although the differences between mouse models and actual human SCD are acknowledged (Al-Samkari and van Beers, 2021; Matte et al., 2021).

Dual- and triple-action drugs for SCD: allosteric modulation, anti-polymerization, and vasoregulatory

Therapeutic approaches to anti-sickling have focused on both measures to disfavor facile deoxygenation and methods to inhibit polymerization. Hydroxyurea is an established therapy in SCD that induces the production of fetal hemoglobin (HbF). HbF has higher O_2 affinity than adult Hb (accounting for the ability of the fetus to extract O_2 from maternal blood), and its presence alongside HbS can prevent deoxyHbS from achieving the critical concentrations necessary for

polymerization. More recently, voxelotor (Oxbryta) gained FDA approval, and this aromatic aldehyde raises O_2 affinity, disfavoring the deoxygenation-dependent polymerization process. Next-generation aromatic aldehydes such as VZHE-039 (Abdulmalik et al., 2020), developed and synthesized by Dr. Martin Safo et al., not only raise O_2 affinity (thus preventing HbS polymerization through an "O_2-dependent" anti-sickling mechanism), but also have direct anti-polymerization action through direct interactions with the alpha subunits of HbS. Safo et al. went further and incorporated into VZHE-039 a nitric oxide (NO)-donor moiety by synthesizing the nitrate ester derivative of VZHE-039, VZHE-039-NO (Figure 1) (Huang et al., 2022). This molecule retains both the O_2-dependent (allosteric) and O_2-independent (direct) anti-polymerization properties while introducing antiadhesive effects on the treated SCD RBCs by delivering the NO group (Huang et al., 2022). We have also demonstrated antiadhesive actions of NO/SNO repletion using simple NO donors in SS RBCs (McMahon et al., 2019).

RBC ATP and malaria: the dark side of RBC-derived ATP

Following parasitic infection with *P. falciparum*, ATP release has been found to contribute to parasitic growth via various mechanisms. ATP release is stimulated by surges in intracellular cyclic adenosine monophosphate (cAMP) concentrations in response to hypoxia or mechanical stress (Table 1). (Sluyter, 2015) Binding of ATP to purinergic receptors, specifically P2Y receptors, on the cell membrane induces the opening of "new permeability pathways (NPP)," channels for osmolytes and anions (Tanneur et al., 2006) whose entry facilitate growth of the parasite as nutrients such as carbohydrates and amino acids can be imported intracellularly and metabolic waste can be removed (Tanneur et al., 2006; Ramdani and Langsley, 2014). Additionally, binding of RBC P2Y receptors by the released ATP has been linked to an upregulation of cAMP production, associated with decreased deformability of malaria-infected cells due to phosphorylated cytoskeletal proteins, establishing positive feedback for the further release of ATP (Ramdani and Langsley, 2014; Sluyter, 2015). The reduced deformability can contribute to pathophysiology by rendering these RBCs more susceptible to the lysis seen in malarial disease.

ATP is normally far more abundant in the RBC than in the plasma. Since increased extracellular ATP content has been associated with increased rates of parasitemia (Alvarez et al., 2014), preventing release of ATP may be a new approach to limiting parasitic growth and infection. ATP is primarily released through pannexin 1 (Px1), a membrane channel or pore that facilitates the passive export of ATP; therefore, blocking the release of ATP could minimize extracellular ATP content (Alvarez et al., 2014). Widely used anti-malaria drugs, such as mefloquine, block the Px1 channel and their success in combating malaria infection appears to be tied to prevention of ATP release (Dahl et al., 2013) in addition to their direct anti-parasite actions. With the rise of parasitic resistance to currently-available anti-malarial drugs (Borges-Pereira et al., 2017), another possible avenue for malaria therapeutics is the use of inhibitors of purinergic P2Y receptors, such as KN-62 and Ip5I, which have been associated *in vitro* with reduced levels of parasitemia in human RBCs (Tanneur et al., 2006; Levano-Garcia et al., 2010). Purinergic receptors have additionally been linked to opening Px1 channels, consequently increasing extracellular ATP (Locovei et al., 2006), so inhibition of P2Y receptors could potentially also limit ATP release by disrupting the feedback loop. Further research regarding selective inhibitors of purinergic receptors could be advantageous for preventing the opening of NPPs and changes in the deformability (fragility) of infected RBCs. Another potential target of therapy are the ectonucleotidases, extracellular enzymes typically located on the surface of RBCs and other cells that can hydrolyze extracellular ATP molecules into AMP, which can then be converted to adenosine, a molecule that signals to increase of cAMP levels within RBCs (Borges-Pereira et al., 2017; Paul et al., 2019). As mentioned, increased intracellular cAMP content stimulates the further release of ATP and additionally increases the rigidity of RBCs (Paul et al., 2019). The genome of *P. falciparum* contains a specific ectonucleoside E-NTPDase whose activity is heightened with higher levels of extracellular ATP (Alvarez et al., 2014). Inhibition of E-NTPDase hinders the development of infected RBCs, emphasizing the link between ectonucleotidases and parasitic growth (Borges-Pereira et al., 2017).

RBC SNO depletion and cardiovascular/cardiopulmonary disease

RBC vasoactivity and SNO

The binding and release of NO by RBC Hb are allosterically controlled by the oxygenation and deoxygenation-induced toggling between the R (relaxed) and T tense) conformations of Hb. Upon oxygenation, an SNO adduct forms from precursor NO at the reactive and highly conserved β93 Cys thiol residue of Hb. Conversely, and in keeping with basic thermodynamics, the SNO moiety is released from Hb upon the allosteric transition to the deoxygenated, T structure. The released SNO can exit the RBC, unlike precursor NO whose affinity for the heme groups in RBC Hb so great that escape is exceedingly rare. SNO-Hb displays higher O_2 affinity and a leftward shift in the O_2 dissociation curve relative to unmodified Hb. This elevated O_2 affinity acts to disfavor profligate SNO release but has no meaningful impact on aggregate blood O_2 affinity because only about 1 per 1000 Hb molecules carries a SNO group, and the ODC shift is not huge. Stated otherwise, blood (RBC) Hb is densely concentrated (millimolar), but RBC Hb-bound SNO is in low abundance (~1 μM). Nevertheless, given the high vasoregulatory potency of SNOs, nanomolar fluxes of this vascular signal resulting from the release of only a small fraction of RBC Hb-derived SNO are sufficient to effect blood flow-regulating vasodilation. We recently identified the type 1 system L amino acid transporter (LAT1) as the conduit responsible for SNO export by RBCs (Figure 1) and its import by endothelial cells. LAT1 inhibitors diminish the extracellular accumulation of SNOs that is typical when RBCs are deoxygenated, and in a mouse deficient in endothelial LAT1 ($LAT1^{ECKD}$), cellular uptake of CSNO is impaired (Dosier et al., 2017). The broad vasoregulatory purview of RBC-derived SNOs is underscored by the observation that when $LAT1^{ECKO}$ mice are transfused, recipient RBCs are sequestered in the lungs and blood oxygenation is depressed. These findings are reminiscent of the impaired oxygenation typical of patients transfused with stored RBCs, which are depleted of SNOs.

Some investigators questioned the importance of SNO-Hb in vasoregulation. In particular, RBCs from a mouse model bearing human hemoglobin in which the β93 Cys residue was mutated to Ala (alanine) were reported to function normally. But this mouse was

also engineered to express gamma hemoglobin [a component of fetal hemoglobin (HbF)], which we have shown is also reversibly S-nitrosylated (Riccio et al., 2016); this rescue may account for the lack of phenotype in this mouse. By contrast, Zhang and coworkers demonstrated that even the persistence (or presence by knock-in) of SNO-susceptible fetal hemoglobin does not fully compensate for the mutation of the critical Cys normally present at residue 93 of the beta-globin subunit of hemoglobin (Zhang et al., 2015). In mice where β93 Cys is mutated to Ala, peripheral blood flow is depressed at baseline and declines during hypoxia, rather than increasing, which is the classic adaptive peripheral vascular response. Accordingly, tissue oxygenation is lower at baseline in the C93A mice than in transgenic controls expressing non-mutated human Hb and declines further during hypoxia. In humanized mouse models of myocardial infarction and heart failure (Zhang et al., 2016), mutation of Hb at the relevant Cysβ93 residue rendering it incapable of forming and transferring the SNO group led to greater cardiac injury and mortality. Also underscoring the essential nature of this RBC activity was that in the mutant mice, coronary vessel collateralization was demonstrated (but did not suffice to prevent injury and mortality) (Zhang et al., 2016).

The regional nature of the hypoxic vasodilatory reflex is exemplified in reactive hyperemia, in which blood flow to an organ (a leg, for example) rebounds higher than baseline flow following the release of a briefly enforced arterial occlusion (e.g., by tourniquet). Reynolds and coworkers found RH responses, and the associated post-reperfusion rebound in tissue oxygenation, to be deficient in C93A mutant mice as compared to mice expressing wild-type (C93) human Hb. In humans, the time needed for tissue reoxygenation upon reactive hyperemic responses correlated inversely with both SNO-Hb absolute values and with the ratio of SNO-Hb to total Hb-bound NO. In patients with peripheral arterial disease, tissue reoxygenation was slowed and SNO-Hb values were depressed. Taken together these findings indicate a role for SNO-Hb in the metabolite-driven (and O_2-sensitive) hyperemic response to reperfusion, a clinically relevant adaptive response involving hypoxic vasodilation and RBCs (Reynolds et al., 2023).

In an elegant test of the role of RBCs, NO and SNO in human hypoxic vasodilation, Hoiland et al. (2023) demonstrated that changes in cerebral blood flow in response to hypoxia were associated with increases in the transcerebral [arterial-to-jugular venous (A-V)] SNO gradient, but not associated with a cerebral A-V nitrite gradient. Cerebral hypoxic vasodilation was augmented during hemodilution in both lowlanders and in polycythemic native Andeans living at high altitude (4300 m), underscoring the apparent role of vasoregulatory mediators downstream of the exquisite O_2 sensor hemoglobin. Taken together, these findings support the assertion that the hypoxia-driven release of SNOs (perhaps ultimately formed from precursor NO by endothelial-type NO synthase) from RBCs contributes critically to the characteristically O_2-sensitive vasoregulation typical of the brain.

Modulation of RBC-dependent vasoregulation by SNO donors

Deficient RBC-based SNO-dependent vasoactivity contribute to pathology in disease states including SCD, pulmonary arterial hypertension, and ischemic cardiovascular disease (McMahon et al., 2005; Pawloski et al., 2005; Zhang et al., 2015; Sonveaux et al., 2007). RBC transfusion for anemia only benefits a subset of patients: those with moderate or severe anemia (Hb < 7 gm/dL in several randomized studies) (Hebert et al., 1999; Lacroix et al., 2007), and the early, deficient vasoregulatory capacity of stored blood secondary to depletion of SNO and ATP appears contributory. One possible exception to the general lack of benefit of more aggressive RBC transfusion is the patient with acute myocardial infarction, with the recently reported MINT trial showing a strong trend in outcomes (Carson et al., 2023) interpreted by some (Bloch and Tobian, 2023) as supporting a more liberal transfusion strategy in these patients and, by extension, a recognition that one size does not fit all in RBC transfusion decision-making. In the heart, a high O_2 utilization downstream of flow-limiting stenosis and/or thrombosis may contribute to benefits of RBC transfusion outweighing its potential harms.

Restoration of RBC vasoactivity

Decreased vasoactivity due to diminished RBC export of SNO can be restored to more physiologic levels by either direct exposure of the RBCs or by administration to patients of SNO precursors. In banked human RBCs deficient in SNO, exposure to NO donors under the appropriate conditions is sufficient to regenerate SNO using the ability of Hb to form SNO from NO (Riccio et al., 2015). In stored RBCs this SNO restoration improves RBC deformability and attenuates RBC adhesivity (Riccio et al., 2015). RBCs exposed to the SNO donor ethyl nitrite (ENO) regain their ability to effect hypoxic vasodilation (Reynolds et al., 2007). In adults PAH patients breathing ENO, RBC SNO and RBC vasoactivity are restored, with parallel improvements in pulmonary hemodynamics (phenocopying that seen in animals) (McMahon et al., 2005; Moya et al., 2001). Newborns with persistent pulmonary hypertension see similar pulmonary hemodynamic benefits (Moya et al., 2002).

Author contributions

TW: Writing–original draft, Writing–review and editing, Conceptualization. MO: Writing–original draft, Writing–review and editing. MJ: Writing–original draft, Writing–review and editing. IW: Writing–original draft, Writing–review and editing, Conceptualization. CD: Writing–original draft, Writing–review and editing. TM: Conceptualization, Funding acquisition, Project administration, Resources, Writing–original draft, Writing–review and editing.

Funding

The author(s) declare financial support was received for the research, authorship, and/or publication of this article. Funding was from VA (BX-003478) and NIH (HL-161071 and HL-156440) to TM, and T32 HL-007057 supporting MJ. TM received research funding from NIH (current), VA (current), Hemanext (2020–2021), and Forma/Novo Nordisk (2022–23) on related topics. The funders were not involved in the study design, collection, analysis, interpretation of data, the writing of this article, or the decision to submit it for publication.

Conflict of interest

The authors declare that the research was conducted in the absence of any commercial or financial relationships that could be construed as a potential conflict of interest.

The author(s) declared that they were an editorial board member of Frontiers, at the time of submission. This had no impact on the peer review process and the final decision.

Publisher's note

References

Abdulmalik, O., Pagare, P. P., Huang, B., Xu, G. G., Ghatge, M. S., Xu, X., et al. (2020). VZHE-039, a novel antisickling agent that prevents erythrocyte sickling under both hypoxic and anoxic conditions. *Sci. Rep.* 10, 20277. doi:10.1038/s41598-020-77171-2

Al-Qudsi, O., Reynolds, J. M., Haney, J. C., and Welsby, I. J. (2023). Voxelotor as a treatment of persistent hypoxia in the ICU. *Chest* 164, e1–e4. doi:10.1016/j.chest.2023.01.036

Al-Samkari, H., and van Beers, E. J. (2021). Mitapivat, a novel pyruvate kinase activator, for the treatment of hereditary hemolytic anemias. *Ther. Adv. Hematol.* 12, 20406207211066070. doi:10.1177/20406207211066070

Alvarez, C. L., Schachter, J., de Sa Pinheiro, A. A., Silva Lde, S., Verstraeten, S. V., Persechini, P. M., et al. (2014). Regulation of extracellular ATP in human erythrocytes infected with Plasmodium falciparum. *PLoS One* 9, e96216. doi:10.1371/journal.pone.0096216

Ayi, K., Min-Oo, G., Serghides, L., Crockett, M., Kirby-Allen, M., Quirt, I., et al. (2008). Pyruvate kinase deficiency and malaria. *N. Engl. J. Med.* 358, 1805–1810. doi:10.1056/NEJMoa072464

Balcerek, B., Steinach, M., Lichti, J., Maggioni, M. A., Becker, P. N., Labes, R., et al. (2020). A broad diversity in oxygen affinity to haemoglobin. *Sci. Rep.* 10, 16920. doi:10.1038/s41598-020-73560-9

Bardyn, M., Crettaz, D., Borlet, M., Langst, E., Martin, A., Abonnenc, M., et al. (2021). Hypoxia and hypocapnia storage of gamma-irradiated red cell concentrates. *Blood Transfus.* 19, 300–308. doi:10.2450/2020.0075-20

Barshtein, G., Rasmusen, T. L., Zelig, O., Arbell, D., and Yedgar, S. (2020). Inter-donor variability in deformability of red blood cells in blood units. *Transfus. Med.* 30, 492–496. doi:10.1111/tme.12725

Bencheikh, L., Nguyen, K. A., Chadebech, P., Kiger, L., Bodivit, G., Jouard, A., et al. (2022). Preclinical evaluation of the preservation of red blood cell concentrates by hypoxic storage technology for transfusion in sickle cell disease. *Haematologica* 107, 1944–1949. doi:10.3324/haematol.2021.279721

Bennett-Guerrero, E., Veldman, T. H., Doctor, A., Telen, M. J., Ortel, T. L., Reid, T. S., et al. (2007). Evolution of adverse changes in stored RBCs. *Proc. Natl. Acad. Sci. U. S. A.* 104, 17063–17068. doi:10.1073/pnas.0708160104

Bloch, E. M., and Tobian, A. A. R. (2023). Optimizing blood transfusion in patients with acute myocardial infarction. *N. Engl. J. Med.* 389, 2483–2485. doi:10.1056/NEJMe2312741

Borges-Pereira, L., Meissner, K. A., Wrenger, C., and Garcia, C. R. S. (2017). Plasmodium falciparum GFP-E-NTPDase expression at the intraerythrocytic stages and its inhibition blocks the development of the human malaria parasite. *Purinergic Signal* 13, 267–277. doi:10.1007/s11302-017-9557-4

Cabrales, P., Tsai, A. G., and Intaglietta, M. (2008). Modulation of perfusion and oxygenation by red blood cell oxygen affinity during acute anemia. *Am. J. Respir. Cell Mol. Biol.* 38, 354–361. doi:10.1165/rcmb.2007-0292OC

Carson, J. L., Brooks, M. M., Hébert, P. C., Goodman, S. G., Bertolet, M., Glynn, S. A., et al. (2023). Restrictive or liberal transfusion strategy in myocardial infarction and anemia. *N. Engl. J. Med.* 389, 2446–2456. doi:10.1056/NEJMoa2307983

Dahl, G., Qiu, F., and Wang, J. (2013). The bizarre pharmacology of the ATP release channel pannexin1. *Neuropharmacology* 75, 583–593. doi:10.1016/j.neuropharm.2013.02.019

D'Alessandro, A. (2023). Red blood cell omics and machine learning in transfusion medicine: singularity is near. *Transfus. Med. Hemother* 50, 174–183. doi:10.1159/000529744

D'Alessandro, A., Anastasiadi, A. T., Tzounakas, V. L., Nemkov, T., Reisz, J. A., Kriebardis, A. G., et al. (2023). Red blood cell metabolism *in vivo* and *in vitro*. *Metabolites* 13, 793. doi:10.3390/metabo13070793

Darbari, D. S., Sheehan, V. A., and Ballas, S. K. (2020). The vaso-occlusive pain crisis in sickle cell disease: definition, pathophysiology, and management. *Eur. J. Haematol.* 105, 237–246. doi:10.1111/ejh.13430

Donovan, K., Meli, A., Cendali, F., Park, K. C., Cardigan, R., Stanworth, S., et al. (2022). Stored blood has compromised oxygen unloading kinetics that can be normalized with rejuvenation and predicted from corpuscular side-scatter. *Haematologica* 107, 298–302. doi:10.3324/haematol.2021.279296

Dosier, L. B. M., Premkumar, V. J., Zhu, H., Akosman, I., Wempe, M. F., and McMahon, T. J. (2017). Antagonists of the system L neutral amino acid transporter (LAT) promote endothelial adhesivity of human red blood cells. *Thromb. Haemost.* 117, 1402–1411. doi:10.1160/TH16-05-0373

Dumbill, R., Rabcuka, J., Fallon, J., Knight, S., Hunter, J., Voyce, D., et al. (2023). Impaired O2 unloading from stored blood results in diffusion-limited O2 release at tissues: evidence from human kidneys. *Blood* 143, 721–733. doi:10.1182/blood.2023022385

Evans, B. A., Ansari, A. K., Srinivasan, A. J., Kamyszek, R. W., Stoner, K. C., Fuller, M., et al. (2020). Rejuvenation solution as an adjunct cold storage solution maintains physiological haemoglobin oxygen affinity during early-storage period of red blood cells. *Vox Sang.* 115, 388–394. doi:10.1111/vox.12910

Forsyth, S., Schroeder, P., Geib, J., Vrishabhendra, L., Konstantinidis, D. G., LaSalvia, K., et al. (2022). Safety, pharmacokinetics, and pharmacodynamics of etavopivat (FT-4202), an allosteric activator of pyruvate kinase-R, in healthy adults: a randomized, placebo-controlled, double-blind, first-in-human phase 1 trial. *Clin Pharmacol Drug Dev* 11, 654–665. doi:10.1002/cpdd.1058

Gehrke, S., Shah, N., Gamboni, F., Kamyszek, R., Srinivasan, A. J., Gray, A., et al. (2019). Metabolic impact of red blood cell exchange with rejuvenated red blood cells in sickle cell patients. *Transfusion* 59, 3102–3112. doi:10.1111/trf.15467

Gehrke, S., Srinivasan, A. J., Culp-Hill, R., Reisz, J. A., Ansari, A., Gray, A., et al. (2018). Metabolomics evaluation of early-storage red blood cell rejuvenation at 4°C and 37°C. *Transfusion* 58, 1980–1991. doi:10.1111/trf.14623

Hay, A., Nemkov, T., Gamboni, F., Dzieciatkowska, M., et al. (2023). Sphingosine 1-phosphate has a negative effect on RBC storage quality. Blood Adv. *Transfusion* 7(8), 1379–1393. doi:10.1182/bloodadvances.2022008936

Hazegh, K., Fang, F., Bravo, M. D., Tran, J. Q., Muench, M. O., Jackman, R. P., et al. (2021). Blood donor obesity is associated with changes in red blood cell metabolism and susceptibility to hemolysis in cold storage and in response to osmotic and oxidative stress. *Transfusion* 61, 435–448. doi:10.1111/trf.16168

Heaton, A., Keegan, T., and Holme, S. (1989). *In vivo* regeneration of red cell 2,3-diphosphoglycerate following transfusion of DPG-depleted AS-1, AS-3 and CPDA-1 red cells. *Br. J. Haematol.* 71, 131–136. doi:10.1111/j.1365-2141.1989.tb06286.x

Hebert, P. C., Wells, G., Blajchman, M. A., Marshall, J., Martin, C., Pagliarello, G., et al. (1999). A multicenter, randomized, controlled clinical trial of transfusion requirements in critical care. Transfusion Requirements in Critical Care Investigators, Canadian Critical Care Trials Group. *N. Engl. J. Med.* 340, 409–417. doi:10.1056/NEJM199902113400601

Hoiland, R. L., MacLeod, D. B., Stacey, B. S., Caldwell, H. G., Howe, C. A., Nowak-Fluck, D., et al. (2023). Hemoglobin and cerebral hypoxic vasodilation in humans: evidence for nitric oxide-dependent and S-nitrosothiol mediated signal transduction. *J. Cereb. Blood Flow. Metab.* 43, 1519–1531. doi:10.1177/0271678X231169579

Holst, L. B., Haase, N., Wetterslev, J., Wernerman, J., Guttormsen, A. B., Karlsson, S., et al. (2014). Lower versus higher hemoglobin threshold for transfusion in septic shock. *N. Engl. J. Med.* 371, 1381–1391. doi:10.1056/NEJMoa1406617

Howard, J., Ataga, K. I., Brown, R. C., Achebe, M., Nduba, V., El-Beshlawy, A., et al. (2021). Voxelotor in adolescents and adults with sickle cell disease (HOPE): long-term follow-up results of an international, randomised, double-blind, placebo-controlled, phase 3 trial. *Lancet Haematol.* 8, e323–e333. doi:10.1016/S2352-3026(21)00059-4

Huang, B., Ghatge, M. S., Donkor, A. K., Musayev, F. N., Deshpande, T. M., Al-Awadh, M., et al. (2022). Design, synthesis, and investigation of novel nitric oxide (NO)-Releasing aromatic aldehydes as drug candidates for the treatment of sickle cell disease. *Molecules* 27, 6835. doi:10.3390/molecules27206835

Isiksacan, Z., D'Alessandro, A., Wolf, S. M., McKenna, D. H., Tessier, S. N., Kucukal, E., et al. (2023). Assessment of stored red blood cells through lab-on-a-chip technologies for precision transfusion medicine. *Proc. Natl. Acad. Sci. U. S. A.* 120, e2115616120. doi:10.1073/pnas.2115616120

Jensen, M., Shohet, S. B., and Nathan, D. G. (1973). The role of red cell energy metabolism in the generation of irreversibly sickled cells in vitro. *Blood* 42, 835–842.

Kirby, B. S., Hanna, G., Hendargo, H. C., and McMahon, T. J. (2014). Restoration of intracellular ATP production in banked red blood cells improves inducible ATP export and suppresses RBC-endothelial adhesion. *Am. J. Physiol. Heart Circ. Physiol.* 307, H1737–H1744. doi:10.1152/ajpheart.00542.2014

Koch, C. G., Li, L., Sessler, D. I., Figueroa, P., Hoeltge, G. A., Mihaljevic, T., et al. (2008). Duration of red-cell storage and complications after cardiac surgery. *N. Engl. J. Med.* 358, 1229–1239. doi:10.1056/NEJMoa070403

Lacroix, J., Hebert, P. C., Hutchison, J. S., Hume, H. A., Tucci, M., Ducruet, T., et al. (2007). Transfusion strategies for patients in pediatric intensive care units. *N. Engl. J. Med.* 356, 1609–1619. doi:10.1056/NEJMoa066240

Levano-Garcia, J., Dluzewski, A. R., Markus, R. P., and Garcia, C. R. (2010). Purinergic signalling is involved in the malaria parasite Plasmodium falciparum invasion to red blood cells. *Purinergic Signal* 6, 365–372. doi:10.1007/s11302-010-9202-y

Li, H., Fang, K., Peng, H., He, L., and Wang, Y. (2022). The relationship between glycosylated hemoglobin level and red blood cell storage lesion in blood donors. *Transfusion* 62, 663–674. doi:10.1111/trf.16815

Lilly, L. E., Blinebry, S. K., Viscardi, C. M., Perez, L., Bonaventura, J., and McMahon, T. J. (2013). Parallel assay of oxygen equilibria of hemoglobin. *Anal. Biochem.* 441, 63–68. doi:10.1016/j.ab.2013.06.010

Liu, Y., Hesse, L. E., Geiger, M. K., Zinn, K. R., McMahon, T. J., Chen, C., et al. (2022). A 3D-printed transfusion platform reveals beneficial effects of normoglycemic erythrocyte storage solutions and a novel rejuvenating solution. *Lab. Chip* 22, 1310–1320. doi:10.1039/d2lc00030j

Locovei, S., Wang, J., and Dahl, G. (2006). Activation of pannexin 1 channels by ATP through P2Y receptors and by cytoplasmic calcium. *FEBS Lett.* 580, 239–244. doi:10.1016/j.febslet.2005.12.004

Lopez Domowicz, D. A., Welsby, I., Esther, C. R., Jr., Zhu, H., Marek, R. D., Lee, G., et al. (2020). Effects of repleting organic phosphates in banked erythrocytes on plasma metabolites and vasoactive mediators after red cell exchange transfusion in sickle cell disease. *Blood Transfus.* 18, 200–207. doi:10.2450/2020.0237-19

Matte, A., Federti, E., Kung, C., Kosinski, P. A., Narayanaswamy, R., Russo, R., et al. (2021). The pyruvate kinase activator mitapivat reduces hemolysis and improves anemia in a β-thalassemia mouse model. *J. Clin. Invest.* 131, e144206. doi:10.1172/JCI144206

McMahon, T. J., Ahearn, G. S., Moya, M. P., Gow, A. J., Huang, Y. C., Luchsinger, B. P., et al. (2005). A nitric oxide processing defect of red blood cells created by hypoxia: deficiency of S-nitrosohemoglobin in pulmonary hypertension. *Proc. Natl. Acad. Sci. U. S. A.* 102, 14801–14806. doi:10.1073/pnas.0506957102

McMahon, T. J., Shan, S., Riccio, D. A., Batchvarova, M., Zhu, H., Telen, M. J., et al. (2019). Nitric oxide loading reduces sickle red cell adhesion and vaso-occlusion *in vivo*. *Blood Adv.* 3, 2586–2597. doi:10.1182/bloodadvances.2019031633

Melzak, K. A., Muth, M., Kirschhofer, F., Brenner-Weiss, G., and Bieback, K. (2020). Lipid ratios as a marker for red blood cell storage quality and as a possible explanation for donor gender differences in storage quality. *Vox Sang.* 115, 655–663. doi:10.1111/vox.12924

Mendelson, A., Liu, Y., Bao, W., and Shi, P. A. (2024). Effect of voxelotor on murine bone marrow and peripheral blood with hematopoietic progenitor cell mobilization for gene therapy of sickle cell disease. *Blood cells, Mol. Dis.* 105, 102824. doi:10.1016/j.bcmd.2024.102824

Metcalf, B., Chuang, C., Dufu, K., Patel, M. P., Silva-Garcia, A., Johnson, C., et al. (2017). Discovery of GBT440, an orally bioavailable R-state stabilizer of sickle cell hemoglobin. *ACS Med. Chem. Lett.* 8, 321–326. doi:10.1021/acsmedchemlett.6b00491

Meyer, E. K., Dumont, D. F., Baker, S., and Dumont, L. J. (2011). Rejuvenation capacity of red blood cells in additive solutions over long-term storage. *Transfusion* 51, 1574–1579. doi:10.1111/j.1537-2995.2010.03021.x

Moody, A. T., Narula, J., and Maurer, T. S. (2024). Quantitative model-based assessment of multiple sickle cell disease therapeutic approaches alone and in combination. *Clin. Pharmacol. Ther.* 115, 1114–1121. doi:10.1002/cpt.3175

Moya, M. P., Gow, A. J., Califf, R. M., Goldberg, R. N., and Stamler, J. S. (2002). Inhaled ethyl nitrite gas for persistent pulmonary hypertension of the newborn. *Lancet* 360, 141–143. doi:10.1016/S0140-6736(02)09385-6

Moya, M. P., Gow, A. J., McMahon, T. J., Toone, E. J., Cheifetz, I. M., Goldberg, R. N., et al. (2001). S-nitrosothiol repletion by an inhaled gas regulates pulmonary function. *Proc. Natl. Acad. Sci. U. S. A.* 98, 5792–5797. doi:10.1073/pnas.091109498

Nakagawa, A., Cooper, M. K., Kost-Alimova, M., Berstler, J., Yu, B., Berra, L., et al. (2022). High-throughput assay to screen small molecules for their ability to prevent sickling of red blood cells. *ACS Omega* 7, 14009–14016. doi:10.1021/acsomega.2c00541

Nazemian, R., Matta, M., Aldamouk, A., Zhu, L., Awad, M., Pophal, M., et al. (2022). S-Nitrosylated hemoglobin predicts organ yield in neurologically deceased human donors. *Sci. Rep* 12(1), 6639. doi:10.1038/s41598-022-09933-z

Needleman, J. P., Setty, B. N., Varlotta, L., Dampier, C., and Allen, J. L. (1999). Measurement of hemoglobin saturation by oxygen in children and adolescents with sickle cell disease. *Pediatr. Pulmonol.* 28, 423–428. doi:10.1002/(sici)1099-0496(199912)28:6<423::aid-ppul7>3.0.co;2-c

Nemkov, T., Stephenson, D., Earley, E. J., Keele, G. R., Hay, A., Key, A., et al. (2024). Biological and genetic determinants of glycolysis: phosphofructokinase isoforms boost energy status of stored red blood cells and transfusion outcomes. bioRxiv, 2023.09.11.557250. doi:10.1101/2023.09.11.557250

Nemkov, T., Yoshida, T., Nikulina, M., and D'Alessandro, A. (2022). High-throughput metabolomics platform for the rapid data-driven development of novel additive solutions for blood storage. *Front. Physiol.* 13, 833242. doi:10.3389/fphys.2022.833242

Newman, T. V., Yang, J., Suh, K., Jonassaint, C. R., Kane-Gill, S. L., and Novelli, E. M. (2023). Use of disease-modifying treatments in patients with sickle cell disease. *JAMA Netw. Open* 6, e2344546. doi:10.1001/jamanetworkopen.2023.44546

Nielsen, N. D., Martin-Loeches, I., and Wentowski, C. (2017). The effects of red blood cell transfusion on tissue oxygenation and the microcirculation in the intensive care unit: a systematic review. *Transfus. Med. Rev.* 31, 205–222. doi:10.1016/j.tmrv.2017.07.003

Paul, A., Ramdani, G., Tatu, U., Langsley, G., and Natarajan, V. (2019). Studying the rigidity of red blood cells induced by Plasmodium falciparum infection. *Sci. Rep.* 9, 6336. doi:10.1038/s41598-019-42721-w

Pawloski, J. R., Hess, D. T., and Stamler, J. S. (2005). Impaired vasodilation by red blood cells in sickle cell disease. *Proc. Natl. Acad. Sci. U. S. A.* 102, 2531–2536. doi:10.1073/pnas.0409876102

Pittman, R. N., Yoshida, T., and Omert, L. A. (2022). Effect of hypoxic blood infusion on pulmonary Physiology. *Front. Physiol.* 13, 842510. doi:10.3389/fphys.2022.842510

Quezado, Z. M. N., Kamimura, S., Smith, M., Wang, X., Heaven, M. R., Jana, S., et al. (2022). Mitapivat increases ATP and decreases oxidative stress and erythrocyte mitochondria retention in a SCD mouse model. *Blood cells, Mol. Dis.* 95, 102660. doi:10.1016/j.bcmd.2022.102660

Rab, M. A. E., Van Oirschot, B. A., Kosinski, P. A., Hixon, J., Johnson, K., Chubukov, V., et al. (2021). AG-348 (Mitapivat), an allosteric activator of red blood cell pyruvate kinase, increases enzymatic activity, protein stability, and ATP levels over a broad range of PKLR genotypes. *Haematologica* 106, 238–249. doi:10.3324/haematol.2019.238865

Rabcuka, J., Blonski, S., Meli, A., Sowemimo-Coker, S., Zaremba, D., Stephenson, D., et al. (2022). Metabolic reprogramming under hypoxic storage preserves faster oxygen unloading from stored red blood cells. *Blood Adv.* 6, 5415–5428. doi:10.1182/bloodadvances.2022007774

Ramdani, G., and Langsley, G. (2014). ATP, an extracellular signaling molecule in red blood cells: a messenger for malaria? *Biomed. J.* 37, 284–292. doi:10.4103/2319-4170.132910

Reynolds, J. D., Ahearn, G. S., Angelo, M., Zhang, J., Cobb, F., and Stamler, J. S. (2007). S-nitrosohemoglobin deficiency: a mechanism for loss of physiological activity in banked blood. *Proc. Natl. Acad. Sci. U. S. A.* 104, 17058–17062. doi:10.1073/pnas.0707958104

Reynolds, J. D., Posina, K., Zhu, L., Jenkins, T., Matto, F., Hausladen, A., et al. (2023). Control of tissue oxygenation by S-nitrosohemoglobin in human subjects. *Proc. Natl. Acad. Sci. U. S. A.* 120, e2220769120. doi:10.1073/pnas.2220769120

Riccio, D. A., Malowitz, J. R., Cotten, C. M., Murtha, A. P., and McMahon, T. J. (2016). S-Nitrosylated fetal hemoglobin in neonatal human blood. *Biochem. Biophys. Res. Commun.* 473, 1084–1089. doi:10.1016/j.bbrc.2016.04.019

Riccio, D. A., Zhu, H., Foster, M. W., Huang, B., Hofmann, C. L., Palmer, G. M., et al. (2015). Renitrosylation of banked human red blood cells improves deformability and reduces adhesivity. *Transfusion* 55, 2452–2463. doi:10.1111/trf.13189

Saraf, S. L., Hagar, R. W., Idowu, M., Osunkwo, I., Cruz, K., Kuypers, F. A., et al. (2024). Multicenter, phase 1 study of etavopivat (FT-4202) treatment for up to 12 weeks in patients with sickle cell disease. *Blood Adv.* doi:10.1182/bloodadvances.2023012467

Schroeder, P., Fulzele, K., Forsyth, S., Ribadeneira, M. D., Guichard, S., Wilker, E., et al. (2022). Etavopivat, a pyruvate kinase activator in red blood cells, for the treatment of sickle cell disease. *J. Pharmacol. Exp. Ther.* 380, 210–219. doi:10.1124/jpet.121.000743

Shah, N., Lipato, T., Alvarez, O., Delea, T., Lonshteyn, A., Weycker, D., et al. (2022). Real-world effectiveness of voxelotor for treating sickle cell disease in the US: a large claims data analysis. *Expert Rev. Hematol.* 15, 167–173. doi:10.1080/17474086.2022.2031967

Shrestha, A., Chi, M., Wagner, K., Malik, A., Korpik, J., Drake, A., et al. (2021). FT-4202, an oral PKR activator, has potent antisickling effects and improves RBC survival and Hb levels in SCA mice. *Blood adv.* 5, 2385–2390. doi:10.1182/bloodadvances.2020003604

Sluyter, R. (2015). P2X and P2Y receptor signaling in red blood cells. *Front. Mol. Biosci.* 2, 60. doi:10.3389/fmolb.2015.00060

Smethurst, P. A., Jolley, J., Braund, R., Proffitt, S., Lynes, T., Hazell, M., et al. (2019). Rejuvenation of RBCs: validation of a manufacturing method suitable for clinical use. *Transfusion* 59, 2952–2963. doi:10.1111/trf.15426

Sonveaux, P., Lobysheva, I. I., Feron, O., and McMahon, T. J. (2007). Transport and peripheral bioactivities of nitrogen oxides carried by red blood cell hemoglobin: role in oxygen delivery. *Physiol. (Bethesda)* 22, 97–112. doi:10.1152/physiol.00042.2006

Soule, L. D., Skrajewski-Schuler, L., Branch, S. A., McMahon, T. J., and Spence, D. M. (2024). Toward translational impact of low-glucose strategies on red blood cell storage optimization. *ACS Pharmacol. Transl. Sci.* 7, 878–887. doi:10.1021/acsptsci.4c00018

Srinivasan, A. J., Kausch, K., Inglut, C., Gray, A., Landrigan, M., Poisson, J. L., et al. (2018). Estimation of achievable oxygen consumption following transfusion with rejuvenated red blood cells. *Semin. Thorac. Cardiovasc Surg.* 30, 134–141. doi:10.1053/j.semtcvs.2018.02.009

Stewart, G. M., Chase, S., Cross, T. J., Wheatley-Guy, C. M., Joyner, M. J., Curry, T., et al. (2020). Effects of an allosteric hemoglobin affinity modulator on arterial blood gases and cardiopulmonary responses during normoxic and hypoxic low-intensity exercise. *J. Appl. Physiol. (1985)* 128, 1467–1476. doi:10.1152/japplphysiol.00185.2019

Suhail, M. (2024). Biophysical chemistry behind sickle cell anemia and the mechanism of voxelotor action. *Sci. Rep.* 14, 1861. doi:10.1038/s41598-024-52476-8

Tanneur, V., Duranton, C., Brand, V. B., Sandu, C. D., Akkaya, C., Kasinathan, R. S., et al. (2006). Purinoceptors are involved in the induction of an osmolyte permeability in malaria-infected and oxidized human erythrocytes. *FASEB J.* 20, 133–135. doi:10.1096/fj.04-3371fje

Thomas, T., Cendali, F., Fu, X., Gamboni, F., Morrison, E. J., Beirne, J., et al. (2021). Fatty acid desaturase activity in mature red blood cells and implications for blood storage quality. *Transfusion* 61, 1867–1883. doi:10.1111/trf.16402

Tzounakas, V. L., Anastasiadi, A. T., Drossos, P. V., Karadimas, D. G., Valsami, S. E., Stamoulis, K. E., et al. (2021). Sex-related aspects of the red blood cell storage lesion. *Blood Transfus.* 19, 224–236. doi:10.2450/2020.0141-20

Valeri, C. R., and Hirsch, N. M. (1969). Restoration *in vivo* of erythrocyte adenosine triphosphate, 2,3-diphosphoglycerate, potassium ion, and sodium ion concentrations following the transfusion of acid-citrate-dextrose-stored human red blood cells. *J. Lab. Clin. Med.* 73, 722–733.

van Manen, L., Deurvorst, J. M., van Hezel, M. E., Boshuizen, M., van Bruggen, R., and Juffermans, N. P. (2020). Severity of illness influences the microcirculatory response to red blood cell transfusion in the critically ill: an observational cohort study. *Crit. Care* 24, 498. doi:10.1186/s13054-020-03202-z

Vardaki, M. Z., Schulze, H. G., Serrano, K., Blades, M. W., Devine, D. V., and Turner, R. F. B. (2021). Non-invasive monitoring of red blood cells during cold storage using handheld Raman spectroscopy. *Transfusion* 61, 2159–2168. doi:10.1111/trf.16417

Vichinsky, E., Hoppe, C. C., Ataga, K. I., Ware, R. E., Nduba, V., El-Beshlawy, A., et al. (2019). A phase 3 randomized trial of voxelotor in sickle cell disease. *N. Engl. J. Med.* 381, 509–519. doi:10.1056/NEJMoa1903212

Vlahakis, N., Dixon, S., Lehrer, J., and Beck, K. (2019). Voxelotor, which left shifts the oxy-hemoglobin dissociation curve, improves oxygen desaturation in IPF patients during maximal exercise. *Eur. Respir. J.* 54. doi:10.1183/13993003.congress-2019.pa1636

Wang, X., Gardner, K., Tegegn, M. B., Dalgard, C. L., Alba, C., Menzel, S., et al. (2022). Genetic variants of PKLR are associated with acute pain in sickle cell disease. *Blood Adv.* 6, 3535–3540. doi:10.1182/bloodadvances.2021006668

Wang, D., Sun, J., Solomon, S. B., Klein, H. G., and Natanson, C. (2012). Transfusion of older stored blood and risk of death: a meta-analysis. *Transfusion* 52, 1184–1195. doi:10.1111/j.1537-2995.2011.03466.x

Wang, Y., Giebink, A., and Spence, D. M. (2014). Microfluidic evaluation of red cells collected and stored in modified processing solutions used in blood banking. *Integr. Biol. (Camb)* 6, 65–75. doi:10.1039/c3ib40187a

Williams, A. T., Jani, V. P., Nemkov, T., Lucas, A., Yoshida, T., Dunham, A., et al. (2020). Transfusion of anaerobically or conventionally stored blood after hemorrhagic shock. *Shock* 53, 352–362. doi:10.1097/SHK.0000000000001386

Wong, A.-K. I., Charpignon, M., Kim, H., Josef, C., de Hond, A. A. H., Fojas, J. J., et al. (2021). Analysis of discrepancies between pulse oximetry and arterial oxygen saturation measurements by race and ethnicity and association with organ dysfunction and mortality. *JAMA Network Open* 4, e2131674–e2131674. doi:10.1001/jamanetworkopen.2021.31674

Xu, J. Z., Conrey, A., Frey, I., Gwaabe, E., Menapace, L. A., Tumburu, L., et al. (2022). A phase 1 dose escalation study of the pyruvate kinase activator mitapivat (AG-348) in sickle cell disease. *Blood* 140, 2053–2062. doi:10.1182/blood.2022015403

Yoshida, T., Blair, A., D'Alessandro, A., Nemkov, T., Dioguardi, M., Silliman, C. C., et al. (2017). Enhancing uniformity and overall quality of red cell concentrate with anaerobic storage. *Blood Transfus.* 15, 172–181. doi:10.2450/2017.0325-16

Yoshida, T., Prudent, M., and D'Alessandro, A. (2019). Red blood cell storage lesion: causes and potential clinical consequences. *Blood Transfus.* 17, 27–52. doi:10.2450/2019.0217-18

Zhang, Y., Dai, Y., Wen, J., Zhang, W., Grenz, A., Sun, H., et al. (2011). Detrimental effects of adenosine signaling in sickle cell disease. *Nat Med* 17, 79–86. doi:10.1038/nm.2280

Zhang, R., Hess, D. T., Qian, Z., Hausladen, A., Fonseca, F., Chaube, R., et al. (2015). Hemoglobin βCys93 is essential for cardiovascular function and integrated response to hypoxia. *Proc. Natl. Acad. Sci. U. S. A.* 112, 6425–6430. doi:10.1073/pnas.1502285112

Zhang, R., Hess, D. T., Reynolds, J. D., and Stamler, J. S. (2016). Hemoglobin S-nitrosylation plays an essential role in cardioprotection. *J. Clin. Invest.* 126, 4654–4658. doi:10.1172/JCI90425

Frontiers in Physiology

Understanding how an organism's components work together to maintain a healthy state

The second most-cited physiology journal, promoting a multidisciplinary approach to the physiology of living systems - from the subcellular and molecular domains to the intact organism and its interaction with the environment.

Discover the latest Research Topics

See more →

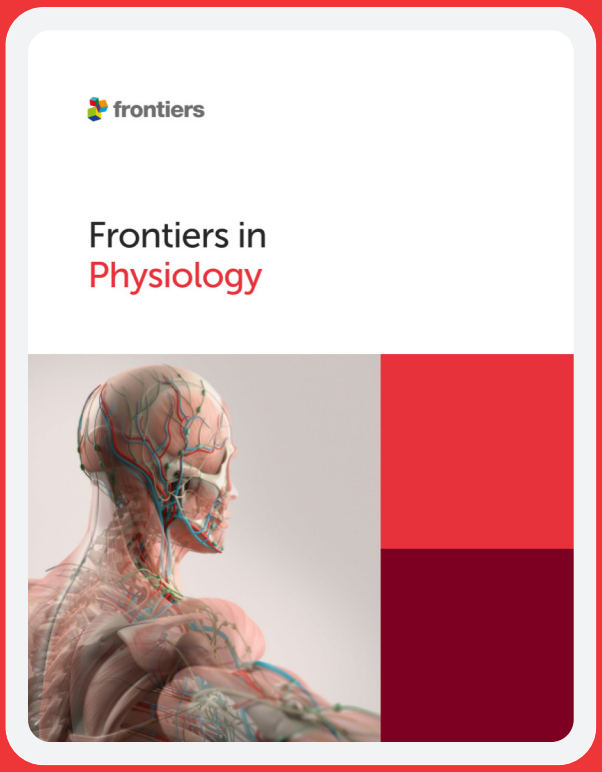

Frontiers

Avenue du Tribunal-Fédéral 34
1005 Lausanne, Switzerland
frontiersin.org

Contact us

+41 (0)21 510 17 00
frontiersin.org/about/contact